Title: Cell identity allocation and optimisation of handover parameters in self-organised LTE femtocell networks

Name: Xu Zhang

Cell Identity Allocation and Optimisation of Handover Parameters in Self-organised LTE Femtocell Networks

by Xu Zhang

A thesis submitted to the University of Bedfordshire in partial fulfilment of the requirements for the degree of Doctor of Philosophy

16-09-2013

Abstract

Femtocell is a small cellular base station used by operators to extend indoor service coverage and enhance overall network performance. In Long Term Evolution (LTE), femtocell works under macrocell coverage and combines with the macrocell to constitute the two-tier network. Compared to the traditional single-tier network, the two-tier scenario creates many new challenges, which lead to the 3rd Generation Partnership Project (3GPP) implementing an automation technology called Self-Organising Network (SON) in order to achieve lower cost and enhanced network performance.

This thesis focuses on the inbound and outbound handovers (handover between femtocell and macrocell); in detail, it provides suitable solutions for the intensity of femtocell handover prediction, Physical Cell Identity (PCI) allocation and handover triggering parameter optimisation. Moreover, those solutions are implemented in the structure of SON.

In order to efficiently manage radio resource allocation, this research investigates the conventional UE-based prediction model and proposes a cell-based prediction model to predict the intensity of a femtocell's handover, which overcomes the drawbacks of the conventional models in the two-tier scenario. Then, the predictor is used in the proposed dynamic group PCI allocation approach in order to solve the problem of PCI allocation for the femtocells. In addition, based on SON, this approach is implemented in the structure of a centralised Automated Configuration of Physical Cell Identity (ACPCI). It overcomes the drawbacks of the conventional method by reducing inbound handover failure of Cell Global Identity (CGI). This thesis also tackles optimisation of the handover triggering parameters to minimise handover failure. A dynamic hysteresis-adjusting approach for each User Equipment (UE) is proposed, using received average Reference Signal-Signal to Interference plus Noise Ratio (RS-SINR) of the UE as a criterion. Furthermore, based on SON, this approach is implemented in the structure of hybrid Mobility Robustness Optimisation (MRO). It is able to offer the unique optimised hysteresis value to the individual UE in the network.

In order to evaluate the performance of the proposed approach against existing methods, a System Level Simulation (SLS) tool, provided by the Centre for Wireless Network Design (CWiND) research group, is utilised, which models the structure of two-tier communication of LTE femtocell-based networks.

Contents

Acknowledgement

I would like to give my deepest thankfulness to my supervisor Dr. Enjie Liu for her patient guidance, kind encouragement and responsible supervision throughout my PhD study. Without her help, I would be unable even to finish my PhD.

To my co-supervisor Prof. Jie Zhang and his wife Dr. Joyce Wu, I would like to give my deepest appreciation, for their kind help, especially the financial aspect. Without their help, I might have already left the University and stopped my PhD study.

I would like to give my deepest gratitude to Prof. Carsten Maple and Prof. Edmond Prakash, for their kind help during my PhD study.

For assistance with proofing the final manuscript, I would like to thank Dr. Peter Norrington.

My thanks to the all researchers in the Centre for Wireless Communication for their valuable support and also my thanks to the University of Bedfordshire for providing me with the working environment.

Last but not least, I would like to thank my parents for their continuing emotional and practical support throughout my PhD study, and I appreciate my friends for their selfless help.

Declaration

I declare that the works described in this thesis is my own unaided work for the degree of Doctor of Philosophy at the University of Bedfordshire. It has not been submitted for any degree or in any other University or college of advanced education.

This thesis is written by me and produced using LATEX.

Name of candidate: Xu Zhang Signature:

List of Figures

List of Tables

List of Publications

- X. Zhang, D.B. Zhou, Z. Xiao, E.J. Liu, J. Zhang, and A.A. Glasunov, "Dynamic Group PCI Assignment Scheme," *Seventh International Conference on Wireless and Mobile Communications(ICWMC)*, pp. 101-106, 2011.

- Z. Xiao, P. Wang, X. Zhang, S. Mahato, L. Chen, and J. Zhang, "Incentive mechanism for uplink interference avoidance in two-tier macro-femto networks," *Vehicular Technology Conference (VTC Spring), IEEE*, pp. 1-6, 2012.

- X. Zhang, Z. Xiao, E.J. Liu, and J. Zhang, "Dynamic PCI assignment in two-tier networks based on cell activity prediction," *IET Electronics Letters*, vol.49, No.24, Nov.2013, pp.1570-1572.

- X. Zhang, Z. Xiao, S. B. Mahato, E. Liu, B. Allen, and C. Maple, "Dynamic UE-based Hysteresis-adjusting Algorithm in LTE Femtocell Network," *IET Communication*, 2014. (Accepted by IET Communication)

Acronyms

3GPP 3rd Generation Partnership Project

ACPCI Automatic Configuration of Physical Cell ID

ANR Automatic Neighbour Relation

APG Average Path-Gain

ARP Allocation Retention Priority

BER Bit Error Ratio

BCCH Broadcast Control CHannel

BFemtocell Busy Femtocell

BUGs Bayesian inference Using Gibbs sampling

CAPEX Capital Expenditure

CI Cell Identity

CCO Coverage & Capacity Optimisation

CDF Cumulative Distribution Function

CQI Channel Quality Indication

CSG Closed Subscriber Group

CN Core Network

CTI Cross-Tier Interference

CGI Cell Global Identity

DCCH Dedicated Control CHannel

DM-RS Demodulation Reference Signals

DRX Discontinuous Reception

DGPAS Dynamic Group PCI Allocation Scheme

DUHA Dynamic UE-based Hysteresis-adjusting Algorithm

EHO Early Handover

EPS Evolved Packet System

E-UTRAN Evolved Universal Terrestrial Radio Access Network

EPC Evolved Packet Core

eICIC enhanced Inter-Cell Interference Coordination

F-GW Femtocell Gateway

FN False Negative

FP False Positive

GBR Guaranteed Bit Rate

HAPI Handover Aggregate Performance Indicator

HAP Handover Additional Parameter

HetNet Heterogeneous Networks

HPIs Handover Performance Indicators

HMM Hidden Markov Model

HSS Home Subscriber Server

LHO Late Handover

ICMP Internet Control Message Protocol

ITU International Telecommunications Union

ITU-R International Telecommunications Union Radio communication Sector

LAC Local Area Code

LTE Long Term Evolution

MCMC Markov Chain Monte Carlo

MBR Maximum Bit Rate

MRO Mobility Robustness Optimisation

MLB Mobility Load Balancing

MUE Macrocell UE: a UE is serving by Macrocell

MRP Markov Renewal Process

MIB Master Information Block

MME Mobility Management Entity

MCC Mobile Country Code

MNC Mobile Network Code

MCS Modulation and Coding Scheme

NCL Neighbour Cell List

OAM Operation Administration and Maintenance

OPEX Operating Expenditure

OFDM Orthogonal Frequency Division Multiplexing

OFDMA Orthogonal Frequency Division Multiple Access

OSS Operation Support System

PCI Physical Cell Identity

PCRF Policy Control and Charging Rules Function

PCEF Policy and Charging Enforcement Function

PDN Packet Data Network

P-GW Packet Data Network Gateway

POT Physical Cell Identity Optimisation Tool

PPT Physical Cell Identity Planning Tool

PUSCH Physical Uplink Shared Channel

PSS Primary Synchronization Signal

QoS Quality of Service

QCI Quality of Service Class Indicator

RACH Random Access Channel

RLF Radio Link Failure

RSS Received Signal Strength

RSSI Received Signal Strength Indicator

RSRQ Reference Signal Received Quality

RS-SINR Reference Signal-Signal to Interference plus Noise Ratio

RSRP Reference Symbol Received Power

RB Resource Block

RE Resource Element

RE Radio Frequency

RP Revise Parameter

SBs Scheduling Blocks

SFN System Frame Number

SSS Secondary Synchronization Signal

SON Self-Organizing Network

S-GW Serving Gateway

SIB1 System Information Block Type 1

SC-FDMA Single-Carrier Frequency Division Multiple Access

SINR Signal to Interference plus Noise Ratio

SFN System Frame Number

SIBs System Information Blocks

TTT Time-To-Trigger

TBS Transport Block Size

TN True Negative

TP True Positive

TPM Traffic Prediction Model

UE User Equipment

VoIP Voice-over-IP

ZMHB Zoned Mobility History Base

Chapter 1

Introduction

This introductory chapter describes the basic information of the research scenario such as the Long-Term Evolution (LTE) single-tier and LTE femtocell (two-tier) network. Then, it explains the motivations that drive this research, aims and objectives, the main research questions, key contributions and the organisation of this thesis.

1.1 LTE Single-tier Network

Mobile and wireless communications have undergone sustained and ever-increasing growth in the first decade of this century. It attracts researchers to work with comprehensive new technologies in order to meet the growing requirements of high-speed mobile broadband.

LTE refers to Long-Term Evolution, a standard developed by the Third Generation Partnership Project (3GPP) standardisation body at Release 8 [1]. It is commonly marketed as 3rd Generation (3G) beyond LTE or 3.9G and represents wireless communication of high-speed data for data terminals and mobile phones. There are several advantages of LTE when compared with existing 3G networks:

The first advantage is LTE offers faster data transfer rates which turn to higher download and upload rates. Generally, when LTE operates at the 20 megahertz (MHz) bandwidth, it should provide at least 100 Mega bits Per

Second (Mbps) in the downlink and 50 Mbps in the uplink [2].

The second advantage is LTE provides better spectrum efficiency and flexibility than 3G systems by allowing spectrum allocations for cells from 1.4 MHz up to 20 MHz [2]. In LTE, Orthogonal Frequency-Division Multiple Access (OFDMA) is used for the downlink and Single-Carrier Frequency Division Multiple Access (SC-FDMA) is used for uplink and they have the ability to allocate the Resource Block (RB) for users in the limited spectrum [3]. As a multiple access, both of them provide diverse time and frequency channel. They enhance the spectrum efficiency of networks by assigning distinct Orthogonal Frequency Division Multiplexing (OFDM) symbols to distinct users.

The third advantage is that LTE considers both Frequency Division Duplexing (FDD) and Time Division Duplexing (TDD) modes for uplink and downlink duplexing [4]. FDD is a method for establishing a full-duplex communications link. It applies two different radio frequencies for transmitter and receiver operation. Therefore, a defined frequency offset is used to separate the transmit and receive frequencies. On the other hand, TDD is a method for emulating full-duplex communication over a half-duplex communication link. It uses the same frequency on both the transmitter and receiver direction. However, the transmit and receive traffic is separated by a defined time.

The last advantage is LTE supports the load management of the neighbouring cells to achieve inter-cell interference coordination by providing information concerning resource use and traffic load conditions [5]. Further information regarding LTE/LTE-Advanced (LTE-A) will be introduced in Section 2.1.

A macrocell is a high-power base station (cellular) in a mobile phone network which provides radio coverage service [6]. It has large service coverage, generally a 1 to 2.5 kilometre (km) radius. If macrocell work with LTE solutions, its coverage can be up to a 100 km radius. However, due to large coverage, there are two problems which can occur in the network [6]:

- Blind spot problem. Due to the shadow fading during the signal wave propagation, the service of macrocell cannot cover a number of specific areas.

- Hot spot problem. Due to the uneven distribution of traffic load of the cells, the service of macrocell cannot cover a number of specific areas.

In order to solve these problems (extend the coverage of wireless service), the standard [7] defines that term macrocell is used to describe the widest range of cell sizes and provide a large area service coverage. Over a smaller cell area, a microcell (micro) is used in a densely populated urban area with about 100-500 metres coverage. Picocell (pico) is used for areas even smaller than those of microcell, about 10 to 80 metres coverage. Femtocell (femto) is used for areas smaller than those of micro and pico, about 10-20 metres (indoor coverage).

Moreover, in an LTE network, if the micro, pico and femto are all deployed within the coverage of the macrocell, this structure of network is called a heterogeneous network. Further information concerning heterogeneous LTE will be introduced in Chapter 2. If the LTE network only consists of macrocell, this is known as a single-tier network. Moreover, if the LTE network consists of both the macrocell and femtocell, it is known as a two-tier network. The single-tier network structure is shown in Figure 1.1.

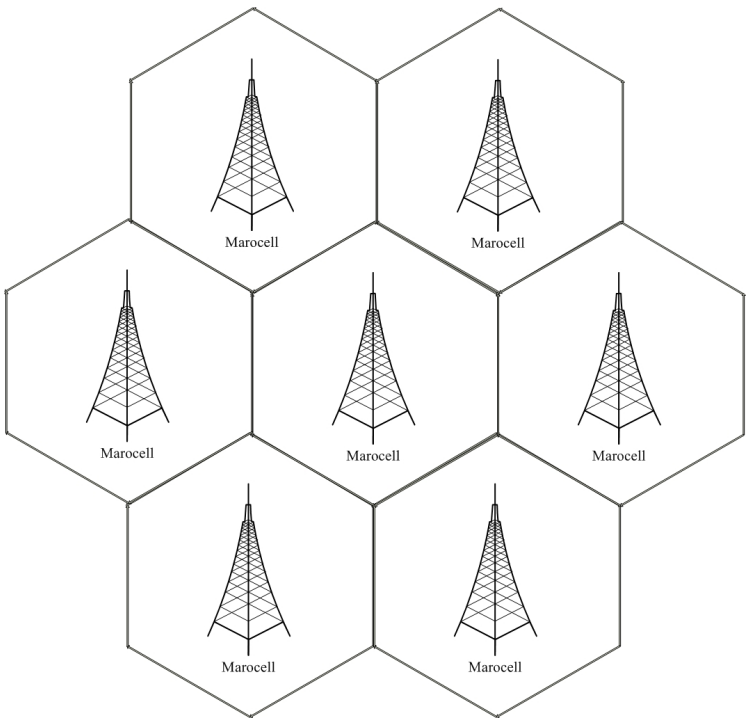

Figure 1.1: The structure of LTE macrocell single-tier network

As shown in Figure 1.1, all users are located in the coverage of the macrocell and only the macrocell offers wireless communication service for the users in the network.

1.2 Femtocall Two-tier Network

In mobile communication, it is estimated that nearly 2/3 [6] of calls and over 90% [6] of data services occur in an indoor scenario. Unfortunately, many indoor users experience poor coverage problems according to some surveys [6]. If this problem cannot be solved satisfactorily, it would seriously impact the Quality of Service (QoS) to users and result in operators losing their clients.

However, even with advances in 4G technology, the traditional macro cellular network simply cannot satisfy the growth in demand for mobile data whether in an indoor or outdoor scenario [8]. This is due to the limitations of the macrocell, such as:

- Limitation of the number of macro stations that can be built due to macro sites being particularly costly.
- Limitation of the location of the macro due to the new site not being located at the optimal area.
- Limitation of the spectrum can satisfy the requirements of the network due to the increase in demand.
- Limitation of the usage of macro cell backhaul due to cost.

Therefore, a small wireless base station, femtocell, has been considered an important radio access technology which extends the service of macrocell and which has received wide attention in recent years. Since the femtocell has a small size, low power, cost-effective and high-performance features [6], it is a talented solution not only to enhance indoor coverage but also to satisfy the fast-growing traffic requirements within current cellular networks.

The femtocell is typically located inside larger cells served by nearby macrocell base stations. As a result, this network structure is divided into two clearly-separated tiers as shown in Figure 1.2.

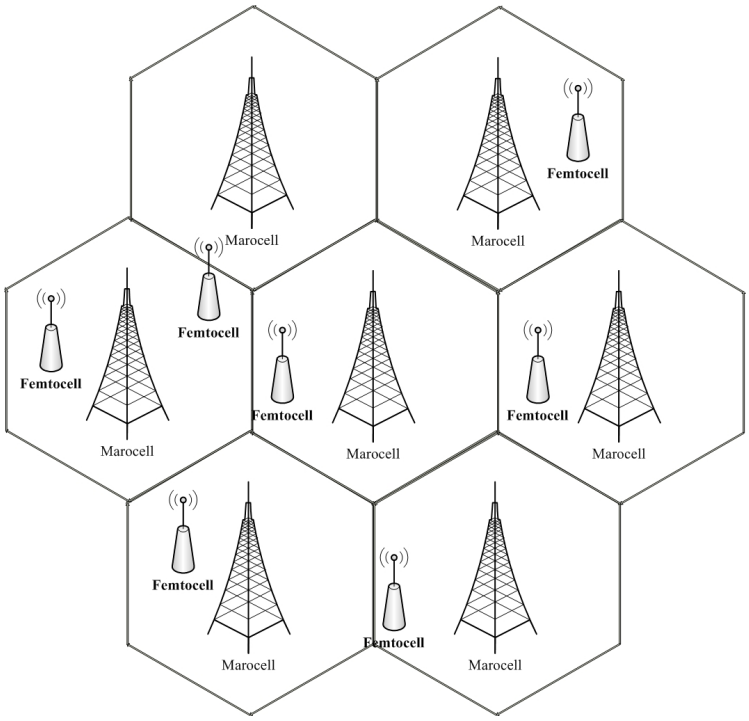

Figure 1.2: The structure of LTE femtocell two-tier network

As shown in Figure 1.2, all users and femtocells are located within the coverage of macrocell. The macrocell tier that provides cellular coverage to mobile users and to the femtocell tier that is used to enhance the coverage of wireless service in an indoor scenario (blind spot or hot spot). Therefore, this kind of network with an LTE solution is known as an LTE femtocell two-tier network.

Moreover, the three network elements that are common to any femtocell network architecture are listed below and the femtocell network architecture itself is shown in Figure 1.3 [9].

- The Femtocell Access Point (FAP): FAP is the primary node in a femtocell network. It implements the functions of the base station and base station controller. Through an Internet connection, FAP is able to connect to the operator network.

- Security Gateway (SeGW): The SeGW is a network node which ensures the security of the Internet connection between femtocell users and the mobile operator core network.

- femtocell Device Management System (FMS): The FMS is located in the operator network (core network). It can remotely configure the FAP and play an important role in the operational management, provisioning and activation of the FAP.

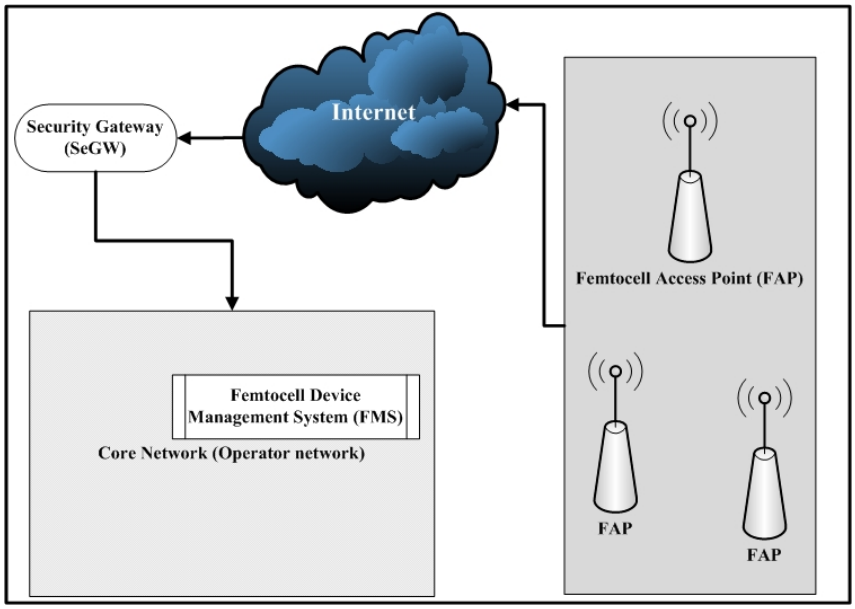

Figure 1.3: The femtocell network architecture

In addition, due to the two-tier network structure, femtocells need to avoid or mitigate any interference with macrocells and provide a seamless experience to users within the wireless service coverage. However, the femtocell is designed to be randomly deployed by the customer (femtocell is a plug-and-play device). Therefore, this technique brings several technical challenges when working with the traditional macrocell [10], such as:

Mobility and Handover: The coverage area of an individual femtocell is small; it is essential to support seamless handovers to and from femtocells to provide continuous connectivity. Handover scenarios include femto-to-macro (outbound mobility), macro-femto (inbound mobility) and possibly femto-to-femto.

Self-Organizing Networks: femtocell networks are largely installed by customers or private enterprises often in an ad-hoc manner without traditional Radio Frequency (RF) planning, site selection, deployment and maintenance by the operator. In that sense, femtocells are sometimes referred to as a Self-Organizing Network (SON).

Interference Coordination: Interference introduced by the femtocell can be featured as: stronger, less predictable, and more varied interference. Interference occurs predominantly when femtocells are deployed in the same spectrum as the legacy (outdoor) wireless network, but can also occur even when femtocells are in a different but adjacent frequency band due to out-of-band radiation, particularly in dense deployments.

Cell Association and Biasing: Assigning users to a proper base station is a key challenge in a heterogeneous network with a wide variety of cell sizes. A solution called 'biasing' has been introduced, whereby users are actively pushed onto small cells. Despite a potentially significant SINR hit for that mobile station, this has the potential for a win-win scenario because the mobile gains access to a much larger fraction of the small cell time and frequency slots. On the other hand, the macrocell reclaims the time and frequency slots that the user would have occupied.

1.3 Motivations

The two-tier network offers a flexible solution that benefits both users and operators, and has been widely deployed in current wireless network systems. However, the random deployment of femtocells (femtocell is a plug-and-play device) and the complex architecture of a two-tier network brings several technical challenges as mentioned earlier.

1.3.1 Physical Cell Identity (PCI) Allocation

Since the coverage area of an individual femtocell is small, it is essential to support seamless handovers to and from femtocells to provide continuous con-

nectivity [6]. During the handover, in an LTE network, the PCI is used to identify the serving and target femtocells. Moreover, the PCI is also used to achieve channel synchronisation between a UE and newly detected cell [11]. Therefore, the PCI value must be unique during the handover and synchronisation process.

Unfortunately, the number of PCIs is limited to 504 due to the limited bytes allocated in the standard [12]. The number is insufficient in cases when introducing large numbers of femtocells. Reflecting this, 3GPP release 9 [12] introduces (Cell Global Identity) CGI to work together with PCI as a solution. However, there are unavoidable drawbacks for using CGI. For example, CGI is obtained by reading system information, which is easily done when UE is in idle mode. When UE is in connected mode, it uses the autonomous gap to read the system information, which takes at least 150 ms as mentioned in release 10 [11]. During that period, UE cannot exchange information with its serving cell, which may lead to service interruption or a call-drop.

Moreover, in LTE, the trigger of handover is only dependent on the UE measurement report [11], the longer the cell identity measurement period, the higher the chance that the UE misses the opening to implement the handover process, which may also result a serious growth of call-drop ratio. Therefore, the PCI allocation problem remains crucial to ensuring a successful handover process.

1.3.2 Triggering Handover Parameter Optimisation

Due to the two-tier structure of femtocell and macrocell deployment, the handover scenario differs considerably from conventional LTE networks, e.g. the coverage of the femtocell is much smaller than the macrocells, the handover between macrocell and femtocell would experience more severe Signal-to-Interference Noise Ratio (SINR) degradation than the handover between macrocells. Therefore, handover from macrocell to femtocell is the most challenging issue for femtocell network deployment [6]. Reflecting this, 3GPP LTE has proposed Mobility Robustness Optimisation (MRO) which focuses

on autonomous selection and optimisation of handover triggering parameters to overcome these issues [12].

In terms of the handover triggering parameters, during the handover process, non-optimal handover triggering parameters such as hysteresis and Time-To-Trigger (TTT) may cause unexpected handover failure, which is quite destructive to the network's continuous connectivity. Currently most research, such as [13] and [14], provide centralised optimal hysteresis for all UEs. However, the centralised optimised parameters algorithm only considers enhancing the average handover performance for the overall system and ignores the nature of the problem: UE's mobility. Therefore, centralised optimal parameter techniques cannot offer the optimised individual hysteresis to each UE.

As a result, it is anticipated that by designing a more flexible approach, a unique, optimised hysteresis value for every UE in the network can be provided.

1.3.3 Self-Organizing Networks

As mentioned earlier, femtocell networks are largely installed by customers or small business often in an ad-hoc manner without the planning, site selection, deployment or maintenance by the operator. In that case, femtocells are referred to as a Self-Organizing Network (SON) [12].

SON has been accepted by 3GPP as the technology for LTE femtocell network development [15]. Compared with SON, traditional manual methods may not be adequate to solve these challenges, or may solve them but while introducing higher costs to operators. The core idea of SON is to automatically sense and react to changes in the network. The reactions include the planning, configuration, management, optimisation and healing of network system. Currently, 3GPP has summarised the self-organisation functions in two-tier networks as shown in Figure 1.4 [12].

Figure Figure 1.4 shows that many functions have been summarised by standards to solve the specific issues in LTE two-tier networks. Automated Configuration of Physical Cell Identity (ACPCI) and Regarding Mobility Robustness Optimisation (MRO) have been defined in SON by 3GPP standard,

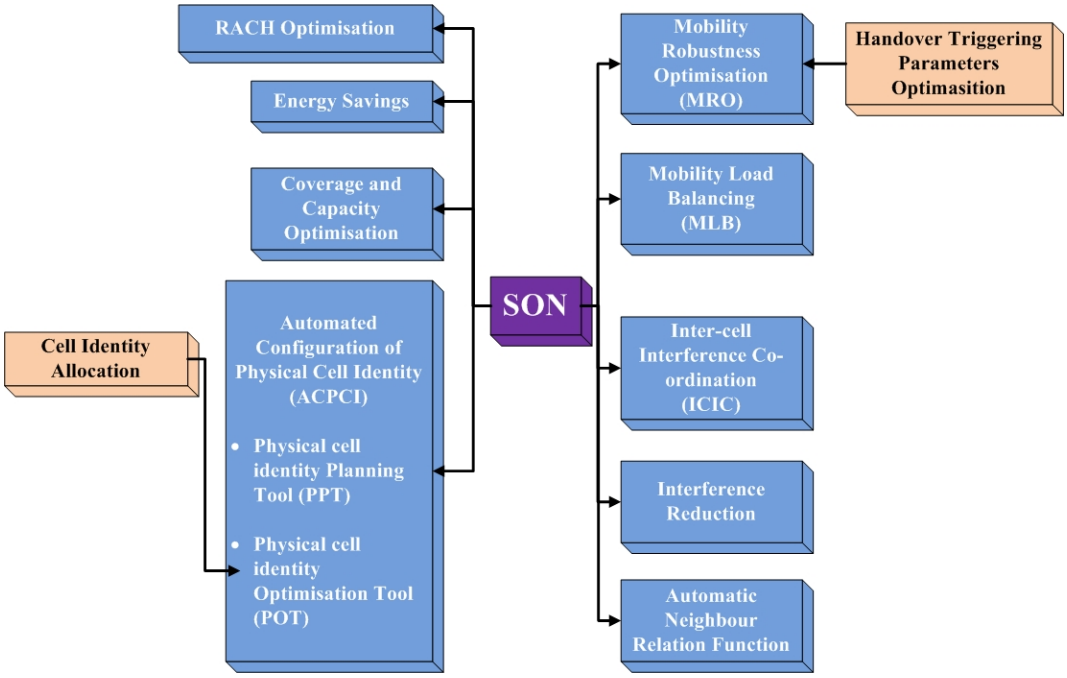

Figure 1.4: The contents of self-organising network

in order to solve the issues mentioned earlier, such as cell identity allocation and handover triggering parameter optimisation.

ACPCI is used for PCI self-planning and provides functions such as PCI allocation situation collection as well as report and PCI management to support the specific PCI allocation approach. Moreover, ACPCI can be separated into two parts [16]. The first part is the Physical cell identity Planning Tool (PPT), and it is used to initialise a Physical Cell Identity (PCI) to the new powered-up femtocell. The other part is the Physical cell identity Optimisation Tool (POT), used to update the PCI value of a femtocell which needs to be changed due to a confusion or collision problem.

Regarding MRO, it is used to optimise handover triggering parameters and provides functions such as handover information collection and reporting as well as the adjustment of those parameters.

Since standards have provided the structure and function of the issues described earlier, it is desirable to design the solutions based on SON.

1.3.4 Traffic Behaviour Prediction Model

Thorough understanding of traffic behaviours leads to a more efficient allocation and management of network radio resources [17]. Reflecting this, most of the current researches on traffic behaviour prediction models are UE-based in a single-tier scenario (marcocell only). For instance, in [18] and [19], the authors propose a traffic behaviour model using the Markov process and Hidden Markov Model (HMM). A state is modelled when a user remains within a particular cell's coverage. If this user stays in on another cell, the state is changed correspondingly.

Those approaches work well in the single-tier deployment, however, it is not suitable for two-tier networks with macrocells and femtocells. One vital reason is that, as mentioned earlier, femtocells are plug-and-play device and it could turn on and off frequently at any time, therefore, it is impossible to obtain an accurate transition probability for each state. The other is that, in the two-tier scenario, a larger number of femtocells also leads to large and unmanageable states in the analysis, which leads to the lower accuracy of the prediction [20]. As a consequence, it is necessary to design a new prediction model for the two-tier network scenario.

1.4 Aims and Objectives

The aim of this thesis is, based on the SON structure, to develop two novel approaches that overcome the issues which occur at the handover between femtocell and macrocell. In addition, to design an optimal traffic behaviour prediction model for the two-tier scenario in order to obtain the necessary system information to associate with those approaches.

The following is a list of objectives that have to be met in order to achieve the research aims:

- To study details all the proposed issues and drawbacks of conventional approaches and prediction models.

- To present how the proposed approach and prediction model can be implemented in the system, especially under the SON structure.
- To analyse why the proposed approach and prediction model were chosen carefully and can achieve better performance than conventional approaches.

1.5 Proposed Solution

The proposed approaches are achieved from the following considerations. The detailed descriptions of those approaches are discussed in Chapters 3, 4 and 5.

Traffic Behaviour Prediction Model

In order to provide a proper prediction model in a LTE femtocell network, this thesis proposes a cell-based prediction model to predict the intensity of a femtocell's effective mobility (the number of handovers appearing in a cell over a time period). In this model, based on the HMM, the hidden states are modelled based on learning the femtocell's handover, and the future network situation can be predicted for system management.

The reason for using HMM instead of Markov is that HMM is able to find more predictive information which is hidden in traffic states than the Markov process [19]. The advantages of the proposed approach are: firstly, it avoids the necessity of frequently counting the number of cells as in the UE-based model, due to the large number of femtocells deployment; secondly, regardless of whether the cell turns on or off, which happens frequently with the femtocell, the transition probability and emission probability will not be affected.

Cell Identity Allocation

In order to solve PCI confusion and the drawbacks of reading CGI in a two-tier network, this thesis proposes a centralised dynamic group PCI allocation scheme. This scheme can be described by firstly separating PCI resources into two different groups such as, unique and reused PCI groups. It then uses the proposed prediction model to determine the Busy femtocell (BFemtocell) with a higher intensity of handovers (the number of inbound handovers). After that,

the scheme will assign the unique PCI to those BFemtocells which especially need to be taken care of. Moreover, since unique PCI is the key parameter in the proposed scheme, the PCI release is also proposed in the scheme. Overall, the proposed scheme complies with ACPCI function in the standards and offers optimised PCI allocation in order to achieve better network performance.

Parameter Optimisation for Triggering the Handover Process

In order to provide the optimised individual hysteresis for every UE, this thesis proposes a hybrid dynamic hysteresis-adjusting scheme. This solution is based on each UE's receiving average Reference Signal-Signal to Interference plus Noise Ratio (RS-SINR) and the reserved parameters form the central controller, UE can calculate its individual hysteresis value. The reason the proposed algorithm uses RS-SINR is that UE's mobility is the only basic feature which triggers the handover process (event), and RS-SINR has a close relation with the UE mobility (UE's various speeds cause changes in the RS-SINR scenario). Overall, the proposed scheme provides a self-optimisation ability to offer the unique optimised hysteresis to the individual UE in order to achieve better handover performance.

1.6 Research Questions

This thesis introduces one traffic prediction model and two approaches to improve the QoS for a handover in a two-tier network. By conducting the research work, this thesis tries to answer the following questions.

- What is the traffic prediction in mobility management and why it is important for resource management in a network system? Moreover, what are the current prediction models and why should a novel traffic prediction model for the two-tier scenario be designed?

- What is cell identity allocation and why it is important for the handover process? Moreover, how to design a centralised PCI distribution approach and to associate with the proposed novel traffic prediction model?

- What are the handover triggering parameters and why are the parameters important for the handover process? In addition, what are the current hysteresis optimisation approaches and why design a hybrid hysteresis self-optimisation algorithm for an LTE femtocell network?

1.7 Contributions

The main contributions in this thesis can be illustrated as follows. The detailed evaluation of these contributions is discussed in Chapter 6.

- **Cell-based prediction model**

  A prediction model based on the intensity of a femtocell's handover (the number of handovers) has been presented. It has been designed not only overcome the drawbacks of conventional UE-based prediction models in the LTE femtocell two-tier scenario but also it provides higher accuracy by obtaining the actual traffic behaviour information which hides in the networks. This prediction model results in extremely high accuracy (up to 90%) when compared to other conventional models in the proposed system-level simulation which is described in detail in the Appendix B.1.

- **Dynamic group PCI allocation scheme**

  Based on the centralised SON structure and complying with its ACPCI function, a dynamic PCI group distribution scheme has been introduced which provides a kind of self-planning ability to offer an optimised PCI allocation approach and also a PCI release approach. This work ensures a higher ratio of successful handovers (an increase of about 40% in the proposed system level simulation) for the femtocells with higher intensity handovers. Therefore, this approach results in enhanced network performance overall in the two-tier scenario.

- **Dynamic hysteresis-adjusting approach**

  Based on the hybrid SON structure and functions provided by MRO, a dynamic UE-based hysteresis-adjusting self-optimisation algorithm has

been demonstrated, unlike the conventional approach that all UEs share the same centralised hysteresis value to trigger handover process. This approach offers the unique optimised hysteresis for the individual UE. Moreover, the Handover Aggregate Performance Indicator (HAPI) and Revise Parameter (RP) have been provided to ensure the correctness of the hysteresis in the handover process. In the system-level simulation, it shows better handover performance (lower RLF, improved up to 5%; lower call-drop and redundancy ratios) than the centralised conventional method in the two-tier scenario.

1.8 Thesis Outlines

In this thesis, the outline of the remaining chapters are organised and their relationship is shown in Figure 1.5.

In Figure 1.5, in terms of Chapters 3, 4 and 5, Chapter 4 uses the predicted network information from Chapter 3 to achieve an optimal PCI planning for distribution. Then, the proposed approach in Chapter 4 offers each femtocell the optimal PCI value and also ensures successful handover for the UEs. Moreover, during the handover process, the self-optimisation algorithm in Chapter 5 ensures the UE retains better handover quality. Each chapter is described in detail below:

Chapter 2: Literature Review

This chapter provides the background of this research and an overview of the literature on traffic prediction model, cell identity allocation, handover-triggering parameter optimisation and uplink interference mitigation.

Chapter 3: Cell-based Prediction Model for the Intensity of a Femtocell's handovers

This chapter firstly introduces the existing issues of the UE-based traffic model implemented in the two-tier network scenario. It then describes a cell-based prediction model which is based on the intensity of femtocell's handover. Further, this chapter presents metrics such as accuracy, precision, F-measure,

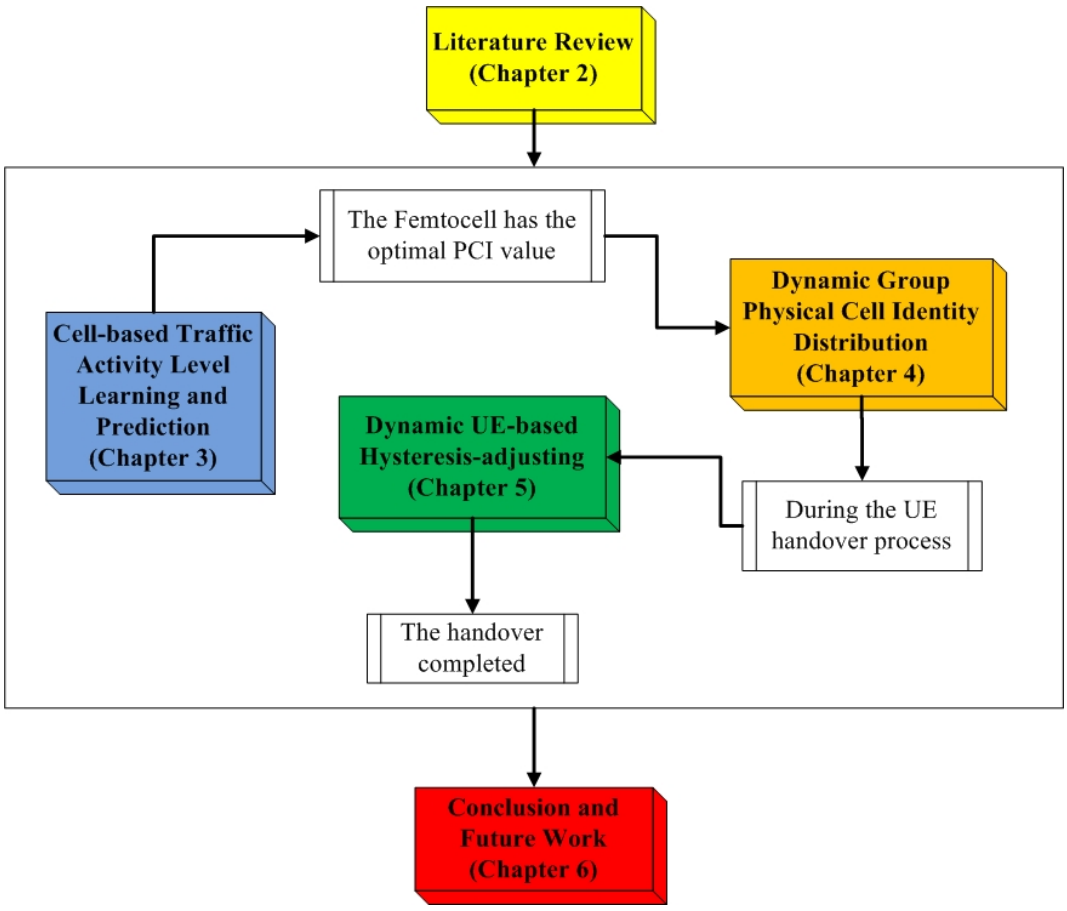

Figure 1.5: The structure of chapters in this thesis

sensitivity and specificity in order to evaluate the prediction performance reasonably. The evaluation and results show the significant advantages of the proposed model in a two-tier network scenario compared to the UE-based prediction model.

Chapter 4: Dynamic Group PCI Allocation Scheme

This chapter firstly presents some important knowledge regarding existing PCI and CGI problems in a two-tier network scenario. Then, it describes the ACPCI functions that have been provided in the SON. Secondly, a dynamic PCI group scheme is proposed which has implemented the predictor that mentioned in Chapter 3. Then, a PCI release approach is designed to associate with the PCI group scheme. Moreover, it also demonstrates how this PCI distribution approach is implemented in the centralised ACPCI framework. Lastly, the evaluation and system level simulation results show that this scheme provides a self-planning ability to offer optimal PCI allocation in order to achieve better network performance.

Chapter 5: Dynamic UE-based Hysteresis-adjusting Algorithm

This chapter firstly describes some important knowledge related to the handover process and failure regarding MRO. Then, it describes the hybrid MRO framework and functions. Through implementing the framework and functionality in MRO, it demonstrates a unique hysteresis-adjusting algorithm for the individual UE depending on the received average SINR. Moreover, it also introduces a handover aggregate performance indicator to evaluate the handover performance. Lastly, the evaluation and results show that this scheme provides a unique optimal hysteresis for the handover event and leads to better overall handover performance in comparison to the conventional centralised hysteresis-adjusting technique.

Chapter 6: Conclusions and Future Works

This chapter summarises the contributions of this thesis and identifies some further research works.

Chapter 2

Background and Related Work

This chapter provides the background and literature review for this thesis. The key aim of this thesis is to tackle the challenges of inbound and outbound handovers for LTE two-tier networks.

The approaches in this thesis comply with Self-Organising Network (SON) functions [12]. Four specific approaches and algorithms are major challenges in inbound and outbound handovers: UE-based traffic prediction model, cell identity allocation and handover triggering parameter optimisation.

As a major conceptual design methodology used in the proposed approaches in this thesis, as described in Chapter 1, core concepts LTE/LTE-Advanced and features of SON are introduced first in this chapter. The chapter then describes the general background and corresponding literature reviews of the above mentioned approaches and algorithm respectively. The sections in this chapter are listed as below:

- LTE and LTE-Advanced
- Self-organisation features in LTE femtocells
- UE-based traffic prediction model
- Cell identity allocation
- Parameter optimisation for triggering handover process.

2.1 LTE and LTE-Advanced

In this section, the LTE and LTE-Advanced and their network architectures are explained. Moreover, the quality of service and the handover process in heterogeneous networks are also described.

2.1.1 LTE Network

Given the ever-increasing growth of wireless network service requirements, Long-Term Evolution (LTE) is a standard developed by 3GPP, the standardisation body, which is used to achieve the improvement of end-user throughput and cell capacity, and reduction of user plane latency [2]. In order to integrate with multimedia services, LTE is designed to support Voice-over-IP (VoIP) and all kinds of IP data traffic.

Since the advantages of LTE compared to 3G networks have been explained in Chapter 1, this section focuses on the network part of LTE. As LTE can support the IP data traffic, a new network architecture has been defined by 3GPP called the Evolved Packet System (EPS) [21]. EPS consists of two parts, the Evolved Universal Terrestrial Radio Access Network (E-UTRAN) or LTE, and the Evolved Packet Core (EPC). The EPS network architecture is shown in Figure 2.1 according to [22].

As shown in Figure 2.1, the network is comprised of an EPC, usually referred to as the CN in LTE and the access network E-UTRAN (LTE). The CN consists of several logical elements: Packet Data Network (PDN) Gateway (P-GW), Serving Gateway (S-GW), Mobility Management Entity (MME), Home Subscriber Server (HSS) and Policy Control and Charging Rules Function (PCRF). LTE is the radio-air interface which consists of the macrocells. A macrocell is used to connect to the UEs and provide the wireless services for them. Those elements showing in the EPS network architecture are connected by the standardised interfaces: S1 and X2 interfaces. This feature enables multi-vendor interoperability which means various network operators can easily add function elements belonging to different vendors to the EPS network

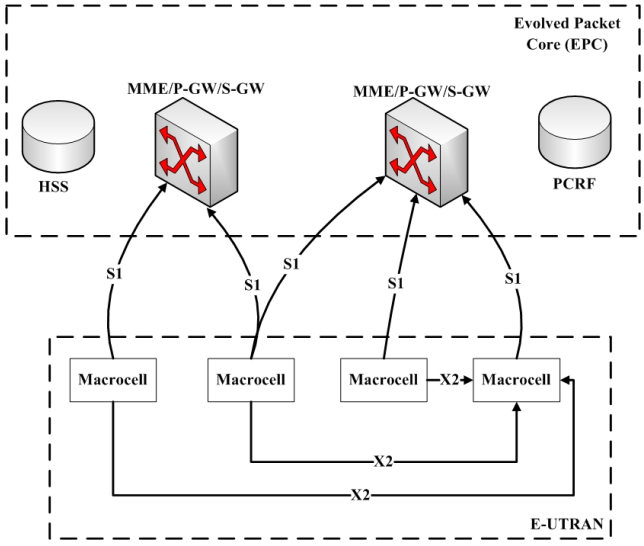

Figure 2.1: The evolved packet system network architecture with S1 and X2 interfaces

[23]. Moreover, in LTE network, two interfaces are used to connect between macrocell and macrocell or LTE and macrocell. S1 is the interface that connects between macrocell and MME and S-GW. X2 is the interface that enables macrocells or small cells which is proposed in LTE-Advanced to communicate directly between each other, which can provide excellent seamless handover and reduce the complexity of interference management (especially in HetNets) [24].

The CN has the ability to control the entire network system and establish bearers [21]. More information about bearers is described in the next section; the elements in the CN are explained below:

- **S-GW:** Serving gateway is used to route and forward user data packets while serving as local mobility anchor point for inter-handover of the macrocell [2].

- **P-GW:** PDN gateway is used to allocate IP address to UEs and provide the service to the external network. Therefore, P-GW also can be treated as local mobility anchor point [2].

- **MME:** Mobility management entity is used to [2]: firstly, select a S-GW or P-GW for an UE at the initial camp in the network; secondly,

control the UE's tracking and paging procedure in idle-mode; thirdly, verify authorisation of a UE to camp on the Public Land Mobile Network (PLMN) which is provided by the service provider; and fourthly, offer management and communication for small cells in LTE-Advanced, e.g. distributing a Physical Cell Identity (PCI) to a femtocell [25].

- **HSS:** Home subscriber server is used to associate with the MME to provide capabilities for: mobile management; user security and identification; access restriction for roaming; service profile and authentication [24].

- **PCRF:** Policy control and charging rules function is used to provide the QoS authorisation which indicates the flow-based charging control decisions [22]. More information about QoS is explained in Section 2.1.2.

2.1.2 LTE Quality of Service (QoS) Management Process

User-experienced Quality of Service (QoS) and its policy management is the 3GPP standards-defined technique that ensures a wireless network with high quality serves and network capacity [26]. Since the network operators like to offer differentiated services to users, manage network congestion and so on, this technique is designed to provide dynamic resource allocation for network use in order to achieve these goals.

In LTE network, the 3GPP standard defines an access-agnostic policy control framework which implements the standardisation of QoS and its policy management [24]. This kind of framework can support multi-vendor deployments and enable operators to offer service to the different UEs. This framework is achieved by the EPS bearer model [27].

As mentioned earlier, in the EPS, the service session-level policy decisions can be made by the PCRF through obtaining the existing network information. The decisions are then sent to the Policy and Charging Enforcement Function (PCEF) located in the PDN-GW [24]. The PCEF forcibly implements the

policy decisions by mapping service data flows to bearers, establishing bearers, and performing traffic managing and shaping. Moreover, a bearer is defined by the 3GPP standard to implement QoS indication between UE and PCRF [27].

Bearer model is the basic traffic separation factor which can enable differential management for traffic with different requirements of QoS [24]. In this model, each bearer works together with a set of QoS parameters which denote the properties of the network system, including bit/bit error rates, packet delay/loss, service interrupt (e.g. call-drop) and scheduling policy in an LTE station. A bearer has four QoS parameters [27]: QoS Class Indicator (QCI); Allocation Retention Priority (ARP); Guaranteed Bit Rate (GBR); and Maximum Bit Rate (MBR).

- **QCI** is used for the forwarding treatment (priority) on a particular bearer. The treatment can be different levels of scheduling weights, admission thresholds, queue management thresholds, link-layer protocol configuration, etc. Then, this bearer is handled by each functional element (for example, a PDN-GW in EPC or femtocells in LTE) [27].

- **ARP** is used in bearer establishment [26]. When a new bearer has been modified or established, it is used to make the decision whether the bearer request should be accepted by considering the current network situation. Moreover, it is a particularly essential parameter to indicate handover situations (e.g. call-drop) [24].

- **GBR/MBR** are used for real-time services, such as conversational voice and video. GBR/MBR is the minimum/maximum guaranteed bit rate per EPS bearer for uplink and downlink [27].

2.1.3 LTE-Advanced Heterogeneous Network

As LTE no longer satisfies the requirements for fast-growing radio link performance, LTE-Advanced Heterogeneous Networks (HetNet) with an evolved

network topology is becoming the next highlight in wireless network technology. Through using joined macro, micro, pico and femto base stations, HetNet permits flexible and economical deployments and provides a consistent wireless service to users in the network [7].

The target of LTE-Advanced is to achieve and exceed the International Telecommunications Union (ITU) requirements and also be compatible with first release LTE equipment and share frequency bands with first release LTE [7]. One of the important LTE-Advanced benefits is the capability to take advantage of advanced topology networks as optimised HetNet with a combination of macrocells and low power small cells such as micro and femto cells [7]. The small cells are the performance leap in wireless networks which bring the network closer to the users. Another LTE-Advanced benefit is that it further improves the network capacity and coverage. It also ensures user fairness in the wireless service [8].

Moreover, LTE-Advanced supports very much higher data rates than LTE. It enables multi-carrier to use ultra-wide bandwidth, up to 100 MHz of spectrum [6]. Therefore, in 2010, 3GPP has determined that LTE-Advanced would meet the International Telecommunications Union Radio communication Sector (ITU-R) requirements for 4G [4].

In terms of micro, pico and femto base stations, a microcell (micro) is used in a densely populated urban area with about 100-500 metres coverage. A picocell (pico) is used for areas even smaller than those of a microcell, about 10 to 80 metres coverage. A femtocell (femto) is used for areas smaller than those of micro and pico, about 10-20 metres (indoor coverage). The structure of HetNet is shown in Figure 2.2 according to [7].

Figure 2.2 shows the macrocell overlaid with micro, pico and femto cells, which are typically deployed in an unplanned manner. Usually, the femtocell uses the Internet as the backhaul to connect to the CN. Macro, micro and pico cells can take other routes, such as, traditional microwave, unlicensed millimetre wave, fibre optics and so on to connect to the CN [28]. Due to their lower transmission power and smaller physical size, micro, pico and femto cells

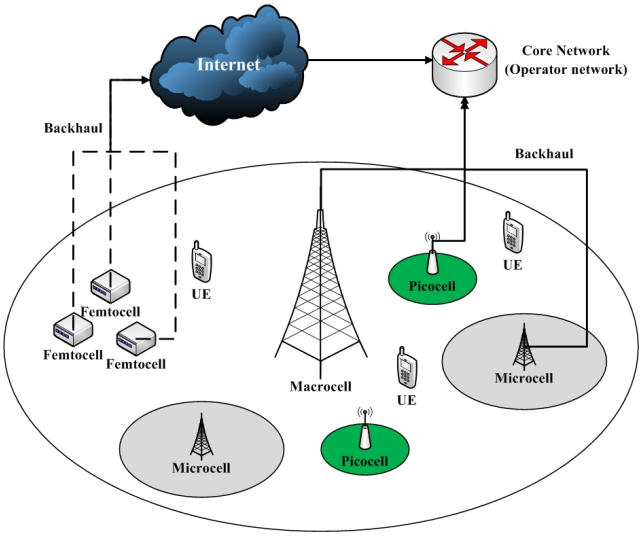

Figure 2.2: The structure of heterogeneous cells in a LTE macrocell

Table 2.1: Cell Types and Characteristics

Characteristic	Macro/Micro cell	Pico/Femto cell
Coverage	Wide area	Hot spot
Type of coverage	Outdoor coverage	Indoor coverage
Desity	Small number of high capacity sites	Large number of lower capacity sites
QoS requirement	High availability	Best effort
Mobility	Seamless mobility	Nomadic mobility
Bandwidth flexibility	Multi-band sectors	Sectors support single band only
Orientation	Designed for voice	Designed for data

can be collectively referred to as small cells, which can provide flexible coverage in order to enhance the wireless services. Table 2.1, from [28], summarises the differences in capabilities and requirements between macro and small cells.

As shown in Table 2.1, macro, micro, pico and femto cells have different services and coverages. Therefore, under the macrocell, the number of pico and femto cells is greater than the number of microcells. Although, the QoS requirement for pico and femto cells is lower than the macro and micro, considering the number of pico and femto cells deployed and the number of UEs that can be served by those cells, pico and femto cells can still offer reliable services to the UEs. Since femto cells are plug-and-play devices and pico cells are deployed randomly, their mobility is nomadic, which depends on the cell's

current location. In terms of the bandwidth, although a microcell belongs to the small cell, its bandwidth distribution is similar to the macrocell which can support more wireless users than pico and femto cells. Moreover, due to the pico and femto cells use to enhance the wireless network service, they can support the data service which needs higher throughput than voice service.

The architecture of a LTE-Advanced system is essentially the same as that of LTE except that LTE-Advanced adopts the deployment of small cells, as shown in Figure 2.3 according to [8].

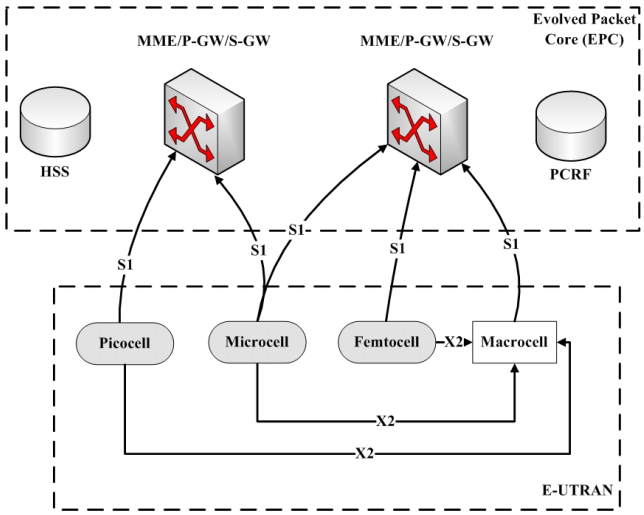

Figure 2.3: The heterogeneous network architecture with S1 and X2 interface

Figure 2.3 shows that similar to the LTE network architecture, the HetNet system comprises two main parts: E-UTRAN which is the radio-air interface of LTE-A; and EPC (CN). The E-UTRAN entity has macrocells as base stations and several small cells. EPC includes MME, S-GW, P-GW, HSS and PCRF. All the functions of those elements are described in the previous section. Moreover, for the femtocell, the HetNet architecture allows three different architecture deployment scenarios [8].

- Femtocell connects to the EPC via S1 interface: the femtocell connects to the EPC like a macrocell and also has S1 connections to MME and S-GW.

- Femtocell connects to the EPC (CN) via a Femtocell Gateway (F-GW):

the F-GW serves as a concentrator for the control plane. It can terminate the user plane towards the femtocell and towards the S-GW, when there is a high number of femtocells deployed in the network. The F-GW occurs towards the MME during S1 setup similar to a macrocell with multiple cells and towards the femtocell similar to a MME.

- Femtocell connects to the EPC (CN) via a F-GW for the control plane only. There are some femtocell-particular functionalities, for example, paging optimisation, defined in the F-GW. If F-GW is less deployed in the network, those functionalities are implemented by the MME.

2.1.4 Handover Process in LTE Heterogeneous Network

In a cellular network, handover is performed between target and serving cells to guarantee that a UE is continually connected to the best serving cell [6]. The general handover process is as follows. A UE measures the signal strength of its neighbouring cells. If the signal strength of a neighbouring cell is higher than that of its serving cell plus a hysteresis for a specific time period called the Time-To-Trigger (TTT), the UE will report this information to its serving cell. The serving cell then initiates the handover process.

In a HetNet, the handover triggering parameters, hysteresis and TTT, are commonly for all cells and all UEs [29]. However, using the same set of parameters for all cells/UEs may lower the mobility performance in the HetNet. Therefore, it is desirable to have a cell-specific handover hysteresis for different small cells. Furthermore, both cell-specific and UE-specific handover functionalities therefore need to be considered for HetNet [30].

In terms of the handover process in HetNet, first of all, the handover is categorised into two parts which differ mainly due to the interference condition. They are intra-frequency and inter-frequency handovers [29].

Intra-frequency handover: This handover denotes that the handover between two LTE cells (including macrocell or small cell) which uses the same frequency carriers, the serving and target cells interfere with each other. When

a UE moves from the serving cell a to a target cell b, the signal strength of the cell a becomes smaller, and the interference caused by the target cell b becomes larger. As a result, a handover is essential if the target cell is stronger than the serving cell, even if the serving cell is still strong.

Inter-frequency handover: This handover denotes that the serving and the target cells use different frequency carriers. Therefore, they do not interfere with each other. In terms of interference situation the handover is from one LTE frequency layer to another.

Handover process in HetNet includes the handover between macro and small cells, the handover between macrocell and macrocell and the handover between small cell and small cell. Therefore, for the handover in macro, micro, pico and femto cells environments, there are 16 different handover processes. It seems that the handover process is very complex in HetNet. However, due to the LTE-particular structure feature mentioned earlier, LTE the network structure enables multi-vendor interoperability which means various network operators can easily add function elements belonging to different vendors to the SPE network. The 16 different handover processes can be summarised in three parts [31].

The first part is Handover Preparation. In this step, UE, serving cell (macrocell or small cell) and target cell (macrocell or small cell) make preparations before the UE connects to the target cell. Particularly, in this step, all the handovers always include four steps [25, 31]:

1. UE measurement control/report. The reason all the handover processes have this step is because all the handover triggering is based on the UE measurement report in the LTE. All the macrocells and small cells require the measurement report from the UE during this step.

2. Handover decision. Once the UE gets the measurement report, it needs to send this report to the serving cell via air interface. Different cells may have different channels and modulations, but it does not affect the communication between the UE and serving cell. When the serving

cell receives the measurement report, it makes the handover decision according to the signal strength of the target cell in the report.

3. Admission control. In this step, the target cell performs the admission control dependent on the QoS information from bearers as mentioned earlier and prepares the handover. As the different cells in HetNet may use different Gateway or MME, therefore, the communication between serving cell and target cell, serving cell and MME (Gateway) and target cell and MME(Gateway) will be different. But, since the integration of the LTE-Advanced network, LTE guarantees the different cells can communicate each other by using S1 or X2 interface [2].

4. Handover response. After communication between serving and target cells has been established and the target cell decides to accept the UE. A handover response will be sent to the serving cell. Once the serving cell receives the handover response, it sends the handover command to the UE.

The second part is Handover Execution. In this part, there are two steps:

1. UE detaching. In this step, once the UE receives the handover command from the serving cell, the UE starts to detach from the serving cell.

2. Service Synchronisation. After the serving cell sends the handover command to the UE, it starts to send the synchronisation information to the target cell by using the established communication channel mentioned in the previous part. As different cell types have different settings, the synchronisation information is different in HetNet. After the target receives the synchronisation information, the UE can start to access the target cell.

The third part is Handover Completion. In this part, there are two steps:

1. Handover confirm and path switch. The Gateway switches the path of downlink/uplink data to the target cell. For this, the Gateway exchanges messages with the MME.

2. Release resource. Once the UE completes the handover process, the target cell changes to the serving cell. The new serving cell sends the release resource request to the old cell. On reception of the release message, the old cell releases the radio and control of related resources. Then, the new serving cell starts the service to the UE which transmits the downlink/uplink packet data to the UE.

The specific LTE femtocell handover information is explained in Sections 5.1.1, 5.1.2 and 5.1.3.

2.2 Self-organisation Features in LTE Femtocell

In recent years, demand for higher data rates increases rapidly, which then results in needs for better QoS requirement for indoor service. Network is considered to be too large to be configured and maintained via regular operation which means it is impossible to achieve by using the classic manual and field trial based design approaches. This is particularly true for femtocells since they are deployed in a random fashion with plug-and-play capability. Complicated structure of two-tier network which causes serious interference and reduce the performance of network service.

From the operator's point of view, femtocell deployment is summarised as higher capacity and QoS comes at the cost of higher Capital Expenditure (CAPEX) and Operating Expenditure (OPEX) [15, 32]. As a result, the trade-off between minimising CAPEX as well as OPEX and providing better QoS as well as capacity is a primary concern for today's operators.

SON is the viable way to achieve optimal resource management in a cost-effective manner, the standards identified SON as not just an optional feature but an inevitable necessity in current femtocell networks as well as in future wireless systems [26, 33]. In a LTE system, SON function has covered many aspects, such as: femtocell automatic registration and authentication; radio

resource management and provisioning; neighbouring cell discovery and synchronisation; cell ID selection and network optimisation.

Specifically, there are nine functions defined in SON:

1. Automated Configuration of Physical Cell Identity (ACPCI)
2. Mobility Robustness Optimisation (MRO)
3. Mobility Load Balancing (MLB)
4. Enhanced Inter-cell Interference Co-ordination (eICIC)
5. Random Access Channel (RACH) optimisation
6. Coverage & Capacity Optimisation (CCO)
7. Interference reduction
8. Energy savings
9. Automatic Neighbour Relation (ANR).

- Considering the MLB, the objective of this function is to intelligently manage the UE traffic across the radio resources of the network system, in order to achieve the redirections of load balancing and overcome unequal traffic load. Moreover, MLB is able to control the system load and the arrival of UEs according to the specific operator policy, to ensure good end-user service quality and performance [30]. For instance, in [10], the biasing is proposed to achieve a win-win scenario for femtocells and macrocell UEs (MUEs), via actively pushing UEs to access the femtocells, in order to mitigate the neighbouring cell interference.

- Considering the eICIC, it provides the intelligent coordination of physical resources between various neighbouring cells (femtocell/macrocell) to reduce interference from one cell to another. This coordination can be considered as restriction and preference for the resource usage in different cells. Moreover, through the eICIC supports, the neighbouring cells

are able to collaborate in terms of bandwidth usage, resource blocks and even the transmission powers across various frequency resource blocks used in each cell.

- Considering the RACH optimisation, RACH is used to carry the random access preamble which a UE sends to access the network in non-synchronised mode. It is also used to allow the UE to synchronise timing with the base station. RACH optimisation aims to minimise the number of attempts from UEs on the RACH channel in order to reduce the interference via an optimised polling mechanism for UEs.

- Considering the CCO, it offers automatic adjustment of the radio frequency parameters (antenna configuration and power) for the base station in LTE network. This method will permit the system to periodically adjust to modifications in traffic (load and location) in addition to any changes in the environment, such as new construction, or new cells being deployed.

- Considering the interference reduction, it is able to switch off those wireless cells (femtocells) which are in idle status for a considerablely long time, in order to achieve interference reduction for other wireless cells.

- Considering energy savings, it offers the wireless cells (femtocells) an ability which can be automatically switched off when the capacity is no longer needed and be re-activated on a need basis. Energy saving can significant reduce the OPEX for operators.

- Considering the ANR, it is able to automatically optimise the neighbour relations if a new femtocell switches on in the network. This will increase the number of successful handovers and result in less disconnection due to missing neighbour relations.

Since this thesis focuses on the ACPCI and MRO functions, more information about them is described in the following sections.

2.2.1 Automated Configuration of Physical Cell Identity (ACPCI)

As a reference signal sequence, PCI is a fundamental parameter for the LTE radio configuration. It is used for cell identity and network synchronisation [25] for two reasons: the PCI can be read within a very short time (20 ms) from the system information [11]; the PCI is a reliable identification as it can avoid interference through its structures. The structure of PCIs is: first, 168 pseudo-random sequences denote the cell identity groups'; second, for each cell identity group, three orthogonal sequences are constructed. Therefore, there are 504 PCI IDs in the LTE system [25]. For more information about the PCI structures, please see Section 4.1.2.

ACPCI is the one of key functions in SON defined by the 3GPP. In a LTE femtocell network, it is obviously more than 504 cells [6, 30]. This leads to a limited resource' with a high reuse-rate' case appearing in the network and PCIs need to be repeatedly re-used. However, a reused PCI would cause a collision or confusion (single-tier confusion) problem due to the neighbouring cells or two closed cells being assigned the same PCIs. There are two reasons why cell PCIs cannot be shared.

Firstly, the configuration of the PCI directly influences the handover process [6]. During the handover, the handover fails if the UE finds that the PCI of the target cells is same as the one in the serving cell or there are many cells have the same PCI as the target cell.

Secondly, the configuration of the PCI directly influences the configuration of other radio parameters [3]. For example, in the uplink reference signals, there are 30 sequence groups. Therefore, neighbouring cells should be assigned different sequence groups (a sequence group is used for resource block allocation) and the sequence group is obtained from the PCI configuration [24].

As a result, ACPCI is proposed to solve those problems with carefully assigned PCIs to the cells by SON. More information about PCI collisions, and single-tier and two-tier confusions is explained in Sections 4.1.2.1 and

4.1.2.2.

ACPCI can be separated into two parts [16]. The first part is the Physical cell identity Planning Tool (PPT), which is used to initialise a Physical Cell Identity (PCI) to the new powered-up femtocell. The other part is the Physical cell identity Optimisation Tool (POT), which is used to update the PCI value of a femtocell which needs to be changed due to a confusion or collision problem. Those functions solve the collision and single-tier confusion by using the same PCI ID with a maximal distance from each other [6, 15]. However, the confusion or collision probability increases when there are multiple deployed small cells which start to overlap within the coverage area of a macrocell in a heterogeneous network. Each of the cells needs to be configured to be collision and confusion free. However, if the two small cell, e.g. femtocells have the same PCI, and a UE handovers from a macrocell to one of the femtocells, in this case, the macrocell will be confused by those femtocells and the handover fails. This confusion is called two-tier confusion [6, 25]. More information about two-tier confusion is explained in Section 4.1.2.2. Therefore, it is essential that the ACPCI provides the collision and single-tier confusion-free assignment for heterogeneous networks, due to the complexity of collision and confusion problems.

In order to achieve the careful PCI assignment in heterogeneous networks, there are some functions already set up in ACPCI.

ACPCI has ability to determine the actual network layout for every cell and also the cell structure changes when new cells are added or closed in coverage of the macrocell [16].

ACPCI has ability to achieve the PCI grouping. Instead of operating with a full set of PCIs, PCIs can be separated and set into many sub-groups. This process can efficiently assign the PCIs to the cells and proactively avoid repetitive reconfigurations [6].

Several approaches which are explained in Section 2.4 have been proposed for automated PCI assignment. Each of these approaches solves different areas of the problem with different characteristics.

2.2.2 Mobility Robustness Optimisation (MRO)

As mentioned in Chapter 1, the general goal of MRO is to ensure the proper handover in connected mode and proper cell re-selection in idle mode for the UE, in order to support the UE's proper mobility [30]. The specific goals of MRO are given below in order of importance.

- **Minimise call-drop:** Call-drop is the worst case that occurs during the handover or re-selection process [30]. This is because that it obviously makes users unhappy and causes lower QoS.

- **Minimise Radio Link Failures (RLF):** RLF is the case of disconnection from serving or target cell during the handover, if the receiving SINR from serving or target cell is lower than -6 dB [11]. If a RLF happens, the UE would re-establish the connection to the serving or target cell. Therefore, RLF would cause redundancy handover and waste wireless radio resources. Moreover, this connection re-establishment is only possible inside a LTE [30]. In many cases, the RLF is less critical than the call-drop problem due to it having a connection re-establishment function, but it is still an important MRO issue.

- **Minimise unnecessary handovers:** Unnecessary handovers includes the ping-pong effect and handover to the wrong cell. Ping-pong effect occurs when there are repeated handovers between two cells within a very short time [7]. Handover to the wrong cell means the UE has not handed over to the target cell, but another cell [12]. Unnecessary handovers lead to inefficient use of wireless radio resources. Therefore, this issue is still important to MRO.

- **Minimise idle mode problem:** Suitable re-selection is necessary such that a connection between a UE and the base station can immediately be set up at any time [30]. Therefore, the MRO should guarantee that the users can camp on a suitable cell at any time.

However, the idle model problem will be not considered in this thesis. More detail of call-drop, RLF and unnecessary handovers (ping-pong effect and handover to wrong cell) and how the ratios of these are calculated is described in Sections 5.1.4 and 5.2.5. The works on MRO by previous authors are summarised below:

- **Call-drop report:** the MRO can easily generate the call-drop report depending on the Key Performance Indicators (KPI) [34].The one of the most important KPIs is the call-drop ratio. Every cell counts the identified handover problems caused by itself over a certain period of time. Then the cell generates the call-drop report (including in the KPIs) which is collected by the MRO.

- **RLF report:** the MRO can generate a RLF report for the wireless system [12]. The process description is: when a RLF happens during the handover between cell A and B, the UE disconnects from cell A. The UE then sends the re-establishment request to cell B. Cell B informs cell A about the RLF, cell A checks the situation of that lost UE and then reports RLF to wireless system. Moreover, the case of handover to a wrong cell is also reported to SON system by using the RLF report [30].

- **Ping-pong effect report:** the MRO can obtain the ping-pong effect report from the cell via a KPI in the LTE [30]. The ping-pong effect is detected by a cell when it realises a handover repeatedly occurs in a shortly time for the same UE. The MRO can collect this ping-pong effect from that cell report (including in the KPI).

- **Mobility parameters correction:** Mobility parameters correction is an actual optimisation process for the MRO [30, 34]. The handover triggering parameters, hysteresis and Time-To-Trigger (TTT) are important mobility parameters need to be chosen correctly during the handover. The correction process is vendor-specific, and in this process, centralised, distributed and hybrid solutions are possible. For more information about the hysteresis optimisation, please see Chapter 5.

2.2.3 The Structures of SON Function in a LTE

According to [33], three different structures of SON function in a LTE two-tier network have been summarised as shown in Figure 2.4.

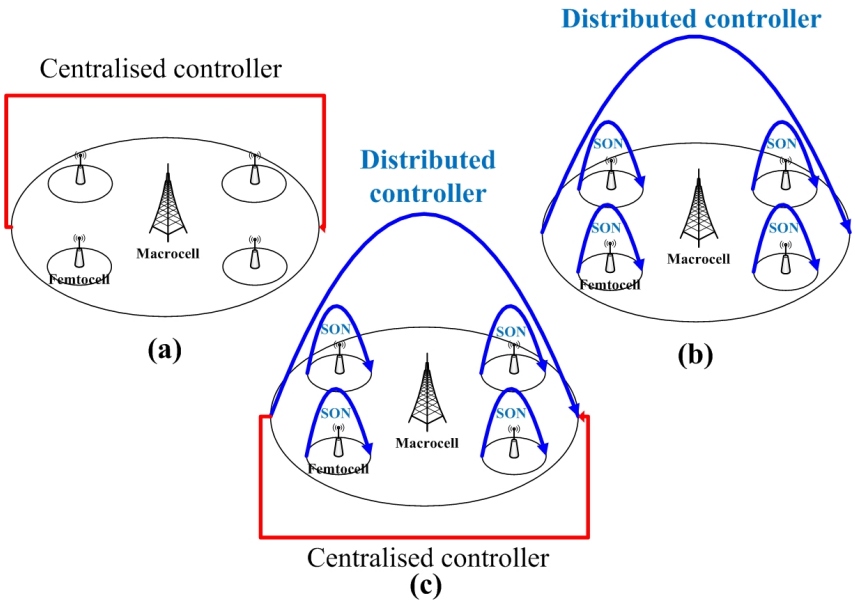

Figure 2.4: Different SON function structure: (a) Centralised, (b) Distributed, and (c) Hybrid

Figure 2.4(a) shows that, in a centralised structure, the SON algorithm resides on a central controller, it first selects all the necessary information from the overall network to this central controller. After an initialisation operation, the controller then outputs the specific parameters or management information to the femtocells or macrocell on a periodic basis or whenever needed.

The advantage of this structure is that it allows the SON algorithm to be considered by the central controller before modifying the setting of the networks. This ensures the fairness of the base stations to obtain the overall optimal network performance. However, there are two disadvantages of this SON structure, namely compatibility and efficiency [26]. A compatibility issue arises as a central controller has difficulty selecting the information from multi-vendor femtocell devices with different system settings. An efficiency issue arises as the individual wireless base station cannot immediately respond to requirements and has to wait for commands from the central controller.

Therefore the centralised SON is slow in terms of response.

Figure 2.4(b) shows that, in a distributed structure, the SON algorithm resides in the individual wireless base station (or UE). It allows the station to make autonomous decisions based on the received UE measurement and additional information from the neighbouring cells.

Compared to the centralised case, this structure obviously overcomes the drawbacks in terms of compatibility and efficiency. Since the SON algorithm resides in the individual base station, it is easily implemented in multi-vendor networks and can immediately respond to the network requirements without any delay. Thus, the distributed SON is fast in terms of system response. However, femtocells are designed to be selfish [6], so it is difficult to achieve fairness for femtocells and at the same time achieve a good overall network performance in the two-tier network.

Figure 2.4(c) shows that, in the hybrid structure, the SON algorithm resides in both the base station and the central controller. This structure ensures base station and central controller work together, in order to be self-organised. Being a combination of centralised and distributed structure, the advantages and disadvantages of this structure also depend on the centralised and distributed algorithms themselves.

Depending on the above description, each structure in SON has its own advantages and disadvantages, therefore the choice of those structures would depend on the specific issues in the two-tier network. Moreover, with regards to the compatibility issue in the hybrid and centralised structures, the SON approach deployment would require the cooperation of the infrastructure vendor, the operator and, possibly, the third party tool company [33]. Thus, operators can choose the optimal SON approach based on the current infrastructure deployment. Reflecting this, in this thesis, the compatibility issue is not considered in the proposed approaches.

To summarise, this section introduces the SON functions and its structures. Those functions and structures are able to support the specific approach to automatically solve the challenges in two-tier networks. Moreover, the scope

of SON functions would be expanded and evolved with upcoming releases of the LTE standard, in order to ensure LTE's continued success in tomorrow's wireless marketplace.

2.3 UE-based Traffic Prediction Model

To cope with the fast growth of mobile networks in terms of user base and network capacity, in order to satisfy the QoS requests, user mobility management becomes one of the hot topics in current wireless network research [35]. In mobility management, traffic behaviour prediction is one of the important aspects which enables the system to predict the further network situation in order to achieve the network radio resource reservation. According to the predicted network situation, the system is able to provide a degree of SON ability to optimise the network radio resource distribution and gain a better network performance [17].

In [36], authors proposed a prediction scheme that offers adaptive bandwidth reservation for handover and admission control. The strategy of this paper is that for each cell, the bandwidth reserved for hand-offs is able to be calculated by optimally estimating the total sum of fractional bandwidths of the expected hand-offs within a mobility-estimation time window. The paper used a Markov process to model user mobility. In this method, based on aggregate history of hand-offs observed in each cell, the future mobiles' directions and hand-off times in a cell were predicted. Based on the prediction, the authors then proposed three different admission-control schemes for new connection requests using bandwidth reservation in order to reduce the handover call-drop ratio.

In [37], authors proposed a prediction approach called Zoned Mobility History Base (ZMHB) to offer correct triggers for handover, in order to improve the handover performance. ZMHB employed a six-sector cell structure and each sector is further divided into three zones based on their handoff probability. The paper exploited cell-zone numbering and intra-cell-basis movement

history, which stores a record of the user's movement in the current cell. In each of those classified cell-zones, the user's movement information is modelled as a Markov process. Through the UE mobility prediction, the approach was able to offer an efficient resource reservation to decrease call dropping probability and shorten handoff latency in a micro-cell structure or a metropolis scenario. The latter normally has a complicated route structure.

Both of the prediction models in [36] and [37] are based on a Markov process. In this model, according to user's movement history, the Markov states are modelled as wireless cells which the user has camped on. Reflecting this, the further user movement situation can be considered as the next state prediction.

In [38], the authors proposed a traffic behaviour prediction model using a k-order Markov process, in order to implement an efficiency and scalability routing protocol for mobile cognitive radio networks. Cognitive radio is a popular technology which is capable of sensing the environmental conditions and automatically adapting its operating parameters in order to enhance network performance. Using cognitive radio technologies, this paper is able to model the UE routing with techniques, such as moving-average, Cumulative Distribution Function(CDF) and static neighbour graph predictor. The authors evaluated the reliability, efficiency and scalability of the routing protocols under the different prediction techniques, the proposed k-order Markov process combined with CDF offers better accuracy than other techniques.

Different from [36] and [37], the prediction model in [38] models the next state prediction not depending on the current state but the i-k time period states, where i is the current time period.

In [18], authors proposed a prediction approach based on the Markov renewal processes in order to achieve efficient network radio resource management and provide a certain level of QoS as perceived by the mobile users. The proposed approach was able to estimate the expected spatial-temporal traffic load and activity at each location in a network's coverage area. The paper computed the likelihoods of the next-cell transition, along with anticipating the

duration between the transitions, for an arbitrary user in a wireless network.

In [35], based on the Markov renewal process, authors presented a framework to predict the subsequent transitions in mobility and activity of network users and to model the traffic population of users with active and idle sessions within a certain time period. The framework is able to optimise the user traffic loads, such as voice and data connectivity, for the future network service requirements. Both single-step and multi-step transitions had been considered in the prediction model in order to enhance the end-to-end QoS up to a certain level.

Similar to [36] and [37], the states in [18] and [35] are modelled as the cells (movement history). However, according to the semi-Markov feature, the next state prediction not only relates to the transition probability between each state, but also depends on the time period in which a user camps on the current serving cell.

The above approaches worked well in the macrocell deployment (single-tier scenario), but are not suitable for LTE femtocell deployment in a two-tier scenario. This is because the feature of random deployment of femtocells; a femtocell could turn on and off frequently at any time. Therefore, it is impossible to obtain the integral states history and correct transition probability for a k-order Markov and semi-Markov.

In [39], the authors proposed an approach to adaptively infer with the system parameters and then estimate the channel quality based on the inferred parameters. This approach uses non-stationary HMM to model the spectrum-sensing process and infer the model parameters through Bayesian inference Using Gibbs sampling (BUGs). BUGs is software that implements the algorithm in computational statistics based on a Markov Chain Monte Carlo (MCMC) method. It can obtain the posteriors for non-conjugate priors numerically [40]. The problems explored suggest that BUGS is able to produce a posterior distribution via the decision maker's true non-conjugate belief; in this case, optimal decision making will be achieved. In this prediction model, the channel occupancy statuses are modelled as hidden states due to their not

being directly observable. The spectrum sensing results which are generated by secondary users are modelled as observation states. Moreover, similar to semi-Markov, in this approach, the transition probability proposed also depends on the current state's lasting time. Therefore, the transition probability is not stationary. Reflecting this, the next prediction state would depend on both current state and state residence time. According to the predicted state of channel occupancy, this approach can estimate the channel quality for a network system.

In [41], based on the history of room visiting, the authors proposed an approach to predict human behaviour within an office building. The prediction model is based on the k-order HMM. It is similar to [38]: since hidden states are a Markov chain, the k-order HMM means that the next period state depends on the i-k time period state, where i is the current time period. The rooms that people entered are modelled as hidden states due to people not entering every room would. The rooms that people arrived in are modelled as observation states. The experimental results show that k-order HMM has better performance than other prediction techniques such as neural network and Markov predictors.

According to [39] and [41], the key contribution is that the states which cannot be observed are modelled as hidden states. Therefore, to model the issue of femtocells turning on and off randomly in a two-tier scenario, the femtocells (states) in a UE movement history model may be modelled as the hidden states.

In [41], it is mentioned that the proposed room visiting prediction model can be used in routing prediction for cellular phone systems, in order to predict the next radio cell for a cellular phone owner based on his previous movement behaviour. In [19], considering both single-tier and two-tier scenarios, the authors proposed to use HMM to model the network traffic behaviours based on a UE moving history model. In this model, the femtocells in which the UE has handover are modelled as hidden states. The user's location cells are modelled as observation states. By predicting the next hidden state, the system can

improve communication conditions and provide better service performance. Moreover, the proposed model in [19] overcomes the drawback of femtocells being randomly deployed by using hidden states to model those cells that cannot be observed, i.e., the number of femtocells cannot be actually observed due to femtocell being a plug-and-play device. Compared to the order-2 Markov process, this model provides higher accuracy in a two-tier scenario.

However, the model in [19] is still not accurate enough since there are a large number of femtocells being deployed which lead to large and unmanageable states in the prediction model in a two-tier scenario [20]. Moreover, in [39], [41] and [19], their prediction models are all based on HMM and the next state prediction is based on the hidden part, since the hidden part is a Markov chain. In contrast to these approaches, the authors in [42] provide a new approach to use HMM in the prediction model.

In [42], authors proposed a model based on HMM for prediction of human behaviour in a ubiquitous environment. In this model, since the human's interest cannot be actually observed, the interests are modelled as the hidden part and the human behaviours are modelled as the observation part. Compared to the above approaches that use the hidden part as the prediction states, this paper models the observation part to predict the next states. The hidden part is used to find the predictive information called weight' (the strength of the relation between the behaviour and interest) which is hidden from the system.

To summarise, all the current UE (in fact, it is also users' behaviour) behaviour prediction models are all based on the UE moving history and model the cells as the states to predict the next visited cell (moving path). However, those UE-based models no longer work well in the two-tier scenario for two reasons: the peculiarity of random femtocell turn on and off which leads the transmit probability matrix to fail; and femtocells being deployed in a large number which leads to large and unmanageable states in prediction model in a two-tier scenario. Therefore, Chapter 3 introduces a cell-based prediction model for LTE femtocell two-tier networks.

2.4 Cell Identity Allocation

In LTE femtocell systems, the PCI is used by UE to identify a femtocell. The number of PCIs is limited to 504 in the standards [6]. They are normally allocated without planning and network operator intervention. Reflecting this, the PCI assignment problems which are called PCI confliction (collision and confusion) has been addressed for single-tier and two-tier network scenarios in the standards [6]. More detail of PCI and Cell Global Identity (CGI) is provided in Chapter 4. In order to comply with the ACPCI, many research works have been proposed to achieve automatically optimal PCI planning.

In [43], the authors proposed a Graph-colouring based mathematical method for PCI auto-planning of a LTE network in a single-tier LTE network. Since each LTE cell is similar to graph nodes and communication between two LTE cells is similar to graph edges, each PCI can be modelled as the colour to assign to the nodes. Moreover, given the feature of Graph-colouring of no identical colour between the neighbour nodes, this approach can easily solve the PCI collision issue.

In [44], the authors proposed a Graph-colouring based mathematical approach for primary component carrier selection and PCI assignment. The authors investigated the possibility to solve these problems in a distributive manner using Graph-colouring algorithms. Moreover, algorithms for real-valued interference pricing of conflicts converge rapidly to achieve the local optimum. The algorithm for binary interference pricing has a chance to find a global optimum. This paper evaluated those algorithms and compared them. The results showed that the binary pricing of interference with an attempt to find a global optimum outperforms the real-valued pricing. Considering the PCI assignment, this approach can significantly reduce the requirement of the number of PCIs, and reduce PCI conflictions.

In [45], the authors proposed an automatic centralised PCI assignment mechanism for a single-tier LTE network, using Operation Administration and Maintenance (OAM) as the central server to collect cell information and build

an abstract graph with this information which reflects the relationship in real world network. Associating this with an enhanced Graph-colouring algorithm greatly reduces time complexity, and meanwhile keeps a high PCI utility ratio to provide confliction-free PCIs for the new cells.

In [46], the authors proposed to use mobile measurements to update the Neighbour Cell List (NCL) in a single-tier LTE network, in order to detect PCI conflict. The problem solution is that if PCI confliction appears, the mobile sends this information to the CN and the Operation Support System (OSS) will require the cells involved in conflict to change their PCIs.

In [47], the authors summarised features in Releases 8 and 9 in a two-tier LTE femtocell network. In Release 8, the inbound-handover is the big issue due to two-tier femtocell confusion. In Release 9, it was proposed to use CGI to replace PCI when the confusion occurred. The general process is that during inbound-handover, if the serving macrocell finds that the PCI of a target femtocell from a UE report is not unique, the serving cell instructs the UE to read system information which includes the CGI-ID of the detected cell and the CGI-ID will be used for this cell identification.

In [48], the authors proposed to use handover to mitigate the interference between macrocell and femtocell. However, this method could fail when the system is fully loaded and no free channel could be offered. Although this paper mentioned about using power control to overcome this drawback, it could still result in UE disconnection. Moreover, these researchers also proposed that using CGI would result in UE disconnection due to it taking a long time to obtain the UE measurement report.

In [49], the authors introduced a femtocell access control strategy in UMTS and LTE. Particularly, they described the problem for cell selection/reselection in three different modes, open, hybrid and closed. It also mentioned the problems for Closed Subscriber Group (CSG)/non-CSG cell inbound-handover due to two-tier PCI confusion in Releases 8 and 9. Moreover, it analysed the drawbacks of using CGI for inbound-handover; using CGI probably leads to unnecessary service interruption and results in the call being dropped in situ-

ations where the signal strength is fading rapidly.

In [50], the authors proposed an approach to reduce the time spent on femtocell cell selection/reselection. This approach uses two groups of PCIs, a femtocell group and a macrocell group, as shown in Figure 2.5. When the UE claims into a new macrocell service, it automatically obtains the network information of this macrocell, which sets the certain PCI numbers for macrocell and femtocell. During handover procedure, the UE easily detects whether the target device is a macrocell or a femtocell by using this information and leads on reducing unnecessary signalling with the CN and identification time.

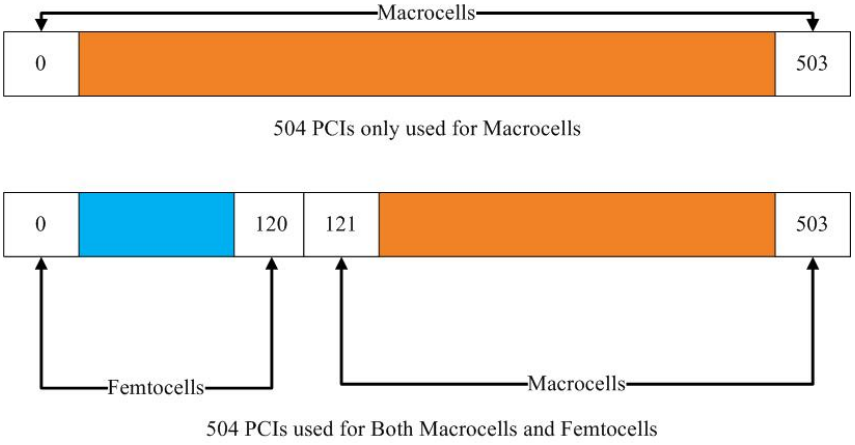

Figure 2.5: PCIs in femtocell and macrocell groups

In [51], the authors analysed the usage of CSG-ID introduced in Release 9. The closed mode cells have a CSG-Identity and CSG-Indication bit set to TRUE; hybrid mode cells have a CSG-Identity and CSG-Indication bit set to FALSE; and open mode cells do not have the CSG-Identity and CSG-Indication bit set to FALSE.

CSG-Identity ID involves using the PCI ID. Both hybrid and close cell modes support CSG-Identity ID. Two-tier LTE femtocells support separate PCI groups. One group of PCIs is reserved for CSG mode deployment (identification), the other group of PCIs is reserved for non-CSG mode. This reserved PCI range is signalled in the system information and UE would easily determine if the target femtocell belongs to CSG cells or non-CSG cells by using this CSG cell's broadcast reserved PCI information. This method is offered to

help the CSG cell selection/re-selection.

In [52], the authors proposed an automated PCI allocation system and ACPCI method to allocate the PCI in a two-tier LTE network in order to reduce the planning time of the PCI. In the paper, the researchers used the cell information, including cell state information, type information and neighbour list information, to create the PCI resource and also allocate the PCIs. Although this method can reduce the planning time of PCI distribution, however, the approach does not solve the CGI problem.

In [53], the authors proposed an automatic assignment of femtocell PCIs depending on different access modes for network optimization in order to reduce the operational expenditure for PCI allocation. In the paper, the researchers proposed a scheme of autonomous planning framework of femtocells which can autonomously detect the neighbouring cells of a target femtocell and send the neighbourhood information to the central controller. By using a central controller, the PCIs can be assigned in the optimal way. Although this method can reduce the operational expenditure for PCI allocation, it does not solve the CGI problem.

In [54], the authors proposed a visual cell ID to extend PCI and tackle the conflict issue. In that paper, the combination of the PCIs and System Frame Number (SFN) is proposed to replace the PCIs to identify the cell. The results show that it can increase the identification to 1024 which is double the time of current PCI number. However, the proposed approach heavily depends on the synchronisation between femtocells and macrocells. This synchronisation is easily undertaken by the system for only a few cells, but considering the densely developed femtocell scenario which brings the PCI conflict issue, it is almost impossible to achieve the synchronisation of a large number of cells at the same time due to the complexity of the synchronisation process.

To summarise, in [43], [44], [45] and [46], the authors analysed the PCI confliction issue in single-tier LTE systems. However, none of them have included the impact of the layered structure of a two-tier network with combination of macrocell and femtocell on PCI auto-planning. In [47], it was proposed that

the CGI assist the PCI to achieve the no-confliction cell identity, however, in [48] and [49], the authors proposed the issue of when UE wants to read the CGI from system information at inbound handover. In DynamicReservation-SchemeofPhysicalCellIdentityfor3GPPLTEFemtocellSystems, [52] and [53], the authors proposed the PCI allocation scheme in two-tier scenarios, but reading the CGI remains a serious issue at inbound handover. Therefore, the research in [54] returns back to PCI and provides the extension PCI IDs to achieve PCI confliction free, but that approach is almost impossible to achieve in a femtocell scenario. Reflecting this, in order to achieve better cell identity performance in inbound handover, in the Chapter 4, a centralised dynamic group PCI allocation in LTE femtocell two-tier network is described.

2.5 Parameter Optimisation for Triggering Handover Process

In LTE, UE is considered to play increasingly important role to support handover procedure [29]. In the handover process, ping-pong effect and Radio Link Failure (RLF) may occur due to many reasons such as: users moving at various speeds and violent change of signal strength. Since ping-pong effect and RLF are significantly affect the handover quality, in the standards, MRO as the solution to automatically detect Ping-pong or RLF and adjust the handover triggering parameters [12].

In [55], the authors proposed an approach using Received Signal Strength (RSS) to decide whether or not to enter a handover process. The paper presents an algorithm based on RSS measurement and Average Path-Gain (APG). By comparing RSS and APG in the hard handover process, the RSS offers better handover quality. Moreover, the paper also proposed a modified RSS-based algorithm with TTT window, which can significantly reduce the average number of handovers with increasing TTT window size while decreasing the average uplink SINR.

In [56], the authors proposed an approach to solve the conflict of handover

parameter judgment between MLB and MRO due to MLB and MRO contradictions with each other (MLB encourages UE to have handover, MRO is contrary). In that paper, the approach was based on restriction on the operation of MLB in the allowed range. The paper provides a scheme that is able to balance the priority of MLB and the MRO in handover parameter judgement. By avoiding the conflicts, this approach offers a better handover performance.

In [57], the authors investigated the handover parameters, such as Reference Symbol Received Power (RSRP) and Reference Signal Received Quality (RSRQ) in inter-frequency handover scenarios. Through evaluation of five handover criteria using RSRP, RSRQ or combinations thereof, the results showed that RSRP-based significantly increases the number of handovers. Conversely RSRQ-based reduces handovers but slightly increases the packet loss rate. Reflecting this, it is desired to use both RSRP and RSRQ which can guarantee signal quality and also handover quality.

The above approaches are proposed to be used in the single-tier LTE network. The approach in [57] only focused on the measurement parameters, such as RSRP and RSRQ. It did not evaluate the handover triggering parameters, such as hysteresis and TTT. The authors in [55] evaluated both RSS and TTT; the paper demonstrated an awareness of the importance of the TTT window in the handover process, but it did not offer an optimal TTT for the handover process. In [56], the authors only evaluated the stationary handover triggering parameters for MLB and MRO, so [56] also does not offer an optimised handover triggering parameter scheme.

In [58], the authors introduced an approach which provides the optimised TTT parameter for a handover process based on macrocell and picocell scenarios. A longer TTT can effectively mitigate the ping-pong effect, but meanwhile, it also causes undesirable Radio Link Failure (RLF) due to later handover. The paper investigated adaptive and group TTTs when UEs move at different speeds with a stationary RLF threshold. The simulation results of this approach showed that the handover performance of the adaptive TTT value is greatly improved compared to that of applying fixed TTT values.

In [14], the authors evaluated impacts and interdependency of handover triggering parameters, such as offset, TTT and hysteresis settings. The paper presented a simulation with different parameter combinations in different UE speeds in a LTE network. In that paper, the authors analyse the RLF and handover frequency using simulation results and provide the best parameter combination for the handover process.

In [13], the authors proposed a cell-type adaptive handover margin in a LTE femtocell network. Similar to [14], the paper investigated RLF and TTT in inbound and outbound handover in the femtocell scenario. It created RLF and TTT ratios in the hysteresis model respectively. It then selects the optimal hysteresis value depending on the minimised ping-pong rate while keeping a reasonable RLF rate. Simulation results showed that the optimal hysteresis values can significantly affect the handover performance in a LTE femtocell scenario.

In [14] and [13], the performance of using various hysteresis and TTT were studied. The results indicated that the optimal hysteresis and TTT are able to reduce the RLF and ping-pong effectively. However, neither of them proposed an efficient algorithm in detail to find the optimal handover triggering parameters.

In [59], the authors presented a rule-based handover optimisation algorithm that tuned the handover parameters TTT and hysteresis values in the LTE networks. Similar to [14] and [13], this paper investigated ping-pong effect, call-drop, and RLF from different hysteresis and TTT combinations. By defining and evaluating Handover Performance Indicators (HPIs) which considered handover failure ratio, ping-pong ratio and call-dropp ratio together, it proposed an integrity self-optimising method to seek the best hysteresis and TTT combination for the current network status. The algorithm is able to improve the overall network performance and diminish negative effects (call-drops and handover failures).

In [60], the authors provided a self-optimisation algorithm for the two handover triggering parameters, i.e., TTT and hysteresis. Similar to [59],

a combination of TTT and hysteresis was evaluated in terms of ping-pong effect, call-drop and RLF. It also proposed another overall performance metric, namely Handover Aggregate Performance (HOAP). This metric includes RLF, handover, and ping-pong ratios with the individual corresponding weightings. Through evaluating the HOAP and weighting function, the system could record and update the performance value at the central controller. As a result, the system is capable of adjusting the hysteresis and TTT to reduce RLF, ping-pong and handover ratios.

To summarise, [56], [57] and [58] did not offer an optimisation scheme for handover triggering parameters. [13] and [14] only investigated the relation between handover performance and handover parameters. They did not propose an efficient algorithm in detail to find those optimal parameters. [59] and SelfOrganizedHandoverParameterConfigurationforLTE provided the integrity self-optimisation algorithm for TTT and hysteresis, however, the algorithm can only offer the centralised handover trigger parameters. The centralised handover trigger parameters mean that the UEs within each cell shares the same handover trigger parameters which are centrally controlled by the base station. However, each UEs moves at different speeds in the real network, so their handover triggering parameters should not be the same. Those centralised values cannot ensure suitable handover performance for the individual UE. Reflecting this, in Chapter 5, a hybrid dynamic hysteresis adjusting algorithm is proposed that is able to offer the unique hysteresis value for the individual UE and gain the overall handover performance.

2.6 Summary

This chapter presents an overview of SON function and its features. The chapter also surveys the current approaches for the related research areas mentioned in Chapter 1, including: traffic activity prediction; cell identity allocation; and parameter optimisation for triggering handover. The critical review summarises the advantages and disadvantages of the reviewed approaches. Some

of the detailed descriptions for each of the related areas are described in later chapters.

Chapters 3, 4 and 5, describe the proposed solutions with regards to the inbound and outbound handovers.

Chapter 3

Cell-based Prediction Model of a Femtocell's Intensity of Handover in Two-tier Networks

Recently, research on mobility management has become one of the hot topics in wireless network systems due to the growth of mobile networking which is required to support a range of QoS levels [61]. Generally, compared to the traditional optimisation approach, the proposed predictive ability enables the equipment (wireless cells) with the intelligence which provides a degree of proactive management (self-organisation) to optimise its network performance for the network system [17]. Moreover, the proposed Dynamic Group PCI Allocation Scheme (DGPAS) is desired to know the further network traffic situation, thus, the improved prediction model is used to assist PCI allocation in Chapter 4.

A number of traffic behaviour prediction approaches have been reported in the literature. Those approaches are applied efficiently allocating and managing of the network radio resources through well understood traffic behaviours. Most of the current research works on traffic behaviour prediction are UE-based schemes which model the UE's historical routes in each cell as the status. For instance, in [37] and [39], authors proposed a traffic behaviour model using a Markov process and a Hidden Markov Model (HMM). A state is modelled

when a user camps on a cell. These approaches work well in the macrocell deployment, but they are not suitable for LTE femtocell scenarios. This is for the following reasons.

Firstly, femtocell is a plug-and-play device. It could turn on and off frequently and unexpectedly at any time, hence, it is impossible to obtain the correct transition probability for each status. The prediction fails if the faulty transition probability is derived.

Secondly, a large numbers of femtocells would be deployed in the macrocell coverage area, which would result in a large and unmanageable status in the prediction model, and consequently make the analysis unachievable [20].

Based on the number of handovers in the femtocells and the HMM, this chapter proposes a Cell-based Prediction Model (CPM) to predict the intensity of a femtocell's handovers in LTE two-tier networks. Compared to the UE-based model, this proposed model overcomes their drawbacks and also provides higher prediction accuracy in the LTE femtocell scenario.

3.1 Overview of UE-based Traffic Prediction Model (UTPM)

Currently, a UE-based Traffic Prediction Model (UTPM) has been widely used in improving tolerant network, call admission, and resource management in mobile communication [18, 61]. Knowing UEs' movements helps the network to better allocate radio resources; the latest developments in this area are described in Chapter 2, and as you can see much research on traffic behaviour prediction model is based on UE activity.

3.1.1 UE-based Traffic Prediction Model

In the UTPM, prediction is based on the user's movement history and each cell which a UE has passed is modelled as a prediction state. The structure of a wireless network can be modelled as regular and irregular node maps as

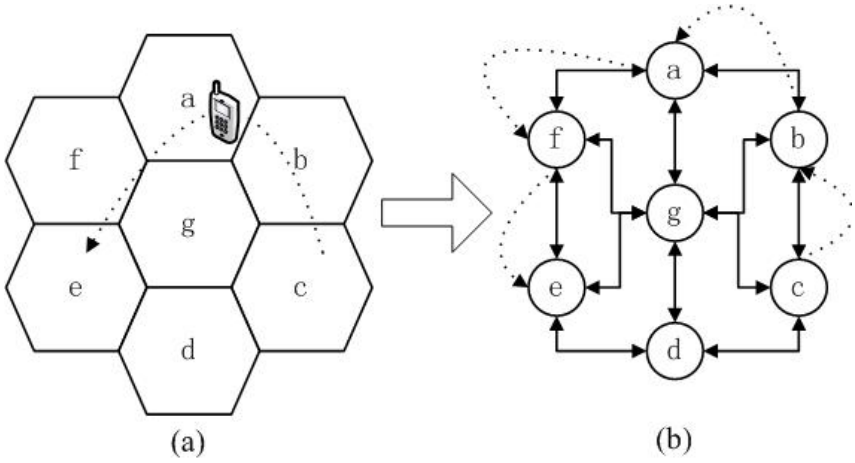

Figure 3.1: Regular wireless network modelling

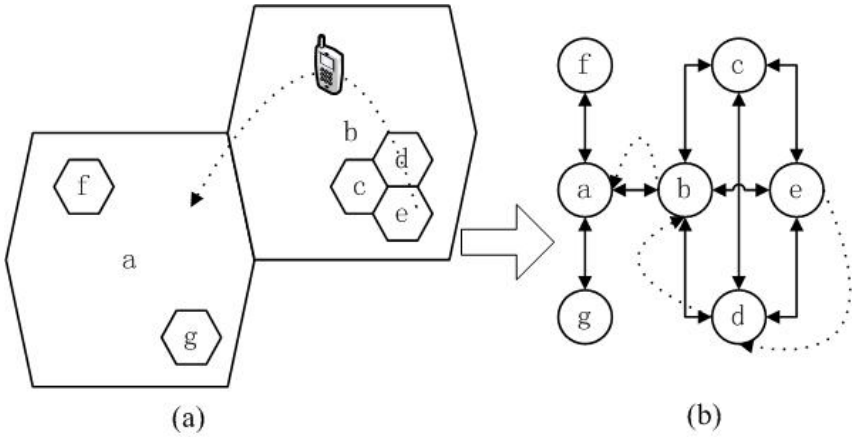

Figure 3.2: Irregular wireless network modelling

shown in Figures 3.1 and 3.2 according to [62].

In Figure 3.1(a), there are seven hexagonal macro stations denoted. Cell g is in the central position. The other cells surround cell g, and this is called a regular structure. Therefore, if the arrow connections denote the neighbouring relationship of the cells, the relationship between the cells can be modelled as the arrow-node map (solid-line arrows) and the cells can be modelled as the nodes as shown in Figure 3.1(b). Moreover, in Figure 3.1(a), a UE movement history from cell c via cells b, a and f to cell e can modelled in the arrow-node map (dotted-line arrow). Therefore, based on this model, that UE movement history can be modelled as a node sequence: $c \Rightarrow b \Rightarrow a \Rightarrow f \Rightarrow e$.

In Figure 3.2(a), there are seven hexagonal stations denoted. Those stations are not regularly located between each other. Some cells, namely *c, d, e,*

f and *g*, are located within the coverage of cells *a* and *b*. Therefore, this non-regular structure is called an irregular wireless network. Cells *a* and *b* can be considered as the macrocells, and the other cells can be considered as femtocells. Thus, this irregular network describes the two-tier network structure, referred to as the LTE femtocell network. Similar to the regular wireless network, if the arrow connections denote the neighbouring relationship of the cells, the relationship between the cells can be modelled as the arrow-node map (solid-line arrow) and the cells can be modelled as the nodes as shown in Figure 3.2(b). Moreover, In Figure 3.2(a), a UE movement history from cell *e* via cells *d* and *b* to cell *a* can be modelled in the arrow-node map (dotted-line arrow). Therefore, based on this model, that UE movement history can be modelled as a node sequence: $e \Rightarrow d \Rightarrow b \Rightarrow a$.

Moreover, from another point of view, these arrow-node maps are exactly the state-transition graphs of every stochastic variable, and every one-step transition must follow the arrows as shown in Figures 3.1(b) and 3.2(b) from one node to another. Therefore, a problem of UE movement prediction (node prediction) in the wireless network can be converted into a problem of stochastic process (finding transition probability between nodes) in the statistics [38, 62].

Based on this model, in Figure 3.1(b), the UE movement history can be modelled as state sequence *c, b, a, f, e* and in Figure 3.2(b), the UE movement history can be modelled as state sequence *e, d, b, a*. Thus, according to the transition probabilities and state sequence of the UE, UTPM will predict its future state which means the cell UE would camp at next step.

3.1.2 Markov Prediction Model

Some papers model the UE mobility history pattern and next cell prediction based on a Markov chain [37, 38].

The multi-order Markov chain can be defined as a sequence of symbols $x_1, x_2, \ldots, x_{n-1}$ as the moving history states of a given UE. Given a variable m, then a new sequence can be written as $x_{n-m}, x_{n-m+1}, \ldots, x_{n-1}$ and $n > m$.

If the probability of future state $X_n = x_n$ depends on the past m states, it can be described as in Equation (3.1) and called an order-m Markov chain [63].

$$\begin{aligned} &Pr(X_n = x_n | X_{n-1} = x_{n-1}, X_{n-2} = x_{n-2}, X_{n-3} = x_{n-3}, \ldots, X_1 = x_1) \\ &\quad = Pr(X_n = x_n | X_{n-1} = x_{n-1}, X_{n-2} = X_{n-2}, \ldots, X_{n-m} = x_{n-m}) \end{aligned} \tag{3.1}$$

According to Equation (3.1), the next cell prediction (future state) can be obtained by using the m past states. If *m=1*, the order-m Markov chain is changed to a normal Markov chain which means that the next cell prediction only depends on the current cell (current state).

[61] and [64], who have studied many cases which use Markov chain to predict the next state, proposed that the order-*2* Markov chain is much more quasi-optimal than other Markov chains. Reflecting this, in this chapter, I only consider the order-*2* Markov chain and Equation (3.1) can be rewritten as Equation (3.2).

$$\begin{aligned} &Pr(X_n = x_n | X_{n-1} = x_{n-1}, X_{n-2} = x_{n-2}, X_{n-3} = x_{n-3}, \ldots, X_1 = x_1) \\ &\quad = Pr(X_n = x_n | X_{n-1} = x_{n-1}, X_{n-2} = X_{n-2}) \end{aligned} \tag{3.2}$$

This mobility prediction usually contains two major steps: parameter learning and next state prediction.

Learning Process of the Markov Model

In this process, the main goal is to find the transition probability matrix. If A denotes the transition probability matrix, in order to create the matrix A, each state transition probability can be calculated by training the data (history states). If sets a_1 and a_2 are the previous states, this model would use them to predict the new state a. Then Equation (3.3) can be obtained according to Equation (3.2) and an order-*2* Markov chain.

$$Pr(X_n = a|X_{n-1} = a_1, X_{n-2} = a_2) \tag{3.3}$$

L denotes the state space and c is the state that consists of a_1 and a_2 in order; c belongs to L. Also $N(s', s)$ denotes the number of times the state s' occurs in the state sequence s. Depending on Equation (3.3), the transition probability for each state can be described as Equation (3.4).

$$Pr(X_n = a|X_{n-1} = a_1, X_{n-2} = a_2) = \frac{N(ca, L)}{N(c, L)} \tag{3.4}$$

where $N(ca, L)$ denotes the number of times the state $c + a$ occurs in the state space L and $N(c, L)$ denotes the number of times the state c occurs in the state space L. After calculating each state transition probability, the matrix A can be created and used for the next state prediction process.

The learning process of the Markov prediction model can be summarised as:

1. Model the UE moving history (cell IDs) to generate the state space.
2. Train the data over a time period.
3. According to the training data, obtain the initial state sequence at time domain, and calculate the initial transition probability for each state by using Equation (3.4)
4. Record the transition probability for each state and create the transition probability matrix A.
5. Each time the new state occurs, update the state sequence at time domain and re-calculate the transition probability for the corresponding state by using Equation (3.4).
6. According to the new transition probability of the state, update the transition probability matrix A.

7. Repeat the process from step 5, which means that the system continually learns the UE moving history and updates the transition probability matrix A in time.

Next State Prediction Process of the Markov Model

In this process, the main goal is to predict the next state. According to the transition probability matrix A which is obtained by the learning process to find the higher probability next state as shown in Equation (3.5).

$$X_{n+1} = argmax Pr(A_{c,a}|X_n = c) \tag{3.5}$$

After the prediction, as soon as the next state (cell) is known, this piece of information is added to the learning process, and used to update the transition probability matrix. Markov parameters in a learning and prediction process can be interleaved and offer the collaborative work for this model in order to achieve better quality of the mobility prediction model.

The prediction process of the Markov prediction model can be summarised as:

1. Obtain the current and previous states (cell ID) due to the order-*2* Markov.

2. Obtain the transition probability matrix A from the learning process.

3. According to Equation (3.5), predict the future state (cell ID) with the highest transition probability.

4. Check the accuracy of the prediction when UE moves to the next cell.

Markov Renewal Processes Prediction Model

In the previous section, the Markov process in UTPM is also called a regular Markov chain. This regular model only considers the state transitions and the

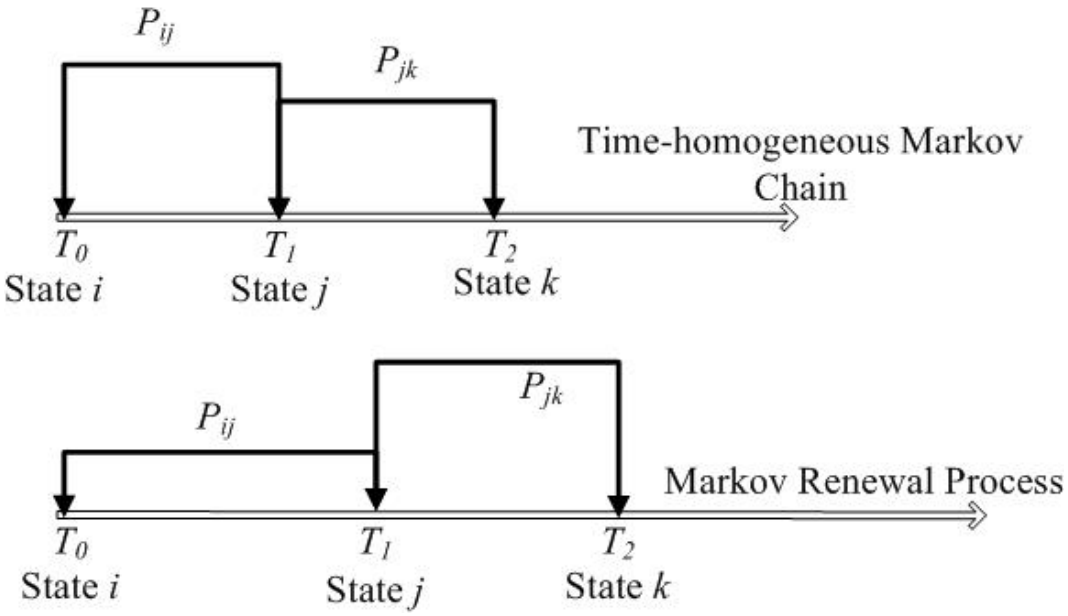

Figure 3.3: Time-homogeneous Markov vs MRP

interval time between states do not affect these transitions. Reflecting this, the regular Markov chain can be called a time-homogeneous Markov chain [20].

However, there is a process called a Markov Renewal Process (MRP), which not only considers the state transitions but also the interval time between states [20]. The comparison with a regular Markov chain is shown in Figure 3.3.

In Figure 3.3, for the time-homogeneous Markov chain, the transition between states is a Markov chain and the interval time between states is constant ($T_2 - T_1 = T_1 - T_0$). The transition probabilities P_{ij} and P_{jk} are not related to the interval time and the next state only depends on the previous state. In the MRP, the interval between states is not constant and the transition between states is modelled as a Markov chain. The transition probabilities P_{ij} and P_{jk} are related to the interval time and the next state not only depends on the previous state but also depends on the future interval time (sojourn time). Reflecting this, the process is not a fully Markov chain, and so it is called a semi-Markov process [18, 20].

According to the above description, a transition probability P_{ij} of a Markov process and the sojourn time in any state depends on both current-state and

the next-state transitions; the MRP can be described as in Equation (3.6).

$$MRP_{ij}(t) = Pr(X_{n+1} = j, T_{n+1} - T_{n<=}t|X_n = i) \tag{3.6}$$

where X_n and X_{n+1} represent the states of the system after the nth and $n+$ 1th transitions respectively and T_n and T_{n+1} represent the interval time when the nth and $n+1$th states occur. $MRP_{ij}(t)$ denotes the probability of making the transition from state j into state i, within t units of time [20].Equation (3.6) can be further rewritten as $MRP_{ij}(t) = P_{ij} * G_{ij}(t)$, where $G_{ij}(t)$ is defined in Equation (3.7).

$$G_{ij}(t) = Pr(T_{n+1} - T_n <= t|X_{n+1} = j, X_n = i) \tag{3.7}$$

In Equation (3.7), $G_{ij}(t)$ denotes the conditional probability that a transition between state i and state j will take place within an amount of time t [20]. If $G_{ij}(t) \to 1$, then $t \to \infty$ and Equation (3.6) can be rewritten as Equation (3.8).

$$P_{ij} = lim_{t\to\infty} MRP_{ij}(t) \tag{3.8}$$

MRP prediction usually contains three major steps: sojourn time learning, transition probability learning and next state prediction process.

Sojourn Time in the Learning Process of the Markov Renewal Model

In this process, the main goal is to find the conditional probability $G_{ij}(t)$ when a UE starts at state i and to state j (cell i and cell j) over the time t.

$N(t)$ denotes the number of transition times $0 < t <= T$ for the $(X_n, T_n), n >=$ 0, where i and $j \in M$, M is the state space. Thus for time t, $G_{ij}(t)$ can be calculated by Equation (3.9).

$$G_{ij}(t) = \frac{N(t)}{N(T)} \tag{3.9}$$

where T is the maximum time for a transition between states i and j . Therefore, for two different states, the maximum time of a transition between them is different.

The learning process of the conditional probability in MRP can be summarised as:

1. Model the UE moving history (cell IDs) to generate the state space.
2. Train the data over a time period.
3. According to the training data, create the initial state sequence at time domain calculate, and create the initial *N(t)* and *N(T)* for each state of a UE at time t.
4. Calculate the initial $G_{ij}(t)$ of the UE by using Equation (3.9) and create the initial conditional probability matrix.
5. Update the *N(t)* and *N(T)* following the new UE moving history.
6. Update the $G_{ij}(t)$ and corresponding value in the conditional probability matrix.
7. Repeat the process from step 4, which means that the system continually learns the UE moving history and update the conditional probability matrix in time.

Transition Probability in the Learning Process of the Markov Renewal Model

In this process, the main goal is to find the transition probability matrix A in $MRP_{ij}(t)$ when UE starts at state i and moves to state j during time t. $MRP_{ij}(t) = P_{ij} * G_{ij}(t)$, as mentioned in the previous section, the transition probability matrix can be obtained from emph$G_ij(t)$ and Pij.

Since P_{ij} is a Markov chain, similar to Section 3.1.2, each state transition probability can be calculated by training the data (history states). Then Equation (3.10) can be derived using Equation (3.1) with an order-*1* Markov chain.

$$Pr(X_n = j | X_{n-1} = i) = \frac{N(i, j, L)}{N(i, L)} \tag{3.10}$$

Where $N(i, j, L)$ denotes the number of times the state $i + j$ occurs in the state space L. $N(i, L)$ denotes the number of times the state c occurs in the state space L. After calculating each state transition probability P_{ij} and $G_{ij}(t)$, the transition probability matrix in $MRP_{ij}(t)$ can be obtained.

The learning process of Transition Probability in MRP can be summarised as:

1. Obtain the information of the state sequence modelling and train the data from the previous learning process.

2. According to the training data, calculate the initial transition probability for each state by using Equation (3.10)

3. Record the transition probability for each state and create the transition probability matrix A.

4. Each time the new state occurs, re-calculate the transition probability for the corresponding state by using Equation (3.10).

5. According to the new transition probability of the state, update the transition probability matrix A.

6. Repeat the process from step 5, which means that the system continually learns the UE moving history and update the transition probability matrix A in time.

Next State Prediction Process of the Markov Renewal Model

In this process, the main goal is to predict the next state. According to the transition probability matrix $MRP_{ij}(t)$ during time t as mentioned earlier, to find the higher probability next state as shown in Equation (3.11).

$$X_{n+1}(t) = argmax Pr(MRP_{ij}(t)|X_n = i) \tag{3.11}$$

After the prediction, as soon as the next state (cell) is known, this piece of information is added to the previous learning process learning process, and to update both P_{ij} and $G_{ij}(t)$. MRP parameters in the learning and prediction process can be interleaved and offer the collaborative work for this model in order to achieve better quality of the mobility prediction model.

The prediction process of MRP prediction model can be summarised as:

1. Obtain the current state (cell ID).
2. Record the duration of UE camps in the current cell as t.
3. Obtain the conditional probability matrix from the learning process.
4. According to the Equation (3.7), current state and the duration t, find the probability value for each of the possible next states.
5. Obtain the transition probability matrix A from learning process.
6. According to the transition probability matrix A and current state, find the probability value for each of the possible next states.
7. Calculate the $MRP_{ij}(t)$ by Equation (3.6) with the values from steps 5 and 6.
8. Predict the future state (cell ID) by using Equation (3.11).
9. Check the accuracy of the prediction when UE moves to the next cell.

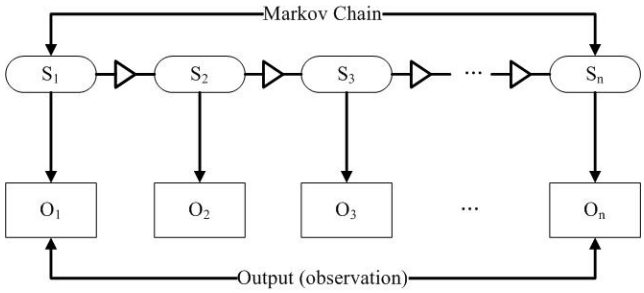

Figure 3.4: The Structure of hidden Markov model

3.1.3 Hidden Markov Prediction Model

Hidden Markov Model (HMM) is defined as relating two kinds of stochastic sequence such as a hidden sequence and an output sequence (observation sequence). The states in the hidden sequence is a Markov chain, but these states cannot be observed due to impossibility, difficulty or imprecision of observation. However, the hidden part reflects other outputs from system, and they can be observed from system. Therefore, the states in the observation sequence are a random sequence and they have the one to one corresponding relationship with the hidden state sequence. If $S_1, S_2, \ldots, S_n$ is a hidden state space and $O_1, O_2, \ldots, O_n$ is the output (observation) state space, $n \in N$, N is the number of states in the space, the structure of HMM is shown in Figure 3.4 according to [63].

HMM can be summarised as (π, A, B), π represents the probability matrix which provides the probability of each hidden state occuring. A represents the transition probability matrix which provides the transition probabilities between hidden states. B represents the emission probability matrix which provides the relationship between hidden and observation states.

According to [19], the UE-based HMM is that UEs' current handovers are modelled as hidden states, such as communication and non-communication. The user's location cells are modelled as observation states. This is because a UE either completes the handover or cannot be observed before the UE moves to the target cell.

The process of UE-based HMM prediction usually contains two major steps:

parameter learning process and next state prediction process, as described below.

Learning process of the UE-based Hidden Markov Model

In this process, the main goal is to learn the network scenario to obtain the optimal (π', A', B') and optimal hidden state sequence due to hidden states which cannot be observed. The optimal (π', A', B') can be obtained by using the learning function defined in the HMM, and observation sequence at time domain $O_t = \emptyset_1, O_2, O_3, \ldots, O_T$, $t \in T, T$ is the duration of the state sequence. The process is described in Equation (3.12):

$$(\pi', A', B') = argmaxPr(O_t|(\pi, A, B)) \tag{3.12}$$

More information about HMM Learning function is described in Section 3.2.2.

The optimal hidden state sequence at time domain $S_t = S_1, S_2, S_3, \ldots, S_T$, $t \in T, T$ is the duration of the state sequence, can be obtained by using the decoding function that defined in HMM, optimal (π', A', B') and observation sequence at time domain O_t. The process is described in Equation (3.13):

$$S_t = argmaxPr(S_t|O_t, (\pi', A', B')) \tag{3.13}$$

More information about the HMM decoding function is described in Section 3.2.2.

The learning process of UE-based hidden Markov prediction model can be summarised as:

1. Model the UE movement history (cell IDs) to generate the observation state space.

2. Train the data over a time period.

3. If this is first time execution of the prediction model, according to the training data, determine the observation state sequence over a time domain. Otherwise update the observation state sequence at time domain.

4. Obtain the optimal (π', A', B') by using Equation (3.12) and the observation state sequence at time domain.

5. Obtain the optimal hidden state sequence by using Equation (3.13), optimal (π', A', B') and the observation state sequence at time domain.

6. Use the current hidden state which is obtained from the optimal hidden state sequence in the next state prediction process.

7. Repeat the process from step 3, which means that the system continually learns the UE moving history (observation state), and updates (π', A', B') and the hidden state sequence.

Next State Prediction Process of UE-based Hidden Markov Model

The next state prediction is defined so as to predict the next hidden state (communication or non-communication), when a UE is moving to the next cell. From the previous learning process, the optimal (π', A', B') and current St can be obtained. Since the hidden states are a Markov Chain, the next hidden state S_{t+1} can be predicted as:

$$S_{t+1} = argmaxPr(A_{S_t,S_{t+1}}|S_t) \tag{3.14}$$

Therefore, S_{t+1} would be the optimal state representing a UE that will handover or not to the new moving target cell at the next time period.

The prediction process of UE-based hidden Markov prediction model can be summarised as:

1. Obtain the current observation state (cell ID).

2. Obtain the emission probability matrix B from optimal (π', A', B') in the learning process.

3. Predict the current hidden state according to the emission probability matrix B and current observation state.

4. Obtain the transition probability matrix A from optimal (π', A', B') in the learning process.

5. Predict the next hidden state according to the transition probability matrix A and current hidden state by using Equation (3.14). If the next hidden state is communication, this means the UE would handover to the cell that it is moving to. Then the system can prepare the network resource for this handover process.

6. Check the accuracy of the prediction when the UE moves to the next cell.

3.2 The Proposed Cell-based Prediction Model (CPM)

The current research on UE-based traffic behaviour is introduced in Chapter 2. Most of the approaches work well in a regular network (macrocell scenario) deployment, but are not suitable for femtocell deployment in a two-tier network scenario. In this chapter, different from those conversional prediction models, a novel combined theoretical and factual cell-based approach is proposed, namely the Cell-based Prediction Model (CPM) for predicting the intensity of a femtocell's handover. This approach overcomes the drawbacks explained in Section 3.3.1 for the UE-based model used in a two-tier network scenario and provides a more accurate prediction compared to these UTPMs.

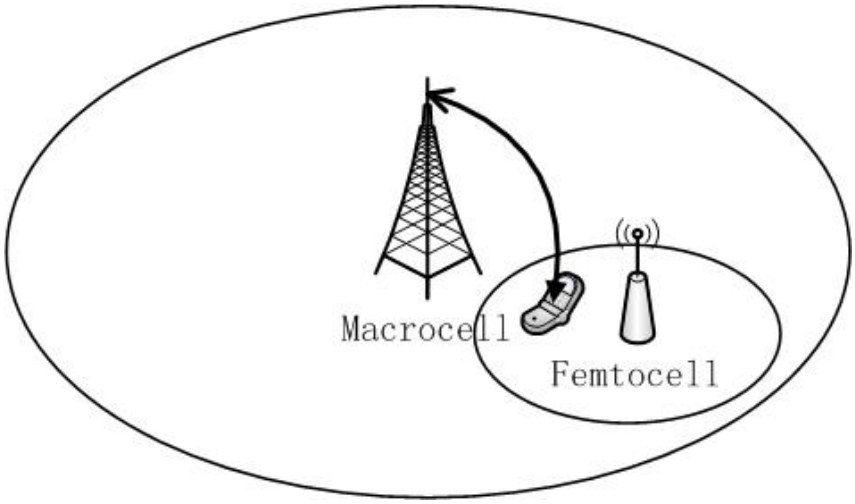

Figure 3.5: A UE served by the macrocell camps in the coverage of a femtocell

3.2.1 The Cell-based Intensity of a Femtocell's Handover Prediction

The intensity of effective mobility in the CPM represents the different number of handovers within a femtocell's coverage. This section introduces how the prediction of the intensity of effective mobility is modelled.

Newly Arrived vs. Handed-over UE in the Femtocell Deployment

Generally, Markov and Markov renewal processes are both used in the scenario of regular wireless networks and work well. However, in the scenario of irregular wireless networks, a serious issue occurs due to the special structure of an irregular network (femtocell and macrocell overlap in two-tier networks) which leads to failure of the Markov and Markov renewal processes. More information regarding the failure is described in Section 3.3.1.

In the regular wireless network, whether a UE is in the idle or connected model, it should camp on a wireless cell and receive the service from this cell. However, in the irregular network structure (two-tier network), a UE can camp on a femtocell but still be connected to the macrocell, as shown in Figure 3.5.

In the case shown in Figure 3.5, when a UE camps on a femtocell, it still retains its connection with the macrocell. Although the UE has already moved into the coverage of the femtocell, the femtocell still has difficulty observing

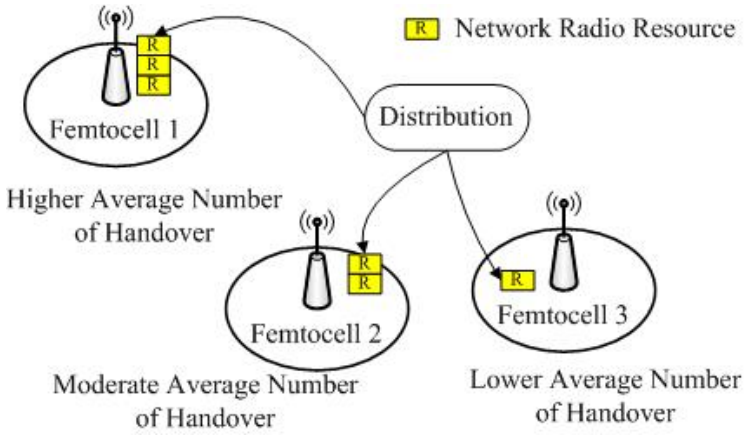

Figure 3.6: The radio resource distribution in LTE Femtocell system

the activity of the UE since that UE does not have any connection with this femtocell. Moreover, in a wireless network, changes to the user's location may not need extra system resources; only the communication process (handover) between UE and cell will lead the system to allocate extra communication channel [19]. Thus, the number of UE handovers is a more meaningful criterion than UE arrivals for the radio resource management.

Hidden Markov Model in the Proposed Prediction Model

As mentioned in Section 3.1.4, a Hidden Markov Model (HMM) is defined as relating two kinds of stochastic sequence such as a hidden sequence and an output sequence (observation sequence). It can be summarised as (π, A, B), π represents the probability matrix which provides the probability of each hidden state occurring; A represents the transition matrix which provides the transition probabilities between hidden states; B represents the emission matrix which provides the relationship between hidden and observation states.

This chapter proposes CPM. Compared to the UTPM, instead of modelling the UE's moving history as states, it models the intensity of a femtocell's handover as the state. The intensity of handovers is defined as the average number of UEs which handover to the target cell. An example is shown in Figure 3.6.

In Figure 3.6, if a femtocell has a higher average number of handovers, the

system would allocate more network radio resources to it in order to guarantee the QoS. This also applies to the femtocells with moderate and lower numbers of handovers. Forecasting the intensity of a femtocell's handovers would achieve more efficient allocation and management of the network's resources. However, the intensity of effective mobility (states) of a femtocell may not follow the Markov chain, therefore, this prediction model needs to be further improved.

According to queuing theory, the number of UEs arriving at a cell in each time period can be modelled by a Poisson distribution. When modelling the varying number of UEs arriving as the states, those states can be formed as a Markov chain [65]. However, the number of UE handovers is not equal to the number of UE arrivals. The relationship between those UE handovers and arrivals can be summarised as: the greater the number of UEs arriving at the cell, the higher the probability a UE handover would happen in this cell; similarly, the lower number of UEs arriving at the wireless cell, the lower the probability of UE handover in this cell. Reflecting this, the number of UE handovers can be set as a sequence. The states in this sequence can be modelled as the different ranges of UE handover numbers (the intensity of handovers). Moreover, this sequence is easily observed by the base station.

Another sequence can be formed for the number of UE arrivals. The states are different ranges of UE arrival numbers. Moreover, the states in this sequence can be modelled as a Markov chain, but arrival as a state is difficult for the base station to identify (observe). Therefore, the cell-based prediction can be modelled as a HMM process. The structure of the proposed HMM model is shown in Figure 3.7.

In Figure 3.7, states S_1, S_2 and S_3 represent the different level of UE arrivals as Busy, Moderate and Idle respectively in the hidden part. The Busy state models a femtocell with a higher number of UE arrivals in a time period. Similarly, Moderate and Idle model medium and lower numbers of UE arrivals respectively. The O_n=$O_1, O_2, \ldots, O_N$ is the observation part, $n \in N, N$ is the number of states in the observation state space; they denote the different

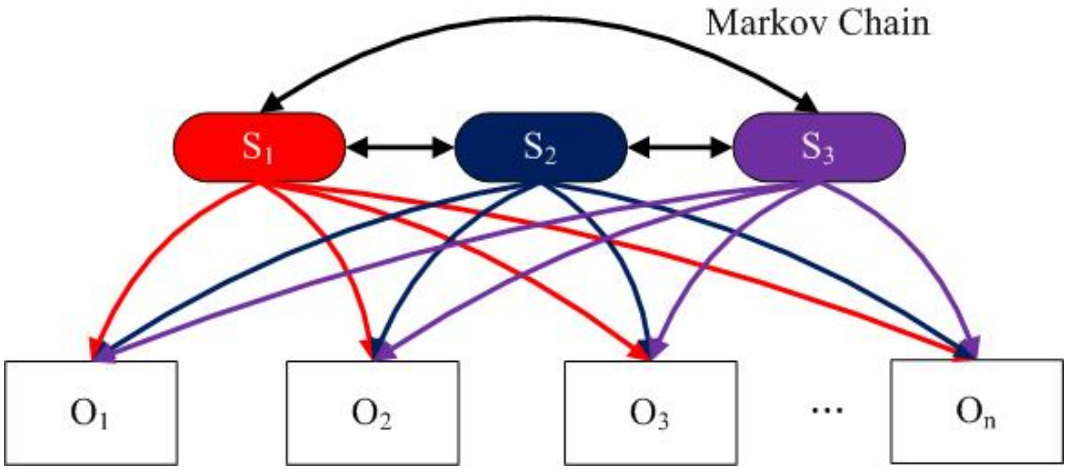

Figure 3.7: The Structure of CPM in hiden Markov model

intensity of a femtocell's handovers. Moreover, depending on the HMM, the relationship between each observation state can be connected via the hidden part.

Proposed Model Prediction Process

As mentioned in the previous section, the system only performs network radio resource allocation on UE handover to the wireless cell, therefore, only the number of UE handovers would lead the system to perform resource distribution. In the proposed CPM, the process will predict the next observation state (intensity of handovers). If O_t=O = $O_1, O_2, \ldots, O_T$ denotes the observation state sequence at time domain and the hidden state sequence at time domain is St=S1, S2, , ST (sequence at time domain means that, any hidden or observation state in state space can appear at time t as O_t or S_t), t is the time period and $t \in T, T$ is the duration of the state sequence, the next state Ot prediction process is shown in Figure 3.8.

As shown in Figure 3.8 the next state prediction depends not only on the current observation state but also the bridge which is made by the hidden states and Markov chain. Moreover, according to [66], HMM can be summarised as (π, A, B), π represents the probability matrix which provides the probability of each hidden state occurring;. A represents the transition matrix which

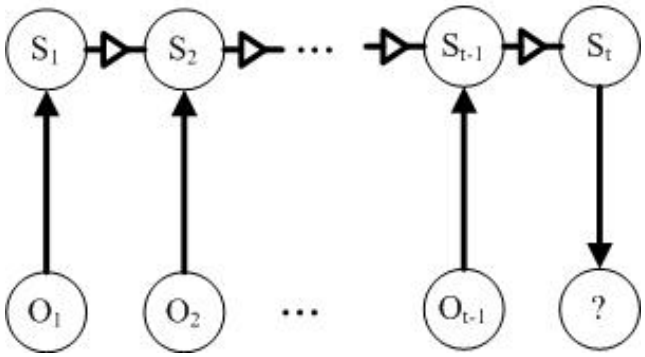

Figure 3.8: Next observation state prediction via hidden states

provides the transition probabilities between hidden states; B represents the emission matrix which provides the relationship between hidden and observation states. The optimal (π, A, B) and hidden state sequence can be obtained by the learning process which is described in detail in the next section. The next observation state process is described as follows:

Firstly, according to matrix A and the hidden states S_{t-1}at time t-1 which is obtained from hidden states sequence at time domain, the next time observation state S_t is calculated by Equation (3.15) which is refer to Equation (3.13), but with different avariables.

$$S_t = argmaxPr(A_{S_t;S_{t-1}}|S_{t-1})(t > 1) \tag{3.15}$$

In the CPM, the intensity of the UE arrivals in a femtocell (hidden part) at time t-1 can be used to predict the next intensity of the UE arrivals at time t. Since only the handover process can cause changes of network resource as mentioned earlier, the next step in the CPM is the prediction of the observation state at time t by using the next intensity of the UE arrivals at time t.

Secondly, according to the S_t and matrix B , the next observation states O_t at time t are calculated by Equation (3.16).

$$O_t = argmaxPr(B_{S_t;O_t}|S_t)(t > 1) \tag{3.16}$$

In the CPM, the O_t is the optimal observation state at time t. Since the O_t represents the intensity of the femtocell's handovers, the system can depend on the value of Ot to optimally distribute the network resource for this femtocell.

3.2.2 Learning process for the intensity of a Femtocell's handover prediction

This section introduces how the CPM approach proposes learning the situation of a femetocell's handover and provides the optimised transition matrix, and the hidden state sequence for the prediction model.

Proposed Model Leaning Process

As mentioned in the previous section, the HMM can be summarised as (π, A, B) and the main goal in this section is to obtain optimal those parameters, based on the given observation sequence and an initial (π, A, B) from the network system.

$O_t = O = O_1, O_2, O_3, ..., O_T$, denotes the observation state sequence at time domain and $t \in T, T$ is the duration of the state sequence. Through the sequence Ot and an initial (π, A, B), the best set of π', A' and B can be found in the learning process. This learning process is described by Equation (3.17).

$$(\pi', A', B') = argmax Pr(O_t|(\pi, A, B)) \tag{3.17}$$

In Equation (3.14), where initial (π, A, B) can be set as various values which would depend on the scenario required. This learning process is achieved by a forward-backward algorithm [66]. The forward and backward intermediate probabilities are derived in Equations (3.18) and (3.19):

$$\alpha(S_{n,t}) = \begin{cases} \pi * B_{S_{n,1},O_1} & (t = 1) \\ \sum_{n=1}^{N} B_{S_{n,t},O_t} * A_{S_{n,t},S_{n,t-1}} * \alpha(S_{n,t-1}) & (t > 1) \end{cases} \tag{3.18}$$

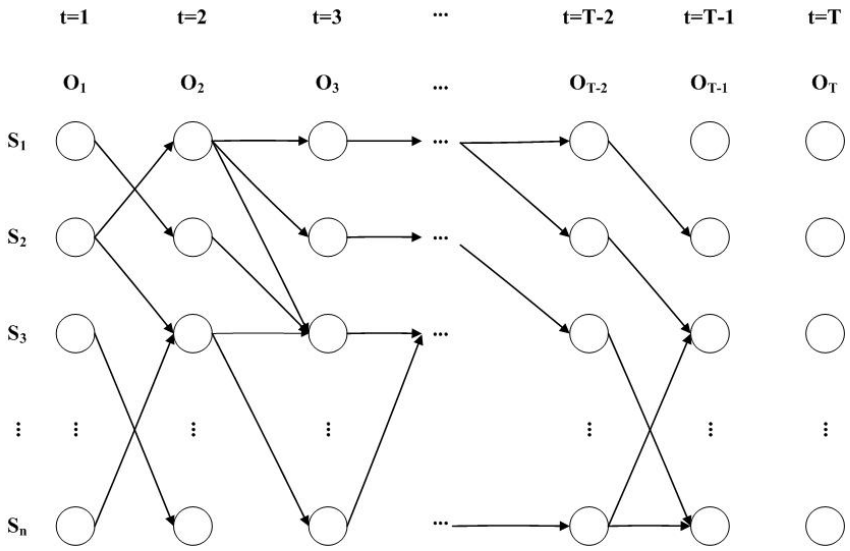

Figure 3.9: Forward process in trellis

$$\beta(S_{n,t}) = \begin{cases} \sum_{n=1}^{N} B_{S_{n,t},O_t} * A_{S_{n,t},S_{n,t+1}} * \beta(S_{n,t+1}) & (1 <= t < T) \\ 1 & (t = T) \end{cases} \tag{3.19}$$

where S_n=$S_1, S_2, S_3, , SN$, $n \in N$ is the hidden state, N is the number of states in the state space. The $\alpha(S_{n,t})$ represents a partial probability which is the probability of reaching state S_n at time t in the forward process. Similarly, $\beta(S_{n,t})$ represents a partial probability which is the probability of reaching state S_n at time t in the backward process. Moreover, the forward process can be modelled as the trellis shown in Figure 3.9.

In Figure 3.9, the circle denotes the partial probability of reaching state S_n at time t. The arrow line denotes the possible path that transition from state S_n at time t to the S_n at time t+1, $n \in N$. Therefore, $\alpha(S_{n,t})$ is calculated as Pr(observation — hidden state is S_n) * Pr(all paths to state S_n at time t) [66], this calculation can be modelled by Equation (3.18). Moreover, when t=1, there are no paths to the state. Thus, the initial partial probability is calculated as the Pr(observation — hidden state is S_n) * π.

Since the backward process is similar as the forward process but in the opposite directions, the $\beta(S_{n,t})$ is calculated as Pr(observation — hidden state

is S_n) * Pr(all paths to state S_n at time t), $n \in N$. This calculation can be modelled by Equation (3.19). Moreover, in the special case where $t = T$, there are no paths to the state, thus, each state has 100% probability to be reached. According to Equations (3.18) and (3.19), another two denotations are introduced.

$$\varepsilon(S_{i,t}, S_{j,t+1}) = \frac{\alpha(S_{i,t}) * \beta(S_{j,t+1}) * A_{S_{i,t},S_{j,t+1}} * B_{S_{j,t+1},O_{t+1}}}{\sum_{i=1}^{N}\sum_{j=1}^{N} \alpha(S_{i,t}) * \beta(S_{j,t+1}) * A_{S_{i,t},S_{j,t+1}} * B_{S_{j,t+1},O_{t+1}}} \quad (3.20)$$

$$\gamma(S_{i,t}) = \sum_{j=1}^{N} \varepsilon(S_{i,t}, S_{j,t+1}) \quad (3.21)$$

where $\varepsilon(S_{i,t}, S_{j,t+1})$ denotes the partial probability of reaching state S_i at time t and state S_j at t+1, $i \in N, j \in N$. According to the forward and backward processes, $\varepsilon(S_{i,t}, S_{j,t+1})$ is calculated by taking the partial probability of reaching state $S_{j,t+1}$ from $S_{i,t}$ (forward process), multiplying it by the partial probability of reaching state $S_{j,t+1}$ from t=T (backward process), then dividing the result by the sum of all possible partial probabilities of reaching state $S_{j,t+1}$ which are obtained from forward and backward processes. This calculation is modelled in Equation (3.20). Moreover, in Equation (3.21), $\gamma(S_{i,t}$ denotes the expected number of transitions from other hidden states to state S_i at time t. According to Equations (3.20) and (3.21), the new $\overline{\pi}, \overline{A}$ and $\overline{B}$ can be obtained as followed:

$$\overline{\pi}_i = \gamma(S_{i,1}) = \sum_{j=1}^{N} \varepsilon(S_{i,1}, S_{j,2}) \quad (3.22)$$

$$\overline{A}_{S_{i,t},S_{j,t+1}} = \frac{\sum_{t=1}^{T-1} \varepsilon(S_{i,t}, S_{j,t+1})}{\sum_{t=1}^{T-1} \gamma(S_{i,t})} \quad (3.23)$$

$$\overline{B}_{S_{j,t},O_t} = \frac{\sum_{t=1}^{T} \gamma(S_{j,t})[s.t.O_t = k]}{\sum_{t=1}^{T} \gamma(S_{j,t})} \tag{3.24}$$

where $\overline{\pi}_i$ is the expected number of times in state S_i at time t=1 as defined in Equation (3.22). A $S_{i,t}, S_{j,t+1}$ is the transition probability calculated as the expected number of transitions from state S_i to state S_j divided by the expected number of transitions from state S_i as denoted in Equation (3.23). $\overline{B}_{S_{j,t},O_t}$ is the emission probability calculated as the expected number of times that state O_t ($O_t = k, k$ is an specific observation state in state space at time t) appears in state j divided by the expected number of times that all hidden states transit to state j. This calculation is summarised in Equation (3.24).

All the $\overline{\pi}_i, i \in N$, can be formed as the $\overline{\pi}$. Then, the new $\overline{\pi}, \overline{A}$ and $\overline{B}$ can be used to execute iteration from Equations 3.20 to 3.21. The iteration process will stop when the difference of current and previous π, A and B reach a threshold, for example, 0.0001. Then, the $\overline{\pi}, \overline{A}$ and $\overline{B}$ are the optimal (π', A' and B').

Proposed Model Decoding Process

The decoding process in this section is used to provide an optimised hidden state sequence for the prediction process in Section 3.3.1.3. Since the hidden state cannot be observed by the network system, it can only be obtained based on the known parameters such as HMM mode π', A' and B' and observation sequence.

Assume $O_t = O_1, O_2, O_3, \ldots, O_T$ is observation state sequence at time domain and $t \in T, T$ is the duration of the state sequence. Assume $S_n = S_1, S_2, ..., S_N$, N is the number of hidden states in the state space and $S_{n,t}$ denotes the hidden state S_n at time $t, t \in T$. The decoding process is described as Equation (3.25).

$$S'_{n,t} = argmax Pr(S'_{n,t}|O_t, (\pi, A, B)) \tag{3.25}$$

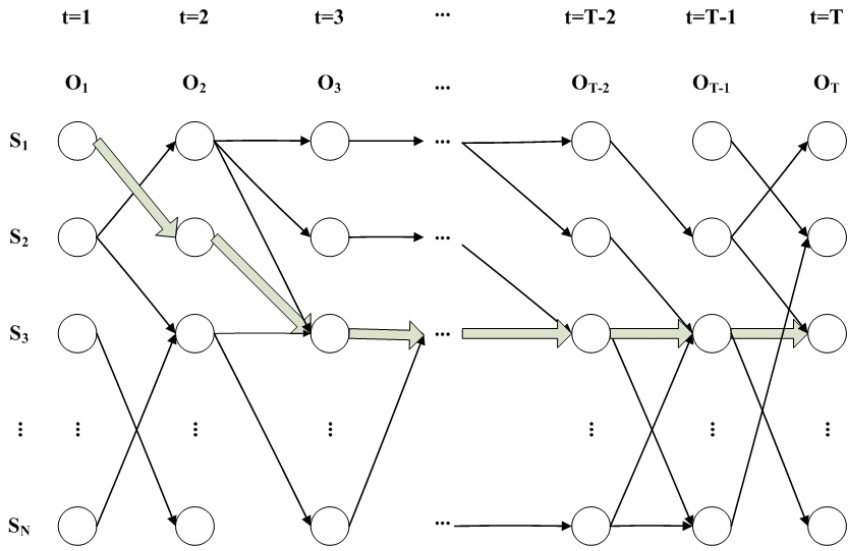

Figure 3.10: Viterbi process in trellis

The decoding process uses the Viterbi algorithm [66] to find the optimal hidden state sequence $S'_{n,t}$, where $\delta_t(S_{i,t})$ denotes the probability of the partial best path to a state $i, i \in N$) at time t when the observation O_t is seen, as shown in Figure 3.10.

In Figure 3.10, the thick arrows show the best path. Therefore, if given a sequence O_t, the best path is chosen by the higher probability of $\delta_t(S_{n,t})$ at time t. This recording (remembering) is done by holding for each state a back pointer $\varphi_t(S_{n,t})$ which points to the predecessor that optimally provokes the current state.

When t=1, since there is no route path, the initial probability of the first path at state $S_{n,1}$ is described as $\delta_1(S_{n,1})$ and $\varphi_1(S_{n,1})$ which are calculated in Equations (3.26) and (3.27).

$$\delta_1(S_{n,1}) = \pi * B_{s_{n,1},o_1}(n \in N, t = 1) \tag{3.26}$$

$$\varphi_1(S_{n,1}) = 0(n \in N, t = 1) \tag{3.27}$$

According to the results from Equations (3.26) and (3.27), the maximum

states probability and route path of states S when $t > 2$ are described as $\varphi_t(S_{n,t})$ and $\varphi_t(S_{n,t})$, as summarised in Equations (3.28) and (3.29).

$$\delta_t(S_{t,n}) = \max_{1 \leq j \leq N} [\delta_{t-1}(j) * A_{S_{i,t},S_{j,t-1}}] * B_{S_{i,t},O_t} (2 \leq t \leq T) \tag{3.28}$$

$$\varphi_t(S_{i,t}) = \operatorname*{argmax}_{1 \leq j \leq N} [\delta_{t-1}(j) * A_{S_{i,t},S_{j,t-1}}] (2 \leq t \leq T) \tag{3.29}$$

If t=T, the current hidden state S_T can be obtained in equation (3.30).

$$S_{n,T} = \operatorname{argmax}(\delta_T(S_{n,T})) \tag{3.30}$$

By using back tracking, the most probable route path can be used to find the rest of the hidden states, as defined in Equation (3.31).

$$S_{n,t-1} = \varphi_t(S_{n,t}) (t = T-1, T-2..., 1) \tag{3.31}$$

Although the network system cannot observe the hidden sequence, the learning and decoding process can work together to train an optimal hidden states sequence for prediction process.

3.2.3 Proposed Cell-based Prediction Model Process

There are five main stages in the proposed CPM, as described below:

1. To collect handover information and determine the detail of the observation states such as number of observation states in model and threshold in observation state. In CPM, the average number of handovers of the femtocells (handover information) can be transferred via backhaul to the Mobility Management Entity (MME) which is the entity used to achieve the femtocell management communication between cells [25]. In MME,

according to the specific system requirement and the handover information from femtocells, the number of observation states in model and threshold in each state can be determined for those femtocells.

2. By using the learning process described in Section 3.3.2.1, initial /current observation states sequences and initial/current (π, A, B) and optimal (π', A', B') can be obtained for each femtocell in MME. If the CPM is executed for the first time in the network, according to the states' detail from stage 1, the initial observation states sequence $O_t = O_1, O_2, O_3, \ldots, O_T$ at time domain could be collected during the training period T. HMM learning is achieved through observing sequence Ot, and the best set of (π', A', B') can be found as described in Section 3.2.2.1.

   If the CPM is not executed for the first time in the network, this stage is only used to add the new state to observation states sequence Ot and obtain the optimal (π', A', B') by using the learning process.

   Moreover, the transition probability A, initial states probability π and emission probability B cannot be gathered since the hidden states are unobserved. According to the maximum entropy principle, the probability distribution can be assumed to be uniform if there is not enough information to decide the distribution of a random variable [67].

   If S_{Busy}, $S_{Moderate}$ and S_{Idle} denote the hidden states respectively and observation states are $O_n = O_1, O_2, O_3, \ldots, O_N$, N is the number of states in the state space, the initial A, and π can be set as [NxN] and [1xN] uniform matrixes with 1/N for the value of elements. The observation states are described as the intensity of a femtocell's handovers. To assume that when an observation state, for example O_N, has higher intensity, the hidden state would have a higher probability to be in state S_{Busy}. Similarly, when the observation state has lower intensity, for example O_1, the hidden state would have a higher probability to be in state S_{Idle}. Based on the number of observation states, the initial emission probability matrix B can be created. Moreover, the initial probabilities in B could have any

value as long as they follow the correct distribution rule.

3. The current hidden state S_t, t is the current time scale, could be obtained by using decode process which has been mentioned in section 3.3.2.2.

4. Based on the current state S_t and optimal (π', A', B'), the next optimal state O_{t+1} can be predicted via prediction process as mentioned in section 3.3.1.3.

5. According to the prediction, a LTE system or MME could manage the network resource for each femtocell in order to achieve the centralised self-organising for the overall network as mentioned in Chapter 2.

   The distribution may controlled by a MME or other entities belonging to the LTE system due to the difference of network resources. In Chapter 3, through the CPM, the PCI distribution is achieved by MME. More information, please see Chapter 3.

The flowchart for this process is summarised in Figure 3.11.

3.3 Theoretical and Simulation Analysis

3.3.1 Comparison of UE-based and Cell-based Prediction Models in the LTE Femtocell network

Compared to the macrocell scenario (regular network), one of the important features in the LTE femtocell is that there is no network planning in developing femtocells [6]. To consider this femtocell feature in the prediction model, comparing with the UE-based predictor, the cell-based predictor has two advantages: firstly, no matter which femtocell turns on or off, the transition and emission probability are affected; secondly, it avoids the complexity of calculation and difficulty of evaluation of transition probabilities.

In terms of the first advantage, the UE-based predictor is based on the transition states and the transition probability matrix. The number of transition states would not be stable. The unstable number of states results in

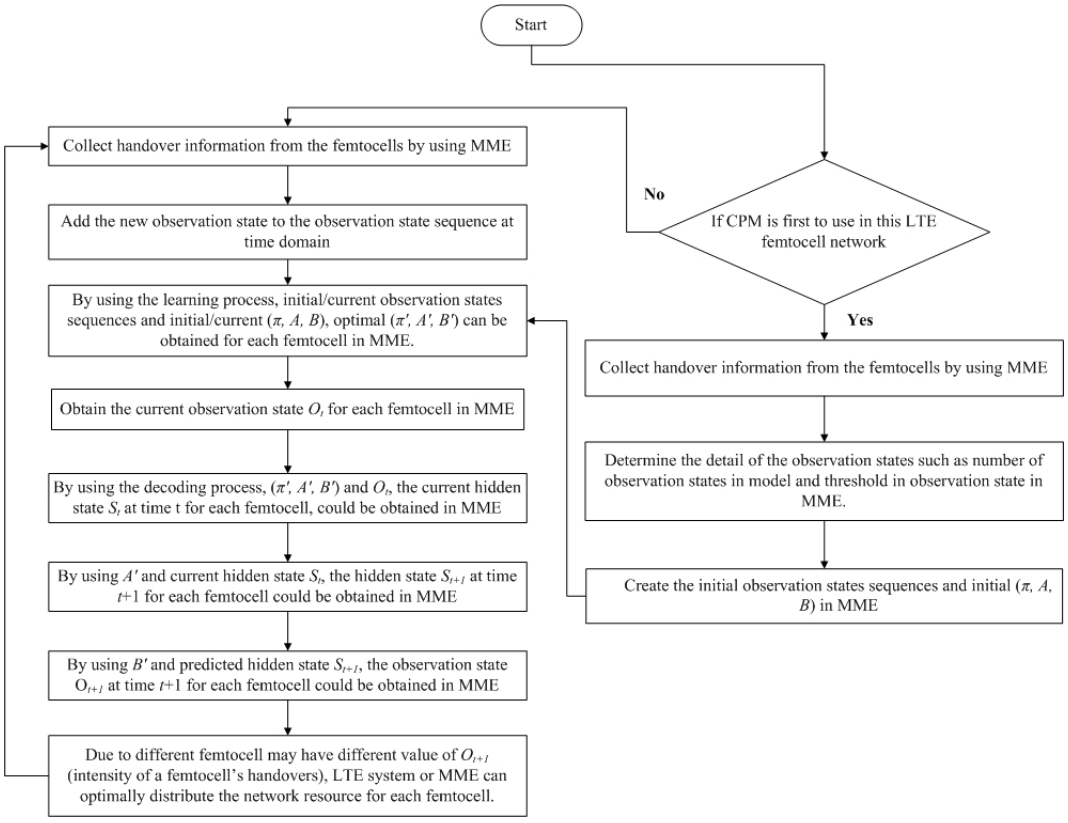

Figure 3.11: Flowchart of the CPM prediction process

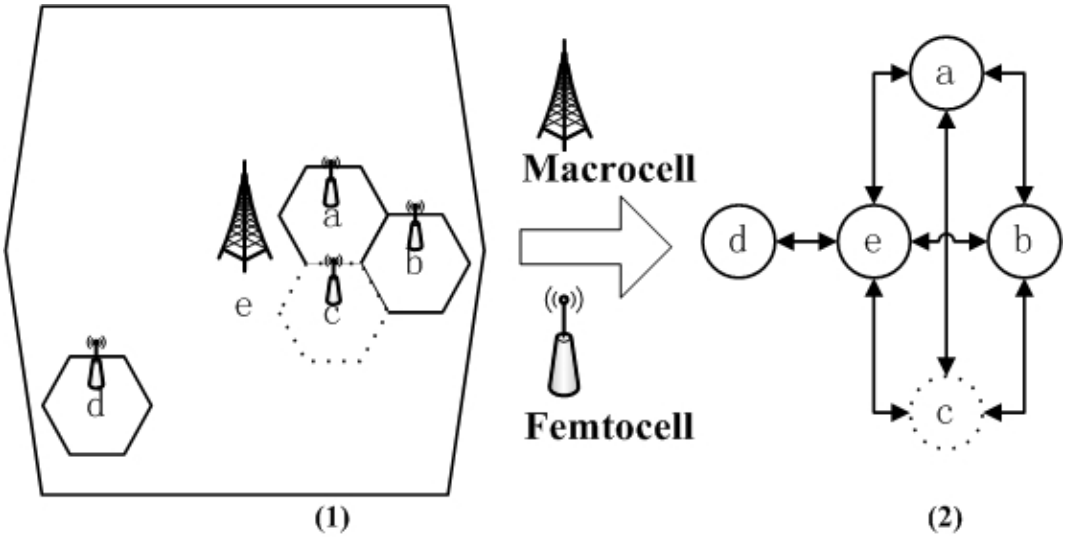

Figure 3.12: A state missing in UE-based prediction model in LTE Femtocell scenario

an incorrect transition probability as well as lower accuracy. This problem is presented in Figure 3.12.

In Figure 3.12(1), there are seven hexagonal stations which are irregularly located between each other, and femtocells *a, b, c* and *d* locate with the coverage of macrocell *e*. This LTE femtocell network can be modelled as arrow-node map as shown in Figure 3.12(2) as mentioned in Section 3.1.1. Therefore, the state sequence can be obtained according to the arrow-node map.

In Figure 3.12(1), assume a UE stays in macrocell e and will arrive in femtocell *c*. Even if the UE-based prediction model gives a right prediction, since femtocell *c* turns off. Therefore, it leads the state *c* is invalid in the state sequence as shown in Figure 3.12(2) and results in the prediction failure.

However, for the CPM, the special femtocell features, such as states, and transition and emission probabilities, are not affected. Depending on the description in the previous sections, unlike the UTPM, the cell-based predictor models the intensity of the handovers as a state. Therefore, this predictor avoids the aforementioned problem caused by a UE-based predictor in a two-tier network.

In terms of the second advantage, since a large number of femtocells may deploy in the network, in the UTPM, the calculation of the transition probabilities would be considerably complex. For instance, if there are 5 states (femtocells) in the network, the transition probability matrix would be a [5x5] matrix with 5^2 transition probabilities. If it increases to 10 states, the number of transition probabilities would be 10^2. Reflecting this, following the growth of number of states, the degree of complexity of transition probability grows geometrically.

Moreover, the larger number of transition probabilities results in little difference between the values of those probabilities, which results in difficulties in evaluation for the transition probabilities and ends up with lower accuracy [20]. Therefore, the number of states should be limited, however, it is difficult to achieve this due to the fact that there is no network planning for femtocell's deployment.

Considering the CPM, the large number of femtocells in deployment does not affect the number of transition and emission probabilities and the number of states of this predictor is related only to the handover. Thus, this predictor overcomes problems in the UE-based predictor in a two-tier network environment.

Overall, CPM has better performance than UTPM due to the two advantages described above.

3.3.2 Metrics used in the Prediction Model

In general, in the bioinformatics and machine learning area, there are many ways, such as accuracy, precision, F-measure, sensitivity and specificity, used to evaluate the quality of prediction model [68]. Thus, those metrics can also be involved in the evaluation of a prediction model for the wireless system.

Description of Evaluation-metrics

In order to describe these metrics in detail, this section involves the confusion matrix as shown in Table 3.1.

Table 3.1: Confusion Matrix for Prediction Evaluation

		Prediction	**Prediction**	
		Positive	Negative	Sum
Reality	Positive	True Positive (TP)	False Negative (FN)	Reality Positive (TP+FN)
Reality	Negative	False Positive (FP)	True Negative (TN)	Reality Negative (FP+TN)
Sum		Prediction Positive (TP+FP)	Prediction Negative (FN+TN)	

In Table B.1, if the reality positive is predicted as the positive, it is called True Positive (TP) and if the reality positive is predicted as negative, it is called False Negative (FN); similarly for False Positive (FP) and True Negative (TN).

According to Table B.1, accuracy, precision, F-measure, sensitivity and specificity are defined as:

- Accuracy is defined as the percentage of predictions that are correct. It is calculated as $(TP + TN)$ / $(TP + TN + FP + FN)$.

- Precision is defined as the percentage of positive predictions that are correct. It is calculated as TP / $(TP + FP)$.

- Sensitivity also called as recall is defined as the percentage of reality positive instances that were predicted as positive. It is calculated as TP / $(TP + FN)$.

- Specificity is defined as the percentage of reality negative instances that were predicted as negative. It is calculated as TN / $(FP + TN)$.

- F-measure is also called as F-score. It is defined as a harmonic mean of precision and sensitivity. A harmonic means that a (50%, 50%) system is often considered better than an (80%, 20%) system. It is calculated as Equation (3.32).

$$F = \frac{(a^2+1)Precision * Sensitivity)}{a^2(Precision + Sensitivity)} \tag{3.32}$$

When a=1, the Equation (3.32) can be rewritten as Equation (3.33) and this is called F1. This is the most-used metric in the prediction system.

$$F_1 = \frac{2 * Precision * Sensitivity}{Precision + Sensitivity} \tag{3.33}$$

Analysis of Proposed Evaluation-Metrics

The different matrices serve the different meaning in the evaluation of the performance of a prediction system, according to the explanation in [20], which are described in practical examples below:

1. Set 100 samples as positive in a data set of 10,000 samples. A prediction model predicts that negative for all the samples. Reflecting this, for this system, it has *TP=0, FN=100, FP=0* and *TN=9900*, according to Table B.1. Then calculate the accuracy as 99%, the precision as 100% (there is no positive predict activity), the sensitivity as 0%, the specificity as 100%, and *F1* as 0%. Note that, although, the accuracy, precision and specificity provide the higher values that indicate this model has very good performance, this prediction model is still useless as to it cannot predict the positive sample. According to this example, sensitivity and *F1* seem to be the actual values that evaluate how well this prediction model performs.

2. The same setting data is used as in example 1. If another prediction model predicts all the samples are positive, then *TP=100, FP=9900, FN=0* and *TN=0*. Reflecting this, the accuracy is 1%, the precision is 1%, the sensitivity is 100%, the specificity is 0% and F1 is 1.98%. Note that, the precision provides the higher value that indicates this model has very good performance. This prediction model is still not good as

other metrics have even lower values. According to this example, the accuracy, specificity precision and F1 seem to be the actual values that evaluate how well this prediction model performs.

3. Similarly to the data used in example 1 but with 10000 samples used, set 9900 out of 10000 as positive. Assume a prediction model predicts all samples as positive, then *TP=9900, FP=100, FN=0* and *TN=0*. Reflecting this, the accuracy is 99%, the precision is 99%, the sensitivity is 99%, the specificity is 0% and F1 is 99%. In this example, the specificity shows the problem that this model cannot predict the negative samples well.

4. In medical diagnostics, sensitivity represents the ability of a test model that correctly identifies people with a disease (*TP* ratio), and specificity represents the ability of a test model that correctly identifies people without the disease (*TN* ratio). For example, say there are 100 people tested by a test model. In fact, 10 people have disease (Positive) and the other 90 people do not have the disease (Negative). After the test, 9 people are tested as having the disease (*TP=9*) and 1 person as not having the disease (FN=1). There are 5 people considered to have the disease (*FP=5*) in 90 people, and the other people do not have the disease (*TN=85*). Reflecting this, the sensitivity is 90% and specificity is 94%. In this example, for the proposed mode, the sensitivity shows the ability to successfully find the actually ill people in the group of ill people, and the specificity shows the ability to find successfully the actually healthy people in the group of healthy people.

According to these examples, the performance of a prediction mode should consider all these metrics.

3.3.3 Simulation and Analysis

This simulation includes the UE-based order-*2* Markov, MRP and HMM predictors from [18], [19] and [38] as well as CPM predictor simulation, and studies

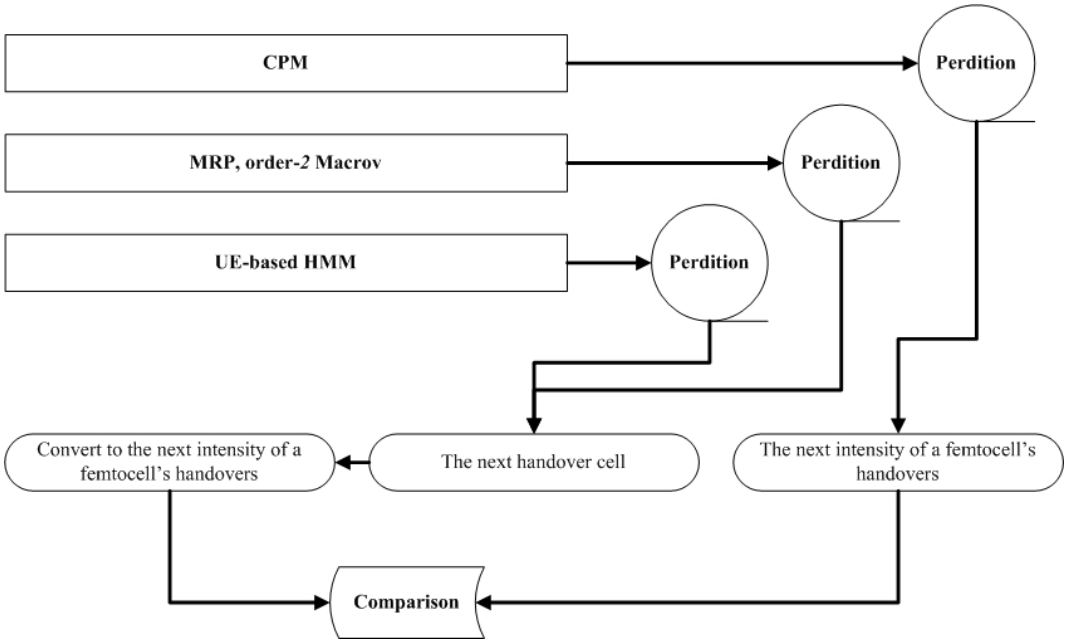

Figure 3.13: The Comparison of different prediction models

the performance of them via accuracy, precision, F-measure, sensitivity and specificity which are proposed in the previous section. These studies give an insight into the effects of performance of different prediction models on the two-tier LTE femtocell network.

The implementation of UE-based in the simulation

In order to compare the performance of UTPM and CPM, the simulation simulates the UE-based order-*2*, MRP and HMM and CPM prediction models together. However, UE-based prediction models can only predict the UE's future location cell or UE's future handover situation. It cannot predict the intensity of a femtocell's handovers. Therefore, the prediction results from UE-base prediction models need to covert to the intensity value as shown in Figure 3.13.

In terms of the order-*2* and MRP prediction model, they can predict the next UE moving cell. In the simulation, the order-*2* and MRP can model the cells which provide the handover process with the UE in the UE moving history as states. Therefore, order-*2* and MRP can predict the next cell which

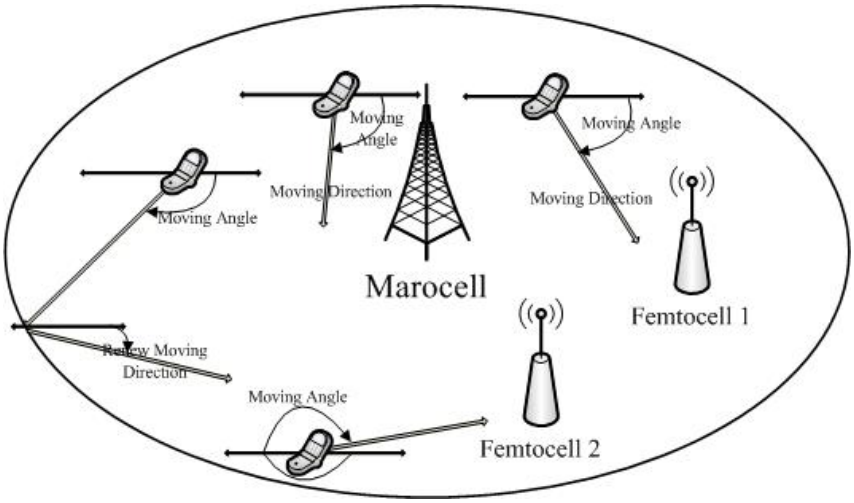

Figure 3.14: The structure of UE randomly mobility pattern scenario

can provide a handover process. In the simulation, the femtocell can collect the predicted information and then count the number of handovers that would happen in a time period. Therefore, the number of handovers can be modelled as the intensity value in order to compare with the intensity value in CPM.

In terms of the UE-based hidden prediction model, it can predict the next cell, UE would handover or not from hidden state (communication and non-communication). Therefore, in the simulation, the femtocell can collect the predicted information and count the number of handovers that would happen in a time period. Therefore, the number of handovers can be modelled as the intensity value in order to compare with the intensity value in CPM.

UE Randomly Mobility Pattern Simulation

In the simulation, it has been configured with 1 macro station; 5 femtocells are randomly located in the macrocell coverage. 20 UEs are firstly randomly located in the macrocell coverage area, then gives the UEs random moving speeds and angles. The UE moving pattern is set as straight and if a UE reaches the threshold of macrocell coverage, it will be given a new angle to ensure it will move around in the macrocell, as shown in Figure 3.14.

In this simulation, if a UE reaches the coverage of a femtocell, it has a probability to handover to the femtocell or remain in the macrocell coverage

Table 3.2: Parameters in UE Randomly Mobility Pattern Simulation

Macro/Femto radius	450/ 20 (m)
UE moving speed (v)	$3 \leq v \leq 14$ (Km/h)
UE moving angles	360 (Degree)
UE moving pattern	Straight
The length of UE camping time in the Femtocell	Negative Exponential Distribution ($3 \leq \lambda \leq 5$)
Femtocell Status (Switched on or off)	Normal distribution

area. When a UE handovers to a femtocell, the time that UE would stay in the femtocell will follow the negative exponential distribution according to queuing theory [65]. Moreover, each femtocell can be turned off and on following a normal distribution. The parameters for the simulation are summarised in Table 3.2.

Every UE records the cells that it has been camped on or handovers to as a ID sequence, such as: 0 represents the macrocell, and 1-5 represent the different femtocells. These IDs are the states used in the Markov chain. Moreover, every femtocell records the number of UE handovers and the number of UE arrivals in a time period. More information about the simulation is provided in Appendix B.1.

According to the discussions in Section 3.3.2, the performance of the prediction model is evaluated via the five metrics: accuracy, precision, F-measure (F1), sensitivity and specificity. Thus, the UE random mobility pattern simulation results are shown in Figures 3.15, 3.16 and 3.17.

According to the results from Figures 3.15, 3.16 and 3.17, the summarised mean results for each metric are provided in Table 3.3.

In Table 3.3, four columns represent the models, CPM, Order-*2* Markov, MRP and HMM prediction, respectively. The rows represent the five different metrics for those prediction models. The elements for each prediction model

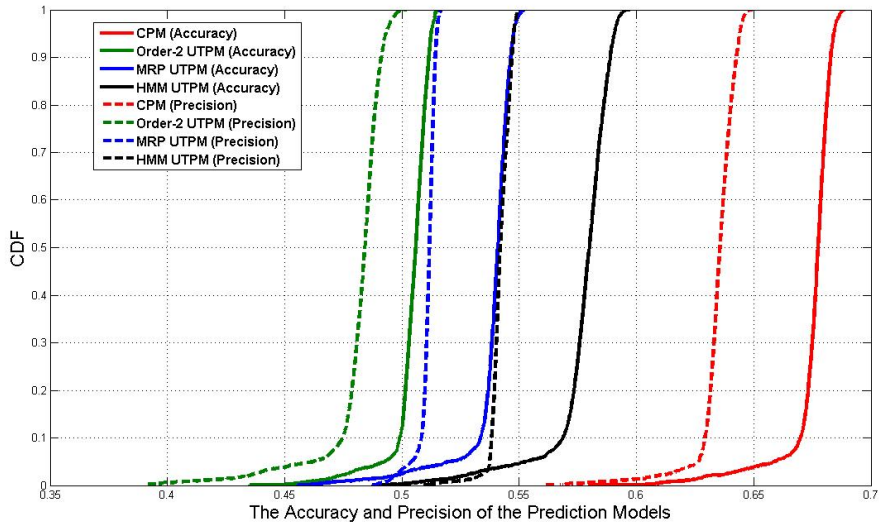

Figure 3.15: The accuracy and precision of the prediction models in cumulative distribution function

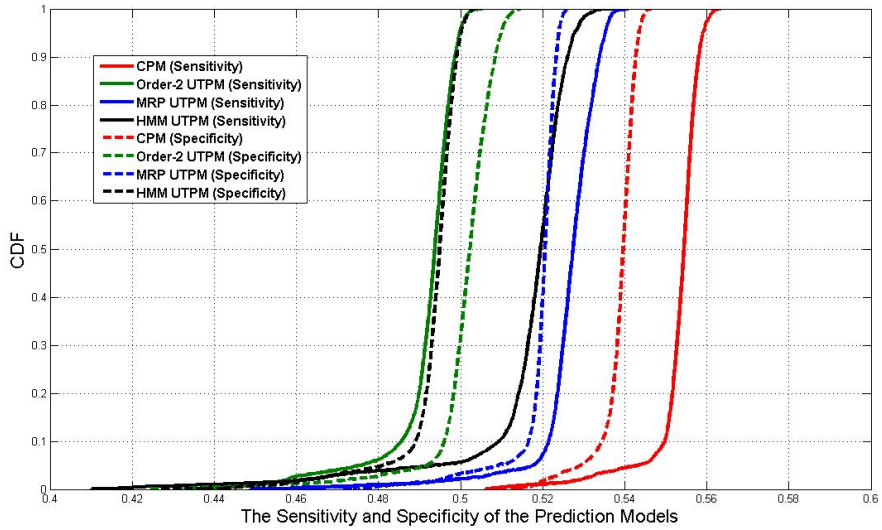

Figure 3.16: The sensitivity and specificity of the prediction models in Cumulative distribution function

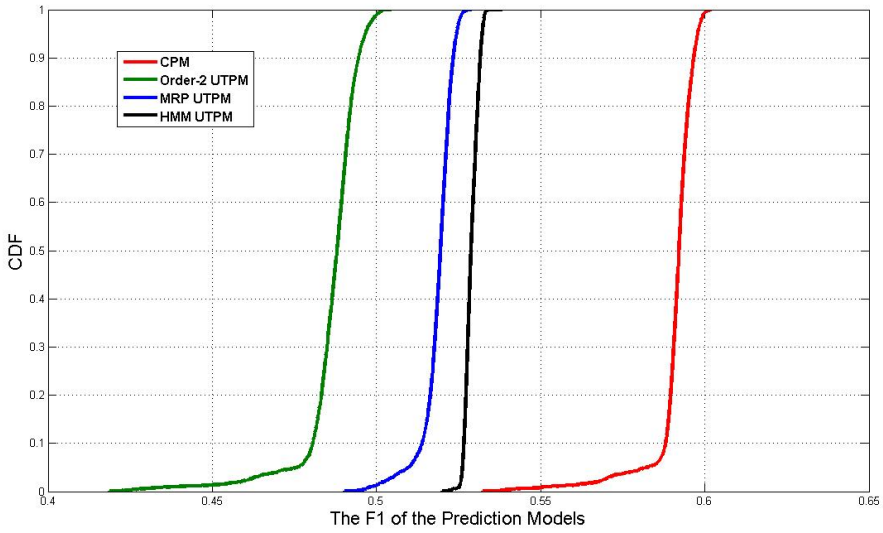

Figure 3.17: The F1 of the prediction models in Cumulative distribution function

Table 3.3: Results List in UE Randomly Mobility Pattern Simulation

Prediction Model	Proposed CPM	Order-2 Markov	MRP	HMM
Accuracy	67.54%	50.45%	53.87%	57.75%
Precision	63.49%	48.17%	51.11%	54.21%
Sensitivity	55.32%	49.19%	52.65%	51.65%
Specificity	53.87%	50.12%	51.93%	49.34%
F1	59.12%	48.67%	51.87%	52.90%

are the mean value of the corresponding metrics which are summarised from the simulation, as shown in Figures 3.15, 3.16 and 3.17.

As mentioned earlier, accuracy is defined as the percentage of predictions that are correct. Precision is defined as the percentage of positive predictions that are correct. Sensitivity, also called recall, is defined as the percentage of reality positive instances that were predicted as positive. Specificity is defined as the percentage of reality negative instances that were predicted as negative. F1 is defined as a harmonic mean of precision and sensitivity

Across the table, in terms of accuracy, precision, sensitivity, specifity and F1, the proposed CPM performed better than the other UTPMs for two reasons: as mentioned earlier, the femtocell plug-and-play feature does not affect the perfomance of CPM; CPM takes into account the UE arrivals and handover issues which occur in the two-tier network scenario. Moreover, the MRP performed better than the order-*2* Markov since it not only considers the state transfers, but also considers the length of time period between two states and the time of the new state appearing. Moreover, HMM performance is better than the other UE-based models, because it considers the UE arrivals and handover issues.

Although the specifity of CPM is the highest value of the predictions, it still has a lower value than its sensitivity. That means CPM is not good at negative prediction, rather than positive prediction. Therefore, the percentage of positive predictions that are correct (precision) has a higher value than specificity. Moreover, F1 is defined as a harmonic mean of precision and sensitivity which described the positive prediction ability of the prediction model. As shown in Table 3.3, CPM provides the highest ability to predict the positive state which is the highest intensity of a femtocell's handovers. Since the network resource distribution should consider the demand of the femtocells, a femtocell with the highest intensity of handovers is desired to obtain more network resource than other femtocells. Therefore, the higher ability of positive prediction is good for network resource distribution. The specific network resource distribution by using CPM is described in Chapter 4.

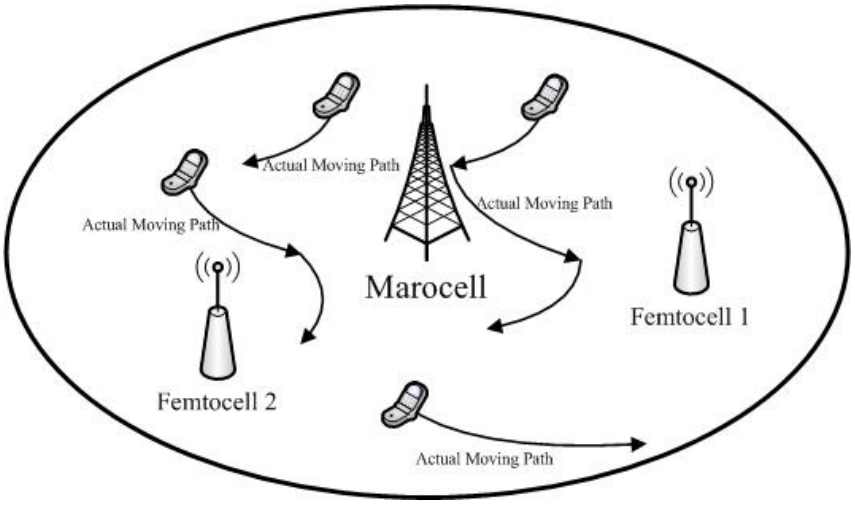

Figure 3.18: The structure of UE Factual mobility pattern scenario

UE Factual Mobility Pattern Simulation

In this section, factual data in this project are used for performance comparison. This data comes from Community Resource for Archiving Wireless Data (CRAWDAD) network trace repository [69], which has recorded the moving history and communication situation of 20 smart phone devices (UEs) over half a month. In the simulation, one macrocell station and five femtocells randomly locate in the macrocell coverage. These 20 UEs' moving patterns are followed by the factual record from CRAWDAD data. The structure of this simulation is shown in Figure 3.18.

In this simulation, if a UE reaches the coverage of a femtocell, it has a probability to handover to the femtocell or still be served by the macrocell. Moreover, each femtocell can be randomly turned off and on.

Similar to the first simulation, every UE will record the cells that it has been camped on or handover to as a ID sequence, such as 0 represents the macrocell, 1-5 represent the different femtocells. Those IDs are the states modelled in the Markov chain. Moreover, every femtocell will record the number of UE handovers and the number of UE arrivals in a time period.

According to the discussions in Section 3.3.3, the performance of the prediction model will be evaluated via the five metrics, accuracy, precision, F-measure, sensitivity and specificity. Therefore, the factual UE mobility pattern

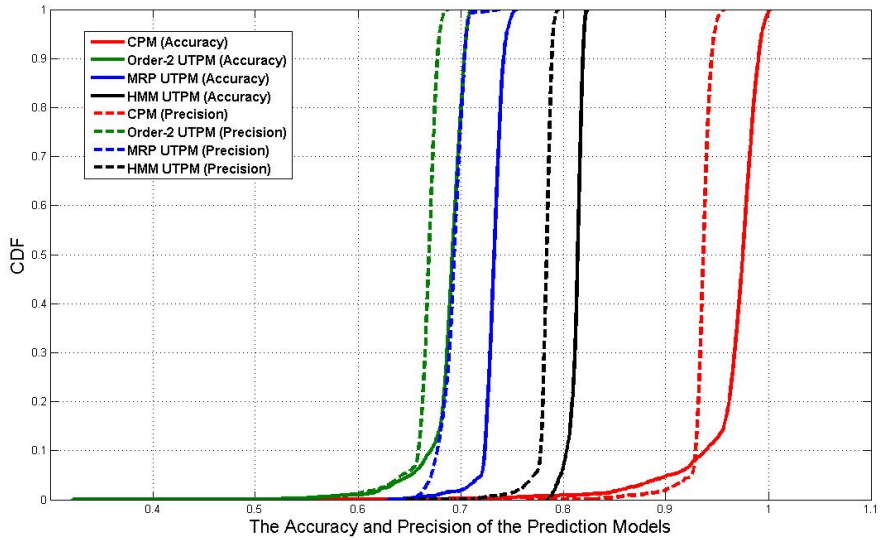

Figure 3.19: The accuracy and precision of the prediction models in cumulative distribution function

Table 3.4: Results List in UE Factual Mobility Pattern Simulation

Prediction Model	Proposed CPM	Order-2 Markov	MRP	HMM
Accuracy	97.78%	68.79%	73.18%	81.27%
Precision	93.54%	66.67%	69.23%	78.27%
Sensitivity	78.34%	59.79%	67.23%	75.61%
Specificity	86.12%	61.30%	66.89%	71.92%
F1	85.27%	63.04%	68.22%	77.25%

simulation results are shown in Figures 3.19 3.20 and 3.21.

According to the results from Figures 3.19, 3.20 and 3.21, the summarised mean results for each metric are provided in 3.4.

In Table 3.4, four columns represent the models, CPM, order-2 Markov, MRP and HMM prediction, respectively. The rows represent the five different metrics for those prediction models. The elements for each prediction model are the mean value of the corresponding metrics which are summarised from the simulation, as shown in 3.19 3.20 and 3.21.

According to Table 3.4, compared with Table 3.3, all the values have increased and the top one almost achieves 97%. This is because in this simulation, more information can be learned from the network and there are fewer

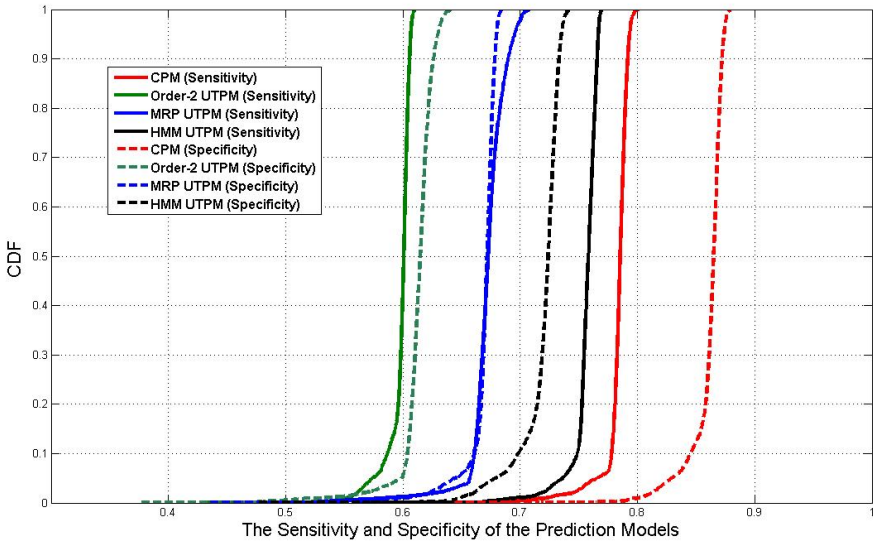

Figure 3.20: The sensitivity and specificity of the prediction models in Cumulative distribution function

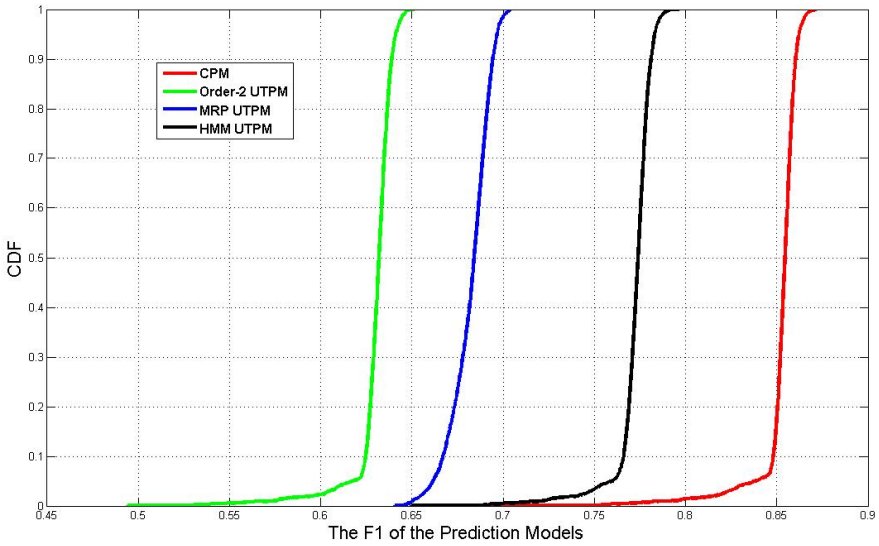

Figure 3.21: The F1 of the prediction models in Cumulative distribution function

random factors in the network due to UE factual mobility patterns. In Table 3.4, the order-*2* Markov still has the worst performance of the prediction models. The MRP performed better than the order-*2* Markov since it considered two factors: the length of states' lasting time and the transition probability of states. The order-*2* Markov chain only considers the state transition probability factor as mentioned in Section 3.1.1.

Moreover, across the table, the simulation results showed that the proposed CPM has better performance compared to the other UE-based prediction models. It overcomes the drawbacks of the UE-based prediction models in the two-tier network scenario. However, the sensitivity of CPM is the lowest value compared to accuracy, precision, specificity and F1. This means that in this simulation, CPM is good at prediction of negative states rather than prediction of positive states. This is because, for the specific data from CRAWDAD, the most frequent state is the negative state (lower intensity of a femtocell's handovers). In the prediction, the state with highest frequency is more predictable than the state with lower frequency [63]. Although, the CPM provides lower ability to predict negative states, the sensitivity of CPM still performs better than the other UTPMs.

3.4 Summary

This chapter presents a cell-based prediction model called CPM, based on the LTE femtocell network in order to predict the intensity of a femtocell's handover. In the tests using both theoretical and actual UE moving patterns, the proposed CPM outperforms the existing UE-based approaches for all five metrics, with higher accuracy, precision, F1, sensitivity and specificity. The proposed approach avoids the drawbacks of UE-based prediction model implemented in the two-tier LTE femtocell scenario, and it provides a better performance than the currently available prediction models. In addition, the intelligence fitted into this approach cooperates with the current trend of selforganisation processes, and therefore, the result of this work may be incorporated

into or potentially contribute to SON technology.

Chapter 4

Dynamic Group PCI Allocation Scheme

In the previous chapter, a Cell-based Prediction Model (CPM) is proposed, in order to achieve a self-organised scheme for network radio resource management. This chapter describes a Physical Cell Identity (PCI) allocation scheme associated with the proposed CPM. In the LTE femtocell network, the PCI is used to identify a cell and also to achieve channel synchronisation between a UE and a newly detected cell [3]. Unfortunately, the number of PCIs is limited to 504 due to the limited byte allocation in the standards [6]. This is insufficient in cases introducing large numbers of femtocells, which brings PCI collision and confusion problems. The PCI cannot be replaced since it is also used to achieve channel synchronisation, 3GPP release 9 [11] introduces CGI together with PCI as a solution. However, there are unavoidable drawbacks. For example, CGI is obtained by reading system information, which is easily done when the UE is in idle mode. When the UE is in connected mode, it uses the autonomous gap to read the system information which takes at least 150 ms. During that period, the UE cannot exchange information with its serving cell, which may lead to service interruptions or call-drops. Due to drawbacks in the CGI implementation, recently, many authors of research works went back to using the PCI and proposed the schemes that have solved PCI collision and confusion in regular network (macrocell) scenarios and PCI

collision in the two-tier network scenario. However, as for the PCI confusion, in the two-tier network scenario, it remains the problem need to be solved. In order to solve the PCI confusion problem and avoid the drawbacks of CGI in the two-tier network scenario and comply with ACPCI function in SON, this chapter introduces a Dynamic Group PCI Allocation Scheme (DGPAS). Via combining with the traffic behaviour learning and prediction model described in Chapter 3, the proposed scheme provides a self-configuration ability to offer an optimal PCI distribution in order to achieve better network performance.

4.1 Cell Identification in the LTE Femtocell

Before introducing the proposed DGPAS, some important background used in the proposed scheme is explained in the following sections.

4.1.1 Inbound Handover

Handovers such as handover or handoff to and from the femtocell is obviously an essential element of the technology. However, this process incurs many problems for the two-tier network scenario presented in detail in this chapter. In 3GPP release 8, three kinds of handovers are defined [3, 70]:

- In the LTE femtocell system, a handover occurs between one femtocell and another nearby femtocell. This process can be called as femtocell-to-femtocell handover.

- In the LTE femtocell system, if a UE handover is from femtocell to macrocell, it is called an outbound handover. For more information about outbound handovers, please check Section 5.1.1.

- In the LTE femtocell system, when a UE handover is from macrocell to femtocell, it is called an inbound handover. In this chapter, the inbound handover will be considered in solving the PCI problems. Inbound handover is one of the most common handover forms in wireless

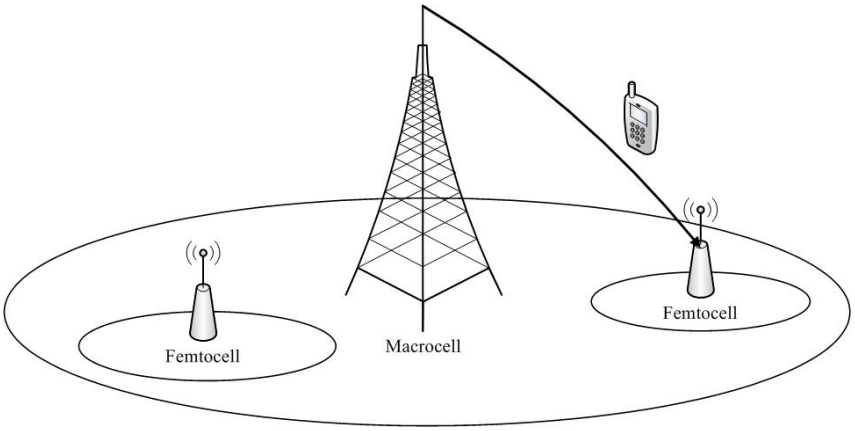

Figure 4.1: Inbound handover in LTE Femtocell

networks with femtocells. But it is also quite challenging due to the efficient communication required between macrocell and femtocell, which exist in different network scenarios. The inbound handover is shown in Figure 4.1.

Figure 4.1: Inbound handover in LTE femtocell

4.1.2 Physical Cell Identity

In the LTE network, Physical Layer Cell Identity (PCI) is used for channel synchronisation and cell identification. According to [3], the PCI consists of two parts:

- Physical layer identity (N_{ID}^{1})
- Physical layer cell identity group (N_{ID}^{2})

The physical layer identity defines the physical layer ID and it has a range from 0 to 2. The physical layer cell identity group defines the group ID that the cell belongs to and it has a range from 0 to 167. PCI is calculated as physical layer ID +3*physical layer cell identity group number which implies 504 possible values as shown in Table 4.1.

Cell synchronisation is an indispensable step if a UE wants to camp on any detected cell [12]. In this case, UE acquires PCI, to achieve synchronisation

Table 4.1: Physical Cell Identity Calculation

Cells	N_{ID}^{1}	N_{ID}^{2}	PCI
Cell A	0	154	462
Cell B	1	134	403
Cell C	2	78	236
...	...	...	...

on both the time slot and frame, in order to enable the UE to read system information blocks from a particular network. In order to communicate with the core network, a UE should first acquire synchronisation with the cell. Then, it can receive and decode system information from the cell. This synchronisation process is defined as cell search. Cell search is performed on the powering-up UE and is repeated whenever the UE intends to move to a new station. Via the public channels, the UE will find that the Primary Synchronization Signal (PSS) blocks in the OFDM symbol at a particular position [3]. Through using PSS, the UE is able to obtain a physical layer ID. Then, a similar process applies to the Secondary Synchronization Signal (SSS). Through using SSS, the UE is able to obtain a physical layer cell identity group number. After the process, by using the physical layer identity and cell identity group number, the UE can obtain the PCI for this cell as mentioned earlier. When the UE obtains the PCI for a given cell, it would also know the location of cell reference signals in the OFDM symbol. Reference signals are used in channel estimation, cell selection / reselection and handover procedures [3]. Cell identification is another function of the PCI developed in the LTE system [3]. PCI is used in cell synchronisation, and it needs to be unique to each cell deployed in the network. Moreover, the PCI can be easily obtained without reading the system information.

Physical Cell Identity Collision

Given both the PCIs are normally allocated without planning and the limitation on the number of PCIs, if the number of cells is higher than the number of PCIs in the network, two problems appear, namely PCI collision and con-

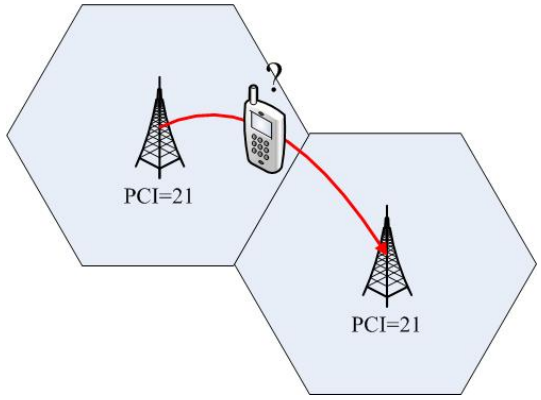

Figure 4.2: PCI collision in regular network(LTE network)

fusion. This section describes the PCI collision in a single-tier and two-tier network scenario. PCI collision happens when a UE starts to handover from a macrocell station (assigned PCI=21) to its neighbour macrocell station (assigned PCI=21). In the handover process in LTE network (regular network), the UE would report the target macrocell PCI to the serving cell to identify the target network, if the serving cell has the same PCI ID with the target cell, then the serving cell cannot distinguish which cell the UE would handover to, and this results in handover failure. The PCI collision in a regular network is shown in Figure 4.2. It is worth noting that, Figure 4.2 is only used to illustrate the PCI collision. In reality, there are many ways to avoid this happening in a single-tier network.

For the two-tier network, the PCI collision applies in a similar way as in the case of the macrocell, the difference is that it happens between the femtocells. If there are two neighbouring femtocells sharing the same PCI ID, the PCI collision would occur when the UE is handed over from the femtocell to another femtocell. According to the descriptions in Chapter 2, some researchers have proposed distribution schemes to solve PCI collision and ensure that there is no repeated PCI assignment between neighbouring cells. Moreover, as mentioned earlier, the reason PCI collision occurs is because of the scarcity of PCIs means they are not as well distributed as the large number of femtocells and the many various relations of the neighbouring femtocells. This case can be treated as the problem of a 'limited resource' assigned with a high 'reuse-ratio'. Therefore,

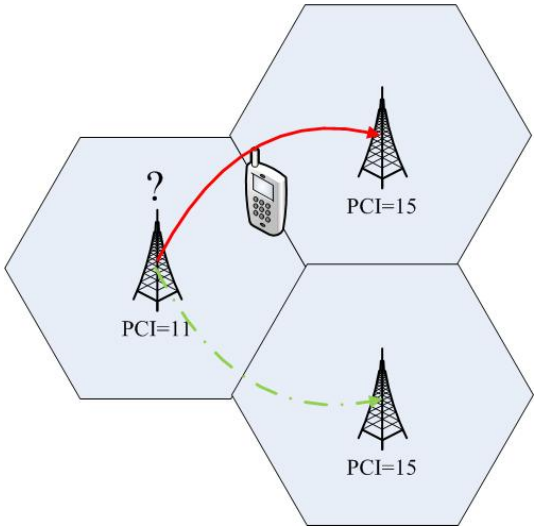

Figure 4.3: PCI confusion in regular network (LTE network)

the frequency of occurrence of PCI collision really depends on the number of and the location of the femtocells deployed in the network.

Physical Cell Identity Confusion

Similar to PCI collision, PCI confusion happens because PCIs are normally allocated without planning. PCI confusion includes two cases: PCI confusion in a single-tier and two-tier network. In terms of PCI confusion in a single-tier network, it happens when a UE starts to handover from a macrocell station (PCI=11) to its neighbouring macrocell (PCI=15) station. In the handover process of the LTE network (regular network), the UE would report the target macrocell PCI to the serving cell to identify the target network, if there is another neighbouring station with the same PCI ID as the target macrocell, then the serving cell cannot distinguish which cell the UE should handover to and this may result in handover failure. PCI confusion in a regular network (single-tier network) is shown in Figure 4.3.

Single-tier PCI confusion can be resolved via optimal PCI allocation. As mentioned in Chapter 2, many researchers have proposed PCI distribution schemes to solve this PCI confusion which ensures that there is no repeated PCI assignment in a cell's neighbouring cells. Moreover, the reason for appearance of PCI confusion is similar to that of PCI collision. Therefore, the

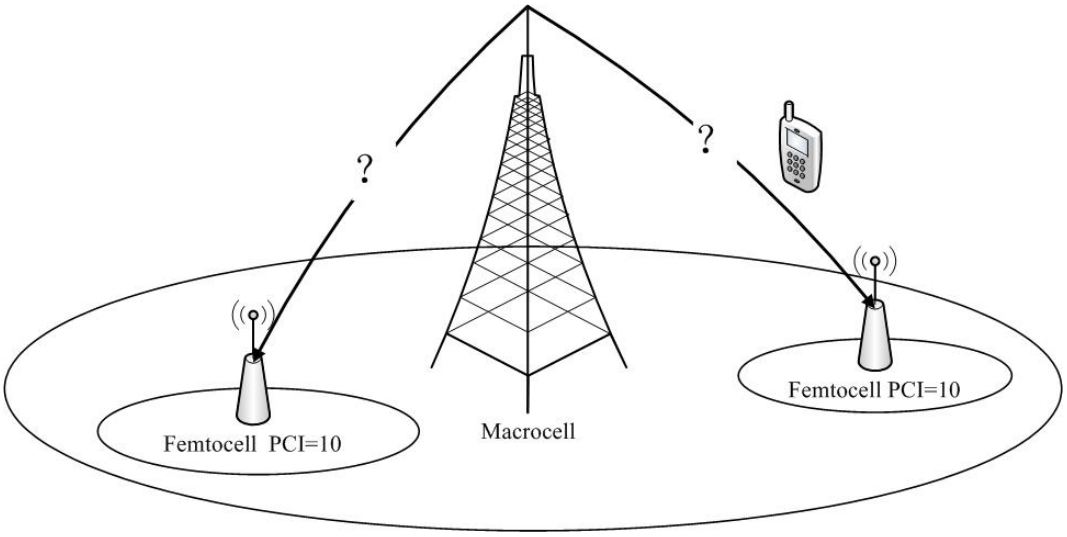

Figure 4.4: Two-tier PCI confusion in inbound handover

frequency of occurrence of PCI single-tier confusion really depends on the number of and the location of the femtocells deployed in the network. In terms of PCI confusion in two-tier networks, it happens in the inbound handover process, and becomes a major problem in the LTE femtocell scenario. This PCI confusion happens during a UE handover from the macrocell to a femtocell when there is another femtocell that has the same PCI as the target femtocell, the macrocell cannot distinguish which cell the UE should handover to and this may lead to handover failure. However, for the inbound handover in the two-tier network, this confusion cannot be resolved as it is in the single-tier network, since the large number of small femtocells are served in the large coverage of macrocell; it is hard to uniquely identify each femtocell. PCI confusion in the inbound handover is shown in Figure 4.4.

The inbound handover is the most common action in an LTE network and the PCI cannot be replaced due to the system needing it to achieve cell synchronization. Reflecting this, in order to solve this problem, in release 9 [3, 12], is proposed a new identity called Cell Global Identity (CGI) to cooperate with the PCI to achieve the inbound handover. The CGI is described in the next section.

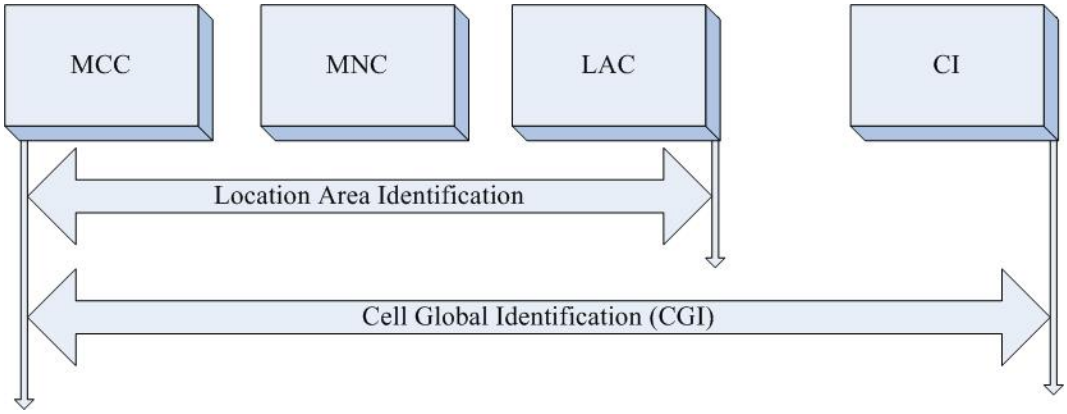

Figure 4.5: The structure of cell global identification

4.1.3 Cell Global Identity

According to 3GPP release 9 [3, 12], Cell Global Identity (CGI) had been introduced. As the name implies, it is a specific ID which can uniquely identify a single cell throughout the whole world. CGI consists of multiple components such a Mobile Country Code (MCC), Mobile Network Code (MNC), Local Area Code (LAC) and Cell Identity (CI) as shown in Figure 4.5.

According to [71], from the MCC, you can figure out in which country (specific country code) the cell is located. From the MNC, you can find out which network operator it belongs to. From LAC, you can find out which location area it belongs to. From CI, you can identify the exact individual cell. Unlike the PCI, a CGI is not a reference signal and cannot be directly read from a public channel. CGI can only be read by the UE via the system information from its corresponding cell. As mentioned in [3], during the inbound handover process, when the UE starts the handover process and PCI confusion occurs, the macrocell would ask the UE to report the CGI. Once the UE receives the CGI request from the macrocell, the UE will read the target cell system information, and then report the CGI to the macrocell. Via this process, the macrocell could obtain the CGI from the target cell and use this CGI instead of PCI to uniquely identify the target cell. The process is shown in Figure 4.6.

However, due to the fact that the PCI can be directly read from a public channel and CGI needs to be read via system information, drawbacks of using

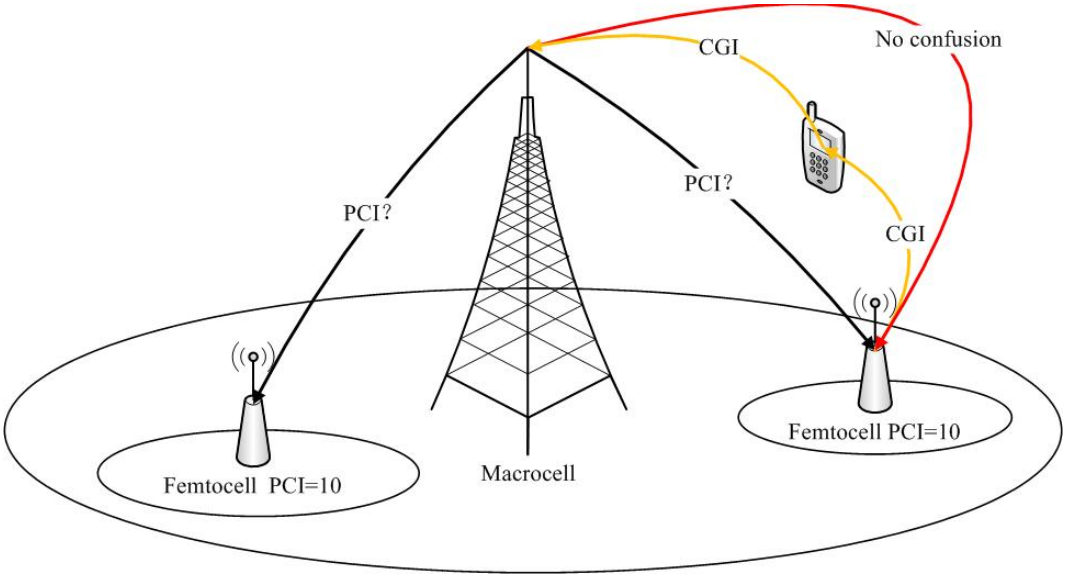

Figure 4.6: CGI in inbound handover

CGI are described in the next section.

Cell Global Identity Reading in UE Idle Mode

The process of a UE read or report CGI can be summarised as a special type of measurement report [25]. Normally measurement control/reports are for detecting the signal strength of the target cell, but a CGI report is not used for measuring signal strength. It is to detect the CGI which uniquely identifies an individual cell throughout the whole world as mentioned an earlier section. For the PCI or signal strength measurement report, the UE has only to switch its tuner to the target cell and measure the signal strength. It does not have to decode any system information of the target cell and therefore, takes a very short time to measure them. But it is a different story in the case of CGI when the UE has to decode the system information of the target cell. It takes up to 160ms for LTE [11]. According to [11], the decoding system is not a big issue if a UE is in idle mode. This is because the UE can read the system information during the Discontinuous Reception (DRX) cycle which implements when the UE is in idle mode. DRX cycle is used in mobile communication by many researchers in power saving [11]. If a UE is in idle mode, the DRX will be

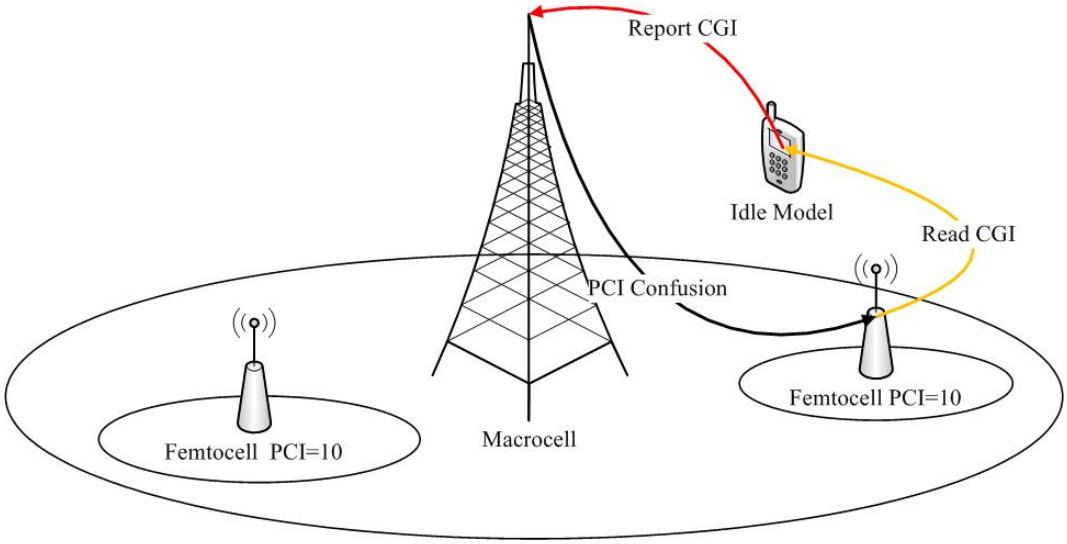

Figure 4.7: Idle UE and CGI reading in inbound handover

activated. In a DRX cycle, it gives the UE enough time to measure the system information of the target cell. The process of a UE read and report CGI in idle mode is shown in Figure 4.7.

As shown in Figure 4.7, if a UE in idle mode wants to do cell reselection (Handover in idle mode is called cell reselection) from macrocell to femtocell, the UE has enough time to read the system information from the target femtocell and cell reselection is more easily achieved for inbound handover in the LTE femtocell scenario. However, if a UE is in connected mode and wants to achieve an inbound handover, a problem would occur, as will be described in the next section.

Cell Global Identity Reading in UE Connected Mode

As mentioned earlier, the 3GPP proposed a new identity as CGI to achieve the cell identity. However, CGI information can only be obtained from the system information and the process will take longer during the inbound handover. When the UE is in connected mode (activity mode), the UE has the ability to transmit data from the network. This action has higher priority than the DRX process [11]. Therefore, the DRX cycle cannot initialise and the UE cannot read the CGI from the system information via DRX and this leads to inbound

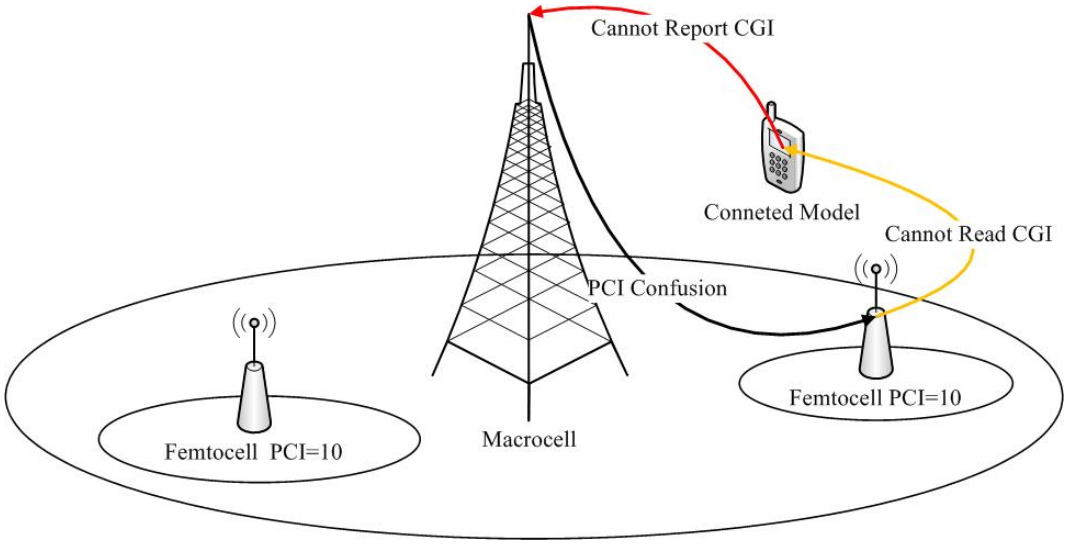

Figure 4.8: Activity UE and CGI reading in inbound handover

handover failure. The process is shown in Figure 4.8.

Due to this problem, in release 10 [11] is proposed an autonomous gap instead of a DRX cycle which is activated during inbound handover to give the UE sufficient time to read the CGI. However, the autonomous gap techniques also bring new challenges which will be described in detail in the next section.

4.1.4 Cell Global Identity vs. Physical Cell Identity

Compared to PCI, using CGI has many serious drawbacks. Firstly, PCI is a reference signal sequence on the signal level which means that the UE reads the identity of the target cell in a very short time (up to 20 ms) in LTE. Whereas, CGI is not a reference signal sequence, and it needs to be obtained by reading the system information which requires a longer measurement time gap, up to 160 ms in LTE. In release 10, when a UE is in connected mode, intended for an inbound handover, the UE then activates the autonomous gap to read the CGI from the system information. However, the autonomous gap requires the UE to temporarily enter into a similar DRX cycle gap to read the CGI. In the autonomous gap, the UE still cannot receive or transmit any data from or to the serving cell [11]. Therefore, it probably results in unnecessary service interruption and consequently results in the call being dropped in a situation

where the signal strength fades rapidly. This becomes more critical in a busy and dense network scenario. This is because that long CGI reading time would lead to the delay of the CGI measurement report which may make the UE miss the optimal handover time. Secondly, the autonomous gap approach is a new approach and currently most UEs do not support this technology. Lastly, a long measurement time is required to obtain the system information which causes concerns regarding UE battery life. The UE battery life is important for battery-hungry multimedia applications. In summary, it is desirable to use PCI rather than CGI to identify cells. However, PCI has a confusion problem, in order to mitigate CGI drawbacks and also to avoid PCI confusion, this chapter proposes an efficient dynamic PCI group scheme.

4.2 The Proposed Dynamic PCI Group Allocation

Firstly, according to the above descriptions, both PCI and CGI drawbacks are caused by PCI reuse in the LTE femtocell scenario. In fact, some femtocells may have a higher number of inbound handovers than others during the same time period and those femtocells are more deserving of having a unique PCI than other femtocells. If those femtocells have a unique PCI, the overall system will have a lower chance to implement the autonomous gap and consequently result in a lower chance of handover failure. In this section, a centralised dynamic group PCI allocation scheme is proposed, the basic framework of centralised Automatic Physical Cell Identity Assignment (ACPCI) in the proposed scheme are described below.

4.2.1 Framework of Centralised Automated Physical Cell Identity Allocation

As mentioned in Chapter 2, the SON functionality architectures are summarised as centralised, distributed and hybrid. In automatic PCI planning,

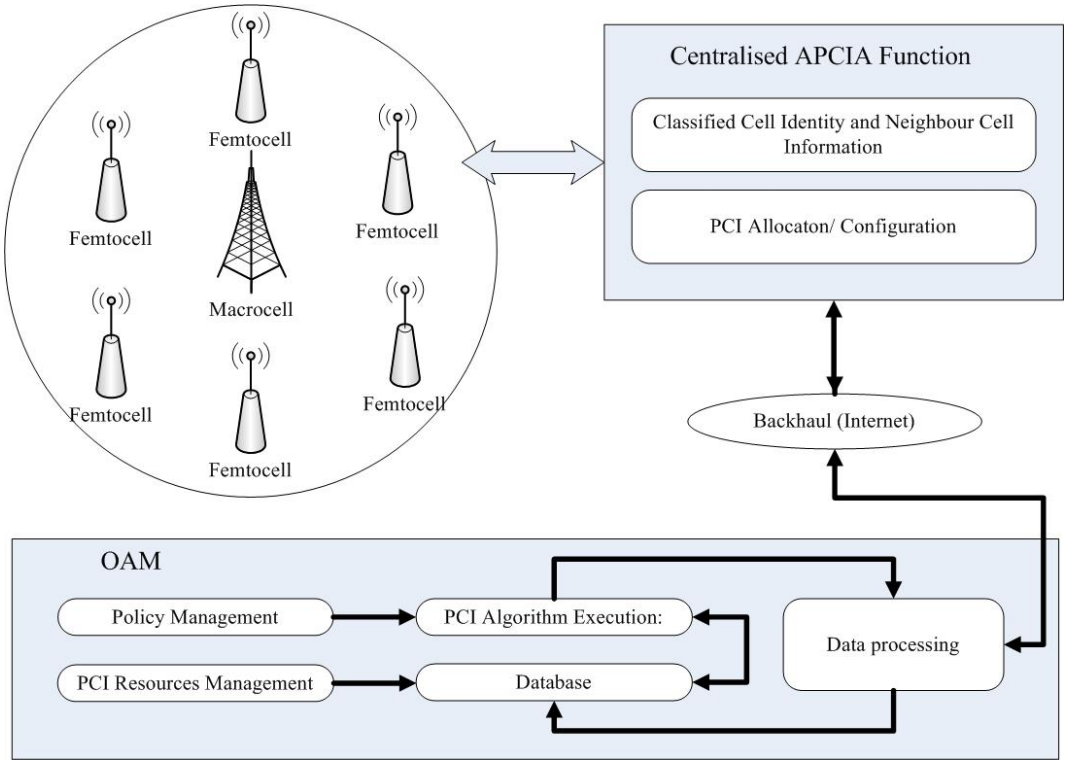

Figure 4.9: Flowchart of dynamic PCI release process

both the centralised and distributed approaches (currently, there is no hybrid approach in PCI planning) have been proposed to achieve PCI assignment via Operation Administration and Maintenance (OAM) system [16]. The OAM system is a tool which is implemented by standards [72] to achieve the operating, administering, managing and maintaining in the SON. Considering the centralised SON structure, ACPCI function and the OAM reside at the network management system level, and the specific SON approach is executed in the OAM system [16]. Moreover, in LTE, MME is the one of network management system blocks and used to achieve the wireless cell management and communication [25]. Therefore, for the centralised ACPCI, the OAM system should reside in MME and the tunnels between wireless cells and the OAM are achieved via MME [73]. The general procedure of centralised ACPCI is shown in Figure 4.9.

- **Centralised SON Function:** the main work of the centralised ACPCI function is to select the network information from all the femtocells in the

two-tier network such as cell identity, cell radius, network traffic situation and neighbourhood information etc. It then classifies the information and sends the necessary information which is required by the specific self-organisation approach to the OAM. Moreover, the necessary information is sent via Backhaul (MME) to the OAM.

- **Data processing:** firstly, this process is to arrange the data which is obtained from the ACPCI function to find the corresponding position in database, in order to transmit the data to database; secondly, after the PCI allocating decision is made, this process indicates the cells to update (allocate); its PCI ID is based on the database record and then sends the decision back to the ACPCI function.

- **Policy Management:** this functional block indicates the policy of the specific self-organisation approach for automatic PCI allocation. Operators can choose different self-organisation approaches and install in this block. Therefore, if the current approach cannot achieve the requirement QoS, it can be easily created, edited and modified by operators in order to improve network performance. Reflecting this, the main part of the proposed PCI allocation scheme in this chapter is located in this functional block.

- **PCI Algorithm Execution:** this functional block used to manage the database depends on the policy from the policy management block. The different approaches lead to different database operations. Database: this functional block indicates the related information obtained from the centralised ACPCI function. The temporary and permanent variables are obtained from the self-organisation approach.

- **PCI Resources Management:** this functional block is used to store the PCI usage status, PCI and CGI map, PCI reuse frequency and the PCI ranges for macrocell and femtocells respectively. Moreover, MME have two functional blocks such as Home Subscriber Server (HSS) and

Neighbour Cell List (NCL). HSS functions include femtocell management, authentication, authorisation and the mapping list for PCI and CGI. NCL stores all neighbouring information for each femtocell. Since the OAM resides at MME, it could easily retrieve all the PCI and CGI information in HSS and NCL and store in its PCI Resources Management.

Overall, in the centralised ACPCI, the OAM system is supposed to have complete knowledge and control over PCIs. It also provides an easy way for the operator to operate the PCI planning approach. The proposed scheme in this chapter will follow the centralised SON structure and comply with ACPCI function.

4.2.2 Busy Femtocells Predicted by Cell-based Prediction Model

In the LTE femtocell scenario, inbound handover is the main cause of two-tier PCI confusion, thus, a higher number of inbound handover events makes things worse. For the sake of the description in this chapter, a concept called Busy femtocell (BFemtocell) is introduced. In Chapter 3, the cell-based Prediction Model (CPM) is proposed based on the intensity of a femtocell's average number of inbound handovers. Therefore, this section defines three different levels of handover intensity. In Chapter 3, the cell-based Prediction Model (CPM) proposed is based on these handover intensities for femtocells in the macrocell coverage area, namely, O_{Busy}, $O_{Moderate}$ and O_{Idle}, where O is the observation state and Obusy represents the BFemtoell state. Similarly, it applies to Omoderate and Oidle, they represent the normal handover states for femtocells. The structure of three intensity levels of a femtocell's handovers in a CPM model is shown in Figure 4.10.

Figure 4.10 shows that the proposed observation states are not related to each other, but they are related to the hidden states. In terms of hidden states in a CPM, they are denoted as S_{Higher}, S_{Mid} and S_{Lower} which each

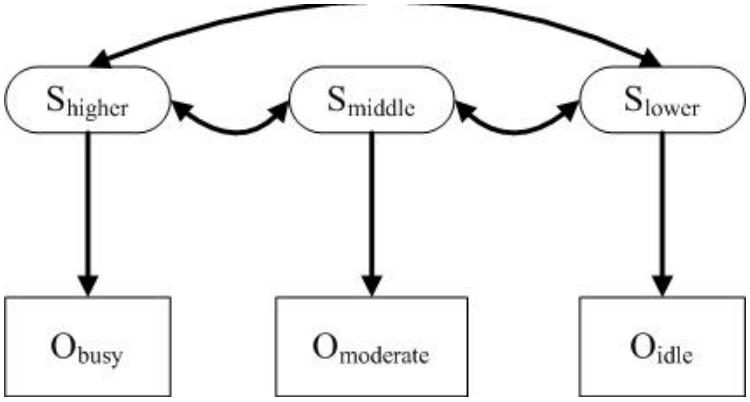

Figure 4.10: The structure of three intensity levels of a femtocells handovers in a CPM model

represent different average numbers of UE arrivals. Depending on the hidden Markov model, the state in the hidden part are modelled as Markov chain, thus, although there is no relation between observation states, the hidden part has created a bridge to connect the observation states.

4.2.3 Dynamic PCI Groups

In the LTE femtocell system, PCIs have already been categorised as two groups: macrocell PCI and femtocell PCI groups [3, 70]. Therefore, through different PCI ranges, the UE can easily determine the type of wireless cell station, whether it is macrocell or femtocell. Moreover, the LTE femtocell defines the Closed Subscriber Group (CSG) as a set of subscribers (registered UEs) which are only allowed to hand over to specific femtocells (CSG femocells). On the other hand, non-CSG femtocells represent the femtocells which allow all UEs to hand over and obtain its service. In order to easily distinguish the CSG and non-CSG femtocells, the standards define a certain range of PCIs to be reserved for CSG femtocells [3, 70]. This process is set in the System Information Block Type 9 (SIB 9), and there are two information elements in SIB 9, csg-PhysCellIdRange.start and csg-PhysCellIdRange.range. System information is the information about the system and the serving cell. The UE could determine the setting of a femtocell via measuring the system information. Assuming csg-PhysCellIdRange.start = n, csg-PhysCellIdRange.range =

Table 4.2: A Certain Range of PCIs for CSG and non-CSG Femtocell

Non-CSG Femtocell	CSG Femtocell	Macrocell
1, 2, 3, ...	n. n+1, n+2, ..., n+k	..., 502, 503, 504

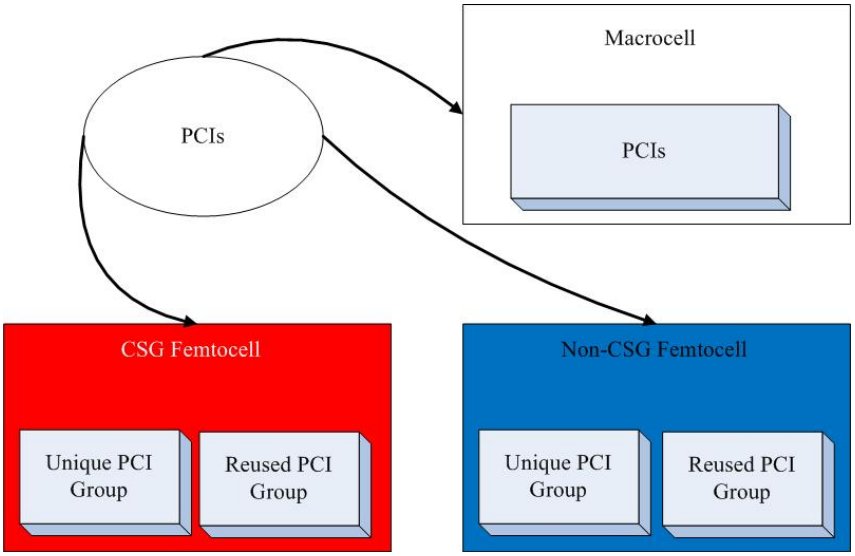

Figure 4.11: The structure of proposed dynamic groups

k. The PCI is distributed between CSG and non-CSG cells as shown in Table 4.2.

Table 4.2 shows that according to the proposed information elements, femtocell PCIs can be well arranged into two groups which easily indicate different femtocell access types. Moreover, the two-tier PCI confusion happens when reusing PCIs deployed under the large range of macrocell service. When an approach guarantees the unique PCIs to be allocated to the Bfemtocells, there is no confusion in the inbound handover. Considering this obvious reason, the PCI resource should be well arranged. Therefore, the femtocell CSG and non-CSG PCI groups in standards need to be further categorised into two sub-groups, such as unique PCI and reused PCI groups as shown in Figure 4.11.

Unique and reused PCI groups are set in each CSG-group/non-CSG group. As the name implies, the PCIs in unique PCI groups are used to identify the CSG or non-CSG mode BFemtocell. The PCIs in reused PCI groups are used to identify the normal CSG or non-CSG mode femtocells. Moreover, the reused

PCI groups are also used to guarantee that the single-tier PCI confusion and PCI collision would not occur in the network, and more information about this can be found in the next section. Since femtocells are deployed randomly in the network, the proposed unique and reused PCI groups would not have a certain PCI range. This is able to be achieved via setting up four information elements in the system information due to system information being flexible and able to contain additional information elements [24]. Similarly, this applies to the two information elements set in SIB 9 as mentioned earlier. Those elements are:

- unique-csg-PhysCellIdRange.start and resued-csg-PhysCellIdRange.range for CSG femtocells
- unique-PhysCellIdRange.start and resued-PhysCellIdRange.range for non-CSG femtocells

Moreover, the dynamic features of the PCI groups are described below: The number of PCIs in the unique PCI group would decrease due to unique PCIs being used to assign the BFemtocells as mentioned in Section 4.2.2. Therefore, after a unique PCI is assigned to the BFemtocell, this PCI would add to the reused PCI group. As a result, the number of PCIs in the unique PCI group would become 0 which would make the proposed approach unachievable. In order to solve this problem, a PCI release function has been proposed in the next section. This function can collect the redundant PCI usage in the system. Then it releases the unique PCIs, and fills the unique PCI group. Therefore, via distribution or release function, the PCIs are dynamically located in either the unique or reused PCI group which means that the PCI groups are dynamic.

4.2.4 PCI Release Functions

As mentioned earlier, unique PCIs are one of the key factors for PCI confusion mitigation, therefore, the proposed scheme provides an enhanced function called PCI release to seek the unique PCIs in the network and supplement them into the unique PCI groups. The PCI release function includes two methods:

one is static PCI release; the other one is dynamic PCI release. Moreover, due to CSG and non-CSG femtocells having the same structure of dynamic PCI groups as mentioned in the previous section, the PCI release functions in those femtocells are also the same. In terms of static PCI release, it is able to obtain the PCIs from those femtocells which have been switched off. Then, those released PCIs would be sent to the OAM, and the OAM would filter out the unique PCIs. Moreover, since *Ping* transmits in very small packages only up to 220 bits for ICMP (Internet Control Message Protocol), it will not cause any large signal overload. As a result, using ping to check the status of femtocells is suggested. Therefore, the femtocells in the network can be clearly separated into two lists: Femtocellon and Femtocelloff. The process of static PCI release is described in Figure 4.12:

In terms of dynamic PCI release, it is able to obtain the unique PCIs from the general network PCI resource update. This updating means that in a specific time interval, the network would check all the relations of femtocells and PCI usage situations. It then reallocates the PCIs to those non-BFemtocells with a minimised number of reused PCIs. Proposed dynamic PCI release can be modelled as Graph-Colouring mathematics as shown in Figure 4.13.

Figure 4.13 shows that different PCIs are modelled as different colours and the relations between femtocells are modelled as the connections of different nodes in the Graphs Colouring mathematic. The goal of Graph-Colouring mathematic is to use the minimal number of colours to colour the nodes and make sure that two nodes are connected with an edge are not assigned the same colour. This process can be applied for the problem of PCI collision and single-tier confusion. Moreover, in order to achieve confusion-free PCIs in the single-tier network, the rules of assigning colours would be changed to ensure the different colours not only appear between neighbouring nodes, but also the neighbour's neighbour of those nodes. The strategy of this process is to use the PCI set in the target femtocell's neighbour's neighbour's neighbour to assign the target femtocell, this structure is shown in Figure 4.14.

As shown in Figure 4.14, the nNeighbour represents the target femto-

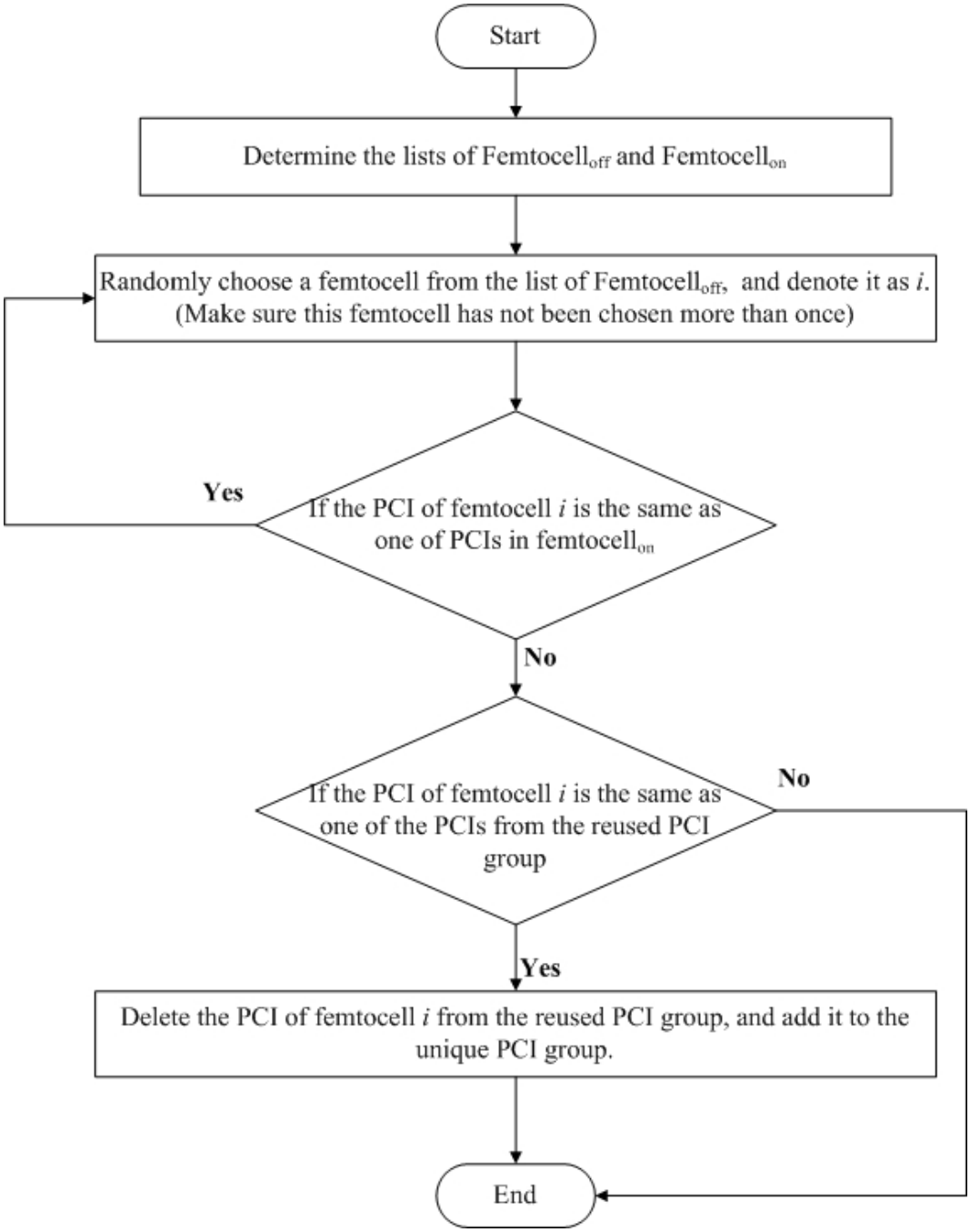

Figure 4.12: Flowchart of static PCI release

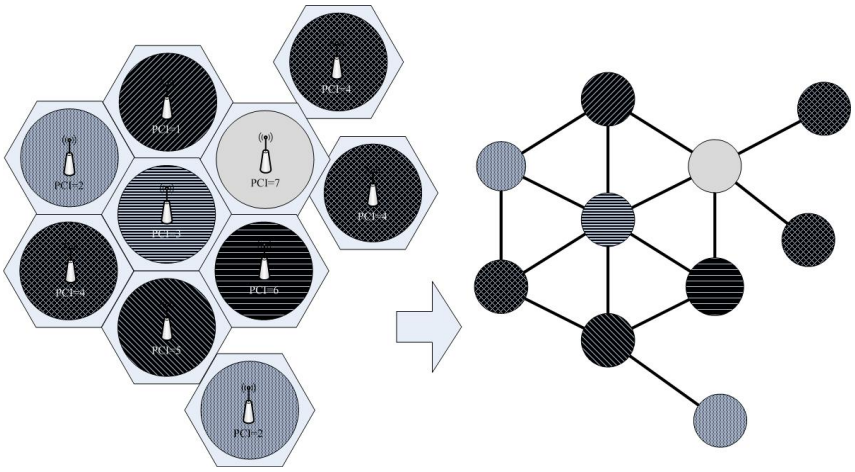

Figure 4.13: Dynamic PCI release in Graphs Colouring

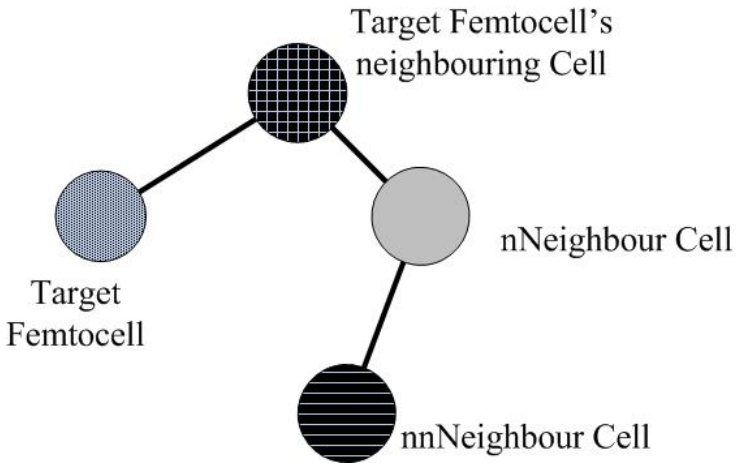

Figure 4.14: Femtocell neighbouring structure

cell's neighbour's neighbour femtocell and nnNeighbour represents the target nNeighbour's neighbour femtocell. The process of dynamic PCI release function is described in Figure 4.15.

However, there is a problem. The dynamic PCI release requires that all femtocells to update their PCIs at the same time, this would cause extreme complexity in the implementation, especially when the network is quite busy. As a result, this is different from a static function that is able to be implemented frequently. This function can only be implemented at a chosen time, for instance, at midnight. Overall, PCI release and PCI assignment provide the functions of unique PCI supplementation and consumption. Those functions ensure the dynamic features of the proposed unique and reused PCI groups.

4.2.5 Dynamic Group PCI Allocation Scheme

As mentioned earlier, the proposed strategy is to use the PCIs in the unique group (PCI_{unique}) to assign the femtocells which have a higher average of inbound handovers (BFemtocells) and PCIs in the reused group (PCI_{reused}) to assign the other femtocells via dynamic unique and reused PCI groups.

There are six processing stages in the proposed DGPAS, described below:

1. PCI group operation. According to the PCI usage in PCI resources management, to determine the unique PCI and reused PCI and create PCI groups in PCI resources management as mentioned in section 4.2.3 (PCI algorithm execution).

2. Threshold for each state determination (belongs to PCI algorithm execution and Centralised SON Function in the proposed centralised framework). In this chapter, the proposed scheme implements the average threshold for each state and the detail of observation states in the proposed scheme is calculated as below:

   After receiving the handover information from the femtocells, If Nk denotes the average number of successful inbound handovers for the kth

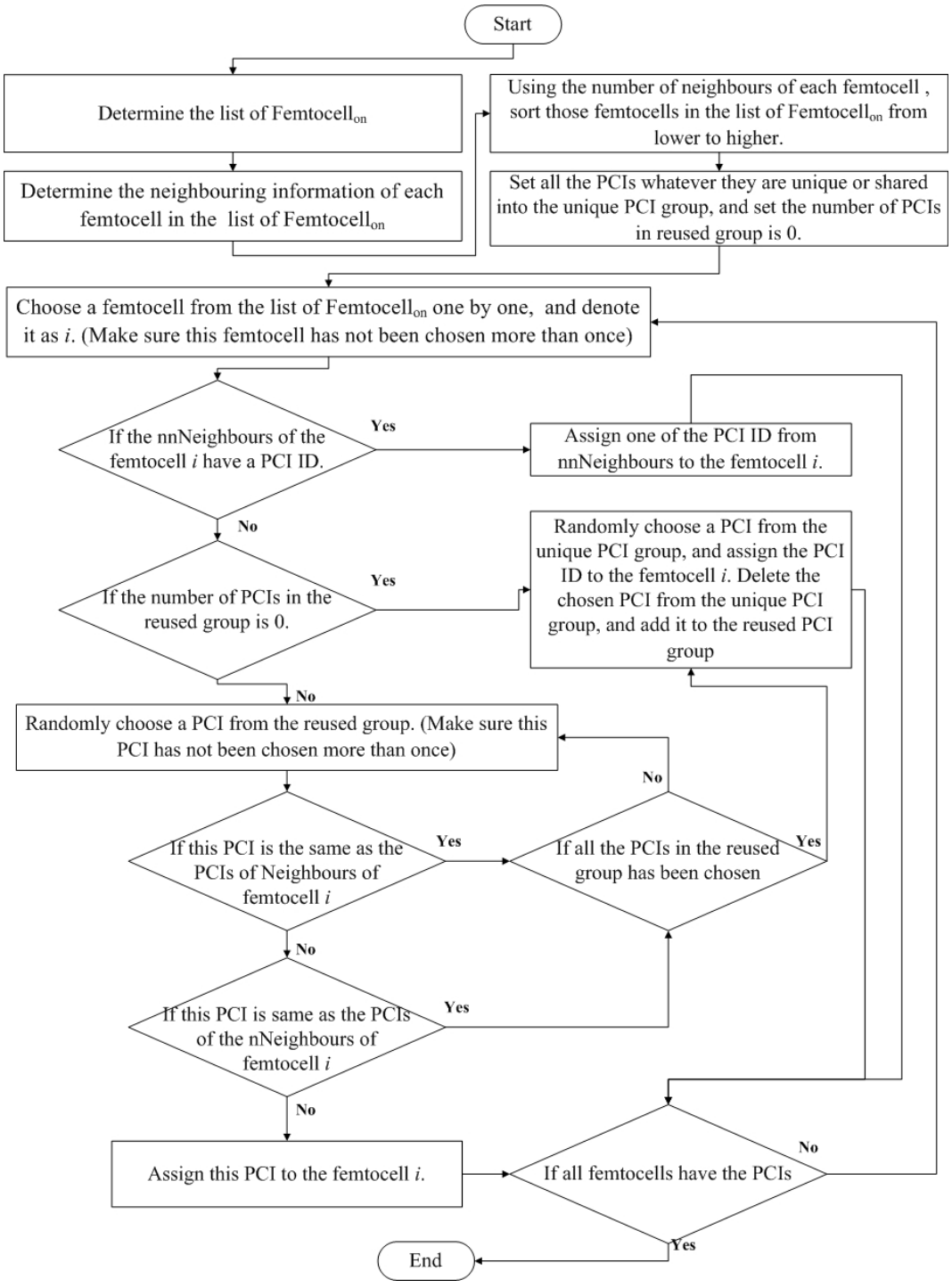

Figure 4.15: Flowchart of dynamic PCI release process

femtocell and the function $f_{Max}(N_k)$ denotes the maximum value of N_k, the threshold of each observation state is calculated with Equation (4.1)

$$Threshold = (|\frac{f_{Max}(N_k)}{N_s}| + 1) * N_{s\_th} \tag{4.1}$$

where N_s is the number of states and N_{s_th} represents the threshold indicator, for example, for the first state, the value of N_{s_th} are 0 and 1, for the second state, the value of N_{s_th} are 1 and 2. Based on the approach described in Section 4.2.2, three observation states, $O_{Idle}, O_{Moderate}$ and O_{Busy}, are proposed. For the observation Idle state, where N_s=3, N_{s_th} ranges from 0 to 1; so substituting them in (4.1), the Idle state can be written as Equation (4.2).

$$0 \leq O_{Idle} < |\frac{f_{Max}(N_k)}{3}| + 1 \tag{4.2}$$

Similar calculations apply to Moderate and Busy states in Equation (4.3) and (4.4):

$$|\frac{f_{Max}(N_k)}{3}| + 1 \leq O_{Moderate} < (|\frac{f_{Max}(N_k)}{3}| + 1) * 2 \tag{4.3}$$

$$(|\frac{f_{Max}(N_k)}{3}| + 1) * 2 \leq O_{Busy} \tag{4.4}$$

3. PCI group operation (belongs to PCI Resource Management, Data processing and Database in the proposed centralised framework). According to the PCI usage in PCI resource management, determine the unique PCI and reused PCI and create PCI groups in PCI resource management as

mentioned in Section 4.2.1.

4. BFemtocell Determination (belongs to PCI algorithm execution and Centralised SON Function in the proposed centralised framework). After the threshold of states has been determined, MME depends on this information to implement the CPM proposed in Chapter 3. In order to predict the next state (the Intensity of a femtocell's average successful inbound handover) for each femtocell. Once the predictions have finished, the femtocells which have the Busy predicted state are defined as Bfemtocell.

5. Centralised PCI distribution in OAM (belongs to PCI algorithm execution in the proposed centralised framework). As mentioned earlier, for the centralised ACPCI, the OAM system should reside in the MME and the tunnels between wireless cells and the OAM are achieved via the MME. Therefore, after BFemtocell determination, MME transfers all the prediction information to the OAM. The PCI distribution process in the OAM can be described thus:

   In the PCI distribution, $P_{Busy}(k)$ denotes the probability of the kth femtocell being in the Busy state, and similarly this can be applied to $P_{Moderate}(k)$ and $P_{Idle}(k)$. $P^k_{Busy,t+1}$ denotes probability of the kth femtocell in Busy state at *t+1* time period, similarly for $P^k_{Moderate,t+1}$ and $P^k_{Idle,t+1}$. Then $P_{Busy}(k)$, $P_{Moderate}(k)$ and $P_{Idle}(k)$ can be calculated in Equations (4.5), (4.6) and (4.7) respectively:

$$P_{Busy}(k) = P^k_{Busy,t+1}(O_{t+1} = O_1 | S_{t+1} = [S_1, S_2, S_3]) \tag{4.5}$$

$$P_{Moderate}(k) = P^k_{Moderate,t+1}(O_{t+1} = O_2 | S_{t+1} = [S_1, S_2, S_3]) \tag{4.6}$$

$$P_{Idle}(k) = P^{k}_{Idle,t+1}(O_{t+1} = O_3 | S_{t+1} = [S_1, S_2, S_3]) \tag{4.7}$$

According to Equations (4.5), (4.6) and (4.7), the three Equations (4.8), (4.9) and (4.10) can be defined thus:

$$Busy(x) = sort(P_{busy}(k) \geq [P_{moderate}(k), P_{Idle}(k)]) \tag{4.8}$$

$$Moderate(y) = sort(P_{Moderate}(k) \geq [P_{Busy}(k), P_{Idle}(k)]) \tag{4.9}$$

$$Idle(z) = sort(P_{Idle}(k) \geq [P_{Busy}(k), P_{Moderate}(k)]) \tag{4.10}$$

Let $Busy(x)$ denotes the sequences of the xth BFemtocells in ascending order and similar denotation applies to $Moderate(y)$ and $Idle(z)$. Since the BFemtocells are the likely sources of the so-called PCI confusion during the inbound handover, the unique PCIs are first be assigned to the xth BFemtocell. If the number of sequences in $Busy(x)$ is greater than PCIunique, the rest of the BFemtocells will use PCIreused. If the number of sequences in $Busy(x)$ is smaller than PCI_{unqiue}, the rest of the unique PCIs will be assigned to Moderate femtocells. If the number of values in $Busy(x)$ and $Moderate(y)$ are both smaller than PCIunqiue, the rest of the unique PCIs will be assigned to Idle femtocells. Moreover, if PCI_{unique}=0, the proposed scheme will not assign the PCI to femtocells until $PCI_{unique} > 0$.

After the PCI distribution, the OAM updates the PCI information in the PCI resource management.

6. PCI Allocation in the femtocell (belongs to Centralised SON Function in the proposed centralised framework). After the PCI distribution process in the OAM, the OAM sends the new PCI allocation command back to

the femtocells via the MME. The femtocells with unique PCIs will not be involved in PCI confusion and their performance improvement leads to an overall network performance improvement.

7. PPCI Release (belongs to PCI algorithm execution in the proposed centralised framework). Considering static PCI release, the network will often check the femtocells' status as mentioned in Section 4.2.4. If the femtocell has been turned off, its PCI would be released and meanwhile the released PCI information would be updated in the PCI resource management via the MME.

   Considering dynamic PCI release, the general femtocell PCI update would be executed by the OAM at an optimal time and released PCI information would be updated in the PCI resource management via the MME.

The flowchart of the proposed DGPAS is shown in Figure 4.16.

4.3 Simulation and Analysis

This simulation presents the conventional PCI distribution and proposed dynamic PCI group scheme, and then studies the performance of reading CGI reduction and successful inbound handover specificity. These studies give an insight into the effects on performance of the proposed PCI allocation scheme regarding two-tier PCI confusion.

4.3.1 Simulation using Theoretical Data

The parameters for simulation are summarised in Table 4.3. Figure 4.17 shows the arriving rate (Homogeneous Poisson distribution) of femtocells for each hour in a day, which approximately corresponds with the human life timetable. The total number of PCIs is set to 20. Since the minimum arrival rate of femtocells is larger than 20, according to Figure 4.17, the two-tier PCI confusion takes place in most cases of inbound handovers. Moreover, the number of UEs

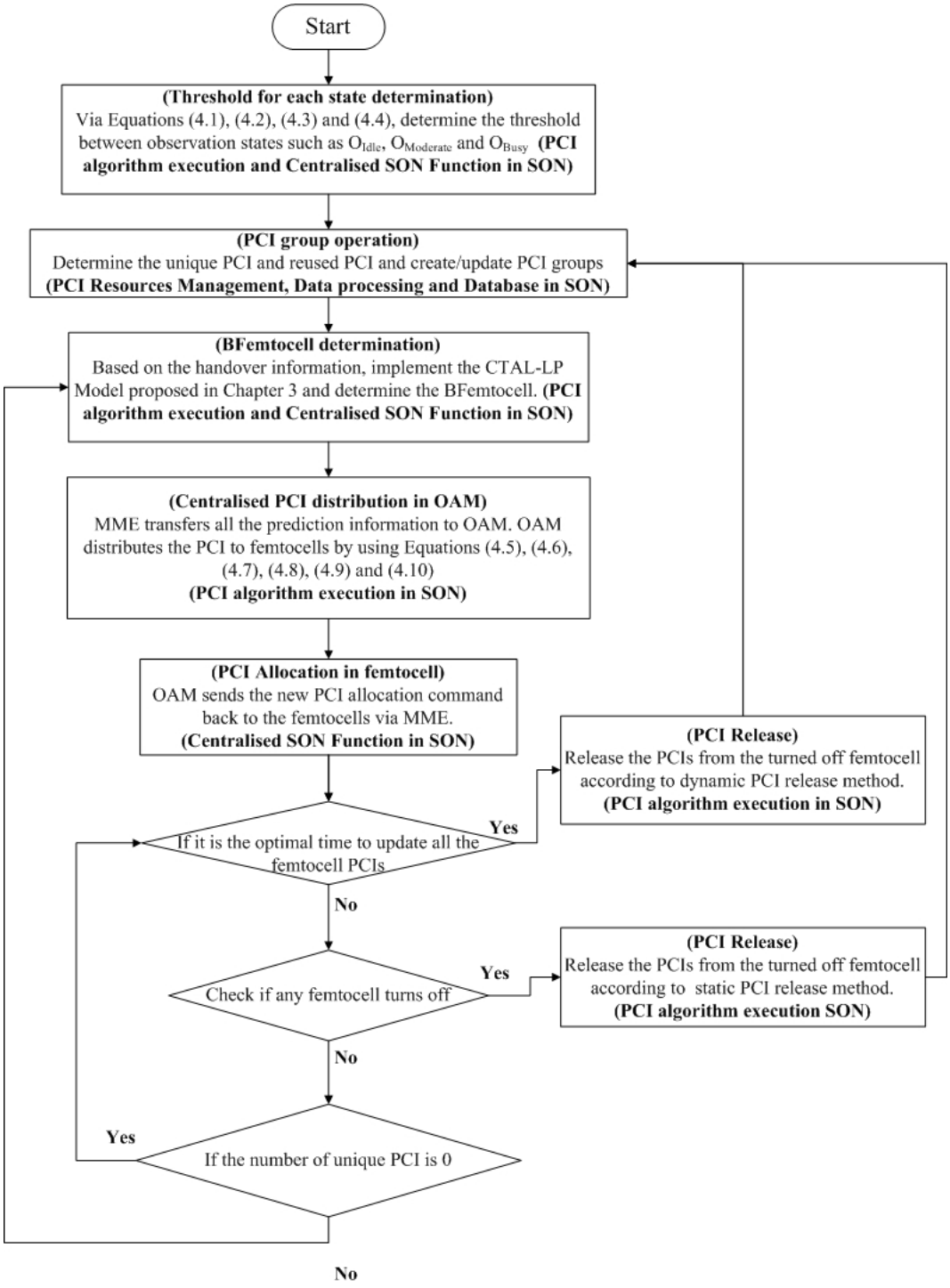

Figure 4.16: Flowchart of dynamic group PCI allocation scheme

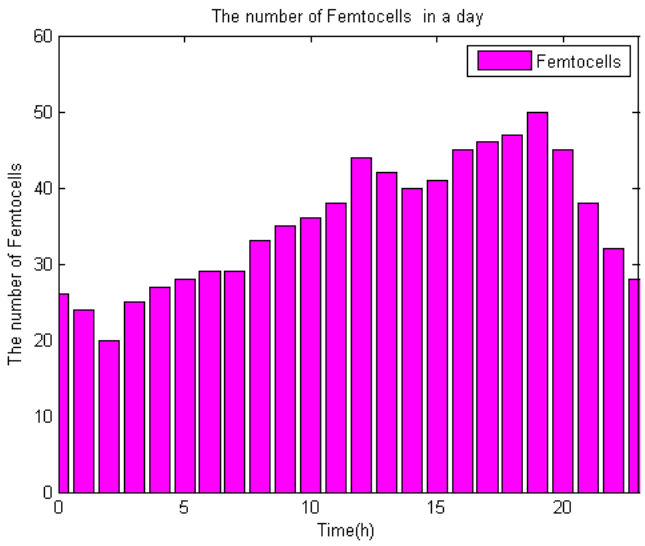

Figure 4.17: The Poisson distribution of the number of active femtocells

arriving at each femtocell depends on the Poisson process according to the queuing theory [65]. For more information of this simulation, especially the OAM and MME modelling, please check Appendix B.2.

The proposed PCI allocation scheme aims to reduce the usage of CGI in the inbound handover due to the drawbacks of using CGI. Hence, the number of CGI readings is the metric which is chosen to evaluate the performance in this simulation. The evaluations are undertaken in two cases, the only non-CSG femtocell scenario case and the blended CSG and non-CSG femtocell scenario case. The number of CGI readings is presented in Figure 4.18 and 4.19, where the proposed DGPAS schemes (Case1 and 2) are compared with the conventional method in Release 9 [3, 70] which uses the CGI to solve the two-tier PCI confusion.

The proposed PCI allocation scheme aims to reduce the usage of CGI in the inbound handover. Hence, number of CGI reading as the metric is chosen to evaluate the performance in this simulation. The evaluations are undertaken in two cases, such as only CSG Femtocell scenario case and blended CSG and non-CSG Femtocell scenario case.

The number of reading CGI is presented in Figure 4.18 and 4.19, where the proposed DGPAS scheme is compared with the conventional method in

Table 4.3: The Parameters in Configurations for the Simulation

Parameter	**Description**
Coverage of Macro/Femto	400/20 (m)
Location of Femtocells	Normal Distribution
Least distance of two Femtocells	5 (m)
Arriving model of Femtocells	Possion Distribution
Maximum UEs in a CSG Femtocell	5
Maximum UEs in a non-CSG Femtocell	10
Arriving rate of CSG Femtocells in case 1	20-50
Arriving rate of Femtocells in case 2	20-50
Ratio of CSG and non-CSG Femtocells in case 2	0.3
Arriving model of UEs	Possion Distribution
The length of a UE camping in the Femtocell	Negative Exponential Distribution ($3 \leq \lambda \leq 5$)
Available PCIs in total	20

Release 9 which uses the CGI to solve the cross-tier PCI confusion.

As can be seen in Figure 4.18 and 4.19, across the board, in both cases, the proposed DGPAS scheme consistently performs better compared to conventional approaches. This is because the proposed scheme has dynamically assigned the unique PCIs to those BFemtocells which are seriously suffering from two-tier PCI confusion. It can also be observed that the performance differs according to the varying time in Figure 4.18. This is because the larger the number of femtocells deployed, the more handovers may occur and the more CGIs have to be read. In addition, in Figure 4.19, it clearly shows that the performance does not proportionally increase with the number of femtocells (reduction appears at in the square area), but with the number of inbound handovers. This is perfectly understandable, because inbound handover is directly related to the located PCI and CGI reading.

In terms of Case 1 and 2, the performance in Case 2 is significantly better than Case 1. This is because CSG and non-CSG femtocells support a different

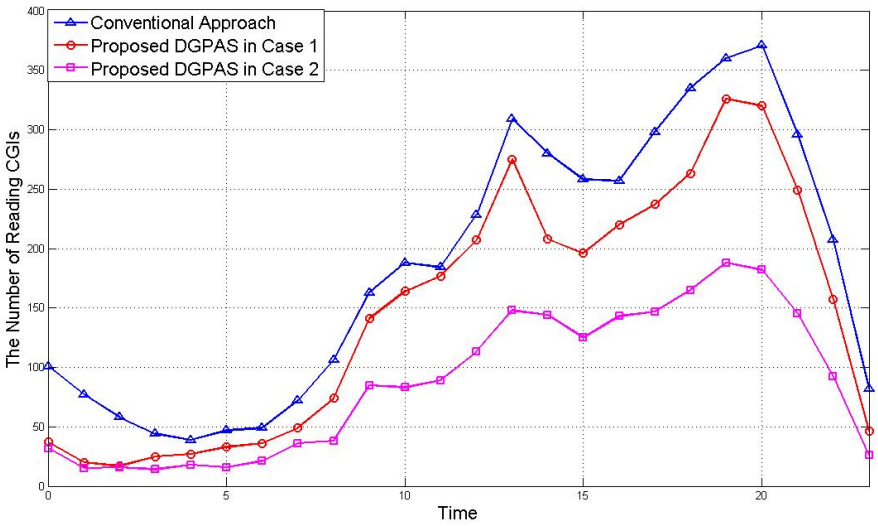

Figure 4.18: Time-based Comparison of DGPAS and Approach proposed in Release 9

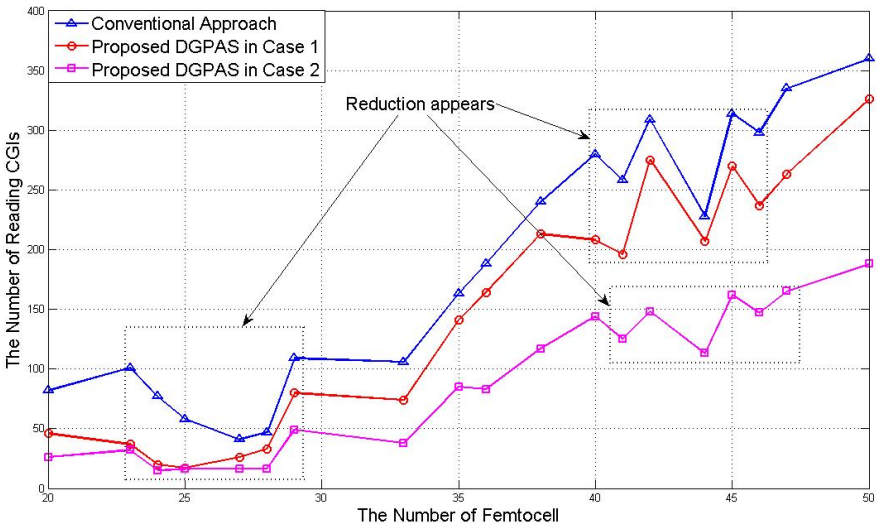

Figure 4.19: Number of femtocells-based Comparison of DGPAS and Approach proposed in Release 9

number of UEs. In Case 1, considering the home usage scenario, the lower number of UEs would be supported and less handovers would occur in the CSG femtocell. This leads to the boundaries of Busy or non-Busy CSG femtocells not being clear and results in the lower accuracy of BFemtocell determination. On the contrary, in Case 2, non-CSG BFemtocells can be determined by CPM with higher accuracy. Reflecting this, the scheme is more suitable for non-CSG femtocells which are currently the highly favoured femtocell deployment method. Moreover, in practice, the hot spot, small shop or public area for example, it is desired to secure fixed unique PCIs from operators, in order to have a better quality of wireless service for their customers.

4.3.2 Simulation using Real Dataset

In this simulation, one macro station and five non-CSG femtocells are randomly located in within the macrocell's coverage. Community Resource for Archiving Wireless Data (CRAWDAD) network trace repository [69] is used as a traffic model to record historical movement and communication situations of 20 smart phone devices over half a month. Moreover, for each time period, the system recorded the number of handovers in each cell and the movement history of each UE. In the simulation, handover between femtocells is not considered. The parameters for simulation are summarised in Table 4.4. These parameters are recommended by [30]. For more information on this simulation, please check Appendix B.2.

Since the worst drawback of CGI reading is the call-drop (the quality of inbound handover), in this section, with the real dataset, the average number of successful inbound handovers is chosen to evaluate the performance of this scheme. Moreover, the call-drop criterion is defined as the receiving SINR from the target of a serving cell below -6 dB [11]. For more information about call-drops, please check Section 5.1.4.

Figure 4.20 shows the average number of successful inbound handovers in the coverage of the femtocell (Femtocell radius is 20 m). For a clearer visualisation, the left side is the results of the proposed DGPAS scheme, and

Table 4.4: The Parameters in Real Dataset Simulation

Parameter	**Description**
System bandwidth	20 (MHz)
Macro/Femto transmit power	46/20 (dBm)
Macro/Femto radius	500/20 (m)
Hysteresis	5 (dB)
TTT/Autonomous gap	100 (ms)
Macro log-normal shadowing	Standard deviation: 8 (dB)
Femto log-normal shadowing	Standard deviation: 4 (dB)
Macro/Femto antenna gain	14/5 (dBi)
Macro path loss	$15.34+37.6 \times \log 10^(d[m])$
Femto path loss1	$38.46 + 20 \times \log 10^(d[m]) d \leq 20(m)$
Femto path loss2	$15.3 + 37.6 \times \log 10^(d[m]) d \geq 20(m)$
CGI/PCI reading length	160/20 (ms)
Call-drop criterion	$SINR - 6(dB)$

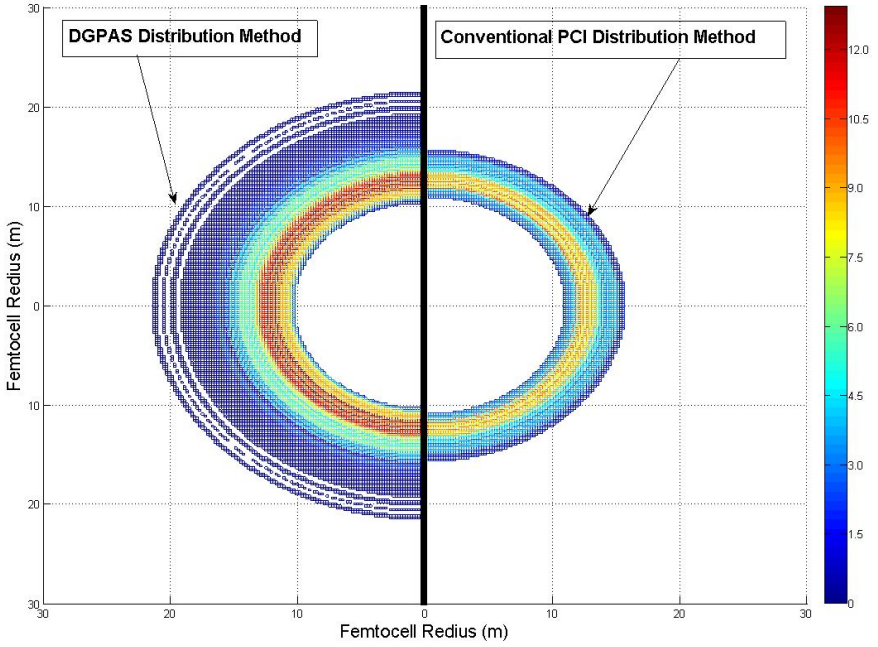

Figure 4.20: DGPAS vs. Approach Proposed in Release 9 Conventional Method at a Femtocell Coverage

on the right side is the results of the conventional method. The shaded bar represents the various average numbers of successful inbound handovers in a time period. Compared to the conventional approach, it is obvious to see that the successful handover area in DGPAS is larger than that of the conventional method. This is because the time cost of the CGI reading leads to the handover procedure triggering late. Therefore, as shown on the right side of Figure 4.20, most of the handovers happen in the area already deeply within the coverage of the femtocell. Moreover, the late handover leads the receiving SINR from the serving cell to easily drop lower than -6 dB [11], and cause a call-drop during the handover procedure. In other words, the proposed DGPAS method reduces the number of CGI readings, thus enhancing the handover area as shown on the left side of Figure 4.20. Moreover, the DGPAS method has a higher number of successful inbound handovers (Results are up to 12 appearances at radius of 13 to 11 metres from the femtocell) than the one in the conventional method (Results only reach 10.5 appearances at radius of 13 to 11 metres from the femtocell). This is because: firstly, most inbound handovers happen in the at area of the radius 13 to 11metres from the femtocell in this simulation; secondly, the reason is same as mentioned earlier, the reduction of CGI reading leads to the lower probability of appearance of call-drop in the areas of most inbound handovers. Therefore, the DGPAS method can reach 12.

4.4 Summary

In this chapter, a dynamic group PCI allocation scheme has been proposed which implements a cell-based prediction model. This scheme is based on the centralised SON structure and complies with ACPCI functions. It includes the concept of the Busy femtocell (BFemtocell), dynamic PCI groups, dynamic PCI allocation and PCI release functions. Through the cooperation of these proposed concepts and functions, this scheme is able to mitigate two-tier PCI confusion and offer enhanced handover quality. The proposed scheme has been tested, the simulation results are positive and its advantages are listed as

follows:

- By reducing CGI reading times, the approach outperforms the existing approach by reducing the possibility of handover failure and also achieving dynamic PCI allocations in the two-tier environment.
- By reducing CGI reading times, the proposed scheme reduces battery consumption for today's evermore demanding multimedia mobile applications.
- To assign unique PCIs to Busy femtocells (BFemtocells) does not affect the steadiness of the current system due to unique PCIs not causing any conflict with other cells.

Chapter 5

Dynamic UE-based Hysteresis-adjusting Algorithm

In the previous chapter, it introduces a centralised dynamic PCI group scheme, in order to achieve better inbound handover quality when UE is in the connected mode. However, PCI allocation happens during the handover preparation stage, this chapter focuses on tackling challenges at a later stage of the handover process, such as Radio Link Failure (RLF) and ping-pong effect. In this chapter, a hybrid dynamic UE-based hysteresis optimisation algorithm is proposed, which provides the optimal handover parameters to improve system performance.

In LTE femtocell system, the handover decision is made in the source cell. However, UE also needs to provide assistance for the hard handover procedure. During the handover process, non-optimal handover triggering parameters may cause more handover failure, which is quite destructive. The existing handover optimisation algorithms focus on dynamically optimising handover parameters, such as hysteresis and Time-To-Trigger (TTT) from the cell-side. Those techniques provide the centralised optimal parameters to UE. However, the centralised optimal parameters algorithms only improve the average handover performance for the entire system but ignor the performance of each individual UE.

UE Mobility is the unavoidable feature in the handover process. Since each

UE moves at various speeds and it may suffer from the violent change of signal strength. Both stationary and centralised optimal parameters techniques cannot offer the suitable parameters for different speeds of UE, which may lead to degraded handover quality. Therefore, it is desired to provide individual parameters for every UE.

Based on the hybrid SON architecture as mentioned in Chapter 2, in this chapter, Dynamic UE-based Hysteresis-adjusting Algorithm (DUHA) for inbound and outbound handover in LTE femtocell system is proposed. It offers distributed optimal hysteresis for every UE and provides a better overall performance than the centralised optimal hysteresis approach.

5.1 Handover in the LTE femtocell

Before introducing the proposed DUHA, some important background knowledge used in this algorithm are described in this section.

5.1.1 Outbound Handover

In the LTE femtocell system, when UE hands off from macrocell to femtocell, it is called inbound handover. On the other hand, if UE hands off from femtocell to macrocell, it is called outbound handover. For the inbound handover, due to the limited number of PCI and drawback of CGI, the handover suffers the confusion and collision issues. Conversely, for the outbound handover, there is no collision or confusion issue. The goal of this chapter is to setup MRO function in SON which has mentioned in Chapters 1 and 2 and solve the handover issues for inbound and outbound handover.

The protocol interfaces between the femtocell and macrocell are listed below [25]:

- MME interface with the MME for control plane traffic.
- S1-U interface with the Serving Gateway (S-GW) for user plane traffic. Collectively the S1- MME and S1-U interfaces are known as the S1

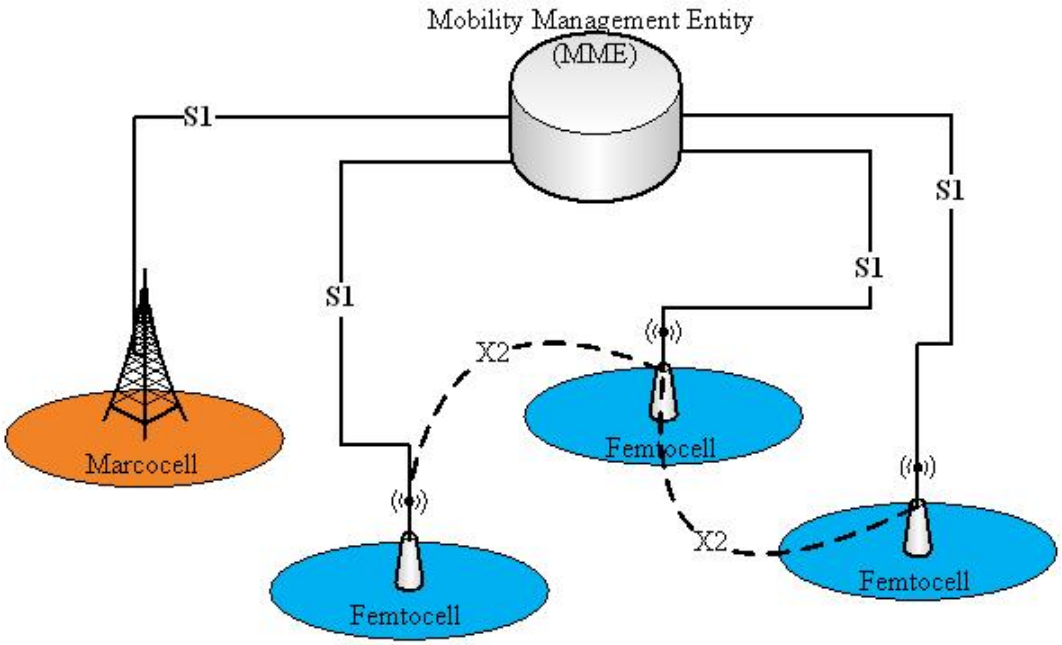

Figure 5.1: communication interface in LTE femtocell

interface.

- X2 interface with macrocell or femtocell elements.

The X2 interface is used to communicate between femtocells. S1 interface (S1-MME) is used to communicate between macrocell and femtocells as shown as Figure 5.1.

X2 interface supports the two cells to communicate directly without the MME. S1 interface supports two cells to communicate with the MME. Since inbound handover and outbound handover happen between macrocell and femtocell, only the S1-MME interface (It is called as S1 for convenience) will be considered in this chapter.

5.1.2 Handover A3 Event

In the LTE femtocell system, the source cell configures the UE to take measurements of the Reference Symbol Received Power (RSRP) and Reference Signal Received Quality (RSRQ) of the serving cell and the neighbouring cells. After the measurement is completed, if the entry event has been maintained for the

duration of time equal to the TTT, UE would send a handover measurement report and handover request to serving cell. This entry event is called A3 event. This chapter will only consider the handover with A3 event. A3 event can be applied using the following equations [29]:

$$RSRP_{target} \geq RSRP_{serving} + Hysteresis \tag{5.1}$$

$$RSRQ_{target} \geq RSRQ_{serving} + offset \tag{5.2}$$

RSRP is a measurement of average reference signal strength for the resource block. RSRQ indicates the quality of the received reference signal. The RSRQ measurement provides additional information when RSRP is not sufficient to make a reliable handover decision. In the procedure of handover, if the system only uses RSRP to trigger A3 event, it results in more frequent handover since it does not consider the signal quality when making the handover decisions. On the other hand, if the system only uses RSRQ to trigger A3 event, it results in higher probability of call-drop. This is because when emph$RSRQ_{target}$ value is suitable, but interference value is high, $RSRP_{serving}$ value may drop down below the threshold, in which case UE can still communicate normally with the serving cell before handover [11].

Received Signal Strength Indicator (RSSI) is effectively a measurement of all of the power contained in the applicable spectrum [25]. This could be signals, control channels, data channels, adjacent cell power, and background noise. As RSSI applies to the whole spectrum, multiply the RSRP measurement by emphN (the number of resource blocks) will effectively applies the RSRP measurement across the whole spectrum. This leads to the Equation (5.3).

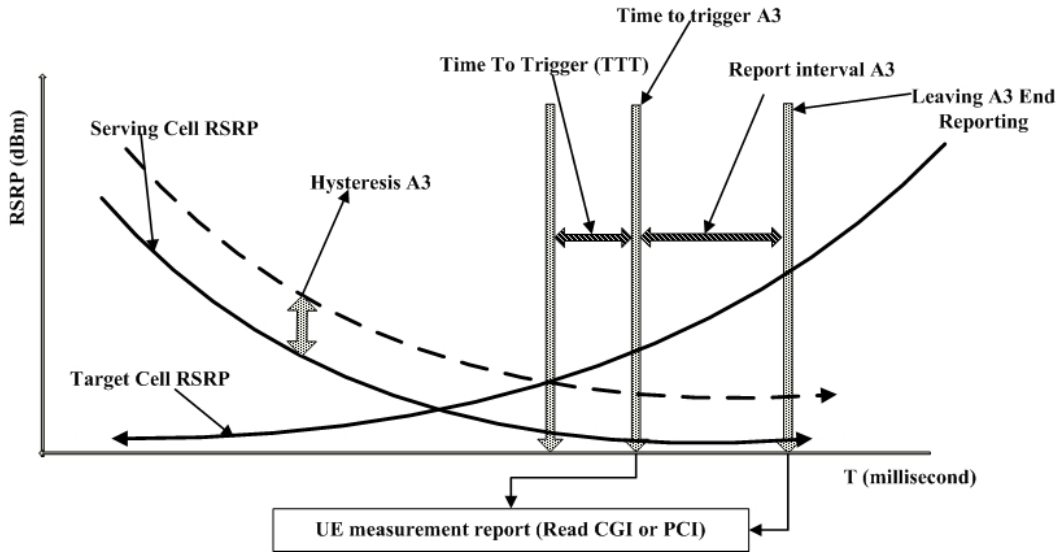

Figure 5.2: The structure of handover process in A3 event

$$RSRQ = \frac{N \times RSRP}{RSSI} \tag{5.3}$$

More details of RSRQ, RSSI and RSRP will be described in Section 5.2.4.

5.1.3 Hysteresis and Time To Trigger (TTT) in Handover

In A3 event, there are two parameters are used to trigger a handover process, Hysteresis and TTT [29].

- In terms of TTT, as mentioned earlier, it delays the A3 event to ensure the signal strength to be more stable, in order to avoid a ping-pong effect.
- In terms of Hysteresis, the role of the hysteresis is to make the measured target cell looks worse than measured. This parameter keeps the signal strength of target cell at a certain level before the UE decides to send a measurement report to initiate a handover process.

The process of the handover in A3 event can be summarised in Figure 5.2.

In the Figure 5.2, TTT event does not start at the intersection point of serving cell RSRP and target cell RSRP since the hysteresis delay the start of TTT. During the A3 report interval, UE would read the PCI from the target cell which cost 20 ms (millisecond) by using measurement report [11, 25]. If there is no confusion happens, the UE would leave the A3 event and finish the handover process. Otherwise, the UE would require the target femtocell to provide the CGI and this cost 160 ms by using measurement report [11]. After UE gets the CGI ID, the UE would leave the A3 event and finish the handover process. Moreover, after UE gets the PCI and CGI, the handover process needs about 300 ms between serving and target cell [74]. Hence, the A3 report interval should include the 300 ms delay till the A3 event finishes.

According to Figure 5.2, the higher the value of hysteresis the more difficult to make the handover decision between serving and target cell. On the other hand, the smaller the value of hysteresis and the faster the calls to be handovered to the neighbouring cells. Therefore, a proper hysteresis value affects the handover performance. However, in the two-tier structure of femtocell and macrocell deployment, the handover scenario differs from the conventional LTE networks, e.g. the coverage of the femtocell is much smaller than the macrocells, the handover between macrocell and femtocell experiences more severe Signal-to-Interference Noise Ratio (SINR) degradation. Therefore, to set an optimal Hysteresis value in the inbound and outbound handover is one of the challenging issues for femtocell network deployment [6]. Moreover, during the handover process, RLF and handover to an incorrect cell may occur as a result of the sub-optimal hysteresis in the system.

5.1.4 Handover Performance Metrics in 3GPP Standards

In this section, three important metrics such as RLF, handover oscillations and call-drop are proposed and used to evaluate handover performance at current network system. These metrics are described below:

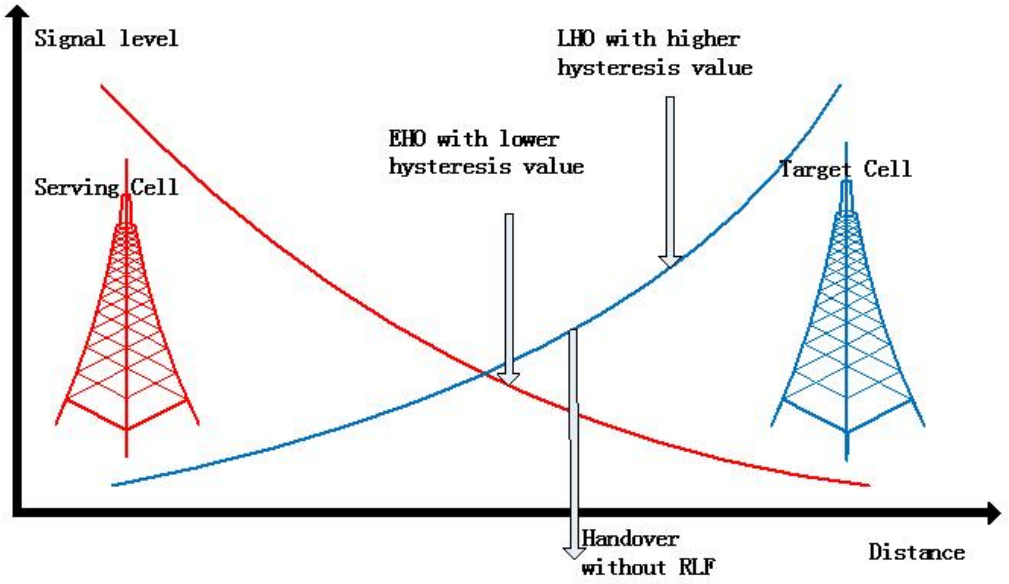

Figure 5.3: RLF during handover

Radio Link Failure

For the RLF, there are two cases of RLF during handover such as: failures due to too late handover (LHO); failures due to too early handover (EHO); failures due to handing over to the wrong cells; LHO and EHO are illustrated in Figure 5.3. If handover is triggered too early, though the signal strength of the target cell is too low, RLF will occur shortly after the handover procedure; UE will re-establish the radio link connection to the serving cell. On the other hand, if handover is triggered too late, though the signal strength of the serving cell is already too low, RLF will occur before the handover is initiated or during the handover procedure; the UE will re-establish the radio link connection to the target cell. Moreover, handover to the wrong cells would not be considered in this chapter.

Figure 5.3 shows that the handover with lower hysteresis value at the serving cell may cause RLFs due to EHO. On the other hand, if handover with higher hysteresis value, LHO would occur. Therefore, efficient values of hysteresis need to be investigated to achieve the lower RLFs simultaneously.

Based on the above mentioned metric, many recent works have provided RLF ratio criteria for system performance evaluation. For instance, [59] has

proposed the handover failure ratio. Handover failure ratio (H_{fr}) is defined as a RLF occurs if SINR stays below a threshold for a duration equivalent to the critical time [11]. If RLF occurs, the handover fails. H_{fr} is the ratio of the number of failed handovers and Nfail is the number of handover attempts. The number of handover attempts $N_{attempt}$ is the sum of the number of successful handover and the number of call-drop Ndropped and the number of incorrect handover (handover to wrong cell):

$$H_{fr} = \frac{N_{fail}}{N_{attempt}} \tag{5.4}$$

Handover Oscillations

For handover oscillations, it is usually called as ping-pong effect. A ping-pong handover is registered due to non-optimal handover parameters, where the UE made a successful handover from a cell B to cell A in a short time period after another successful handover had already occurred from A to B with the same UE. ping-pong causes heavy network traffic and leads to worse quality of service. Non-optimal handover parameters, such as lower hysteresis value, may worsen the ping-pong effect [12].

Based on [12], [59] has proposed the way to calculate ping-pong ratio. Ping-pong ratio (P_{pr}) is defined as the mobile wildly switch links with either base station when UE is in the overlapped area of the base stations. The N_{pp} measures the ratio of handover oscillations. Npp represents the number of ping-pong handovers to the number of handover attempts $N_{attempt}$, thus N_{pp} can be defined as:

$$P_{pr} = \frac{N_{pp}}{N_{attempt}} \tag{5.5}$$

UE Call Drop

According to [12] and [59], call-drop is defined as when the RLF or ping-pong occurs, if UE cannot reconnect to the serving or target cell, and then call-drop happens. The call-drop is the worst event in the handover process, as it leads to interrupted communication.

Call-drop ratio (C_{dr}) is defined as the probability that an existing call is dropped before it was finished, e.g. during handover. It is calculated as the ratio of the number of dropped calls as Ndropped to the number of handover attempts $N_{attempt}$ in the network:

$$C_{dr} = \frac{N_{dropped}}{N_{attempt}} \tag{5.6}$$

As mentioned in MRO [11], the handover parameters need to ensure better performance with these lower criteria value. The multi-parameter optimisation issue is difficult to satisfy three criteria at the same time.

Overall, according to [12], one of the main functions in MRO is that UE needs to report RLF to the serving cell in order to assist MRO in monitoring RLF, such as EHO and LHO. In general, this procedure can be described as: firstly, that report is sent to the target cell by UE when the handover process is completed; Secondly, the target cell will send the RLF report to the serving cell via MME [12].

5.1.5 System Information Block

In 3GPP standard, the system information or broadcast information is information about the system and the serving cell. It is sent to UE by the network in a point-to-multipoint manner. The system information elements are broadcasted in information blocks which consists of System Information Blocks (SIBs) and Master Information Block (MIB). Moreover, Broadcast information is sent via the Broadcast Control CHannel (BCCH) or Dedicated Control CHannel (DCCH). BCCH is a downlink channel for broadcasting sys-

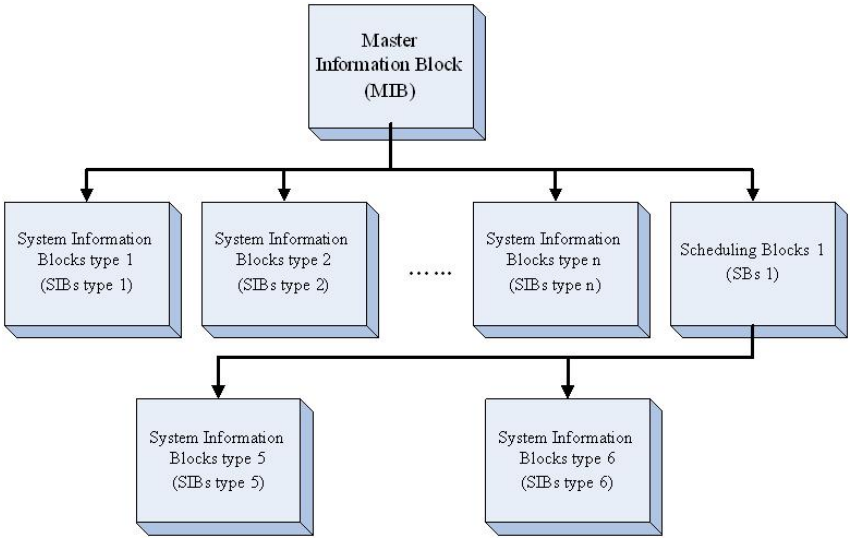

Figure 5.4: Overall structure of SIBs scheduling tree

tem control information and if a UE in the connected mode, DCCH would be used in the network to send system information to the UE [24].

SIBs are contained in broadcast information and are named as SIBs type 1 through 18. SIBs are sent depending on a certain schedule, hence the blocks that are more important than others are sent more often and the less important blocks are sent less often. The schedule is flexible since it can be adjusted by the current loading situation [24].

MIB indicates the identity and the schedule of a number of SIBs. The SIBs may be included in the MIB or Scheduling Blocks (SBs), as illustrated in Figure 5.4.

According to Figure 5.4, the tree starts from a MIB, which must be received and decoded first and then move onto the next stage. The system information is arranged as a blocks tree and UE must maintain this tree in its memory, therefore it can decode only those blocks that are needed and skip the rest. This arrangement avoids the networking redundancy and also provides the possibility to add new types of SIBs to the protocol if such is needed later in the system. Therefore, the length of the system information is flexible.

If UE gets sequences of blocks that it cannot recognise, it simply ignores them, but other mobiles which have updated protocol can successfully access the blocks. Currently, most of femtocell measurement control information is

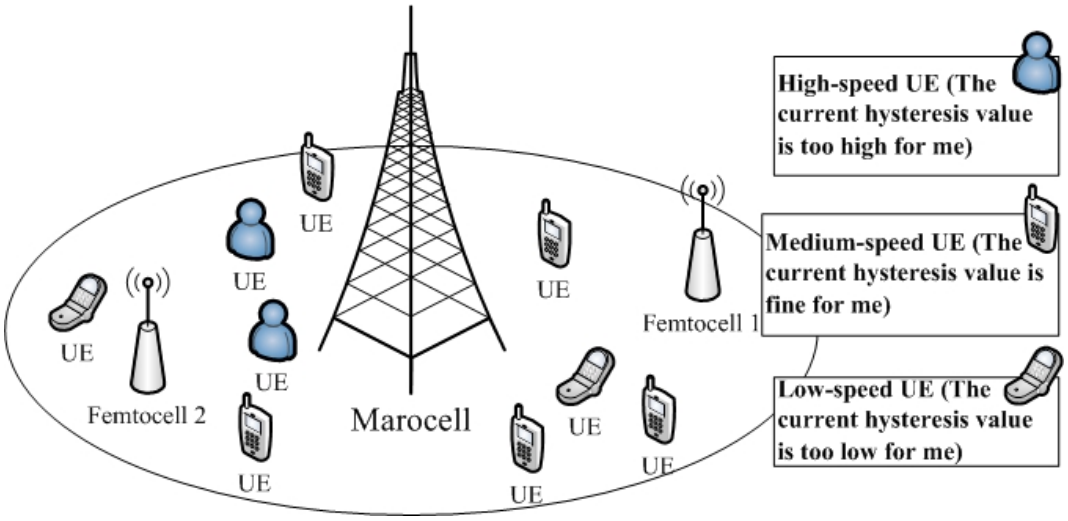

Figure 5.5: Three mobility states and their hysteresis in LTE network

contained in the SIBs type 11 [29].

5.1.6 User Mobility States in Standards

In the real network, users in different moving speeds need to be offered with different hysteresis value [70], the LTE cell provides three different hysteresis parameters to support three user mobility states.

Depending on users' speed, the users can be grouped into three states such as Normal-mobility state, Medium-mobility state and High-mobility state. A cell offers the different corresponding hysteresis to different user ranks as shown in Figure 5.5. However, according to MRO [29], the stationary hysteresis is insufficient to satisfy users' movement at various speeds.

In order to get a better performance, it is desired to give the optimal hysteresis to UE. For example: LHO easily happens when higher speed UE with a higher hysteresis value. In high-mobility states, it offers a lower hysteresis to the high speed UE in order to avoid LHO. Similar applies to medium and normal mobility states. Different hysteresis values should be offered to the different UEs with different speed in order to avoid RLF and ping-pong.

5.2 Proposed Dynamic Hysteresis Algorithm

When UE moves at a different speed, in LTE standards, some common parameters such as the receiving average reference signal Signal-to-Interference-plus-Noise Ratio (RS-SINR), RSRP and RSRQ, would change in different pace in a certain period. To ensure that a hysteresis change according to changes of those three parameters.

UE's moving speed is complicated to obtain by the network system. However, the average RS-SINR (It would be called as SINR for convenience), RSRP or RSRQ is easy to obtain by the UE measurement report. It is desired to use those parameters rather than speed factor. In this section, a hybrid dynamic UE-based hysteresis-adjusting and optimisation algorithm is proposed. Based on the received average SINR, this approach aims to obtain the optimal distributed hysteresis for users who are moving at various speeds and achieve the better overall handover performance.

5.2.1 Framework of Hybrid Dynamic Hysteresis Algorithm

In 3GPP, one of the main targets in SON is the self-optimisation in the handover procedure. The MRO focuses on autonomous selection and optimisation of handover parameters, for instance, hysteresis and TTT. The objective of MRO is to dynamically improve the network performance of handover in order to provide improved end-user experience as well as increased network capacity [12]. The objectives of the MRO can be summarised as listed as follows:

- To detect and reduce RLFs prior, during or after handovers
- To detect and reduce handovers to wrong cells
- To minimise the handover ratio and handover oscillations while achieving 1 and 2 as described above.

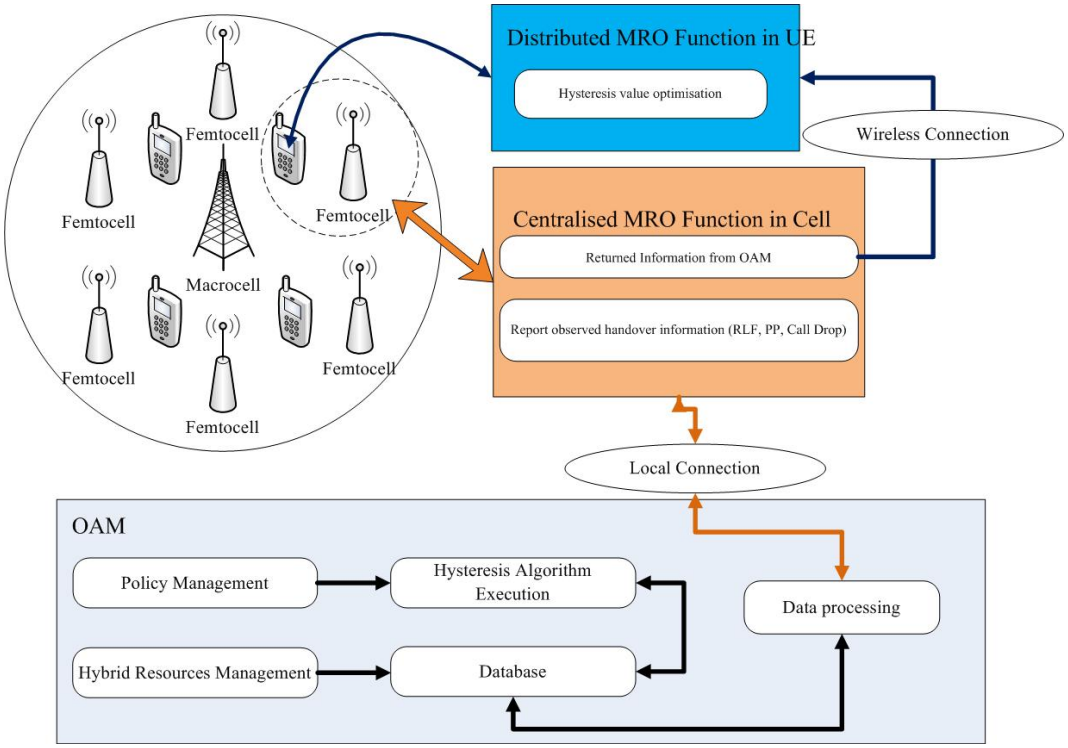

Figure 5.6: The general framework of hybrid hysteresis optimisation

In order to achieve the objectives proposed in MRO, this chapter proposed a hybrid SON approach to obtain an optimised unique hysteresis value for handover process. In terms of the hybrid SON structure, MRO function and OAM reside at the base station, and specific SON approach is executed partly at the OAM system and partly at the network elements (UEs) [16, 39]. The general framework of hybrid MRO is shown in Figure 5.6.

In the following, the main function blocks are described below:

- **Distributed MRO Function:** the distributed MRO function resides in the individual UE. Depending on the received the information from the centralised MRO function, distributed MRO function can provide the unique optimal hysteresis value for its resided UE. Therefore, this function has the ability to execute the specific part of SON approach and fully control the handover triggering parameters such as hysteresis.

- **Centralised MRO Function:** the main task of centralised MRO function is to select the observed handover information such as RLF, ping-

pong and call-drop from each UE within the base station coverage. It then reports them to the self-organisation approach in OAM system via Data Processing. Moreover, since OAM and centralised MRO function reside in wireless cell, the data switching between them is local transmission.

The second task of centralised MRO function is to manage the information that OAM returned and send it to the distributed MRO Function in the specific UE. The communication between distributed and centralised functions is via wireless downlink transmission.

- **Data processing:** there are two functions have implemented in this functional block: firstly, this block arranges the data sent from the centralised MRO function depending on the database pattern in OAM, in order to transmit the data to the Database functional block; secondly, after receiving the necessary information returned from Hysteresis Algorithm Execution, this block would indicate the specific UE and then send it back to centralised MRO function.

- **Policy Management:** the same as mentioned in Chapter 4, this functional block indicates the policy of SON approach for MRO and the specific part of proposed dynamic hysteresis-adjusting algorithm in this chapter is located in this block. The different from the centralised SON structure, the operators need to update algorithm at this block and distributed SON function in UE.

- **Hysteresis Algorithm Execution:** this functional block is used to manage the database depends on the policy from Policy Management block.

- **Hysteresis Resources Management:** this functional block is used to store the default hysteresis values, TTT values and UE IDs for the different user mobility states as mentioned in Section 5.1.6.

- **Database:** this functional block stores the information that obtained

from the centralised MRO function such as RLF, ping-pong, call-drop and UE ID. It also stores the temporary values, for example, the handover performance indicators.

Overall, in the hybrid MRO, as the centralised approach, OAM system is supposed to have a complete knowledge of the handover performance of each UE. On the other hand, as a distributed approach, SON function can fully control the hysteresis value. Depending on cooperation of centralised and distributed functions, the SON approach can be executed and offer an optimised unique hysteresis value for individual UE in the network system. The next section introduces the key information in the proposed hybrid dynamic hysteresis-adjusting algorithm.

5.2.2 Comparison of the Proposed Approach against the Centralised Hysteresis

In 3GPP, the handover parameters such as hysteresis and TTT are all defined in serving cell and are published by RRC measurement configuration to UE to support the event like A3 event as mentioned in Section 5.1.2. However, the handover process is triggered by UE mobility, but the stationary hysteresis and TTT method no longer offers a reliable service. Reflecting this, the MRO in SON focuses on the optimisation of handover parameters.

Papers such as [59] and [60] proposed the optimal algorithms based on the observed handover information to find the optimal hysteresis and TTT at cell side. These algorithms are centralised cell-based method which means they select average optimal handover parameters for the entire networking. It works fine if all the UEs move at the same speed or similar speed. However, in the realistic network, UE moves at various speeds and this cell-based optimal algorithm cannot offer the optimal parameters to every UE as shown in Figure 5.7.

Figure 5.7 shows that, most of UEs with neither high nor low moving speed satisfied with the centralised optimal hysteresis. However, for the UEs with

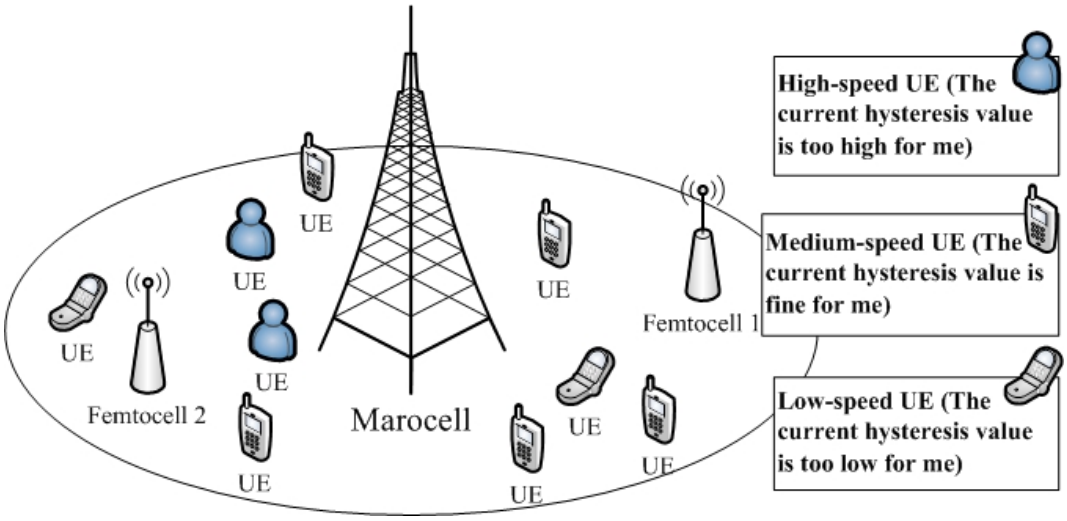

Figure 5.7: The general framework of hybrid hysteresis optimisation

high or low moving speed, they cannot work well with current hysteresis. Some of UEs cause decrease in the system performance. DUHA is proposed based on UE mobility factors (SINR, RSRP and RSRQ from target cell) and it offers the distributed optimal parameters scheme for each UE.

5.2.3 Proposed Algorithm Handover Parameters

To cope with the different changing pace of these parameters and hysteresis, this chapter introduces a Revise Parameter (RP). We also introduce a Handover Additional Parameter (HAP) in the proposed DUHA. In this algorithm, the SINR is used to represent the speed factor and the reason will be described in the next section.

In the proposed algorithm, HAP is defined as a weighted factor of: $RP \times SINR_{target}, n$ (In linear units). If $SINR_{target}$ denotes the received average SINR of the UE from the target cell and $SINR_{serving}$ denotes the received average SINR of the UE from the serving cell, the Equation (5.1) can be rewritten as Equation (5.7), (5.8) and (5.9) in dB units:

$$HAP = RP + SINR_{target} \tag{5.7}$$

$$H_{proposed} = H_{high} - HAP \tag{5.8}$$

$$RSRP_{target} \geq RSRP_{serving} + H_{proposed} \tag{5.9}$$

where H_{high} is the highest hysteresis value which corresponds to the lowest speed boundary. Therefore, in different user mobility states, they have different RP and same H_{high} for handover. The range of RP value must ensure that both $H_{high} >= RP + SINR_{target}$ are true (in dB units). $H_{proposed}$ denotes the optimal hysteresis value for handover and it is obtained by using RP, SINR and H_{high} according to the Equations.

In the proposed algorithm, RP is the public parameter which needs to be defined at cell side and HAP is the UE side private parameter in order to adjust hysteresis value. RP is the public parameter in the centralised MRO function and HAP is defined in the distributed MRO function, therefore, in the hysteresis self-optimisation approach, all UEs should share the same RP but different HAP.

Since RP is the public parameter for the system, it needs to be sent to UE via cell information using SIBs. SIBs can be easily updated, therefore I proposed that RP would be involved in existing SIBs type 11 (SIBs type 11 includes most femtocell parameters) or a new SIBs type.

5.2.4 RSRQ vs SINR vs RSRP

In this section, three LTE common handover parameters are evaluated for DUHA algorithm, in order to achieve better Quality of Service (QoS).

RSRQ vs RS-SINR

Both RSRQ and SINR from the target cell can be used to reflect the UE's speed changes. However, the RSRQ is not more reliable than SINR in the system handover process. According to [1], the reason is described below:

RSRQ is defined as Equation (5.10) and RSSI is defined as Equation (5.11) in linear units.

$$RSRQ = \frac{RSRP \cdot N}{RSSI} \tag{5.10}$$

$$RSSI = P_{interference} + RSRP \cdot N \cdot z + P_{noise\_z\_N} \tag{5.11}$$

where N is the number of resource block (RB) over which the RSSI is measured, typically equal to system bandwidth. The z is the number of resource elements (RE) that are used in the RSSI measured RB. $P_{interference}$ is the total RS interference from adjacent base station for those RBs. $P_{noise\_x\_N}$ is the total noise for these REs that are used in RSSI measured RBs. According to [1] and [3GPPTS36211], one slot has 6 or 7 symbols in time domain, thus, a block consists of 12 sub-carriers on frequency domain and 1 slot in time domain (6-7 symbols). RE refers to 1 sub-carrier on frequency domain and 1 symbol in time domain, as shown in Figure 5.8 according to [3].

When z= 2 (RE/RB), it means that only reference signal power is considered in 2 sub-channels in the serving cell. This means that the resource block is empty since it needs at least 2 REs for reference signal and no power is assigned for the others REs. When z=12 (RE/RB), it means that all REs are carrying data in the 12 different channels, which means the resource block is fully loaded.

Unlike RSRQ, SINR is not defined in the 3GPP standard but defined by the UE vendors. Therefore it is may not be reported to the network (depend

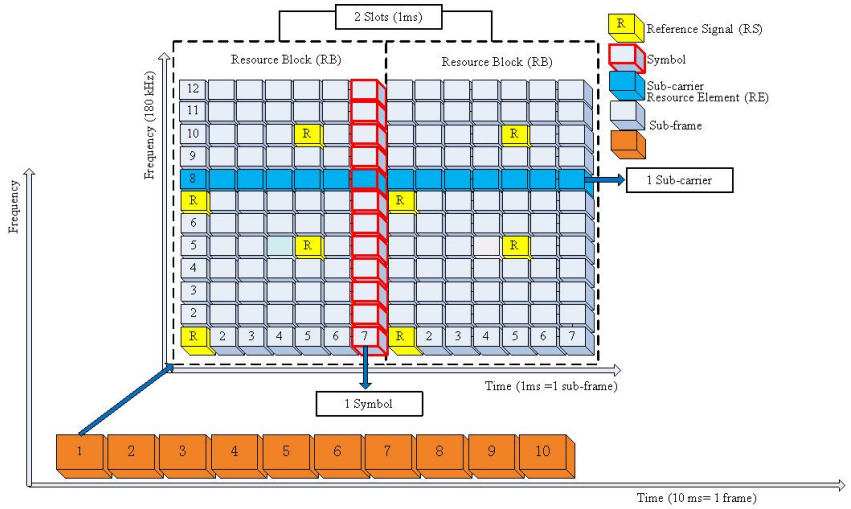

Figure 5.8: LTE downlink frame structure

on vendor's design). SINR is very commonly used by operators and vendors [75]. SINR is equal to the ratio of whole spectrum power that UE is using and RS interference from adjacent base station plus noise power. Thus, it can be described in the Equation (5.12):

$$SINR = \frac{RSRP \cdot 12 \cdot N}{P_{interference} + P_{noise\_z\_N}} \tag{5.12}$$

In Equation (5.12), 12 refers to 12 sub-carries in 1 RB, based on Equation (5.10) and (5.11), the (5.12) can be rewritten as Equation (5.13).

$$SINR = \frac{RSRP \cdot 12 \cdot N}{\frac{RSRP \cdot N}{RSRQ} - RSRP \cdot z \cdot N} = \frac{12}{\frac{1}{RSRQ} - z} \tag{5.13}$$

The relation between SINR and RSRQ through Equation 5.13 are shown in Figure 5.9.

Figure 5.9 illustrates the load-dependent relation between SINR and RSRQ schematically. When the value of z increasing from 2 to 12 (traffic load, the usage of the sub-carries in 1 RB), the RSRQ measurement may differ up to 8 dB depending on the load for the same SINR.

For instance, the RSRQ may reduce 8 dB when UE starts downloading

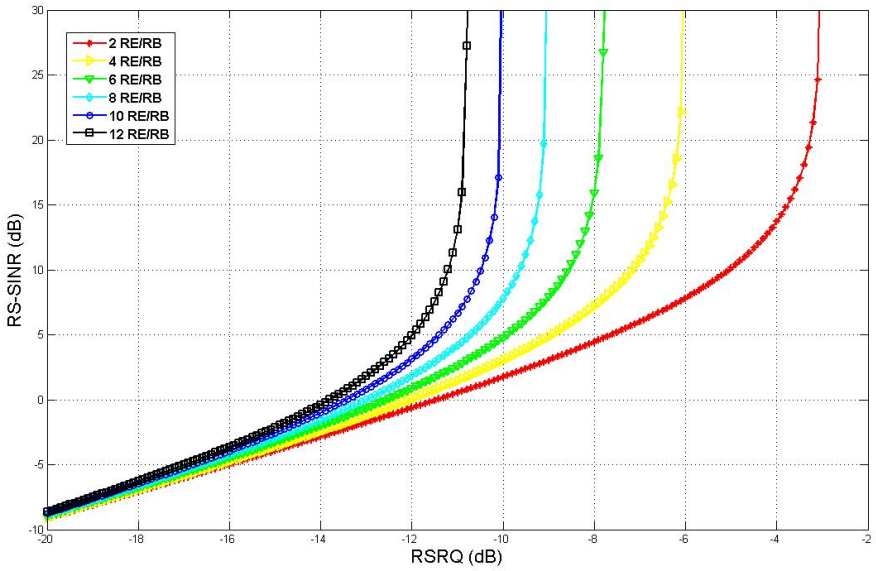

Figure 5.9: Load-dependency of RS-SINR and RSRQ measurement

in an empty cell and has to assign all the REs with data. When UE turns from light traffic load to heavy traffic load, the RSRQ will reduce although neither the SINR nor RSRP have changed [30]. Hence, RSRQ is very sensitive to this cell traffic load, but SINR is not affected by the cell traffic load. This obviously makes RSRQ less attractive to be used to represent the speed factor, in particular in low loaded cells. Reflecting above, SINR is a better parameter to use in DUHA than RSRQ.

RS-SINR vs RSRP

Both RSRP and SINR from the target cell can be used to reflect the changes of UE speed. However, the RSRP is not more reliable than SINR in the system handover process [30]. The reason is described below:

To substitute Equation (5.7) and (5.8) in Equation (5.9), the (5.9) can be rewritten as Equation (5.14) in linear units. Then, through replacing the SINR with RSRP in (5.14), Equation 5.15 can be obtained.

$$RSRP_{target} \geq \frac{RSRP_{serving} \times H_{high}}{RP \times SINR_{target}} \tag{5.14}$$

$$RSRP_{target} \geq \frac{RSRP_{serving} \times H_{high}}{RP \times RSRP_{target}} \tag{5.15}$$

Therefore, Equation (5.15) is RRSP based and Equation (5.14). The (5.15) is easier to be rewritten to Equation (5.16) by moving the right side RSRP-target to the left side and extracting a root at both sides as shown below:

$$RSRP_{target} \geq \sqrt{\frac{1}{RP} \times RSRP_{serving} \times H_{high}} \tag{5.16}$$

Based on Equation (5.12), to rewrite Equation (5.14) to Equation (5.17) as shown below:

$$RSRP_{target} \geq \frac{RSRP_{serving} \times H_{high}}{RP \times \frac{RSRP_{target} \times 12 \times N}{P_{interference} + p_{noise\_z\_N}}} \tag{5.17}$$

To rewrite Equation (5.17) to Equation (5.18) by extracting a root at both sides as shown below:

$$RSRP_{target} \geq \sqrt{\frac{P_{interference} + p_{noise\_z\_N}}{RP \times 12 \times N} \times RSRP_{serving} \times H_{high}} \tag{5.18}$$

Comparing Equation (5.16) and (5.18), it obviously shows that the SINR based algorithm, the inequality is not only dependents on the adjustment by RP, but also depends on interference and noise from the scenario. If there is strong interference or noise, the inequality (5.18) would not be easily satisfied. This means that it would not be easily handover to the heavy interference cell

when use Equation (5.18).

RSRP is not reliable as it cannot represent the signal quality, which leads to the un-reliable handover. The main goal of these equations is to reduce the H_{high} until it reaches to the optimal hysteresis value. Since the femtocell radius is much smaller than the macrocell radius, consequently inbound or outbound handover experience more interference than the handover between macrocells [58]. To use RSRP as the speed factor, obviously makes the handover experiences a higher interference condition, especially in the two-tier femtocell scenario. For instance, forthe RSRP as shown in Equation (5.7), when the UE is close to one neighbour cell, HAP increases quickly as well as RSRP. This means that hysteresis would decrease quickly and UE is easier to handover to the cell which may have higher interference. On the other hand, for SINR as shown in Equation (5.7), when the UE is close to one neighbour cell, the hysteresis would not decrease quickly if the target cell has higher interference. This means that UE would not be easily handover to the cell which has a higher interference and a worse QoS.

RSRP is not good at LTE femtocell system due to the heavy interference. SINR is a better parameter to be used in DUHA than RSRP.

RSRP is not good at LTE Femtocell system due to the heavy interference. SINR is a better parameter to be used in DUHA than RSRP.

5.2.5 Handover Aggregate Performance Indicator (HAPI)

It is complicated to satisfy three criteria together as it involves a multi-parameter optimisation issue. In order to evaluate the performance of proposed DUHA against the existing approach, this chapter proposed a Handover Aggregate Performance Indicator (HAPI), as the overall performance, for evaluation, as defined in Equation (5.19):

$$HAPI = W_1 \times H_{fr} + W_2 \times P_{pr} + W_3 \times C_{dr} + W_4 \times R_{hr} \tag{5.19}$$

$$W_1 + W_2 + W_3 + W_4 = 1 \tag{5.20}$$

R_{hr} represents the redundancy handover rate. It is defined as the ratio of the number of incorrect handover (handover to wrong cell) Nincorrent to and Nattempt which is the sum of the number of successful handover, the number of call-drop Ndropped and the number of incorrect handover Nincorrent as shown in Equation (5.21).

$$R_{hr} = \frac{N_{incorrect}}{N_{attempt}} \tag{5.21}$$

R_{hr} reflects the efficiency handovers in the network, thus according to MRO, the lower Rhr provides lower handover number rate and also offers lower associated signalling load for the network.

In Equation (5.19) and (5.20), the W_1, W_2, W_3 and W_4 are defined as weights and the sum of the values of them should be equal to 1. This is because of that, for instance, some of the systems would carefully consider ping-pong rather than RLF or call-drops and number of handovers. In that case, I can set the W_1, W_4 and W_3 with smaller values or set them to 0. If W_1, W_3 and W_4, W2 would be equal to 1, thus HAPI would be same as R_{hr}. In the other cases, W_1, W_3 and W_4 may set the value as 1 separately and correspondingly HAPI would represent H_{fr}, C_{dr} and R_{hr}.

The values of W_1, W_2, W_3 and W_4 would various but depend on the specific requirement. In this chapter, the scenario of normal LTE femtocell is considered, therefore, in general, W_1 should outweigh W_2 since RLF has more pronounced effect than ping-pong for user experience and introduces more signalling overhead [12, 60]. Call-drop has more prominent effect on system performance than RLF [12, 59], so W_3 should outweigh W_1. This is because when RLF occurs the UE can reconnect to a good quality cell instead, and therefore maintains the call connection. For the W_4, Rhr reflect the efficiency

handover ratio which is the third object in MRO as mentioned in Section 3.3.1, therefore the value of W4 should be smaller than W_3 and greater than W_1 and W_2.

Overall, the values of weights can be changed depending on the system requirements in order to achieve a better performance for specific system.

5.2.6 Proposed Hybrid Hysteresis Algorithm

There are two processes in DUHA, preparing process and optimising process. Preparing process is used to create the initial HAPI-RP table and optimising process is for updating the optimal hysteresis for system handover.

HAPI-RP Table

According to Equation (5.7) and (5.8) in Section 5.2.3, (5.7) and (5.8) can be transferred to Equation (5.22) and (5.23) in linear units, as shown below:

$$H_{high} \geq RP \times SINR_{target} \tag{5.22}$$

$$0 < RP \leq \frac{H_{high}}{SINR_{target}} \tag{5.23}$$

The range of SINR and H_{high} can be measured by the operators for the specific cell, thus the range of RP can be calculated by using these information from system. For instance, the H_{high} is 8 dB, the SINR is from -15 to 30 dB. The range of RP would be from -22 to 23 in dB units. Moreover, in dB units, since $HAP >= 0$, if $H_{high} - (RP + SINR) < 0$, the HAP will be set back to 0.

Once the system has determined the range of RP, the HAPI-RP table can be created in OAM database and the range of RP is the row ID to be saved in table. The HAPI values will be obtained from preparing process and optimising

process in proposed algorithm.

Proposed Algorithm in Handover Process

There are two processes have been proposed in the algorithm, preparing and optimising process.

Preparing Process: In this preparing process, the main goal is to train all RPs and obtain their initial corresponding HAPI in order to complete the initial HAPI-RP table in the OAM Database. The main process is described below:

1. Set the range of RP and H_{high} from experience of the cell system network as mentioned in the previous section. (OAM Database)

2. Create a HAPI-RP empty table. Record all RP values in the table as row IDs. This table needs to be stored on the cell (macro or femto) and then the system randomly chooses a RP from the recording to be $RP_{current}$. (OAM Database)

3. Send $RP_{current}$ and H_{high} to the UE via SIBs (Centralised MRO Function). The UE would use these two values and the measured receiving SINR to calculate the hysteresis value via Equations (5.7) and (5.8) (Distributed MRO Function). This hysteresis will be used to trigger an A3 event and the UE will require the serving cell to allow it to handover.

4. When the handover is completed, the UE reports the RLF and ping-pong effect by using an observed handover information report to the serving cell (Centralised MRO Function). At the cell side, the OAM system calculates the H_{fr}, P_{pr}, C_{dr} and R_{hr} depending on this report and provides the HAPI value by using Equation (5.6) (Hysteresis Algorithm Execution).

5. The OAM system calculates the HAPI based on observed handover information from the UE and records it in the HAPI-RP table. After a time period, the cell chooses another RP from the table row and seeks its

corresponding HAPI until training with all RP values in table has been finished. (Hysteresis Algorithm Execution)

6. Once the initial HAPI-RP table is completed, the preparing process stops; in the meanwhile the optimising process will start.

Optimising Process: In the optimising process, the main goal is to update $RP_{current}$ according to online the HAPI-RP table in order to have the online distributed optimal hysteresis for UEs.

1. According to the HAPI-RP table created in the preparing process, if the HAPI which corresponds to $RP_{current}$ is not the minimum value, then pick the $RP_{optimal}$ which corresponds to the minimum HAPI value in the table as the $RP_{current}$. Else, the $RP_{current}$ is not changed and its HAPI is trained and updated in the HAPI-RP table. (Hysteresis Algorithm Execution)

2. Send $RP_{current}$ and H_{high} to the UE via SIBs. The UE uses these two values to calculate HAP via Equation (5.7) (Distributed MRO Function).

3. After the UE obtains the HAP, the private hysteresis can be calculated using Equation (5.8) (Distributed MRO Function). In DUHA, the UE needs to use this hysteresis value into an A3 event which is represented in Equation (5.9). In an A3 event, the measured $RSRP_{serving}$, $RSRP_{target}$ and private hysteresis are used to trigger the event. If UE has a higher speed, which is evaluated by its changes of SINR, this hysteresis value decreases quickly, which is the same as $RSRP_{target}$ increasing quickly. Reflecting this, the A3 event is triggered early to avoid the LHO as the UE has higher speed. On the other hand, if the UE has a lower speed, this hysteresis value would decrease slowly, which is the same as the $RP_{current}$ increasing slowly to avoid the EHO and ping-pong effect.

4. In the case when an A3 event is triggered, the UE sends the handover request to the serving cell requesting a handover. The serving cell will decide whether to attempt the handover or not.

5. When the handover procedure is completed, the UE reports observed handover information to the serving cell, as mentioned in Section 5.2.3. The cell calculates the H_{fr}, P_{pr} and C_{dr} depending on this report and provides the HAPI value by using Equation (5.6). (Hysteresis Algorithm Execution)

6. Update the HAPI value in the table and check the HAPI, which corresponds to $RP_{current}$, if it is the minimum value. (Hysteresis Algorithm Execution)

7. Repeat the process from step 1 in optimising process.

The flowchart of the proposed algorithm including preparing and optimising processes is shown in Figures 5.10 and 5.11.

5.3 Simulation and Analysis

In this simulation, performance of HAPI, RLF ratio, ping-pong ratio and Call-drop ratio, for the centralised optimal hysteresis algorithm proposed in [59] and proposed DUHA in three different user mobility states are evaluated. These studies give an insight in the effects of various handover Hysteresis affect the system performance.

5.3.1 Simulation Description

In the simulation, one macro station and 20 femtocells are randomly located in the macrocell coverage. 300 UEs are randomly located in macrocell coverage area with random moving speeds. Since only inbound and outbound handover are considered in this algorithm, the handover between femtocells is not considered. Furthermore, the hysteresis is only considered in this chapter, thus the TTT will be set a constant value during the simulation. This chapter also assumes that each UE can easily decide its serving cell: either macro or femto and sets that the RLF occurs when SINR from serving cell drops below -6 dB

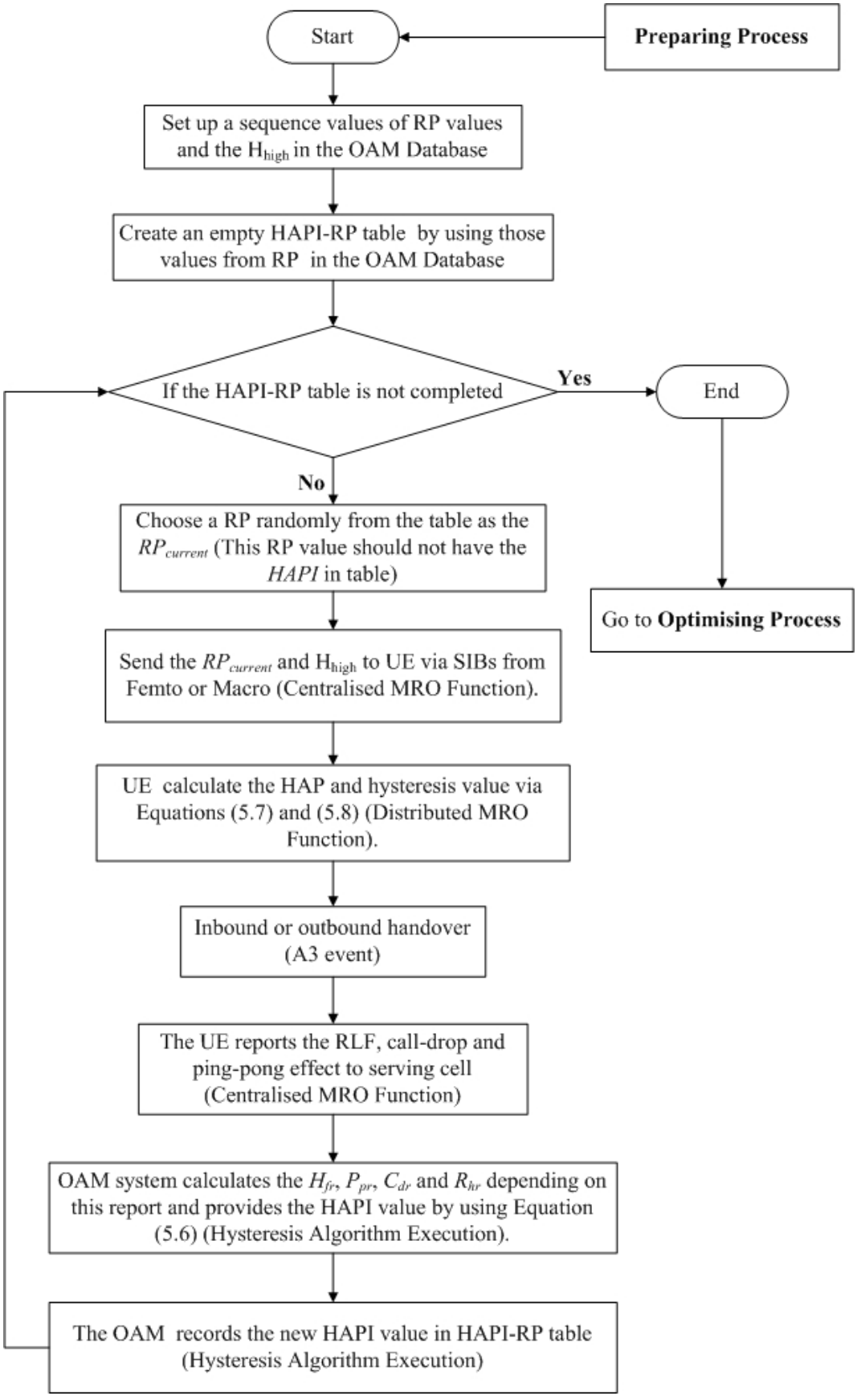

Figure 5.10: The flow chart of preparing process

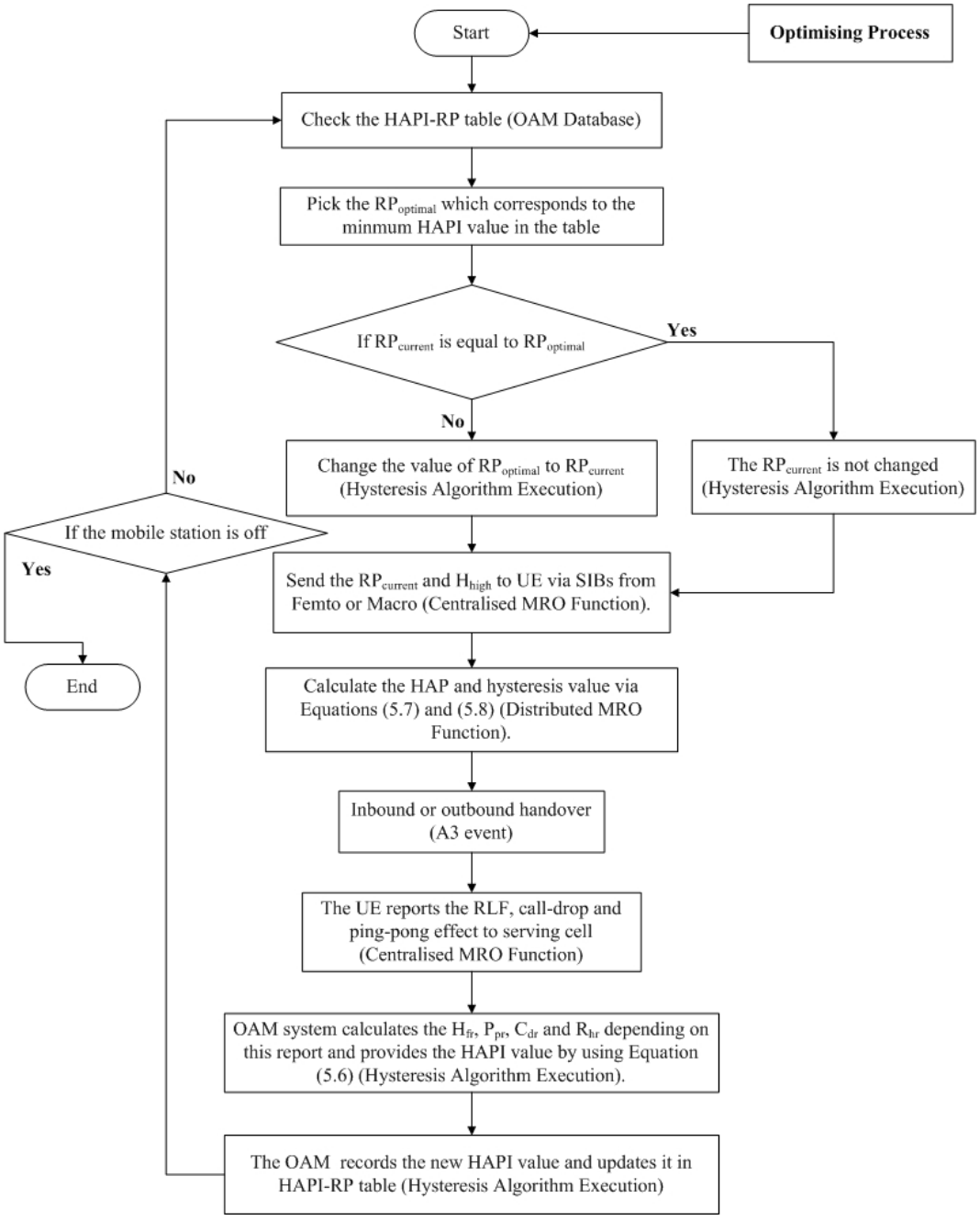

Figure 5.11: The flow chart of optimising process

Table 5.1: The Parameters in Real Dataset Simulation

Parameter	**Description**
System bandwidth	20 (MHz)
Macro/Femto transmit power	46/20 (dBm)
Macro/Femto radius	500/20 (m)
H_{high}	8 (dB)
Hysteresis	0, 1, 2, ..., 9, 10 (dB)
RP	-20, -19, ..., 25 (dB)
TTT	100 (ms)
Macro log-normal shadowing	Standard deviation: 8 (dB)
Femto log-normal shadowing	Standard deviation: 4 (dB)
Macro/Femto antenna gain	14/5 (dBi)
Macro path loss	$15.34+37.6 \times \log 10^(d[m])$
Femto path loss1	$38.46 + 20 \times \log 10^(d[m]) d \leq 20(m)$
Femto path loss2	$15.3 + 37.6 \times \log 10^(d[m]) d \geq 20(m)$
Macro/Femto noise figure	5/8 (dB)
High speed user mobility state	$10 < v \leq 14$ (km/h)
Medium speed user mobility state	$7 < v \leq 10$ (km/h)
Low speed user mobility state	$3 \leq v < 7$ (km/h)
UE's speed	$3 \leq v \leq 14$ (km/h)
UE moving pattern	straight
Call-drop criterion	SINR -6 (dB)

before the handover procedure completes [11]. The parameters for simulation are summarised in Table 5.2. These parameters are recommended by [74].

5.3.2 The trend of average hysteresis value in inbound handover

In the simulation, $W_1 = 0.2, W_2 = 0.1, W_3 = 0.5$ and $W_4 = 0.3$. Since the outbound handover is happened in randomly location within the coverage of macrocell, it is difficult to show the trend of changes of the average dynamic hysteresis value based on the macrocell (outbound handover). As illustrated in Figure 5.12, this result only shows the average dynamic hysteresis value of the UEs at different locations of the femtocell in inbound handover.

In Figure 5.12, the curve with circle points represents the hysteresis changes with the optimal RP and the optimal hysteresis value depends on the HAPI in

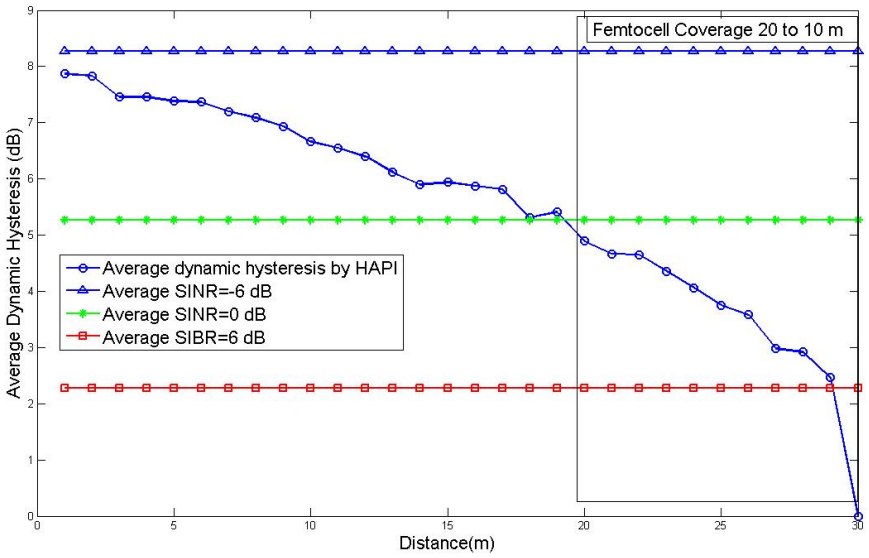

Figure 5.12: The trend of average UE hysteresis value in inbound handover

DUHA. The hysteresis value drops down faster when the UE is closer to the centre of femtocell. This is because when the UE is far away from the target cell, the receiving SINR from target cell changes smoothly. When the UE is closer to the target cell, the receiving SINR of this UE from target cell would increase violently.

Moreover, according to the optimal RP, it is able to draw three boundaries, such as early, late and critical. According to the Section 5.1.4, early handover boundary denotes the receiving SINR from target femtocell is lower than -6 dB. Therefore, it could calculate the hysteresis value when SINR= -6 dB via Equation (5.7) and (5.8). Similarly, this applies to late handover boundary SINR = 6 dB (received SINR from macrocell = -6 dB) and critical handover boundary SINR= 0 dB. Critical boundary represents the line of RSRPtarget is equal to PSRPserving. Due to the definition of hysteresis, in the ideal case, most of the handover should happen after this critical boundary.

According to Figure 5.12, it is obviously that using DUHA, the hysteresis is able to reach the higher value while the UE resides on earlycritical handover boundary in order to avoid EHO. Meanwhile, the hysteresis is able to reach

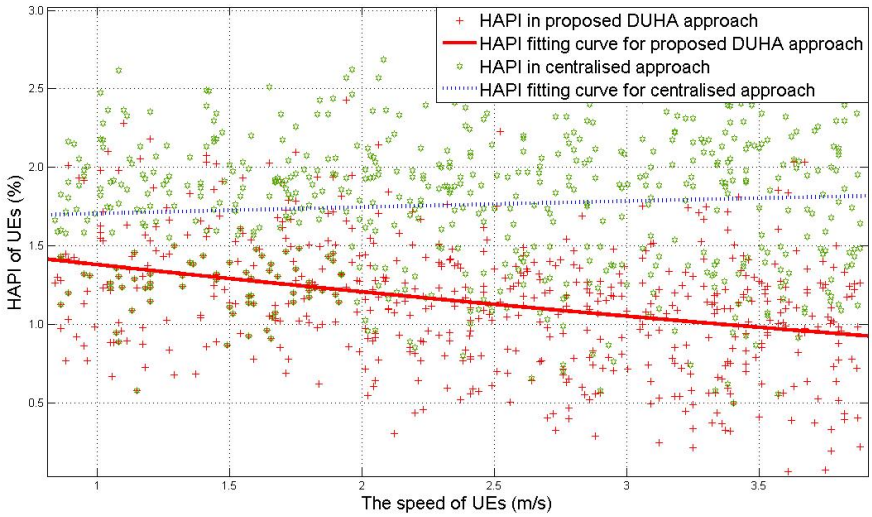

Figure 5.13: The HAPI of each UE in different speeds

the lower value while the UE is closed to the late handover boundary in order to avoid LHO.

5.3.3 HAPI without Redundancy Handover Ratio

When set the $W_4 = 0$, this means that scheme has the same equation as the conventional method proposed in [59] which only considers the redundancy handover ratio. According to [HandoverparameteroptimizationinLTEselforganizingnetworks], if $W_1 = 0.3, W_3 = 0.6$ and $W_2 = 0.1$, that means that RLF, call-drop and ping-pong effect are ordered by priority, thus the weight factors would be considered in normal LTE femtocell scenario as mentioned in Section 5.2.5. The results are shown in Figure 5.13 in three ranges of speed which are defined in the user mobility states.

In Figures 5.13, the solid and broken lines represent the HAPI fitting curve for centralised and DUHA approaches. Those lines are fitted from the HAPI points by using quadratic polynomial in Matlab. The results show that compared to the conventional methods (centralised optimal hysteresis algorithm), the proposed DUHA obviously improves the overall system performance. In the conventional methods, even if the hysteresis updates according to the per-

formance indicator of HAPI values, without taking into account the individual UE side speed factor, it only provides the centralised hysteresis for all UEs. However, in DUHA, every UE can have the distributed optimal hysteresis and performance would gain from every UE side. Reflecting above, it summarises that a compromised centralised hysteresis is to blame for declined overall system performance.

Furthermore, in three different user mobility states, the handover in higher speed user mobility state has better performance than other user mobility states. This result shows that DUHA has the higher ability to adjust hysteresis value. This is because that, for the DUHA, the hysteresis value is adjusted by SINR (UE speed factor). Therefore, if UE moves at a higher speed, the SINR and HAP would experience a higher drop, where $HAP = RP + SINR$ in dB unit. According to Equation (5.8), the HAP with a higher value changes leads the higher ability to adjust hysteresis value.

5.3.4 Result of Ping-pong Effect Metric is Measured

When $W_2 = 1$, this means that the ping-pong effect is the only factor to be considered in this scenario. The results during optimising process period are shown in Figure 5.14 and 5.15 with three different user mobility states.

In Figure 5.14 , it shows that the ping-pong ratio of each speed UE. Most of the UEs with lower speed have higher ping-pong ratio compared to the UEs with higher speed. This is because the lower speed may lead the UE to trigger the A3 event after TTT with received non- stable signal strength.

In Figure 5.15, it shows that compared to the conventional centralised method, the proposed DUHA does not quite improve the ping-pong effect in the three user mobility states (about 0.02%). This is because that hysteresis is not effective parameter to reduce the ping-pong effect issue compared to TTT. TTT is considered as the main factor to reduce the ping-pong ratio [58, 76].

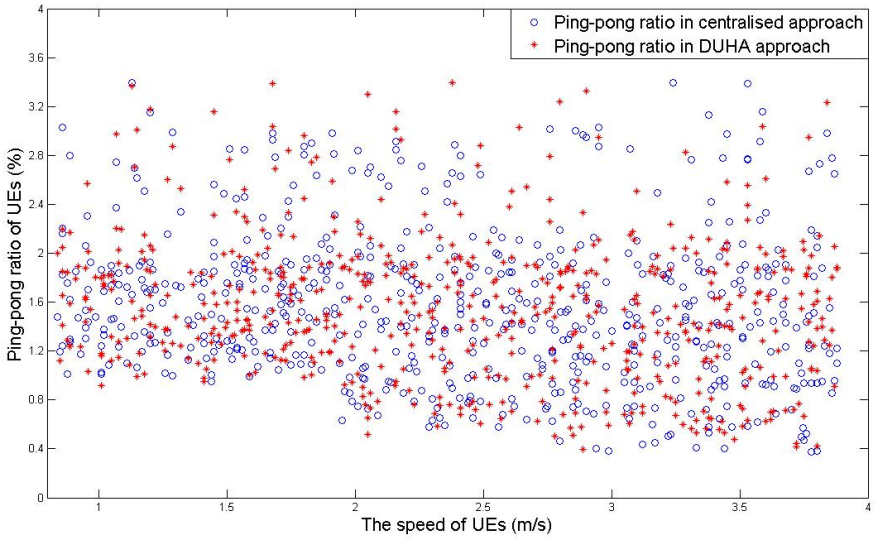

Figure 5.14: The ping-pong ratio of each UE in different speeds.

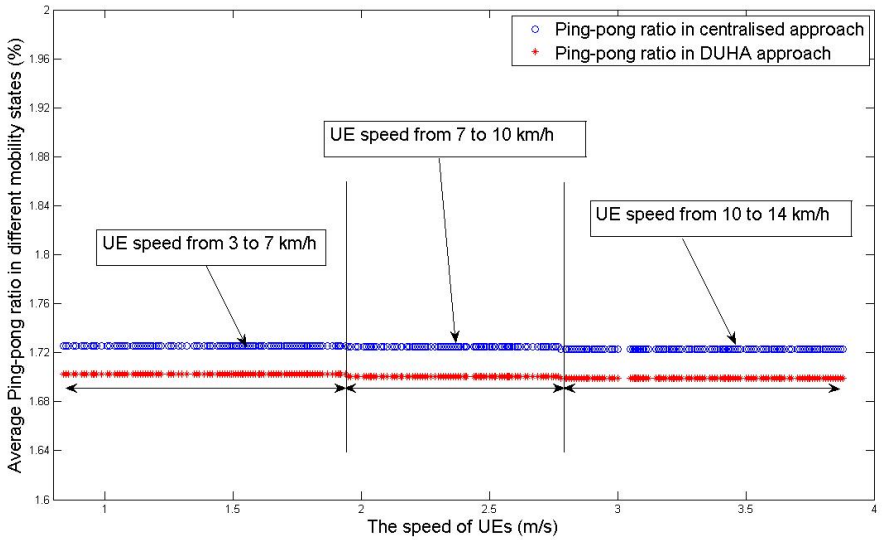

Figure 5.15: The average ping-pong ratio in different mobility states

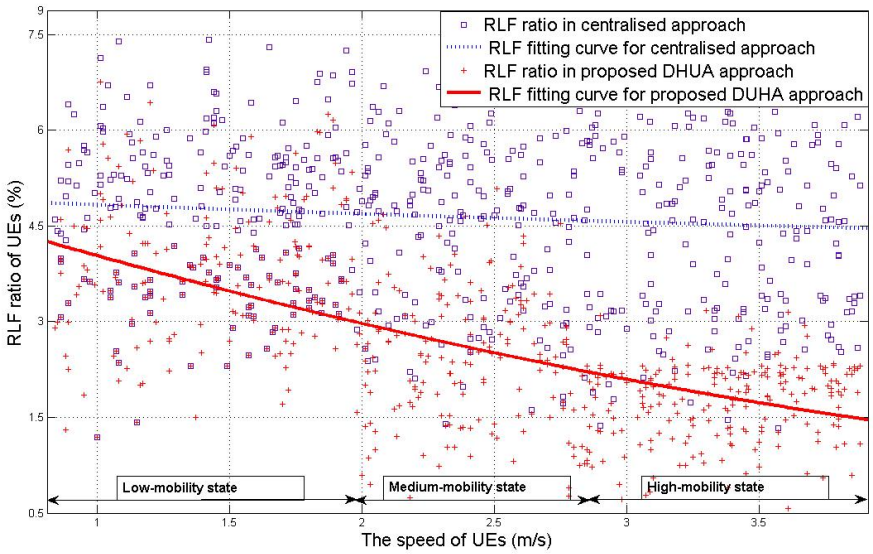

Figure 5.16: The RLF ratio of each UE in different speeds

5.3.5 Result of Radio Link Failure Metric is Measured

When set the $W_1 = 1$, this means the RLF is the only factor to be considered in this scenario. The results during optimising process period are shown in Figures 5.16 at three different user mobility states.

In Figures 5.16, the solid and broken lines represent the RLF ratio fitting curve for centralised and DUHA approaches. Those lines are fitted from the RLF ratio points by using quadratic polynomial in Matlab. The results show that compared to the conventional method, the proposed DUHA obviously improve the RLF performance up to 5%. This is because of that the optimal hysteresis value directly influent the EHO and LHO as mentioned in Section 5.1.4 and the faster changes of SINR (speed factor) values causes the higher ability to adjust hysteresis as mentioned in Section 5.3.2. In addition, since HAPI calculation takes into account of the ping-pong ratio, the RLF ratio performances better than the HAPI result.

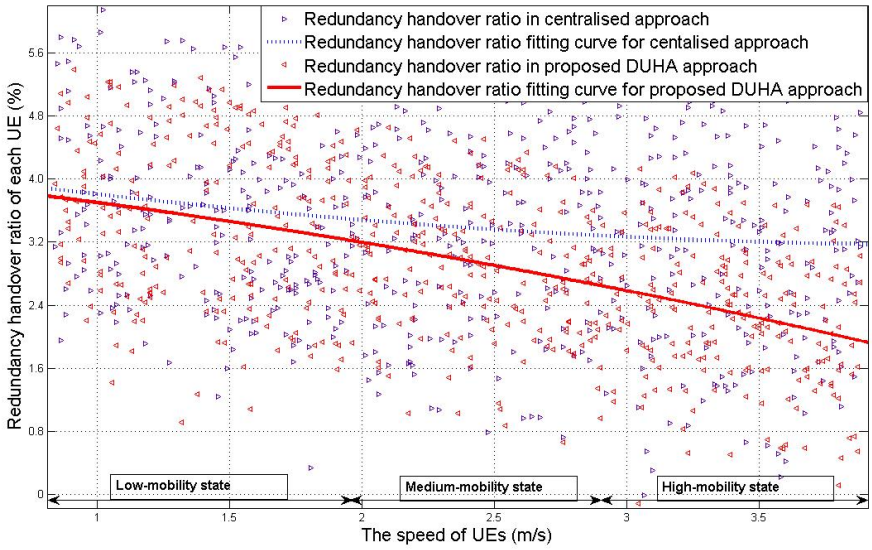

Figure 5.17: The redundancy handover ratio of each UE in different speeds

5.3.6 Result of Redundancy Handover Metric is Measured

When $W_4 = 1$, this means the redundancy handover ratio is the only factor to be considered in this scenario. The results during optimising process period are shown in Figures 5.17 at three different user mobility states.

In Figures 5.17 , the solid and broken lines represent the redundancy handover ratio fitting curve for centralised and DUHA approaches. Those lines are fitted from the redundancy handover ratio points by using quadratic polynomial in Matlab. Both of the solid and broken lines are reduced from the lower to higher speeds. This is because the UE may frequently receive the similar RSRP values from the neighbour cells due to its slow moving. As a result, those received RSRP leads UE has a higher chance to trigger the A3 event and handover to a wrong cell. In other words, when UE moves at a higher speed, the received RSRP from target cell and the other neighbour cell would be much different. As a result, UE would trigger the A3 event and handover to the target cell with higher signal strength.

Moreover, the Figure 5.14 also shows that compared to the conventional

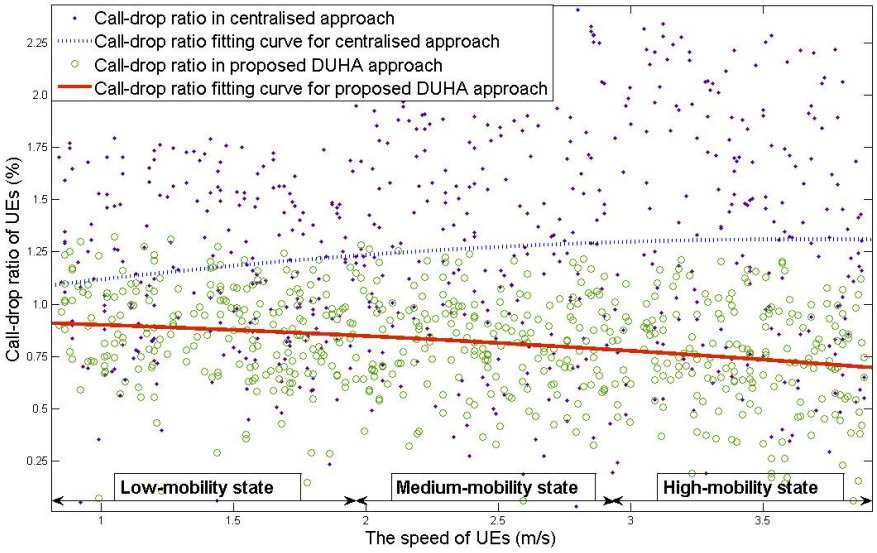

Figure 5.18: The call-drop ratio of each UE in different speeds.

method, although the DUHA has the similar performance with the centralised approach in the lower mobility state, the proposed DUHA obviously reduces the redundant handover ratio in the higher mobility state. This is because, in DUHA approach, when the UE with higher speed and close to the target cell, this leads the receiving SINR of the UE from target cell would increase violently. The increased UE's receiving SINR causes the optimal hysteresis decrease according to Equation (5.7), (5.8) and (5.9). This leads the UE easily triggers the A3 event and handover to the target cell compare to the other neighbour cell with a higher hysteresis.

5.3.7 Result of Call-Drop Metric is Measured

When $W_3 = 1$, this means the call-drop ratio is the only factor to be considered in this scenario. The results during optimising process period are shown in Figure 5.18 in three different user mobility states.

In Figures 5.18, the solid and broken lines represent the call-drop fitting curve for centralised and DUHA approaches. Those lines are fitted from the call-drop ratio points by using quadratic polynomial in Matlab. The results

show that compared to the conventional methods, the proposed DUHA obviously reduce the call-drop ratio. This is because reduction of RLF and incorrect handover causes unexpected handovers which consequently decreases the chance of call-drop. Moreover, most of the higher call-drop ratios happen in higher mobility states for the centralised approach and the degree of call-drop ratio reduction is not very obviously for the proposed DUHA. This is because when RLF and ping-pong effect or incorrect handover occur, the UE with higher speed is not easily to reconnect to the serving or target cell due to its receiving SINR is easier to drop lower than -6 dB.

5.4 Summary

In this chapter, DUHA algorithm is proposed to assist handover in the two-tier network for users moving at various speeds. It avoids the drawbacks of the conventional centralised hysteresis adjustment approach, as a hybrid approach which implements MRO functions requested in the standards. DUHA outperformed the existing approach with the feature of online unique hysteresis adjusting mechanism.

In addition, the simulation results also showed that, in different scenarios, the proposed DUHA has not only outperformed the existing approach with a less combined evaluation parameter HAPI but also provides a better RLF performance with a lower call-drop ratio. Furthermore, for these high speeds UEs, DUHA has higher ability to obtain the optimal hysteresis value than UE moving at a lower speed.

Chapter 6

Conclusions and Future Work

This chapter presents the conclusions consisting of a brief summary, answers to the research questions and contributions, and suggestions for future work.

6.1 Conclusions

6.1.1 Summary

Self-Organising Network (SON), as the new technology, not only reduces Operating Expenditure (OPEX) and Capital Expenditure (CAPEX), but also improves performance of the networks. In the two-tier network, since femtocells are randomly deployed by end users (femtocell is a plug-and-play device), SON structures are desired to be used in the algorithms developed in the LTE two-tier network.

In order to comply with SON, this thesis proposes the SON architecture, namely the centralised, hybrid and distributed architecture as well as its functions, particularly, Automated Configuration of Physical Cell Identity (ACPCI) and Mobility Robustness Optimisation (MRO) functions. In a centralised architecture, the SON Algorithm developed under the SON structure resides in the central controller which is able to control and monitor the overall network. In the distributed architecture, the SON algorithm controller resides in the individual wireless base station or UE which is able to respond faster to

network change or requirement than a centralised architecture. The selection of any particular architecture would depend on the specific approach.

ACPCI and MRO functions are used to support the implementation of the proposed approaches. In this thesis, three approaches are presented, Cell-based Perdition Model (CPM), Dynamic Group PCI Allocation Scheme (DGPAS), and Dynamic UE-based Hysteresis-adjusting Algorithm (DUHA).

The summary of each approach is as follows:

- **Summary of the Cell-based Perdition Model (CPM)**

  Being aware of the drawbacks of conventional UE-based Traffic Prediction Models (UTPM) implemented in the two-tier LTE femtocell scenario, Chapter 3 presents the CPM which can learn and predict the intensity of the handovers for femtocells. The proposed predictor is based on a HMM (Hidden Markov Model) to model the different intensities of handovers for a femtocell as observation states. Through using the learning and decoding functions in the HMM, the CPM can predict the femtocell's future handover situation. Both theoretical and real data based UE moving patterns have been used in the simulations. Their results show that the proposed CPM outperform the existing UTPM approaches with higher accuracy, precision, F1, sensitivity and specificity.

- **Summary of the Dynamic Group PCI Allocation Scheme (DGPAS)**

  The strategy of the proposed scheme is based on the different intensity of femtocell inbound-handovers and PCI groups to allocate specific PCIs to specific femtocells, in order to mitigate two-tier PCI confusions and avoid call-drop by reading the CGI. Since the proposed prediction model can be used to find the femtocells (BFemtocells) which have a higher intensity of femtocell inbound-handovers at next time period, it is desired to implement this predictor in proposed PCIs allocation scheme to determine those BFemtocells. Moreover, PCI is the key radio resource in the PCI allocation, so the idea of dynamic group is designed in the proposed

scheme. The PCIs are well managed by the PCI groups, e.g., unique and reused. In order to achieve the dynamic feature for the groups, the PCI release functions are also provided.

In addition, the proposed approach also complies with the centralised SON architecture and was implemented using ACPCI functions. The functions include necessary information transmitted between femtocells and the macrocell, including: knowledge of PCI confliction, control of PCI assignment in the network and a centralised controller in Operation Administration and Maintenance (OAM).

Both theoretical and real UE moving patterns have been implemented in the simulations. The results show that the proposed PCI allocation scheme outperforms the existing approach by reducing the frequency of CGI reading and also the possibility of handover failure.

- **Summary of the Dynamic UE-based Hysteresis-adjusting Algorithm (DUHA)**

  In chapter 5, the dynamic hysteresis-adjusting scheme is presented which complies with the hybrid MRO functionality to assist handover in two-tier networks for users moving at various speeds. Given the drawbacks of conventional centralised optimal hysteresis methods, this algorithm provides an optimal unique hysteresis value for each individual UE which moves at various speeds. The strategy of the proposed scheme is to use a combination of centralised and distributed functions to obtain the unique hysteresis for the UE: the centralised SON function offers the public parameter Revise Parameter (RP) to UEs; the distributed SON function depends on the RP and Reference Signal-Signal to Interference plus Noise Ratio (RS-SINR) to calculate the unique hysteresis value for the specific UE. The SON functions include necessary handover information transmitted between base stations and UEs, knowledge of ping-pong effect, RLF, redundancy handover and call-drop, full control of handover parameters such as hysteresis in the network, and a hybrid controller in

OAM.

Moreover, the combined evaluation parameter Handover Aggregate Performance Indicator (HAPI) is also proposed in the scheme to evaluate the overall handover performance. Users move at different speeds are modelled in the simulation, and results show that the proposed scheme has not only outperformed the existing approach with the HAPI, but also provides lower ping-pong effect, RLF, redundancy handover and call-drop ratios than the centralised hysteresis approach.

6.1.2 Answers to the Research Questions

The following summarises the answers to the research questions as proposed in Chapter 1.

1. **What is the traffic prediction in mobility management and why it is important for resource management in a network system? Moreover, what are the current prediction models and why should a novel traffic prediction model for the two-tier scenario be designed?**

   As described in Chapter 3, traffic prediction is used to predict future traffic situations, such as, the future handover, the future quality of channels and the future usage of the resource blocks etc., and depends on the current traffic behaviour. The predictive ability equips the femtocell with intelligence which provides a degree of proactive SON ability for the cell to optimise its network radio resource [17]. Therefore, it is desired to implement a kind of predictor for network radio resource self-optimisation in a two-tier scenario.

   The current traffic prediction model is UE-based and it models every cell that the UE has camped in as the states. This model is usually used in a single-tier scenario, for instance, a LTE network. Implementing this model in a two-tier scenario would cause many drawbacks, such as incorrect transition probability and would predict large and unmanageable

states, as mentioned in Chapters 2 and 3. Those drawbacks lead to lower accuracy due to the femtocell plug-and-play feature which is deployed in a large number of two-tier scenarios [20]. Reflecting this, this thesis proposes a CPM for a two-tier scenario.

2. **What is cell identity allocation and why it is important for the handover process? Moreover, how to design a centralised PCI distribution approach and to associate with the proposed novel traffic prediction model?**

   As described in Chapter 4, cell identity allocation includes PCI and CGI which are used to identify the cell. During the handover process, if PCI conflict occurs, the UE reports the target cell CGI to the serving cell. The serving cell then depending on that ID, communicates with the target cell via the X2 or S1 interfaces. However, to read the CGI of the target cell with connected model needs at least 150 ms from system information. During this fairly long time period, the handover process is easily triggered late and this leads to handover failure.

   Higher intensity of a femtocell's handovers represents the higher number of inbound handovers within that femtocell. Therefore, if allocating the unique PCI to those femtocells with higher intensity value, during the inbound handover process, the UE would not need to read the CGI of the targeted cell from system information. As a result, handover failure can be largely avoided.

   Since one of the core parts in the centralised PCI distribution approach is to find the different intensity level of the femtocell's handovers, the CPM proposed for a two-tier scenario in Chapter 3 is used to predict the handover situation for the femtocells in the network. Therefore, in the centralised PCI distribution approach, the CPM provides the information of the handover intensity level of the femtocells, then this information is associated with the PCI distribution approach.

3. **What are the handover triggering parameters and why are the**

parameters important for the handover process? In addition, what are the current hysteresis optimisation approaches and why design a hybrid hysteresis self-optimisation algorithm for a LTE femtocell network?

As described in Chapter 5, A3 event is the entry that allows the UE to send a handover measurement report and handover request to the serving cell. A3 event is triggered by handover trigger parameters, such as hysteresis and Time-To-Trigger (TTT). The optimal handover triggering parameters largely reduce handover failure from ping-pong effect, RLF and call-drop, thus the parameters are desired to be optimised for handover Quality of Service (QoS).

The current hysteresis optimisations are all centralised approaches, which means that the serving cell uses only one centrally determined hysteresis value for all the UEs to trigger a handover.

As the handover in two-tier scenarios differs from conventional LTE single-tier network, e.g. the coverage of the femtocell is much smaller than the macrocells, the handover between macrocell and femtocell experiences more severe Signal-to-Interference Noise Ratio (SINR) degradation than the handover between macrocells. Thus, as the UE moves at various speeds, it would more seriously suffer from the violent change of signal strength, and the centralised hysteresis value is not suitable for that individual UE. As a result, a unique optimal hysteresis should be provided to achieve better performance.

6.1.3 Contributions

The contribution of each approach is as follows:

- **Contribution of the Cell-based Perdition Model (CPM):** The cell-based perdition model is designed for LTE femtocell two-tier networks. It not only overcomes the drawbacks of the conventional UE-based prediction model, such as, incorrect transition probability matrix

and large and unmanageable state issues, but also provides an intelligence to present a thorough understanding of the future femtocell handover situation. This understanding could provide the necessary system information for SON to distribute the network resources carefully. As a result, CPM enhances the SON in a two-tier network system. Compared to the existing UTPM approaches, CPM can offer, particularly, higher accuracy (up to 97%) and also provide the best ability for both positive and negative perditions with higher precision, F1, sensitivity and specificity.

- **Contribution of the Dynamic Group PCI Allocation Scheme (DGPAS):** The dynamic group PCI allocation scheme is designed for LTE femtocell two-tier networks. It complies with a centralised ACPCI functionality proposed by standard [16] and introduces an optimal PCI assignment which offers a self-planning ability for PCIs allocation. This work ensures a higher ratio of successful handovers (an increase of about 40%) for the femtocells with higher intensity handovers. Therefore, this approach mitigates significantly the two-tier confusion issue in the inbound handover process and results in enhanced network performance overall in the two-tier scenario.

- **Contribution of the Dynamic UE-based Hysteresis-adjusting Algorithm (DUHA):** The dynamic UE-based hysteresis-adjusting algorithm is designed for LTE femtocell two-tier networks. It complies with a hybrid MRO functionality proposed by standard [12] and introduces a UE-side mobility consideration approach. Compared to conventional centralised optimal hysteresis methods which do not consider the UE speed the main factor causing the handover process the proposed approach provides a unique optimised hysteresis-adjusting mechanism for the UEs which suffer seriously from the violent change of signal strength at various speeds. This approach overcomes the drawbacks of the conventional methods and provides lower RLF (up to 5%), redundancy han-

dover and call-drop ratios. Moreover, in a high-speed user mobility state, the proposed approach can offer a higher ability to obtain the optimal hysteresis value for UEs than in a low-speed user mobility state.

Overall, the proposed approaches can significantly overcome the two-tier handover issues and offer better performance than conventional approaches in LTE femtocell two-tier networks.

6.2 Future Works

Two-tier LTE femtocell networks remains an interesting research area, especially in terms of inbound and outbound handovers. Although the proposed approaches can provide better performances than conventional methods, further research is required to improve the current works. The following outlines some thoughts on possible future works:

- **Extend the Cell-based Prediction Model**

  Chapter 3 proposed a CPM based on the normal Hidden Markov Model. The main challenges for the CPM is how to improve the ability for both positive and negative predictions. Therefore, in future work, the k-order HMM would be considered in this predictor.

  Moreover, this proposed CPM can offer the ability to support the system to obtain the future network radio resource requirement situation. This kind of feature is similar to the function of cognitive radio networks [38], thus, future work would be to extend prediction into the cognitive radio resources in order to achieve optimal radio resource management such as frequency distribution, power control etc.

- **Improve the Dynamic Group Physical Cell- identity Allocation**

  There are two main challenges in the proposed scheme, namely, the optimal time period to predict the future intensity of a femtocell's handovers

since a different time period would affect the perdition results. The optimal dynamic PCI release method due to the unique PCI is the key parameter in the proposed scheme.

Therefore, the work will be carried out on optimising the parameter time period and also to optimise the dynamic PCI release method to obtain the more unique PCI resource for network.

- **Enhance the Dynamic UE-based Hysteresis Optimisation**

  Since the current approach only considers the hysteresis value optimisation, the main challenge of the approach is to consider the TTT with hysteresis together. Therefore, in future, work, both TTT and hysteresis would be combined to achieve a hybrid dynamic TTT and hysteresis optimisation for inbound and outbound handovers. Moreover, the research work can be applied where inter-femtocell handovers are allowed, and is particularly desired in order to reduce non-necessary handovers.

In addition, recently, the small cell concept has been introduced, where in terms of the usages scenario, considering their sizes, small cells are clarified as femtocells, picocells, metrocells and microcells. In fact, the underlying technologies for these types of small cell are based on the femtocell technologies, and use the same standards, software, open interfaces and chipset technology. In addition, small cells also facilitate new applications of mobile services, such as location detection. Therefore, when talking about small cells, many standards and discussions are centred on femtocells. In which case, the research in this project can still be applied in the small-cell scenario.

References

[1] "LTE; Evolved Universal Terrestrial Radio Access (E-UTRA); Long Term Evolution (LTE) physical layer; General description," 3GPP ETSI TS 136 201, Tech. Rep., 2009, version 8.3.0, Release 8.

[2] "Lte:an introduction," ERICSSON, Tech. Rep., 2011, white paper. [Online]. Available: http://www.ericsson.com/res/docs/2011/lte_an_introduction.pdf

[3] "LTE; Evolved Universal Terrestrial Radio Access (E-UTRA); Physical channels and modulation," ETSI TS 136 211, Tech. Rep., 2010, version 9.1.0, Release 9.

[4] "Universal Mobile Telecommunications System (UMTS); Feasibility study for evolved Universal Terrestrial Radio Access (UTRA) and Universal Terrestrial Radio Access Network (UTRAN)," ETSI TR 125 912, Tech. Rep., 2008, version 8.0.0, Release 8.

[5] "Technical Report Universal Mobile Telecommunications System (UMTS); LTE; Requirements for Evolved UTRA (E-UTRA) and Evolved UTRAN (E-UTRAN)," ETSI TR 125 913, Tech. Rep., 2010, version 9.0.0, Release 9.

[6] J. Zhang and G. de la Roche, *Femtocells: Technologies and Deployment*, 1st ed. UK: John Wiley & Sons, Ltd., 2011. ISBN 1119965659, 9781119965657

[7] "3rd Generation Partnership Project; Technical Specification Group Radio Access Network; Evolved Universal Terrestrial Radio Access (E-

UTRA); Mobility enhancements in heterogeneous networks," 3GPP TR 136 839, Tech. Rep., 2012, version 11.0.0, Release 11.

[8] S. Yi, S. Chun, Y. Lee, S. Park, and S. Jung, *Radio Protocols for LTE and LTE-Advanced*, 1st ed. John Wiley & Sons, Ltd., 2012. ISBN 1118188551

[9] "Femtocellsarchitecture & netowrk aspects," QUALCOMM, Tech. Rep., 2010, white paper. [Online]. Available: https://www.google.co.uk/search?q=Femtocell+Device+Management+System&oq=Femtocell+Device+Management+System&aqs=chrome.69i57.711j0j4&sourceid=chrome&ie=UTF-8

[10] J. G. Andrews, H. Claussen, M. Dohler, S. Rangan, and M. C. Reed, "Femtocells: Past, present, and future," *Selected Areas in Communications, IEEE Journal on*, vol. 30, no. 3, pp. 497–508, Apr. 2012.

[11] "LTE; Evolved Universal Terrestrial Radio Access (E-UTRA); Requirements for support of radio resource management," 3GPP ETSI TS 136 133, Tech. Rep., 2011, version 10.4.0, Release 10.

[12] "Evolved Universal Terrestrial Radio Access Network (E-UTRAN); Self-configuring and self-optimizing network (SON) use cases and solutions," 3GPP ETSI TR 136 902, Tech. Rep., 2011, version 9.3.0, Release 9.

[13] H.-D. Bae, B. Ryu, and N.-H. Park, "Analysis of handover failures in lte femtocell systems," in *in Proc. IEEE Australasian Telecommunication Networks and Applications Conference (ATNAC)*, Melbourne, Australia, Nov. 2011, pp. 1–5.

[14] P. Legg, G. Hui, and J. Johansson, "A simulation study of lte intra-frequency handover performance," in *in Proc. IEEE 72nd Vehicular Technology Conference (VTC 2010-Fall)*, Ottawa, Canada, Sep. 2010, pp. 10–15.

[15] O. G. Aliu, A. Imran, M. A. Imran, and B. Evans, "A survey of self organisation in future cellular networks," *Communicatopns surveys & tutorials, IEEE*, pp. 336–361, Feb. 2012. ISSN 1553-877X

[16] "Self-optimizing networks: Benefits of son in lte," 4G Americas, Tech. Rep., 2011, white paper. [Online]. Available: http://www.4gamericas.org/documents/Self-Optimizing%20Networks-Benefits%20of%20SON%20in%20LTE-July%202011.pdf

[17] Y. Y. Li and E. S. Sousa, "Cognitive femtocell: A cost-effective approach towards 4g autonomous infrastructure," *Wireless Personal Communications*, vol. 64, no. 24, pp. 65–78, 2012. doi: 10.1007/s11277-012-0517-6

[18] H. Abu-Ghazaleh and A. S. Alfa, "Application of mobility prediction in wireless networks using markov renewal theory," *Vehicular Technology Society, IEEE Transactions on*, vol. 59, no. 2, pp. 788–802, Feb. 2010.

[19] H. Si, Y. Wang, J. yuan, and X. ming Shan, "Mobility prediction in cellular network using hidden markov model," in *in Proc. IEEE 7th Consumer Communications and Networking Conference (CCNC)*, Las Vegas, United States of America, Jan. 2010, pp. 1–5.

[20] G. F. Lawler, *Introduction to Stochastic Processes*, 2nd ed., ser. Chapman & Hall/CRC Probability. UK: Taylor & Francis Ltd., 2006. ISSN 158488651X

[21] "Universal Mobile Telecommunications System (UMTS); LTE; Non-Access-Stratum (NAS) protocol for Evolved Packet System (EPS); Stage 3," ETSI TS 124 301, Tech. Rep., 2011, version 10.3.0, Release 10.

[22] "The lte network architecture," alcatel-lucent, Tech. Rep., 2009, white paper. [Online]. Available: http://www.cse.unt.edu/~rdantu/FALL_2013_WIRELESS_NETWORKS/LTE_Alcatel_White_Paper.pdf

[23] "Long term evolution (lte):a technical overview," Motorola, Tech. Rep.,

2007, white paper. [Online]. Available: http://www.cse.unt.edu/~rdantu/FALL_2013_WIRELESS_NETWORKS/LTE_Alcatel_White_Paper.pdf

[24] Stefania, Sesia, I. Toufik, and M. Baker, *LTE The UMTS Long Term Evolution: From Theory to Practice*, 2nd ed. John Wiley & Sons, Ltd., 2011. ISBN 9780470978641

[25] "LTE; Evolved Universal Terrestrial Radio Access (E-UTRA) and Evolved Universal Terrestrial Radio Access network (E-UTRAN); Overall description; Stage 2," 3GPP ETSI TS 136 300, Tech. Rep., 2010, version 9.4.0, Release 9.

[26] "Self-optimizing networks in 3gpp release 11: The benefits of son in lte," 4G Americas, Tech. Rep., 2013, white paper. [Online]. Available: http://www.slideshare.net/zahidtg/self-optimizing-networksbenefits-of-son-in-lte-10713

[27] "3rd Generation Partnership Project; Technical Specification Group Services and System Aspects; Policy and charging control architecture," ETSI TS 123 203, Tech. Rep., 2010, version 8.9.0, Release 8.

[28] "Wireless backhaul solutions for small cells," Ceragon Networks, Tech. Rep., white paper. [Online]. Available: http://www.ceragon.com/images/Reasource_Center/Solution_Briefs/Ceragon_Solution_Brief_Wireless_Backhaul_Solutions_for_Small_Cells.pdf

[29] "LTE; Evolved Universal Terrestrial Radio Access (E-UTRA); Radio Resource Control (RRC); Protocol specification," ETSI TS 136 331, Tech. Rep., 2011, version 8.16.0, Release 8.

[30] S. Hamalainen, H. Sanneck, and C. Sartori, *LTE Self-Organising Networks (SON): Network Management Automation for Operational Efficiency*, 1st ed. John Wiley & Sons, Ltd., 2011. ISBN 978-1-119-97067-5

[31] J. Lim and D. hong, "Mobility and handover management for heterogeneous networks in lte adcanced," *Wireless Personal Communications*, vol. 72, no. 4, pp. 2901–2912, Oct. 2013.

[32] "NGMN recommendations on SON and O&M requirements," NGMN, Tech. Rep., 2008, white paper. [Online]. Available: http://www.ngmn.org/uploads/media/NGMN_Recommendation_on_SON_and_O_M_Requirements.pdf

[33] "Universal Mobile Telecommunications System (UMTS); LTE; Telecommunication management; Self-Organizing Networks (SON); Concepts and requirements," 3GPP ETSI TS 132 500, Tech. Rep., 2011, version 10.1.0, Release 10.

[34] "LTE; Telecommunication management; Key Performance Indicators (KPI) for the Evolved Packet Core (EPC); Definitions," ETSI TS 132 455, Tech. Rep., 2012, version 11.0.0, Release 11.

[35] H. Abu-Ghazaleh and A. S. Alfa, "Mobility prediction and spatial-temporal traffic estimation in wireless networks," in *in Proc. IEEE Vehicular Technology Conference (VTC)*, May 2008, pp. 2203–2207.

[36] S. Choi and K. G. Shin, "Adaptive bandwidth reservation and admission control in qos-sensitive cellular networks," *Parallel and Distributed Systems, IEEE Transactions on*, vol. 13, no. 9, pp. 882–897, Sep. 2002.

[37] S. Kwon, H. Park, and K. Lee, "A novel mobility prediction algorithm based on user movement history in wireless network," *Proceeding AsiaSim'04 Proceedings of the Third Asian simulation conference on Systems Modeling and Simulation: theory and applications*, pp. 419–428, Feb. 2005.

[38] I. Butun, A. C. Talay, D. T. Altlar, M. Khalid, and R. Sankar, "Impact of mobility prediction on the performance of cognitive radio networks," in *in Proc. IEEE Wireless Telecommunications Symposium (WTS)*, Tampa, USA, Apr. 2010, pp. 1–5.

[39] X. Xing, T. Jing, Y. Huo, H. Li, and X. Cheng, "Channel quality prediction based on bayesian inference in cognitive radio networks," in *in Proc. IEEE International Conference on Computer Communications (INFOCOM)*, Turin, Italian, 2013, pp. 1465–1473.

[40] "An introduction to markov chain monte carlo methods and their actuarial applications," Department of Mathematics and Statistics, University of Calgary, Tech. Rep., 2012. [Online]. Available: http://www.casact.org/pubs/proceed/proceed96/96114.pdf

[41] A. Gellert and L. Vintan, "Person movement prediction using hidden markov models," *Studies in Informatics and Control*, vol. 15, no. 1, pp. 17–30, Mar. 2006.

[42] W. Kang, D. Shine, and D. Shin, "Prediction of state of user's behaviour using hidden markov model in ubiquitous home network," in *in Proc. IEEE Industrial Engineering and Engineering Management (IEEM)*, Macao, China, May 2010, pp. 1752–1756.

[43] T. Bandh, G. Carle, and H. Sanneck, "Graph coloring based physical-cell-id assignment for lte networks," in *in Proc. ACM International Conference on Wireless Communications and Mobile Computing (IWCMC)*, Macao, China, Jun. 2009, pp. 116–120.

[44] F. Ahmed, O. Tirkkonen, M. Peltomaki, J.-M. Koljonen, C.-H. Yu, and M. Alava, "Distributed graph coloring for self-organization in lte networks," *Journal of Electrical and Computer Engineering*, vol. 2010, pp. 17–30, Jul. 2010. doi: 10.1155/2010/402831

[45] Y. Liu, W. Li, H. Zhang, and W. Lu, "Graph based automatic centralized pci assignment in lte," in *in Proc. IEEE Computers and Communications (ISCC), IEEE Symposium on*, Beijing, China, Jun. 2010, pp. 919–921.

[46] M. Amirijoo, P. Frenger, F. Gunnarsson, H. Kallin, J. Moe, and K. Zetterberg, "Neighbor cell relation list and physical cell identity self-

orgamization in lte," in *in Proc. IEEE International Conference on Communications (ICC)*, Beijing, China, May 2008, pp. 37–41.

[47] "LTE Home Node Bs and its enhancements in Release 9," Elie Saad Normor Research, Tech. Rep., 2010, white paper. [Online]. Available: http://www.nomor.de/uploads/fc/lp/fclpAIhtNJQ9zwyD957atQ/2010-05_LTE_HomeNB_Rel9_Overview.pdf

[48] D. Lopez-Perez, A. Valcarce, A. Ladanyi, G. de la Roche, and J. Zhang, "Intracell handover for interference and handover mitigation in ofdma two-tier macrocell-femtocell networks," *EURASIP Journal of Wireless Communications and Networking*, vol. 2010, Feb. 2010. doi: 10.1155/2010/142629

[49] A. Golaup, M. Mustapha, and L. B. Patanapongpibul, "Femtocell access control strategy in umts and lte," *IEEE Communications Magazine*, vol. 47, no. 9, Sep. 2009.

[50] ——, "Dynamic reservation scheme of physical cell identity for 3gpp lte femtocell systems," *Journal of Information Processing Systems, IEEE*, vol. 5, no. 4, May 2009.

[51] "3rd Generation Partnership Project; Technical Specification Group Radio Access Network; Mobility procedures for Home Node B (HNB); Overall description; Stage 2," ETSI TS 125 367, Tech. Rep., 2011, version 10.0.0, Release 10.

[52] T. Wu, L. Rui, A. Xiong, and S. Guo, "An automation pci allocation method for enodeb and home enodeb cell," in *in Proc. IEEE Wireless Communications Networking and Mobile Computing (WiCOM)*, Chengdu, China, Sep. 2010, pp. 1–4.

[53] Y. Wu, H. Jiang, Y. Wu, and D. Zhang, "Physical cell identity self-organization for home enodeb deployment in lte," in *in Proc. IEEE Wire-*

less Communications Networking and Mobile Computing (WiCOM) Meeting, Beijing, China, Sep. 2010, pp. 1–6.

[54] S. Kwon and N.-H. Lee, "Virtual extension of cell ids in a femtocell environment," in *in Proc. IEEE Wireless Communications and Networking Conference (WCNC)*, Cancun, Mexico, Mar. 2011, pp. 428–433.

[55] M. Anas, F. D. Calabrese, P. E. Mogensen, C. Rosa, and K. I. Pedersen, "Performance evaluation of received signal strength based hard handover for utran lte," in *in Proc. IEEE Vehicular Technology Conference (VTC)*, Dublin, Ireland, Apr. 2007, pp. 1046–1050.

[56] Z. Liu, P. Hong, K. Xue, and M. Peng, "Conflict avoidance between mobility robustness optimization and mobility load balancing," in *in Proc. IEEE Global Telecommunications Conference (GLOBECOM)*, Miami, FL, Dec. 2010, pp. 1–5.

[57] M. Kazmi, O. Sjobergh, W. Muller, J. Wiorek, and B. Lindoff, "Evaluation of inter-frequency quality handover criteria in e-utran," in *in Proc. IEEE Vehicular Technology Conference (VTC)*, Miami, USA, Apr. 2009, pp. 1–5.

[58] Y. Lee, B. Shin, J. Lim, and D. Hong, "Effects of time-to-trigger parameter on handover performance in son-based lte systems," in *in Proc. IEEE 16th Asia-Pacific Conference on Communications (APCC)*, Auckland, New Zealand, Nov. 2010, pp. 492–496.

[59] T. Jansen, I. Balan, J. Turk, I. Moerman, and T. Kurner, "Handover parameter optimization in lte self-organizing networks," in *in Proc. IEEE 72nd Vehicular Technology Conference (VTC2010-Fall)*, Ottawa, Canada, Sep. 2010, pp. 1–5.

[60] S. S. Mwanje, N. Zia, and A. Mitschele-Thiel, "Self-organized handover parameter configuration for lte," in *in Proc. IEEE Wireless Communication Systems (ISWCS)*, Paris, France, Aug. 2012, pp. 26–30.

[61] J.-M. Fran, "Performing and making use of mobility prediction," University of Liege, Tech. Rep., 2007. [Online]. Available: ftp://ftp.run.montefiore.ulg.ac.be/pub/RUN-BK07-01.pdf

[62] D. Katsaros and Y. Manolopoulos, "Prediction in wireless networks by markov chains," *Wireless Communications, IEEE Transactions on*, vol. 16, no. 2, pp. 56–64, Apr. 2009.

[63] G. Kochanski, "Markov models, hidden and otherwise," Tech. Rep., 2005. [Online]. Available: http://kochanski.org/gpk/teaching/0401Oxford/HMM.pdf

[64] L. Song, D. Kotz, R. Jain, and X. He, "Evaluating location predictors with extensive wi-fi mobility data," in *in Proc. IEEE the 23rd Annual Joint Conference of the IEEE Computer and Communications Societies (INFO- COM)*, Mar. 2004, pp. 1414–1424.

[65] T. Slater, "Basic queueing theory," Tech. Rep., 2000. [Online]. Available: http://homepages.inf.ed.ac.uk/jeh/Simjava/queueing/index.html

[66] L. R. .Rabiner and B. H. Juang, "An introduction to hidden markov models," *ASSP Magazine, IEEE Transactions on*, vol. 3, pp. 4–16, 1986.

[67] J. Lafferty, A. McCallum, and F. C. Pereira, "Conditional random fields: Probabilistic models for segmenting and labelling sequence data," in *in Proc. the Eighteenth International Conference. on Machine Learning, Morgan Kaufmann*, Jun. 2001, pp. 282–289.

[68] Z. Lu, D. Szafron, R. Greiner, P. Lu, D. Wishart, B. Poulin, J. Anvik, C. Macdonell, and R. Eisner, "Predicting subcellular localization of proteins using machine-learned classifiers," *Journal Bioinformatics*, vol. 20, no. 4, Mar. 2004.

[69] "Crawdad data set st andrews/locshare accessed 18nd june 2013," CRAWDAD, Tech. Rep., database. [Online]. Available: http://www.citeulike.org/user/theshadowhost/article/10103173

[70] "LTE; Evolved Universal Terrestrial Radio access (E-UTRA); User equipment (UE) procedures in idle mode," ETSI TS 136 304, Tech. Rep., 2010, version 9.1.0, Release 9.

[71] "3rd Generation Partnership Project; Technical Specification Group Core Network and Terminals; Numbering, addressing and identification," ETSI TS 123 003, Tech. Rep., 2009, version 9.1.0, Release 9.

[72] "3rd Generation Partnership Project; Technical Specification Group Services and System Aspects; Telecommunication management; Study of Self-Organizing networks (SON) related Operations, Administration and Maintenance (OAM) for Home Node B (HNB)," ETSI TR 132 821, Tech. Rep., 2009, version V9.0.0, Release 9.

[73] "3gpp femtocells: Architecture & protocol," QUALCOMM, Tech. Rep., 2011, white paper. [Online]. Available: http://www.slideshare.net/allabout4g/3gpp-femtocells-architecture-and-protocols

[74] "Simulation assumptions and parameters for FDD HeNB RF requirements," 3GPP TSG RAN WG4 (Radio) Meeting # 51, R4-092042 2009, Tech. Rep., 2009, alcatel-Lucent, picoChip Designs, Vodafone.

[75] "Physical layer measurements in 3gpp lte," Aalborg University, Tech. Rep., 2012, white paper. [Online]. Available: http://projekter.aau.dk/projekter/files/60737111/diplom.pdf

[76] "3rd Generation Partnership Project; Technical Specification Group Radio Access Network; Improved Network Controlled Mobility between E-UTRAN and 3GPP2/Mobile Wimax Radio Technologies," ETSI TR 136 938, Tech. Rep., 2008, version 8.0.0, Release 8.

[77] A. V. Rial, H. Krauss, J. Hauck, M. Buchholz, and F. A. Agelet, "Empirical propagation model for wimax at 3.5 ghz in an urban environment," *Wiley Microwave and Optical Technology Letters*, vol. 50, no. 2, pp. 483–487, Feb. 2008.

[78] "Next generation mobile networks radio access performance evaluation methodology," NGMN, Tech. Rep., 2008, white paper. [Online]. Available: http://www.ngmn.org/uploads/media/NGMN_Radio_Access_Performance_Evaluation_Methodology.pdf

[79] L. Haring, B. K. Chalise, and A. Czylwik, "Dynamic system level simulations of downlink beamforming for umts fdd," in *in Proc. IEEE Global Telecommunications Conference (GLOBECOM '03)*, vol. 1, Dec. 2003, pp. 492–496. doi: 10.1109/GLOCOM.2003.1258286

[80] E. Dahlman, S. Parkvall, J. Skold, and P. Beming, *3G EVOLUTION HSPA and LTE for Mobile Broadband*, 2nd ed. Elsevier Ltd., 2008. ISSN 0123745381

[81] "LTE; Evolved Universal Terrestrial Radio Access (E-UTRA); Physical layer procedures," 3GPP TS 136 213, Tech. Rep., 2012, version 10.6.0, Release 10.

Appendix A

System-Level Simulation (SLS)

This System-Level Simulation (SLS) tool has been designed by the Centre for Wireless Network Design (CWiND) group since 2010. It has been provided to evaluate the performance of the self-organising network for LTE and LTE femtocell. Since author of the thesis was in CWiND at 2010, he has chance to learn and use this tool.

In SLS, a series of events are modelled as the life' of the network through time [77, 78]. For instance, when a user connects to the network, a UE changes its current position or handover to a cell, an optimisation procedure is triggered in the network, they all can be modelled as the events.

Each event can easily obtain the data from the simulator configuration and also be implemented in the simulation process. The SLS has the main thread process system which can be modified by the research. Moreover, the main process and those events (branch process) are independent threads. Therefore, the research can only change the main process without modifying any events. Each event can report the results to either the main process or the final output.

In SLS, it includes three main blocks, the network configuration, the simulator execution and the output collection. The more detail of those blocks are described below.

A.1 The Network Configuration Block

In the SLS, the network configuration block is used to store the basic modelling and functions which are listed below:

- Traffic behaviour modelling
- Path loss modelling
- Shadow fading modelling
- Signal strength modelling
- Signal quality modelling
- Channel quality indicators
- Throughput modelling
- Neighbourhood modelling
- UE measurement report function
- Network structure modelling

A.1.1 Traffic Behaviour Modelling

In SLS, it has three default traffic behaviour models:

- In each cell, a fix number of User Equipments (UEs) are uniformly distributed within its coverage. Those UEs stay in the network from beginning to end of simulation.
- In each cell, a fix number of UE are uniformly distributed within its coverage. Different from the previous one, there is a holding time that set for every UE. If the time expires, this UE would disappear and a new one would be generated at different location.

- In each cell, a various number of UE are uniformly distributed with its coverage. The number of users is generated in a period of time T, through the homogeneous Poisson process [79].

$$P[N(t+T) - N(t) = N_u] = \frac{(\lambda \cdot T)^{N_u} \cdot e^{-\lambda \cdot T}}{N_u!} \tag{A.1}$$

where N_u is the number of UEs appear and locate in the network. $\lambda \cdot T$ is the mean users' arrival ratio, also known as process intensity'. Moreover, the holding time t_h is provided by exponential distribution (a.k.a. negative exponential distribution). This distribution is described as:

$$f(t_h) = \mu \cdot e^{-\mu \cdot t_h} \tag{A.2}$$

where μ is the mean holding time of users.

A.1.2 Path Loss Modelling

In SLS, it has four default path loss models for LTE:

In terms of macrocell environment, two different models have been used.

- Firstly, this path loss model is recommended by [78], it is an empirical model and works at 2.0 GHz. It can be described in meters unit as:

$$Lp[dB] = 15.34 + 37.6 \cdot \log 10^(d[m]) + W_n \cdot W_L(indoorscenario) \tag{A.3}$$

$$Lp[dB] = 15.34 + 37.6 \cdot \log 10^(d[m])(outdoorscenario) \tag{A.4}$$

where d represents the distance in meter between transmitter and receiver. W_L denotes the mean wall penetration loss and Wn denotes the number of walls.

- Secondly, this path loss model is recommended by [77], it is an empirical

model and works at 3.5 GHz, it can be described in meters units as:

$$Lp[dB] = 15.46 + 39.11 \cdot \log 10^(d[m]) + W_n \cdot W_L(indoorscenario) \quad \text{(A.5)}$$

$$Lp[dB] = 15.46 + 39.11 \cdot \log 10^(d[m])(outdoorscenario) \quad \text{(A.6)}$$

where d represents the distance in meter between transmitter and receiver. W_L denotes the mean wall penetration loss and Wn denotes the number of walls.

In terms of femtocell environment, two different models have been used.

- Firstly, this path loss model is recommended by [74], it works for any frequency except 3.5 GHz. It can be described in meters unit as:

$$Lp[dB] = 38.46 + 20 \cdot \log 10^(d[m]) + 0.7 \cdot d_{min}(indoorscenario) \quad \text{(A.7)}$$

$$Lp[dB] = 38.46 + 20 \cdot \log 10^(d[m]) + 0.7 \cdot d_{min} + W_n \cdot W_L(outdoorscenario) \quad \text{(A.8)}$$

  where d_{min} denotes the minimum distance in meter between transmitter and receiver

- Secondly, this path loss model is determined as Finite-Difference Time-Domain (FDTD) based model. It works on frequency 3.5 GHz and it is based on Maxwell's equations and calibrated with indoor-to-outdoor measurement.

A.1.3 Shadow Fading Modelling

In SLS, the shadow fading between transmitter and the receiver is modelled as the log-normal distribution with the zero mean and different standard deviations σ_s^2.

$$Ls[dB] = \log N(0, \sigma_s^2) \tag{A.9}$$

This shadowing loss complements the path loss and hence they multiply each other. However, this shadowing model does not apply to the Finite-Difference Time-Domain (FDTD) propagation model, due to this model is based on Maxwell's equations which already predicts the shadow effects [6].

A.1.4 Signal Strength Modelling

To assume that the Cell M_m is transmitting to its connected UE U_n in sub-channel k. the strength of the carrier signal received by UE from its serving cell in sub-channel k is modelled as (linear unit):

$$W_{n,k}^m = \frac{P_{m,k} \cdot g_m \cdot g_n}{l_{m,n} \cdot Ls_{m,n}} = P_{m,k} \cdot Cg_{m,n} \tag{A.10}$$

where $W_{n,k}^m$ is the signal strength the UE received from the cell, $P_{m,k}$ the power applied by cell M_m to each of the subcarriers of sub-channel k, $l_{m,n}$ represents the path loss between cell M_m and UE U_n. $Ls_{m,n}$ represents the shadowing between cell M_m and user U_n. The g and l stand for the antenna gains and equipment loses, respectively. The $Cg_{m,n}$ denotes the channel gain between macrocell M_m and Un.

A.1.5 Signal Quality Modelling

The signal quality in terms of SINR $\gamma_{n,k}$ of UE U_n in sub-channel k is thus modelled as:

$$\gamma_{n,k} = \frac{W_{n,k}^m}{W_{n,k}^u + \sigma^2} \tag{A.11}$$

Table A.1: A part of CQI and Modulation and Coding Schemes

CQI indez	Modulation	Code rate x1024	Efficiency
1	QPSK	78	0,1523
2	QPSK	120	0.2344
3	QPSK	193	0.3770
4	QPSK	308	0.6016
5	QPSK	449	0.8770
6	QPSK	602	1.1758
7	16QAM	378	1.4766
8	16QAM	490	1.9141
9	16QAM	616	2.4063
10	64QAM	466	2.7305

Where $W^m_{n,k}$ is the signal strength of UE U_n received in sub-channel k and $W^u_{n,k}$ is sum of the signal strength the U_n received from other macrocell M_u (inter-cell interference). σ^2 is the background noise density.

In SLS, it is assumed that the σ^2 is an additive white Gaussian noise which is a zero-mean Gaussian process and its variance equals the sum of the powers received from all surrounding cells.

A.1.6 Channel Quality Indicators

To calculate the channel quality indicator $C_{n,k}$ of UE U_n in sub-channel$k$ is modelled as:

$$C_{n,k} = F_{map}(SINR_{n,k}) \tag{A.12}$$

F_{map} is a monotonically increasing function, which means that the higher SINR brings higher Channel Quality Indicator (CQI) value and indicates lower interference of the target channel [80].

CQI is an indicator carrying the information on how good/bad the communication channel quality is. In the LTE system, there are 15 different CQI values which are from 1 to 15 and mapping between CQI and modulation scheme as defined in Table A.1 [81].

Efficiency is defined as ratio of information (data) bits per symbol. Due

to channel fading, in order to ensure a lower of Bit Error Ratio (BER), in the standard [81], modulation process sets some redundancy symbols which ensure the resource element cannot achieve the maximum transfer data. As shown in Table A.1, there are 6 efficiency values within the same modulation type, this is because that the same modulation can also offer the different information bits per resource element depends on CQI value.

Code rate x1024 is defined as how many effective modulation symbols can be transmitted when transmitted 1024 symbols. For instance, when CQI value is 1, the code rate can be calculated as 0.1523*1024/2=78%, which the 2 is the QPSK maximum transfer bits per resource element.

A.1.7 Throughput Modelling

To calculate the throughout $TP_{n,k}$ (bits/sec) of user U_n in sub-channel k when using Modulation and Coding Scheme (MCS) is modelled as:

$$TP_{n,k} = TBS_{n,k} \cdot 1000 \tag{A.13}$$

Where $TBS_{n,k}$ denotes the Transport Block Size which is the transport resource block per sub-frame (1 transport resource block per sub-frame = 2 resource blocks) in LTE [80].

The TBS is determined by the MCS index and MCS is determined by CQI. MCS is a table which store the modulation and coding information. In SLS, the cell uses CQI value to select modulation type from Modulation and TBS index table as shown in Table A.2 and the modulation type will be informed UE. After the information has been received, the UE would change its modulation type to achieve the lower BER.

A part of TBS table is shown in Table A.3 [81], N_{PRB} denotes the number of transport Resource Blocks (RBs) per sub-frame.

According to Equation (A.13), to calculate throughput, if the bandwidth is 20 MHz, 10% of 20MHz is used as guard band, thus the effective bandwidth will be 18 MHz. Since a sub-carry is 15 KHz, thus there are 1200 sub-carries

Table A.2: A part of Modulation and TBS index table for PUSCH

MCS Index	Modulation Order	TBS Index
0	2	0
1	2	1
2	2	2
3	2	3
4	2	4
5	2	5
6	2	6
7	2	7
8	2	8
9	2	9

Table A.3: A Part of Transport Block Size Table

TBS Index \N$_{PRB}$	91	92	93	94	95	96	97	98	99	100
0	2536	2536	2600	2600	2664	2664	2728	2728	2728	2792
1	3368	3368	3368	3496	3496	3496	3496	3624	3624	3624
2	4136	4136	4136	4264	4264	4264	4392	4392	4392	4392
3	5352	5352	5352	5544	5544	5544	5736	5736	5736	5736
4	6456	6456	6712	6712	6968	6968	6968	6968	6968	7224
5	7992	7992	8248	8248	8248	8504	8504	8760	8760	8760
6	9528	9528	9528	9912	9912	9912	10296	10296	10296	10296

and 100 RBs (1 RB has 12 sub-carries). If MCS index is 0, look up table, we got the bits value 2792. The hole bandwidth throughput is 2792*1000=2792000 bits/sec and $2792 * 1000 \div 1000000 = 2.792$ Mbits per sec. The average sub-channel throughput is $2.792 \div N_k$ Mbits per sec where N_k is the number of sub-channels.

A.1.8 Neighbourhood Modelling

There are three different neighbourhood models in SLS.

1. Neighbourhood cells. The coverage of the neighbouring cells are adjacent disjoint. In SLS, this model is used in Macro scenario.

2. Overlap neighbourhood cells. The coverage of the neighbouring cells are overlap by their coverage. In SLS, this model is used in macro and femto scenario.

3. Non-neighbourhood cells. The neighbouring cells are not adjacent. In SLS, this model is used in macro-femto scenario.

A.1.9 UE Measurement Report Function

During the cell selection and handover procedures, the Physical Cell Identities (PCIs) are used to identify the different neighbouring cells. However, due to the limitation of the number of PCI, the confusion and collision problems occur and impact the performance of the network. (The more information about PCI problem, please check Section 4.1.2)

In order to avoid confusion or collision, In SLS, it denotes that each UE should report the PCIs of the nearby cells by using Measurement Report (MR) to its serving cell. Then this cell can either change its PCI or report this confusion or collision to the Mobility Management Entity (MME). MME could change the PCIs for those cells which are involved in the confusion or collision.

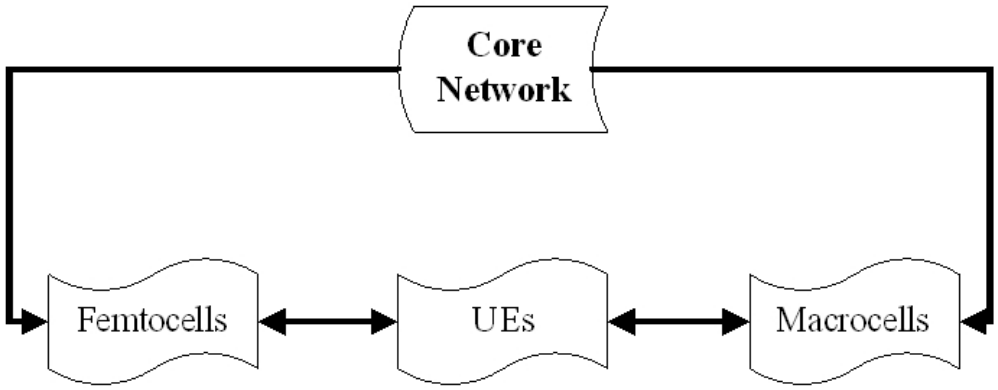

Figure A.1: The structure of the network in system-level simulation

A.1.10 Network Structure Modelling

There are four different network layers in this simulator, such as macrocell, femtocell, UE and core network layer.

As shown in Figure A.1, macrocell layer contains all the activities for the macrocells. Femtoocell layer contains all the activities for the femtocells. UE contains all the activities for the UEs. Core network layer is used to control the entire network and also achieve the communication interface (Section 5.1.1) between macrocell and femtocell. MME is the function that manages the handover, PCI distribution in the core network.

A.2 The Output Collection Block

Each result is collected in this block and output as the XML file. The XML file is imported into Matlab for analysis and to draw the figure and analysis. Moreover, since different approach needs to be simulated in different scenarios and have different output data, the structure of elements in the XML would be different.

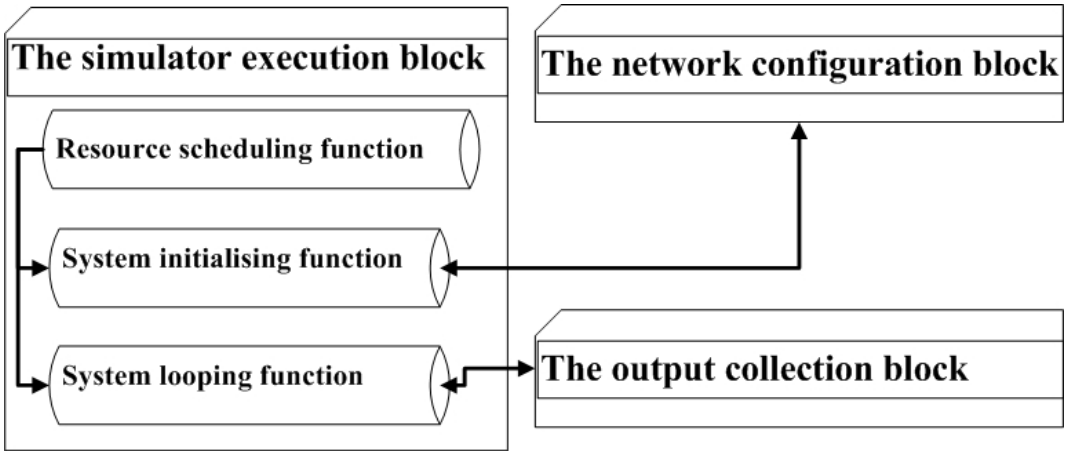

Figure A.2: The relationship of the function blocks in system-level simulation

A.3 The Simulator Execution Block

This block consist three main functions, such as system initialising, system looping and resource scheduling function. The relationship between this block and configuration block is shown in Figure A.2.

In the Figure A.2, resource scheduling function is used to setup the main process and manage the other functions or events in the simulation to implement the proposed approach. System initialising function is used to import the system parameters to the network configuration block. Since the main process of the simulator is the looping process, the looping function would obtain the functions from the network configuration block and meanwhile, provides the results and send to the output collection block. The details of simulation process in this thesis will be described in Appendix B.

Appendix B

Simulations in This Thesis

This section will introduce the simulations for each chapter.

The following assumptions are made in order to evaluate the performance of the system analytically without the loss of generality.

- Hexagonal base station sites (Femtocell or Macrocell) placed at the centre of each hexagon.
- The simulation scenario only considered one Macrocell with many Femtocells due to the research focus on the inbound handover.
- Propagation model is based on 2.0 GHz.
- This thesis only considers the handover simulation. Hence, in the simulation of each chapter, there is always data available to be transmitted to all users and each cell is fully loaded and it does not consider the multiply antenna system (MIMO).
- The sub-channel bandwidth is smaller than the coherence bandwidth, in order to achieve the fading of all subcarriers within a sub-channel due to multipath is constant and flat

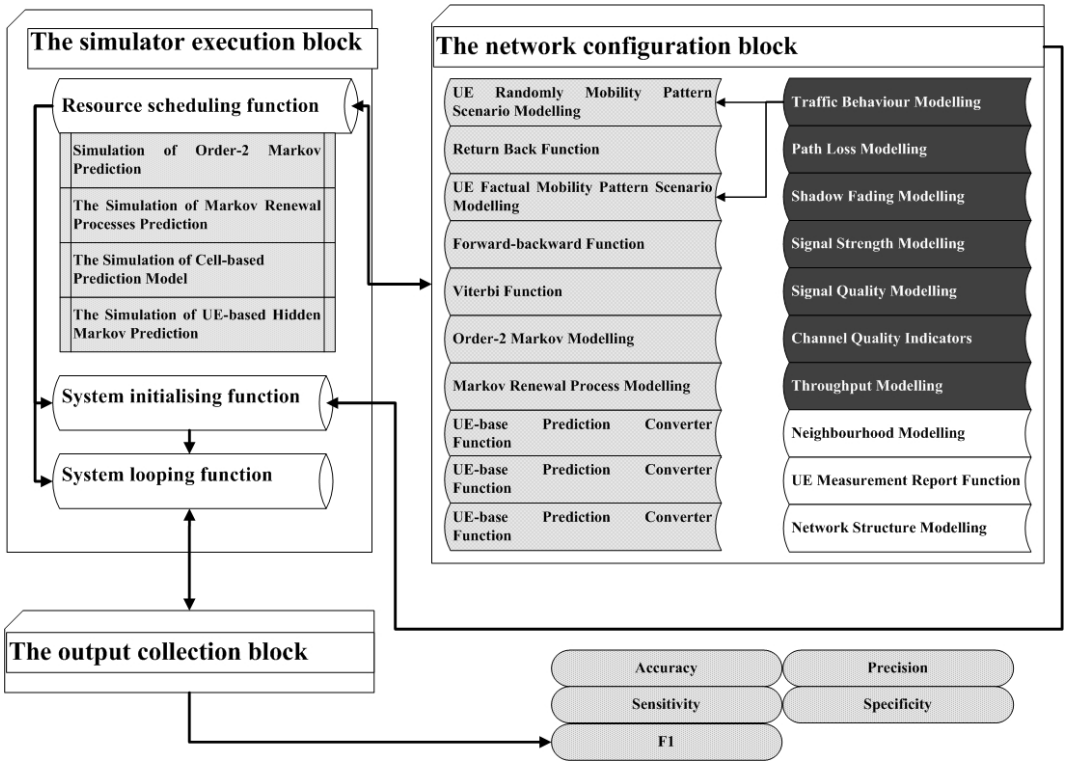

Figure B.1: The structure of simulation in Chapter 3

B.1 Simulation for Cell-based Prediction Model in Chapter 3

The simulation for Cell-based Perdition Model (CPM) can be summarised as Figure B.1. The semi-dark blocks are the custom functions that add to the SLS in order to achieve the simulation requirements.

Due to this simulation doesn't consider the throughput, in SLS, some of the blocks (dark) are disabled or replaced by the other custom blocks which will be described as following sections.

B.1.1 The Modification of the Configuration Block

UE Randomly Mobility Pattern Scenario Modelling

Since this simulation needs to model the UE moving history as states for UE-based Traffic Prediction Model (UTPM), there are many new requirements

need to be achieved:

For the UE object in this simulation:

- The number of UEs in the simulation scenario should be fixed.
- The speeds and directions of UEs should be different.
- UEs should have the camping time in the coverage of femtocell.
- UE should record its moving history (cell IDs) and the status of handover or camping in the serving cell.
- UE should have the ability to calculate the transition and emission probability matrix in order to predict the next cell for CPTM.
- UE should have the ability to walk back to the macrocell, if the UE walk out from the coverage of macrocell.

According to the requirements, the author modifies the traffic behaviour model as a set number of UEs uniform randomly located in the coverage of a macrocell. Add the speed and direction features to the UE object at UE layer and give them uniform randomly value. The camping time of a UE in the femtocell is based on the exponential distribution.

Moreover, the action of handover or camping is based on the uniform randomly value. UE also has the function to record its moving history in order to calculate the transition probability matrix and emission probability matrix.

Return Back Function

In terms of return back function, since the coverage of the macrocell is hexagonal and it difficult to calculate the angle when the UE return back to macrocell. Therefore, the author set the circle as the return back boundary for the coverage of the macrocell as shown in Figure B.2. When a UE arrives at the boundary of the circle, the return back function would be triggered.

However, there are four different cases need to be considered in return back function due to the UE needs different new angles as shown in Figure B.3.

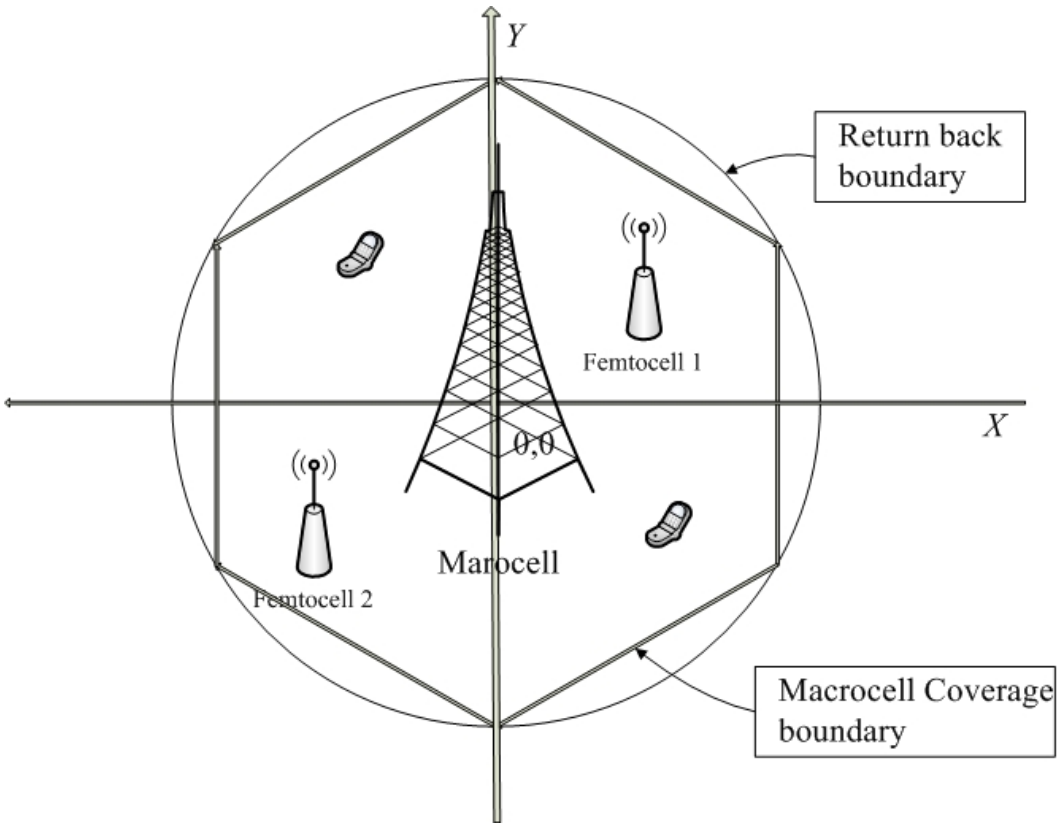

Figure B.2: Four return back cases in macrocell network

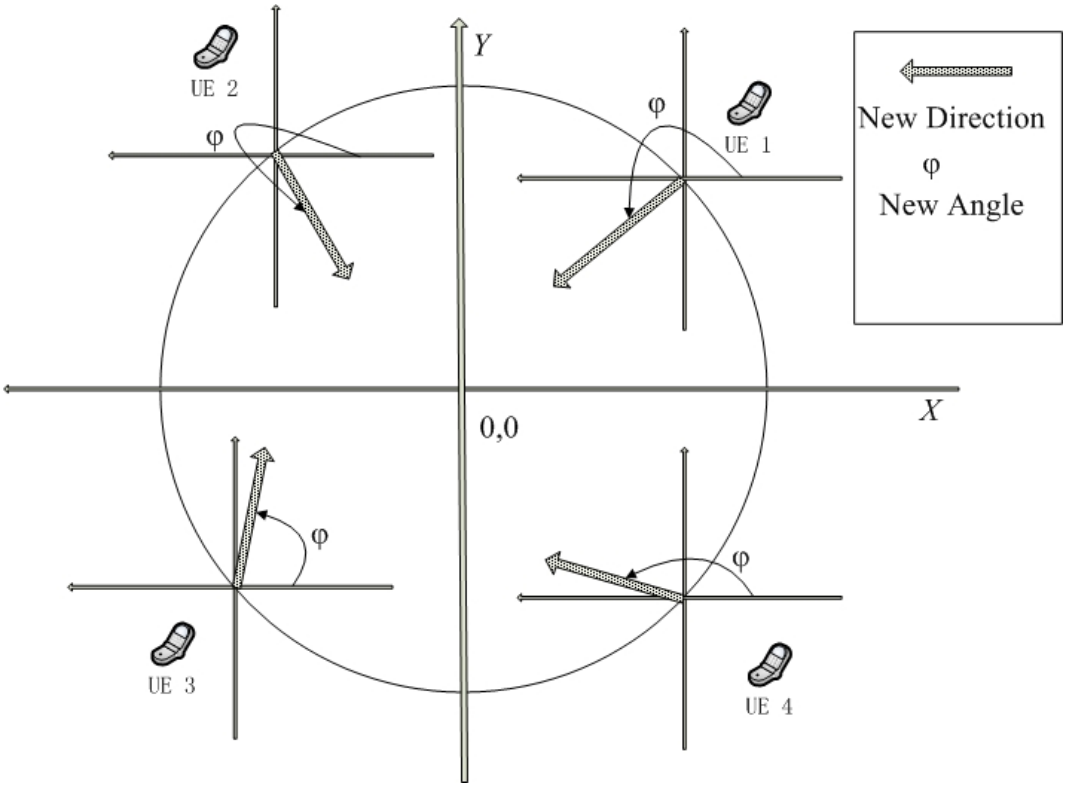

Figure B.3: The return back boundary in macrocell network

In Figure B.3, UE 1 represents the return back case happened at the first quadrant and the new angle would take random value between 180 and 270 degree. UE 2 represents the return back case happened at the second quadrant and the new angle would take random value between 270 and 360 degree. Similar applies to UE 3 and 4 in third and fourth quadrants. When the UEs get the new directions, their speeds would be also changed a new value in this simulation.

Femtocell Modelling

For the femtocell object in SLS:

- The number of femtocells should be changed to simulate the plug and play feature
- Femtocell should have the ability to record the number of handovers (traffic level) and camped UEs in a given time period.

- Femtocell should have the ability to calculate the transition and emission probability matrix in order to predict the next traffic level.

According to the requirements, the author modifies the traffic behaviour modelling as 5 femtocells uniform randomly located in the coverage of a macrocell. During the simulation, location of femtocells are not changed, but the femtocell would turn off or on followed Normal distribution. Moreover, add the recording function to record the number of handovers and camped UEs for each femtocell object at femtocell layer. Moreover, femtocell also has the function to calculate the transition probability matrix and emission probability matrix.

Mobility Management Entity Modelling in Chapter 3

The MME is already modelled in the SLS as mentioned in Chapter 2.1. As mentioned in thesis, MME is the one of network management system blocks and used to achieve the wireless cells management and communication [25]. Therefore, in this simulation, MME is set in the core network layer which can control the other three layers. MME has four main functions:

- Collects all the information from the femtocells. The information includes the number of average handover of the femtocells for CPM and CPTM processes (information of average handover of the femtocells for CPTM, please Section B.1.1.10).

- Models the information from the femtocells as the states, and then executes forward-backward function and viterbi function for CPM.

- Collects the reality states from the femtocells and calculate the prediction accuracy, precision, sensitivity, specificity and F1 for CPM and CPTMs. The calculation of those results is based on the Table B.1 which refers to Table 3.1.

  Since the main purpose of the prediction is to predict the Busy Femtocell (BFemtocell) (Section 4.2.2), this positive is considered as the traffic level

Table B.1: Confusion Matrix for Prediction Evaluation

		Prediction	**Prediction**	
		Positive	Negative	Sum
Reality	Positive	True Positive (TP)	False Negative (FN)	Reality Positive (TP+FN)
Reality	Negative	False Positive (FP)	True Negative (TN)	Reality Negative (FP+TN)
Sum		Prediction Positive (TP+FP)	Prediction Negative (FN+TN)	

at Busy and Negative is considered as the traffic level at Moderate and Idle (not Busy). The calculation rules are:

  - If reality Busy, but predict not busy, it is considered as False Negative.
  - If reality not busy, but predict not busy, it is considered as false positive.
  - If reality Busy, but predict as Busy, it is considered as true positive.
  - If reality not busy, but predict as Busy, it is considered as true negative.

- Send the prediction results to the output collection block.

UE Factual Mobility Pattern Scenario Modelling

In this scenario, the factual data are used in the SLS. This data comes from Community Resource for Archiving Wireless Data (CRAWDAD) network trace repository, and it has recorded movement history and communication situation of 20 smart phone devices (UEs) over half month.

The date from CRAWDAD is saved as excel file. Each UE's position, ID and recording time been recorded as the rows in that excel file in every 20 second. Therefore, each of the UE's moving direction and UE speeds can be calculated and modelled as the UE moving history.

Forward-backward Function

To calculate the optimal parameters in HMM, in this simulation, the author sets the forward-backward function in the simulation. More information about forward-backward algorithm, please check Section 3.2.2.

Viterbi Function

To calculate the sequence of hidden states, in SLS, the author sets the viterbi function in the simulation. More information about viterbi algorithm, please check Section 3.2.2.

Order-2 Markov Modelling

To generate the transition probability matrix in order-2Markov model, the author sets a Makrov function in the simulation. More information about order-2 Markov, please check Section 3.1.2.

Markov Renewal Process Modelling

To generate the transition probability matrix and condition probability in Markov Renewal Process (MRP) model, the author sets a MRP function in ths simulation. More information about MRP, please check Section 3.1.3.

UE-base Prediction Converter Function

UE-base prediction models only can predict the UE future locating cell not the intensity of a femtocell's handovers. Therefore, the UE-base prediction converter is used to convert the prediction results to the traffic level.

In this simulation, the femtocell object has a function to collect the predicted information from UEs. Then it counts the number of that UE predicted take a handover to this femtocell in a given time period.

After the femtocell got the information of the number of UE handovers, it send the all information to MME as mentioned earlier, MME would generate

the prediction process for all CTPMs. More information about the process, you can check the Section 3.3.3.1.

B.1.2 The Modification of the Simulator Execution Block

Simulation of Order-2 Markov Prediction Model

In this simulation, each of the UE moving history (Cell ID) will be record in the UE object and generate the transition probability matrix, each time of UE take a handover to a cell, and this transition probability matrix would be updated. An array [the number of order-*2* states * the number of states] is defined in the UE object to represent the transition probability matrix. In transition probalility matrix table, the percentage numbers are the transition probability from the first column to the top row. When the UE campus time finish and move to the new state (Cell), it could use the transition probability matrix to predict the next state with the highest probability. Once the UE has moved in the new cell, the predicted results and reality results would be save as new an array defined in UE object. Then the femtocell object would load this array to provide the traffic level via UE-base prediction converter function as mentioned earlier. Moreover, during the prediction, if one of the femtocell has been turned off or on, the simulation tool would recalculate the transition probability matrix to predict the next UE's moving location (the next state). More information about order-*2* Markov model, please check Section 3.1.2.

The Simulation of Markov Renewal Processes Prediction Model

In Markov Renewal Processes (MRP) prediction model, the next state prediction is not only based on the transmit probability but also the interval time between two states occurs (condition probability). Hence, there are two arrays [6x6] and [6xT] (T is the time that transition between two states) in the UE object, and represent transition and condition probability matrix.

The transition probability matrix is similar to the previous model but with less elements. in condition probability matrix table in UE object, the percent-

age numbers are the transition probability from the first column to the top row. When the UE campus time finish and move to the new state (Cell), it could use the transition probability matrix and condition probability to predict the next state with the highest probability. Once the UE has moved in the new cell, the predicted results and reality results would be save as new an array defined in UE object. Then the femtocell object would load this array to provide the traffic level via UE-base Prediction Converter function. Moreover, during the prediction, if one of the femtocell has been turned off or on, the simulation tool would recalculate the transition probability matrix and MRP condition probability to predict the next UE moving location (the next state). More information about MRP, please check Section 3.1.3.

The Simulation of Cell-based Prediction Model

In SLS, the Cell-based Traffic Prediction Model (CTM) defined as three hidden states, such as $S_{Busy}, S_{Moderate}$ and S_{Idle} and three observation states, such as $O_{Busy}, O_{Moderate}$ and O_{Idle}. Hence, in the programme, to create three arrays as A [3x3], π [1x3] and B [3x3], where A represents the transition probability matrix which provides the transition probabilities for hidden states. π represents the probability matrix which provides the probability of each hidden state occur. B represents the emission probability matrix which provides the relationship between hidden and observation states.

In CTM, via the forward-backward function to update the (π, A, B) and via the viterbi function to find out the hidden states sequence.

Since the hidden states in CTM are Markov chain, the MME can calculate the next hidden states and predict the observation state via emission matrix B. After that, when the MME receive the reality number of handovers from femtocells, then it sends prediction results to the output collection block.

The Simulation of UE-based Hidden Markov Prediction Model

The UE-based HMM is that UE has present handover are modelled as hidden states. The user's locating cells are modelled as observation states. In SLS, it

defines as 2 hidden states such as communication and non-communication and six observation states (0-5 cell IDs). Hence, in the programme, similar to the CTM to create three arrays as A [the number of current observation states * the number of next observation states], π [1* the number of observation states] and B [the number of hidden states * the number of observation states] due to five femtocells and one macrocell are set in the network.

The initial value of elements in A and pi is 1/ (the number of observation states) and the initial value of elements in B is obtained from small time training.

Similar applies to CTM, this prediction uses the forward-backward function and observation sequence to update the (π, A, B). Then it uses the viterbi function to find out the hidden states sequence.

Since the hidden states is a Markov chain, once the UE object can have the current observation state, and UE start to handover. It then calculates the current hidden state, and predicts the next hidden states via matrix A and also predicts the next cell via matrix B. Therefore, this model provides the communication (handover) probabilities to the cells that UE moving to.

B.1.3 The Modification of the Output Collection Block

After MME send the results of accuracy, precision, sensitivity, specificity and F1 for different models to this block, this block can transfer those data into the XML file. Each element's name is the name of the model, and its children elements are accuracy, precision, sensitivity, specificity and F1. The more information about those evolution results, please check Section 3.3.1 and 3.3.2.

B.2 Simulation for Dynamic Group Physical Cell Identity Distribution in Chapter 4

The requirements in this simulation are described below:

- The number of femtocells and their locations should be changed in order

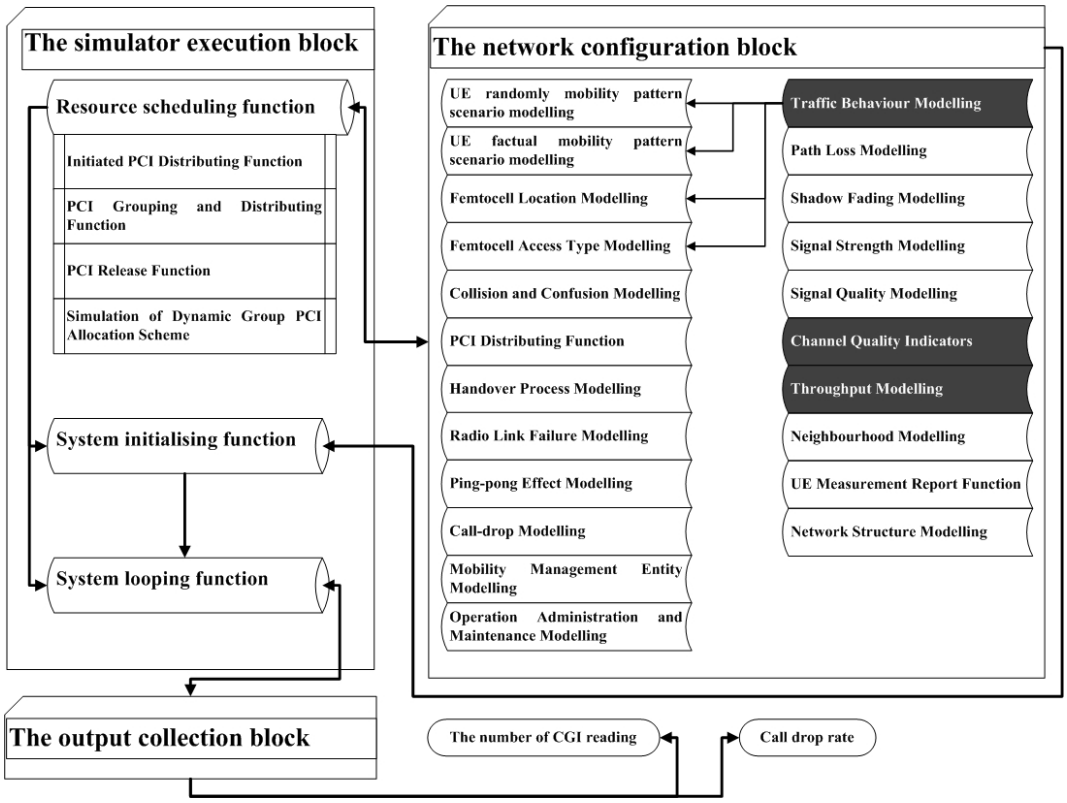

Figure B.4: The structure of simulation in Chapter 4

to simulate the plug-and-play feature.

- The number of PCIs should be less than the number of the femtocells in order to simulate the PCI confusion and collision.
- The handover process should be simulated in the simulation.
- The call-drop event should be recorded in UE objects and then it would be reported to the core network layer.

In order to achieve those requirements, some modelling and functions have been proposed. This simulation can be summarised as Figure B.4. Some blocks (semi-dark) are the custom functions that add to the SLS in order to achieve the simulation requirements.

Due to this simulation doesn't consider the throughput, in SLS, the dark blocks are disabled or replaced by the other custom blocks which will be described below.

B.2.1 The Modification of the Configuration Block

Femtocell Location Modelling

The number of femtocells should be changed to simulate the plug-and-play feature. femtocell location is uniform randomly. In the macrocell, a various number of femtocells are uniformly distributed with its coverage (from 20-50). The number of femtocells is generated in a period of time T, through the homogeneous Poisson process.

$$P[FN(t+T) - FN(t) = FN_u] = \frac{(\lambda \cdot T)^{FN_u} \cdot e^{-\lambda \cdot T}}{FN_u!} \tag{B.1}$$

where FN_u is the number of femtocells appear and locate in the network. $\lambda \cdot T$ is the mean users' arrival rate, also known as 'process intensity'. Moreover, the holding time th is provided by exponential distribution (a.k.a. negative exponential distribution). This distribution is described as:

$$f(t_h) = \mu \cdot e^{-\mu \cdot t_h} \tag{B.2}$$

where μ is the mean holding time of femtocells.

Femtocell Access Type Modelling

There are two access types are considered in this simulation, Closed Subscriber Group (CSG) and non-CSG (Section 4.2.3). In this simulation, some of the UEs would be signed as the registered UE for CSG femtocell.

For the CSG femtocell, if a registered UE arrived at the femtocell, it would take the handover process to the femtocell in 100%. Otherwise, the non-registered UE cannot take the handover process to that femtocell.

For the non-CSG femtocell, all the UEs can have the chance to take the handover to the femtocell, unless the femtocell is fully load (2 RBs are the minimum for one UE).

Collision and Confusion Modelling

According to the neighbourhood model, after the femtocells have been located, the femtocell will record the conflicted femtocell IDs. Moreover, for the one-tier confusion case, femtocell would also record its neighbour, neighbour's neighbour and neighbour's neighbour's neighbour cell IDs in order to achieve the PCI release. The more information about PCI release methods, please check Section 4.2.4.

PCI Distributing Function

This function will achieve two goals:

Firstly, MME could use this function to distribute the PCIs to the femtocells.

Secondly, during the PCI distribution, this function ensures the PCI collision and one-tier confusion free by using the PCI release methods (Section 4.2.4).

Handover Process Modelling

In this simulation, the handover model only considered the RSRP trigger equation as:

$$RSRP_{target} \geq RSRP_{serving} + Hysteresis \tag{B.3}$$

$RSRP_{target}$ and $RSRP_{serving}$ are the measurement of average reference signal strengths for the resource block at target and seving cell. Hysteresis can be used to delay the handover happening until the signal strength become more stable. The more information about handover process is described in Sections 5.1.2 and 5.1.3. Due to no reference signal defined in the simulator, RSRP is calculated from the average power of the whole sub-channels.

The process of the handover can be summarised in Figure B.5.

In the Figure B.5, the hysteresis delay the time that Time-To-Trigger (TTT) happened and TTT is used to delay the A3 event triggering in order

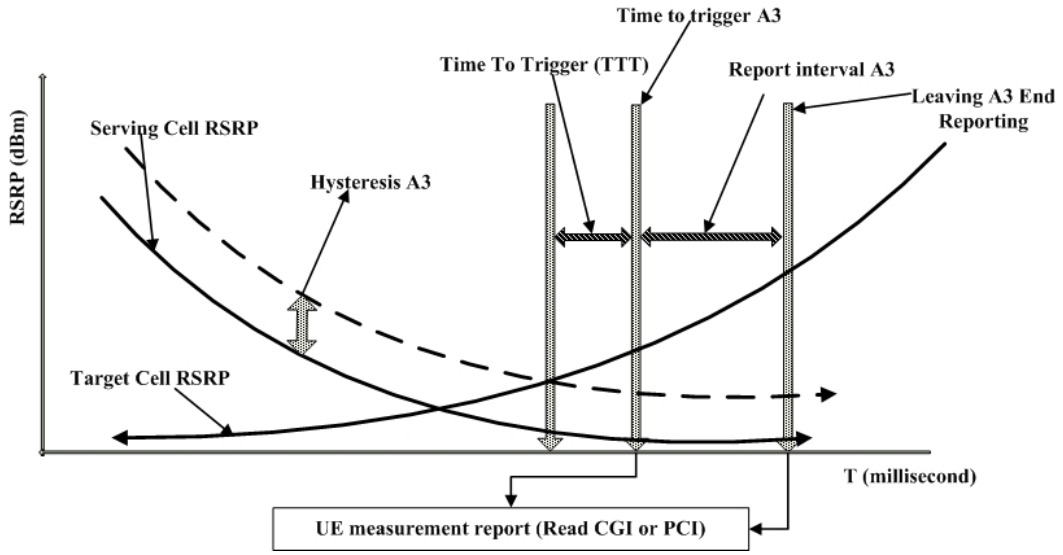

Figure B.5: The stureture of handover process in system-level simulation

to achieve the signal strength become more stable.

During the A3 report interval, UE would read the PCI from the target cell which cost 20 ms by using measurement report. If there is no confusion happened, the UE would leave the A3 event and finish the handover process. Otherwise, the UE would require the target femtocell to provide the CGI and this would cost 160 ms by using measurement report. After UE got the CGI ID, the UE would leave the A3 event and finish the handover process. Moreover, after UE got the PCI and CGI, the handover need about 300 ms to be estimated between serving and target cell [8]. Hence, the A3 report interval should include the 300 ms delay till the A3 event finished. Moreover, in the simulation, the loop function will check the A3 event trigger or not.

Radio Link Failure Modelling

According to the standard [9], if the average received SINR drop below -6 dB, the call of the UE would has higher probability to disconnect to the connected cell and this is defined as Radio Link Failure (RLF). The number of RLF event would be stored in the UE object and then reported to the target cell. After that, the femtocell or marcocell sends the RLF information to MME in core network layer.

Ping-pong Effect Modelling

Ping-pong effect is registered due to non-optimal handover parameters, where the UE made a successful handover from a cell B to cell A in a short time period after another successful handover had already occurred from A to B with same UE. In the simulation, this short time is defined as 5 second [59]. The number of ping-pong event would be stored in the UE object and then reported to the target cell. After that, the femtocell or marcocell sends the RLF information to MME in core network layer.

Call-drop Modelling

When the RLF or ping-pong happened, the UE would try to connect back the serving cell or to the other cells. Therefore, in this simulation, the call-drop model is defined as the UE is fail to connect back the serving cell or to the other cells due to average SINR received from them is lower than -6 dB after RLF or ping-pong effect happened. The number of call-drop events would be store in the UE object and then reported to the target cell. After that, the femtocell or marcocell sends the RLF information to MME in core network layer.

Mobility Management Entity Modelling

MME resides in the core network layer in SLS, core network layer is used to control the entire network and also achieve the communication interface between macrocell and femtocell. MME is the function that manages the handover, PCI distribution in the core network.

In this simulation, Operation Administration and Maintenance (OAM) is reside in MME and can have all the functions from MME. OAM modelling will be described in next section.

Operation Administration and Maintenance Modelling

As mentioned in thesis, OAM is a tool which is implemented by standards to achieve the operating, administering, managing and maintaining in the SON. Considering the centralised SON structure in this simulation, the OAM reside together with MME in the core network layer which can control the other three layers.

In this simulation, the OAM would implements those modelling that have been proposed earlier to achieve some functions which are list below:

- Collect the handover information from the femtocell objects and execute the cell-based prediction for those femtocell objects.
- Manager the PCI groups and PCI IDs in the simulation. In this function, it includes: distributed unique PCI IDs to the BFemtocells; seek the PCI IDs via PCI release method (Section 4.2.4).
- Calculate/collect the prediction results, reading CGI results and call-drop results then send them to the Output Collection Block.

B.2.2 The Modification of the Simulator Execution Block

Initiated PCI Distributing Function

After the all the femtocell located in the simulation, this function could achieve two purposes in this simulation for Chapter 4.

- To initially distribute the PCIs by using PCI distribution model.
- To obtain the reused and unique PCI IDs after the distribution process and then send them to the PCI group function.

PCI Grouping and Distributing Function

After the initiated PCI distribution, this simulation would create the reused and unique PCI groups. The, via the MME (OAM) and proposed approach (Section 4.2), this simulation start to sign the PCI to the new femtocell appears

or get the PCIs from the turned off femtocells. A loop programme will be executed in the simulator to ensure this process and also update the PCI groups.

Moreover, the results of the CPM from OAM are used in this function to find the BFemtocells in the PCI distributing process. During this process, the UE would report the call-drop, ping-pong, RLF to the femtocells. The femtocell would report all the information from UEs and also the number of CGI reading and number of successful handover to the OAM.

PCI Release Function

This function will be executed when fewer femtocell is working in the network. In this function, the whole network PCI distribution would be changed and the PCI groups would be update at same time. Then the simulator can start to process of PCI group function and output the results.

Simulation of Dynamic Group PCI Allocation Scheme

There are two different scenarios have been simulated in this simulation, UE randomly mobility pattern and UE factual mobility pattern scenarios.

In terms of UE randomly mobility pattern scenario, this simulation is focus on the analysis of the CGI reading time between CSG and non-CSG femtocell due to there are higher number of femtocells (20-50) can be generated in the network. Therefore, the femtocell Access Type Model is involved in the process. Moreover, the traffic model uses the same as the previous simulation.

In terms of UE factual mobility pattern scenario, similar applies to the previous factual mobility pattern scenario simulation. In this scenario, the factual data are used in the simulation. 20 UEs are record from the CRAWDAD over half month. This simulation only considers the call drop rate. Therefore, only five non-CSG femtocells are located in the network and Call Drop Model is involved in the process.

In both of the scenarios, the femtocell object implements the femtocell location, collision and confusion and handover process with CGI or PCI models

from the configuration Block. Moreover, the processes of the initiated PCI distribution, PCI groups and PCI release function are involved in both of the simulation.

B.2.3 The Modification of the Output Collection Block

In this simulation, this block collects the number of CGI reading time and successful handover Nsuccessful and the number of call drop Ndrop from the OAM.Then the number of CGI reading and call-drop ratio are saved into the XML file.

B.3 Simulation for Distributed Dynamic UE-based Hysteresis adjustment in Chapter 5

The requirements in this simulation are described below:

- To assume that no two-tier PCI confusions happened during handover, due to the simulation only considers the handover triggering parameter. Therefore, the number of femtocells and their location are fixed.
- The handover process should be simulated in this simulation.
- RP-HAPI table (Reserved Parameter (RP) and Handover Aggregate Performance Indicator (HAPI)) can be calculated and updated in the femtocell object.
- The optimal hysteresis can be calculated in the UE object.
- The RLF, ping-pong effect, redundancy handover and call drop event should be recorded in UE objects and then it would be reported to the femtocell object.

In order to achieve those requirements, some functions have been added to this simulation. Those functions can be summarised as Figure B.6. The

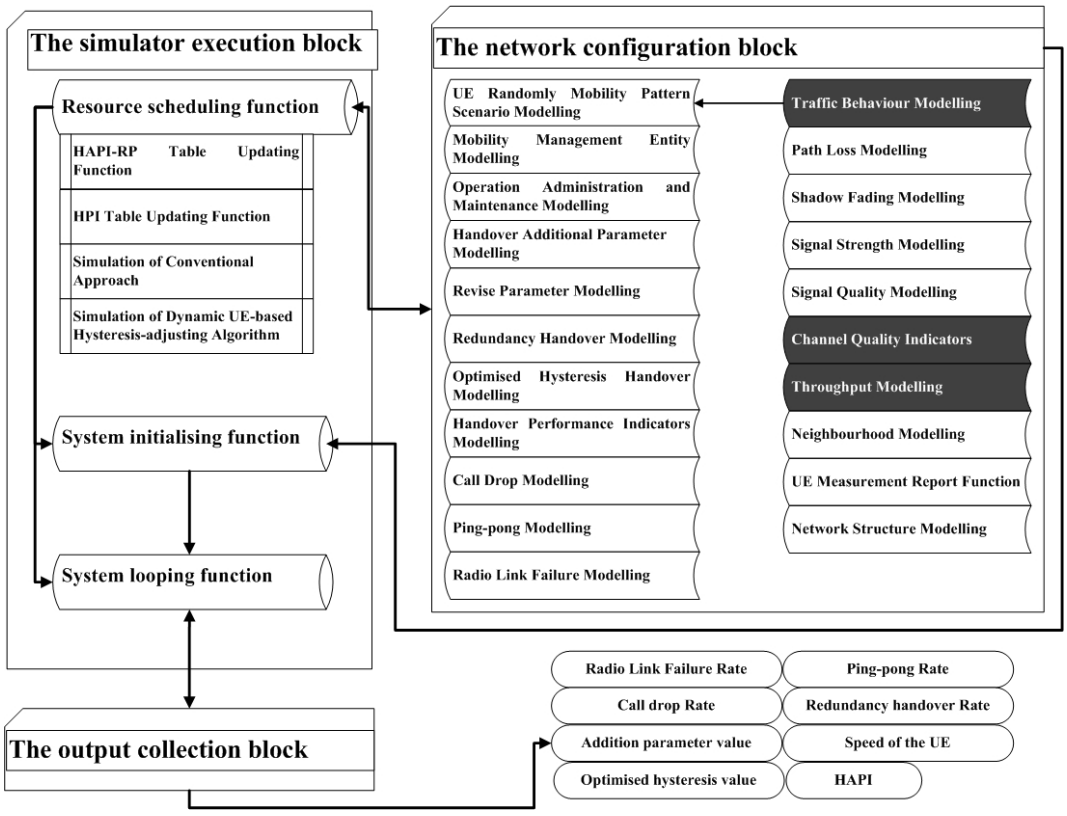

Figure B.6: The structure of simulation in Chapter 5

semi-dark blocks are the custom functions that add to the SLS in order to achieve the simulation requirements.

Due to this simulation doesn't consider the throughput, in SLS, some of the blocks (dark) are disabled or replaced by the other custom blocks.

B.3.1 The Modification of the Configuration Block

Mobility Management Entity Modelling

MME resides in the core network layer in SLS, core network layer is used to control the entire network and also achieve the communication interface between macrocell and femtocell. MME is the function that manages the handover, PCI distribution in the core network.

In this simulation, MME is only used to control the handover process. Centralised and distributed OAMs don't reside in MME.

Operation Administration and Maintenance Modelling

As mentioned in thesis, OAM is a tool which is implemented by standards to achieve the operating, administering, managing and maintaining in the SON. Considering the hybrid SON structure in this simulation, the OAM has been separated into two parts: centralised OAM and distributed OAM. Both of them implement those modelling that have been proposed earlier to achieve some functions are list below:

In terms of centralised OAM, it resides in the femtocell object. The functions are:

1. Collect the handover information from the UE object and calculate the HAPI.
2. Create/update the HAPI-RP table according to the handover information and HAPI.
3. Obtain the optimised RP value and send it to the UEs which are serving by the femtocell.
4. Report the simulation results to the output collection block.

In terms of distributed OAM, it resides in the UE object. The functions are:

1. Collect the handover information during the handover process.
2. Send the handover information to serving femtocell (centralised OAM).
3. Receive the optimal RP value and calculate the optimised hysteresis value.

Handover Additional Parameter Modelling

To calculate the Handover Additional Parameter (HAP) from distributed MRO function (UE object), it can be described as:

$$HAP \geq RP + SINR_{target} \tag{B.4}$$

where RP is the reserved parameter that record in femtocell object (centralised OAM), $SINR_{target}$ is the average SINR received from target femtocell (inbound handover) or macrocell (outbound handover). This HAP then uses in the Equation (B.5) as mentioned in Section 5.2.3 to calculate the optimal hysteresis Hproposed.

$$H_{proposed} \geq H_{high} - HAP \tag{B.5}$$

where H_{high} is a constant value that used for the lowest speed UE in the network, in this simulation, H_{high} is 8 dB according to [13, 74].

Revise Parameter Modelling

Before the creation of HAPI-RP table, this simulation needs to generate a sequence RP values and the steps of this sequence generation are list below:

- Calculate the maximum average received SINRmax,averagefrom the simulation.

- Since the $H_{high} - HAP$ is greater or equal to 0 (Section 5.2.3), according to the Equation (B.5) and (B.6) the RP should be smaller or equal to $H_{high} - SINR_{max}$,average. Therefore, the simulation can calculate the maximum RP value and generate a sequence RPs with a 1dB reduction step. The range of SINR and H_{high} can be measured by the operators for the specific cell, thus the range of RP can be calculated by using these information from system. For instance, the H_{high} is 8 dB, the SINR is from -15 to 30 dB. The range of RP would be from -22 to 23 in dB units. Moreover, in dB units, since $HAP >= 0$, if $H_{high} - (RP + SINR) < 0$, the HAP will be set back to 0.

- During the process, if the $H_{high} - HAP$ smaller than 0, the simulation would set the result as 0. Moreover, RP is the public parameter in the centralised OAM (reside in the femto or macro object) and HAP is defined in the distributed OAM (reside in UE object), therefore, in the

hysteresis self-optimisation approach, all UEs should share the same RP but different HAP.

Redundancy Handover Modelling

Redundancy handover represents the redundancy handover rate. It is defined as the ratio of the number of incorrect handover (handover to wrong cell). In the simulation, if the UE take a handover to the wrong cell which one has the poor signal strength the target cell, the UE would record this as the redundancy handover events in the UE object. Then it will be reported to the target femtocell.

Handover Aggregate Performance Indicator Modelling

To calculate the Handover Aggregate Performance Indicator (HAPI) from femtocell, it can be described as:

$$HAPI = W_1 \times H_{fr} + W_2 \times P_{pr} + W_3 \times C_{dr} + W_4 \times R_{hr} \tag{B.6}$$

$$W_1 + W_2 + W_3 + W_4 = 1 \tag{B.7}$$

where the $H_{fr}, P_{pr}, C_{dr} and R_{hr}$ represent handover link failure, ping-pong, call-drop and redundancy handover ratio, respectively. The W_1, W_2, W_3 and W_4 are defined as weights and the sum of the values of them should be equal to 1. The more information about HAPI and calculation of handover link failure, ping-pong, call-drop and redundancy handover ratio, please check Section 5.1.4 and 5.2.5.

Optimised Hysteresis Handover Modelling

Due to the SLS does not consider the reference signal, the average SINR is calculated by whole sub-channels. This calculation is set in the UE object to trigger the A3 event.

Handover Performance Indicators Modelling

In this simulation, in order to compare with the proposed optimised hysteresis approach, this research simulates the scheme that proposed in [19]. Handover Performance Indicators (HPI) is evaluation which considers the handover failure ratio, ping-pong ratio and call-drop ratio together.

$$HPI = W_1 \times HPI_{hof} + W_2 \times HPI_{hpp} + W_3 \times HPI_{dc} \tag{B.8}$$

where W_1, W_2 and W_3 are the weights and the sum of the values of them should be equal to 1. HPI_{hof}, HPI_{hpp} and HPI_{dc} represent the handover failure ratio, ping-pong ratio and call-drop ratio. The more information about this scheme, please check Section 2.4.

B.3.2 The Modification of the Simulator Execution Block

HAPI-RP Table Updating Function

In the proposed approach, the HAPI-RP table is used to record the RP values and its corresponding HAPI values in the centralised OAM, in order to obtain the optimal RP value. Moreover, the number of RLF, ping-pong, redundancy handover and successful handover events are stored in the UE object. Therefore, during the handover process, centralised OAM could collect that information from UEs and calculate the HAPI value via handover aggregate performance indicator modelling. Then, centralised OAM update the HAPI value in the HAPI-RP table for each RP value.

HPI Table Updating Function

In order to create the HPI table, each of the value in the sequence of given hysteresis would be implemented in the simulation. Then the RLF, ping-pong and call-drop information can be collected by femtocell object to calculate the HPI value via handover performance indicators modelling and create the HPI table with the corresponding hysteresis value. After that, the simulator can

choose a optimal hysteresis with the lower HPI value from table, and wait for the next time HPI table updating.

Simulation of Dynamic UE-based Hysteresis-adjusting Algorithm

In the simulation, UE randomly mobility pattern is implemented with 20 Femtocells and 300 UEs. The handover process with CGI and PCI is involved in this simulation, however, the simulation considers all the network have enough PCIs to sign the femtocells. Therefore, the handover process only considered the 20 ms reading PCI and 300 ms handover signalling time.

The HAPI Table is updated in a fix time period (100 ms). Each femtocell object has its unique RP and the hysteresis value updating for each UE is only implemented after the UE finish the handover process. This is because during the handover process, the hysteresis can be changed.

Each time of the HAPI-RP table updating, the RP may change to the optimal one. Then the centralised OAM sends the information of RLF, ping-pong, call-drop, redundancy handover ratios, HAPI, optimal hysteresis, RP value, UE's speed to the output collection block.

Simulation of Conventional Approach

Since in the simulation, TTT is set as the constant value, the approach [11] only considers the hysteresis value. Same to the previous simulation, UE randomly mobility pattern is implemented with 20 Femtocells and 300 UEs and the handover process only considered the 20 ms reading PCI and 300 ms handover signalling time.

The hysteresis value in the given sequence is used in the simulation and the HPI Table is updated in a fix time period (100 ms). Each femtocell object can obtain the optimal hysteresis value from the HPI table. The hysteresis for each femtocell only can be updated after the UE handover finish.

Each time of the HPI table updating, the hysteresis value may change to the optimal one. In this simulation in order to compare with the proposed approach, this simulation also calculate the HAPI value and redundancy han-

dover rate. Then the fermtocell object sends the information of RLF rate, ping-pong, call-drop, redundancy handover ratios, HAPI to the output collection block.

B.3.3 The Modification of the Output Collection Block

In this simulation, this block collects the RLF, ping-pong, redundancy handover, call-drop ratios, HAPI, optimised hysteresis values, RP values and UEs' speeds from the centralised OAM or femtocell object. Then, this block records the results into the XML file.